

UNITED STATES
DEPARTMENT OF THE INTERIOR
GEOLOGICAL SURVEY

A SCHLUMBERGER RESISTIVITY SURVEY OF THE
AMARGOSA DESERT, SOUTHERN NEVADA

by

Michael R. Greenhaus

and

Charles J. Zablocki

Open-File Report 82-897

1982

Prepared by the U.S. Geological Survey
for the
Nevada Operations Office
U.S. Department of Energy
(Interagency Agreement DE-AI08-78ET44802)

A SCHLUMBERGER RESISTIVITY SURVEY
OF THE
AMARGOSA DESERT, SOUTHERN NEVADA

by

Michael R. Greenhaus

and

Charles J. Zablocki

INTRODUCTION

During 1978-1980, the U.S. Geological Survey carried out a geoelectric survey consisting of 136 Schlumberger resistivity soundings in the Amargosa Desert, Nevada, in support of hydrological studies being performed by the Water Resources Division in this area. These studies are part of the Radwaste Program effort to find a suitable site for nuclear waste storage within the Nevada Test Site, north of the Amargosa Desert. The aim of the geoelectric survey was to define basement structure and basin-fill characteristics, which may or may not be influencing the hydrological systems of the region.

SURVEY DESCRIPTION AND METHODS

Figure 1 shows the region of the geoelectric survey and the locations and azimuths of the 136 Schlumberger resistivity soundings. Maximum electrode separations ranged from $AB/2=4000$ feet (1219 meters) to $AB/2=8000$ feet (2438 meters). Crossed pairs of soundings were made at several locations as a check for anisotropy. Also, several sounding locations were reoccupied in order to sound deeper at locations where the original sounding did not detect the basement.

The resulting sounding curves were processed and interpreted using an automatic interpretation program developed by Adel Zohdy (unpub. program, U.S. Geological Survey, 1973, 1975). The results, plotted on 3 cycle x 4 cycle

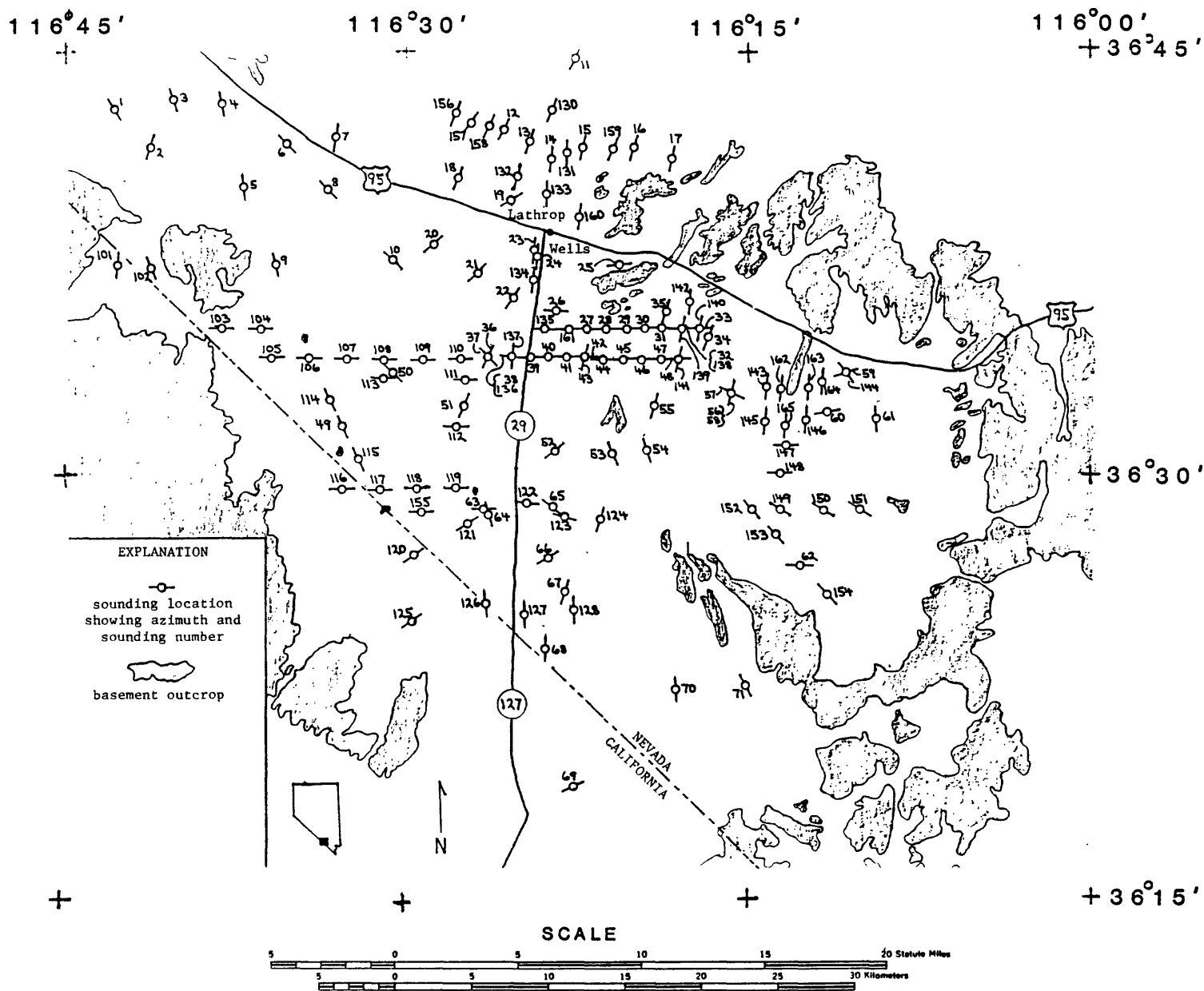


Figure 1. Schlumberger sounding locations, Amargosa Desert region.

log-log graphs, are included in the appendix. The soundings have been numbered AMAR 1 through AMAR 71, and AMAR 101 through AMAR 165. Each graph includes the following:

- (1) The field data, shown by "x" symbols, which plot as a discontinuous curve of offset curve segments.
- (2) A digitized-data curve shown by square symbols. This curve was obtained by shifting the offset segments of the field data with respect to the last segment to produce a continuous curve (Zohdy and others, 1973), and then digitizing this curve at a rate of six points per logarithmic cycle using a subroutine in a computer program for bicubic spline functions (Anderson, 1971).
- (3) The layered model, represented by a solid-line step function, showing layers of various thicknesses and resistivities. This model is obtained by entering the digitized data points into the automatic interpretation program (Zohdy, 1973, 1975) which, through iteration, finds a horizontally layered model, the theoretical sounding curve of which best fits the digitized data curve.
- (4) The best-fitting theoretical sounding curve, shown as a continuous, solid-line curve, computed from the layered model.
- (5) The Dar Zarrouk curve for the layered model, plotted as "+" symbols. This curve has been shifted vertically by one logarithmic cycle in order to avoid confusion due to cluttering of the curves. The Dar Zarrouk curve can be used to simplify the model by reducing the number of layers (Zohdy, 1974).

RESULTS

The Amargosa Desert is a region which is well suited for resistivity soundings. It is basically a sediment-filled basin surrounded by ranges of outcropping basement rocks, the typical structure of the Basin and Range tectonic province.

Basement The basement rocks, composed of Paleozoic carbonates with some Precambrian and Cambrian clastics, will generally have resistivities greater than several hundred ohm-meters. The overlying basin-fill sediments, composed of clay, sand, gravel, and boulders, have much lower resistivities, particularly when clay content is high and when the sediments are saturated. This setting presents a large resistivity contrast between the basement rocks and the overlying sediments, allowing for fairly easy recognition of basement in the resistivity sounding curves. When the high resistivity basement has been reached after sounding through a medium of much lower resistivity, the curve swings up to a slope approaching $+45^{\circ}$, which is the theoretical limit of the slope (for horizontally stratified media) as the resistivity contrast approaches infinity. This can be seen on the deep end of many of the sounding curves in this report.

Figure 2 shows the sounding locations with the corresponding interpreted basement depths in meters. The shaded areas are basement outcrops. At stations where basement was not detected with the maximum electrode spacing, the letters "NB" ("no basement") appear. A question mark (?) indicates a sounding where the basement signature was not clear, or where the last data point (maximum electrode separation) just started to show what may have been basement signature, the uncertainty due to the absence of more data at greater electrode separation.

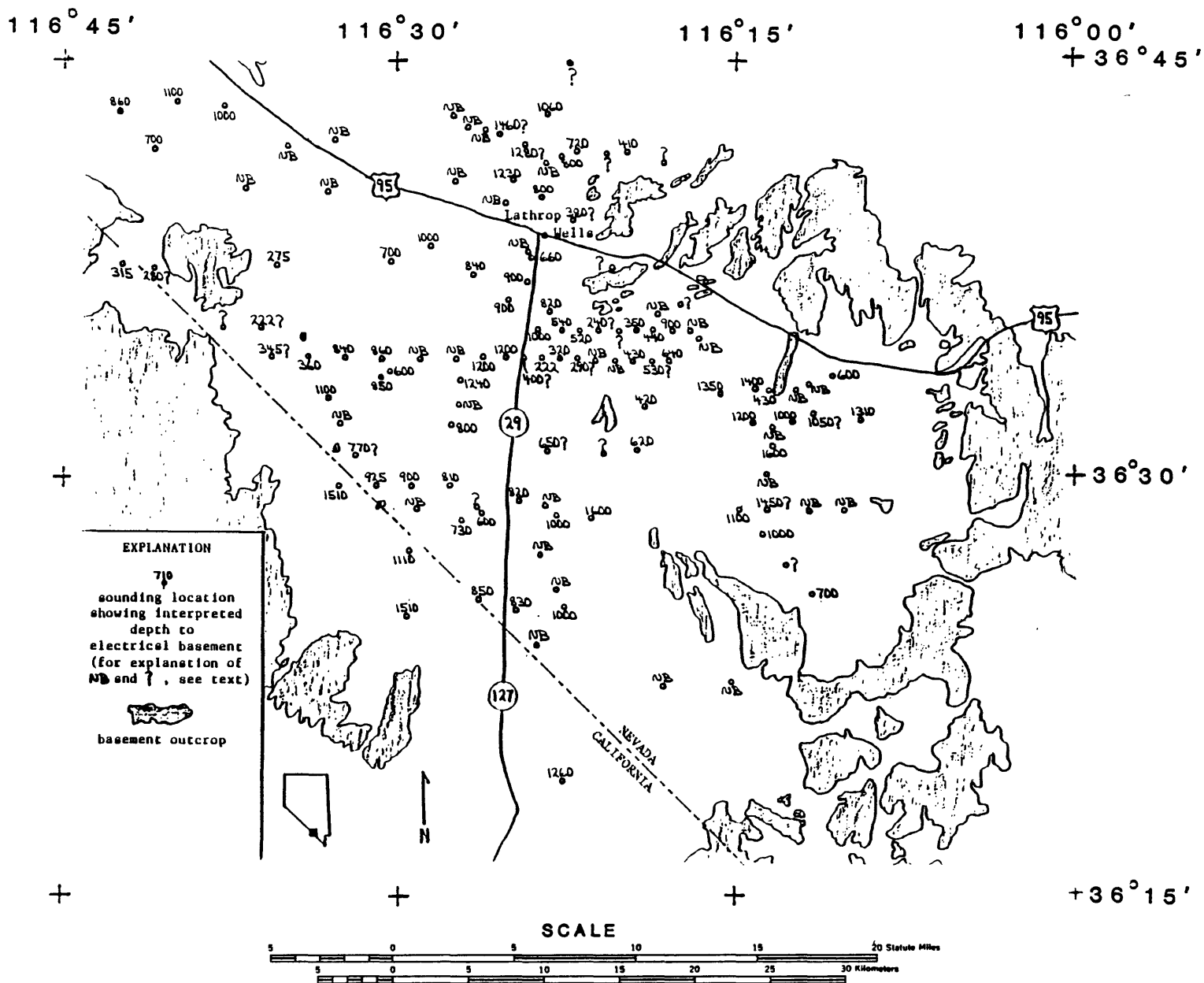


Figure 2. Interpreted depths to electrical basement from Schlumberger sounding results, Amargosa Desert region. Depths are in meters.

A cautionary word is necessary about what is being identified as basement from these sounding curves. As explained above, the basement surface is taken to be at the depth at which the top of the medium of much higher resistivity is encountered. This is commonly referred to as the "electrical basement." In the simplest case, this low resistivity-high resistivity interface would correspond to the actual geological interface between sedimentary fill and basement. However, if the uppermost section of the geologic basement has been fractured extensively, these fractures could be filled with clayey sediments and saturated with water, thus lowering the resistivity of this section. In this case, the top of the electrical basement inferred from the resistivity sounding would be at a greater depth than the top of the actual geologic basement. This is illustrated by an example from this survey. On correlation of one sounding, AMAR 162, with a lithological log for a nearby well (Johnston, 1971), a disagreement in depth to basement was seen. The well log indicated that basement rocks (in this case, dolomite and limestone) were encountered at 189 meters, where as the electrical sounding showed an apparent electrical basement depth of 430 meters. In this case, the depth to electrical basement is probably the depth to coherent basement, which is overlain by a section of highly fractured basement rock.

It should also be noted that when basement is identified by the upswing of only the last few data points in a sounding, and the last and highest resistivity value is still below the expected range of resistivities for the basement, it is possible that this is due to a thick, relatively high resistivity layer within the basin-fill sediments, and that the basement surface is at an even greater depth. However, the existence of such a high resistivity layer within the sedimentary section throughout the entire region of the survey is not likely.

The general picture of basement relief from the soundings shows the expected shallowing of basement toward the basement outcrops, with the greater depths occurring beneath the valleys between outcrops. The most pronounced feature of basement structure made apparent by this survey is the large vertical offset south of Lathrop Wells (figures 2 and 3). This north-south trending feature, downthrown on the west side, and probably the result of normal faulting, was first recognized in a regional gravity survey of the region by Healey and Miller (1971). It is most apparent between soundings 136 and 39, showing about 800 meters of vertical offset within a lateral distance of 2438 meters. The offset is not as abrupt to the north, and probably occurs as a series of sub-parallel, lesser normal faults west of the basement outcrops. To the south, all the soundings appear to be on the down-dropped side of the fault. This offset appears to be the southern continuation of the east side of the Forty-mile Wash graben to the north. Figure 3 shows the approximate location of this feature as derived from the regional gravity data (Healey and Miller, 1971), and its apparent location in one area as determined by three different methods; Schlumberger soundings (this report), tellurics (D. B. Hoover, unpublished data, 1979) and detailed gravity (H. W. Oliver, unpublished data, 1980), all along the same profile. The fairly close agreement in fault location among the three detailed profiles, and their difference from the fault location as modelled from the regional gravity, may be due to the expected lack of accuracy in locating structural features from the sparse distribution of the regional gravity data, or may be an indication that this offset is distributed among several parallel or sub-parallel normal faults.

Basin-fill Due to the complexity of the basin-fill sediments encountered over the large area covered in this survey, the basin-fill characteristics that are

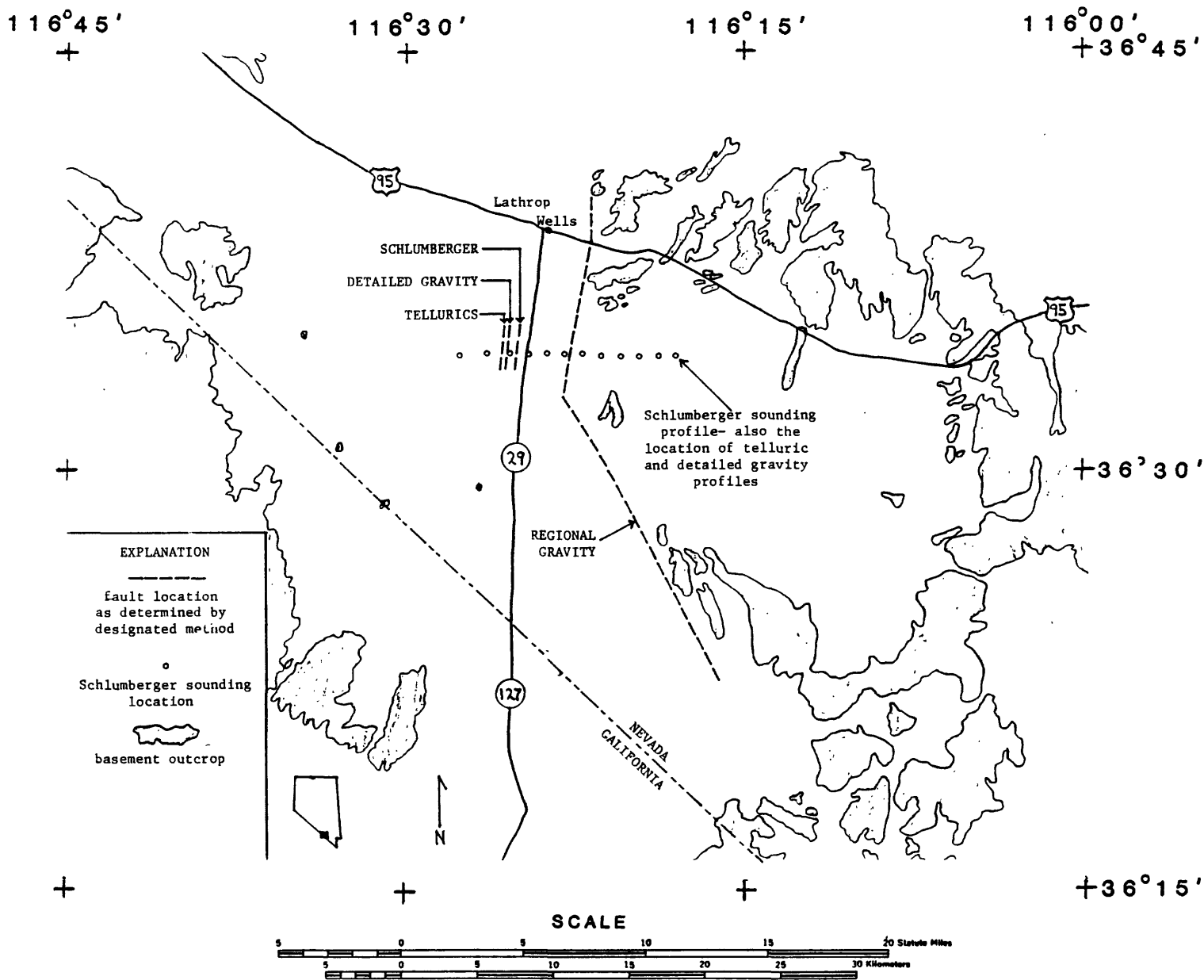


Figure 3. Comparison of four geophysical methods in determining the location of an inferred fault concealed beneath the Amargosa Desert (see text).

reflected in the resistivity soundings will be discussed in general terms. Lithologic logs for wells throughout the Amargosa Desert indicate a basin-fill composed of clay, sand, gravel, and boulders. In the area just south of Lathrop Wells, south of highway 95, a top sedimentary section, varying in thickness from about 7 to 25 meters, with resistivities from several tens to several hundred ohm-meters, can be seen in most of the sounding curves. Beneath this, and down to the top of the basement, is a section with resistivities mostly in the range of 10-100 ohm-meters. This grouping of layers of relatively higher resistivities overlying layers of generally lower resistivities probably represents a section of essentially dry sand and gravel layers at the surface overlying a section of saturated clayey sand, with varying amounts of clay throughout the section. The layers with resistivities less than 10 ohm-meters could be clay beds, or perhaps indicate the presence of saline groundwater. North of the highway, the soundings show a thicker top section of dry sediment, with the saturated and perhaps more clayey sediments starting at a depth of about 100 meters, and continuing down to the basement.

Toward the western margin of the survey area, the soundings show evidence of layers of clay, sand, and gravel. Resistivities range from less than 10 ohm-meters, probably for water-saturated sediment or possibly high clay content, to near 1000 ohm-meters, for dry layers of sand and gravel. Most of the resistivities are between 10 and 100 ohm-meters, most likely representing various layers of the sediment types mentioned above.

The soundings in the southern part of the survey area, near the state border, again show evidence of various layers of clay, sand, and gravel, with resistivities ranging from less than 10 ohm-meters to several hundred ohm-meters. In one sounding AMAR 118, layers of over 1000 ohm-meters (probably caliche) are possible. Again, the high resistivities in this area occur at shallower depths and can thus be attributed to dry layers.

The eastern part of the survey area, in addition to having the typical sounding results discussed thus far, contains three adjacent soundings (AMAR 149, 153, and 62) which show a simple three-layer picture. The uppermost layer, from the surface to a depth of about 25 meters, has resistivities of 1-3 ohm-meters, among the lowest resistivities in this survey. As all three soundings are located within a playa, this thin, top layer most likely consists of playa deposits. The second layer, from 25 meters to about 1000 meters depth, with resistivities from 10 to 30 ohm-meters, probably represents a layer of sand and silt, with varying clay content. The third and deepest layer is the basement, with resistivities over 100 ohm-meters (AMAR 153).

In most of the soundings on the downthrown, western side of the major normal fault discussed earlier, some of the lowest resistivities (10 ohm-meters) occur just before reaching electrical basement. This could indicate several hundred feet of sediments with very high clay content, or the presence of saline groundwater, just above the basement throughout this area.

AEROMAGNETIC SURVEY

An interesting feature in the magnetics of part of the study area sheds some light on the nature of the basin-fill sediments, and thus will be briefly discussed here. In 1978, Aero Service of Houston, Texas, under contract with the U.S. Geological Survey, flew an aeromagnetic survey over the Amargosa Desert at an elevation of 122 meters (400 feet). Figure 4 shows the contoured results of the survey, obtained by running the flight data through projecting, gridding, and contouring programs (Godson and Webring, 1981; Webring, 1981). The contour interval is 50 gammas. With the exception of three isolated anomalies, the aeromagnetics over the Amargosa Desert show little magnetic variation over most of the region, including the surrounding basement outcrops, varying up to about 100 gammas in a few areas, but exhibiting little

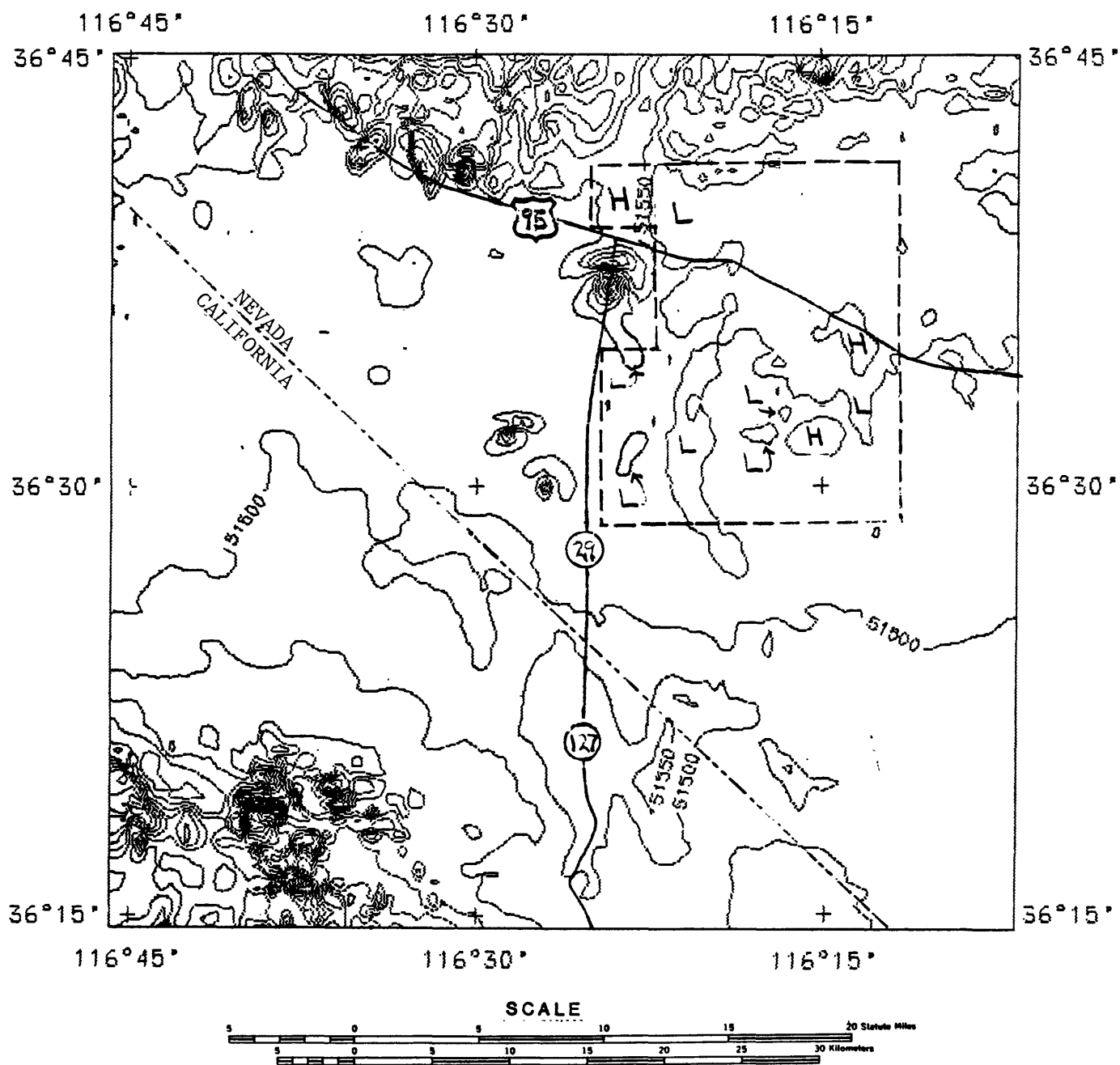


Figure 4. Contoured results of an aeromagnetic survey over the Amargosa Desert region. H = magnetic highs, L = magnetic lows. Dashed border encloses area where "reverse-relief" effect of magnetics is apparent (see text). Contour interval = 50 gammas.

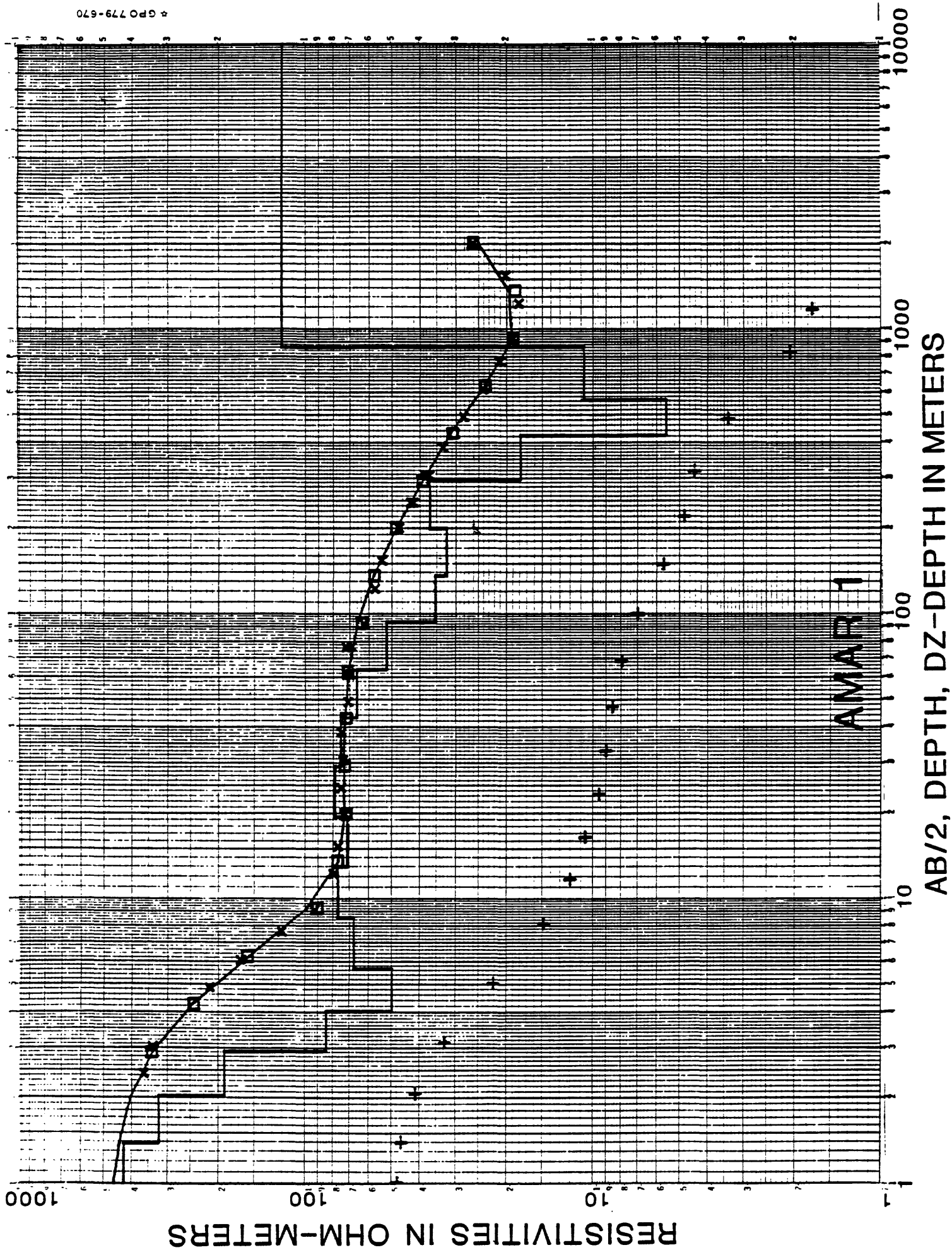
more than about 20 gammas variation (low-frequency background) throughout most of the region, due to the weak magnetic nature of both the basement carbonates and the basin-fill sediments. The three isolated anomalies include one large, reversed anomaly just south of Lathrop Wells (580 gammas max. deflection), and two adjacent anomalies, one normal (220 gammas max. deflection), one reversed (260 gammas max. deflection), about 15 km south-southwest of Lathrop Wells. Also, strong (hundreds of gammas) high-frequency magnetic variation occurs along the northern edge of the Amargosa Desert, indicating the southern edge of the Tertiary volcanics found north of this region.

Although the magnetics over the Amargosa Desert are relatively quiet, the variation in the northeastern part of the desert (bordered area in Figure 4) seems to show a "reverse-relief" effect where basement relief is known. That is, there are magnetic highs where the basement surface is deepest (and thus where the basin-fill sediments are thickest), and magnetic lows where the basement surface is at shallower depths. This indicates that the magnetization producing these variations is within the basin-fill sediments, and that the three-dimensional distribution of magnetic particles within the sediments is uniform enough to produce this effect.

REFERENCES

- Anderson, W. L., 1971, Application of bicubic spline functions to two dimensional gridded data: NTIS (Natl. Tech. Inf. Service), PB-203 579, Springfield, VA.
- Godson, R. H., and Webring, M. W., 1982, CONTOUR: A modification of G. I. Evenden's general purpose contouring program: U.S. Geol. Survey Open-File Report 82-797, 72 p.
- Healey, D. L., and Miller, C. H., 1971, Gravity survey of the Amargosa Desert area of Nevada and California: U.S. Geol. Survey Open-File Report, 30 p.
- Johnston, R. H., 1971, U.S. Geological Survey tracer study, Amargosa Desert, Nye County, Nevada; part 1: exploratory drilling, tracer well construction and testing, and preliminary findings: U.S. Geol. Survey Open-File Report, 64 p.
- Webring, M. W., 1981, MINC: A gridding program based on minimum curvature: U.S. Geol. Survey Open-File Report 81-1224, 41 p.
- Zohdy, A.A.R., 1973, A computer program for the automatic interpretation of Schlumberger sounding curves over horizontally layered media: NTIS (Natl. Tech. Inf. Service), PB-232 703/AS, 25 p., Springfield, Va.
- _____, 1974, The use of Dar Zarrouk curves in the interpretation of VES data: U.S. Geol. Survey Bull. 1313-D, 41 p.
- _____, 1975, Automatic interpretation of Schlumberger sounding curves using modified Dar Zarrouk functions: U.S. Geol. Survey Bull. 1313-E, 39 p.
- Zohdy, A.A.R., Anderson, L. A., and Muffler, L.J.P., 1973, Resistivity, self potential, and induced polarization surveys of a vapor dominated system: Geophysics, v. 38, p. 1130-1144.

APPENDIX



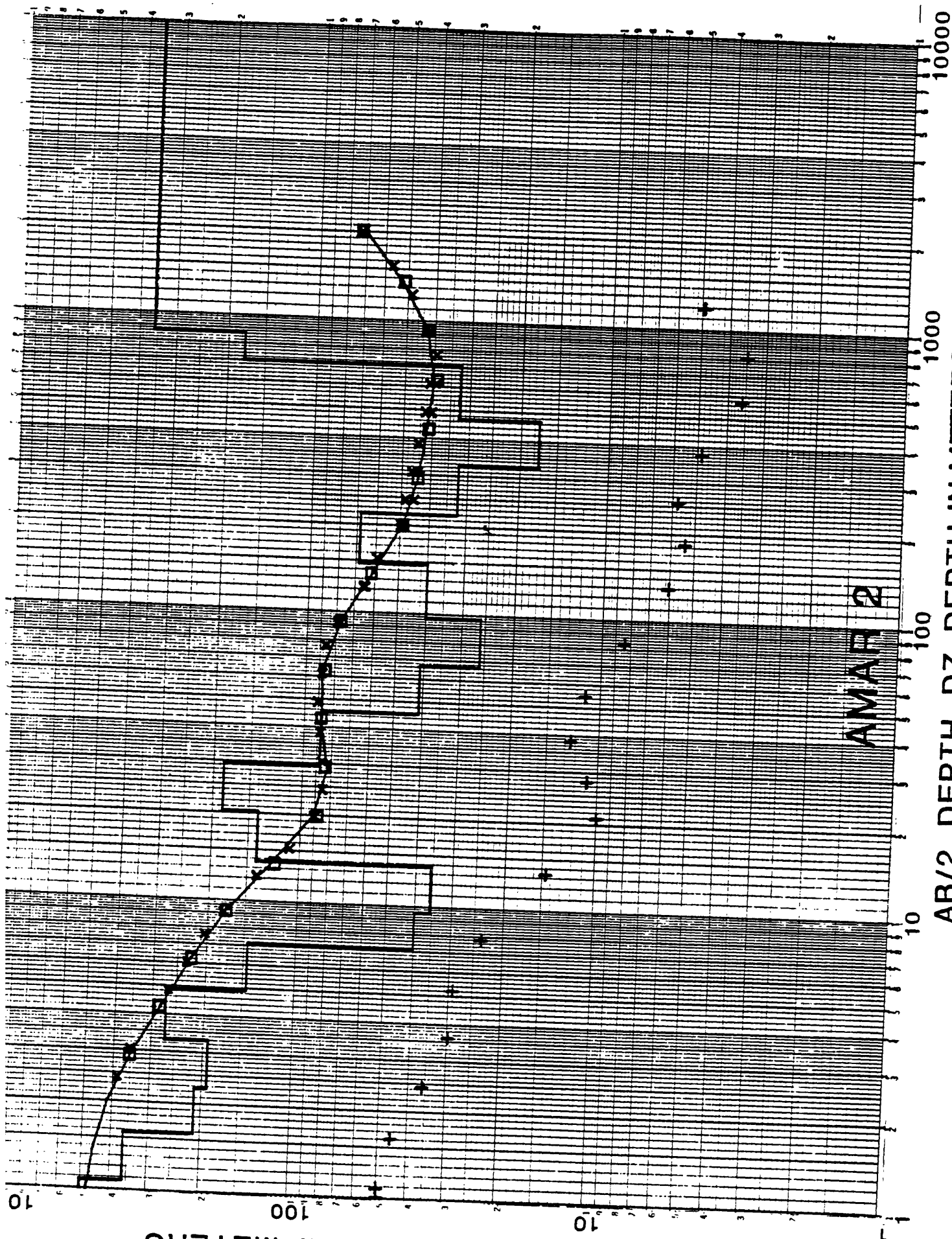
* GPO 779-670

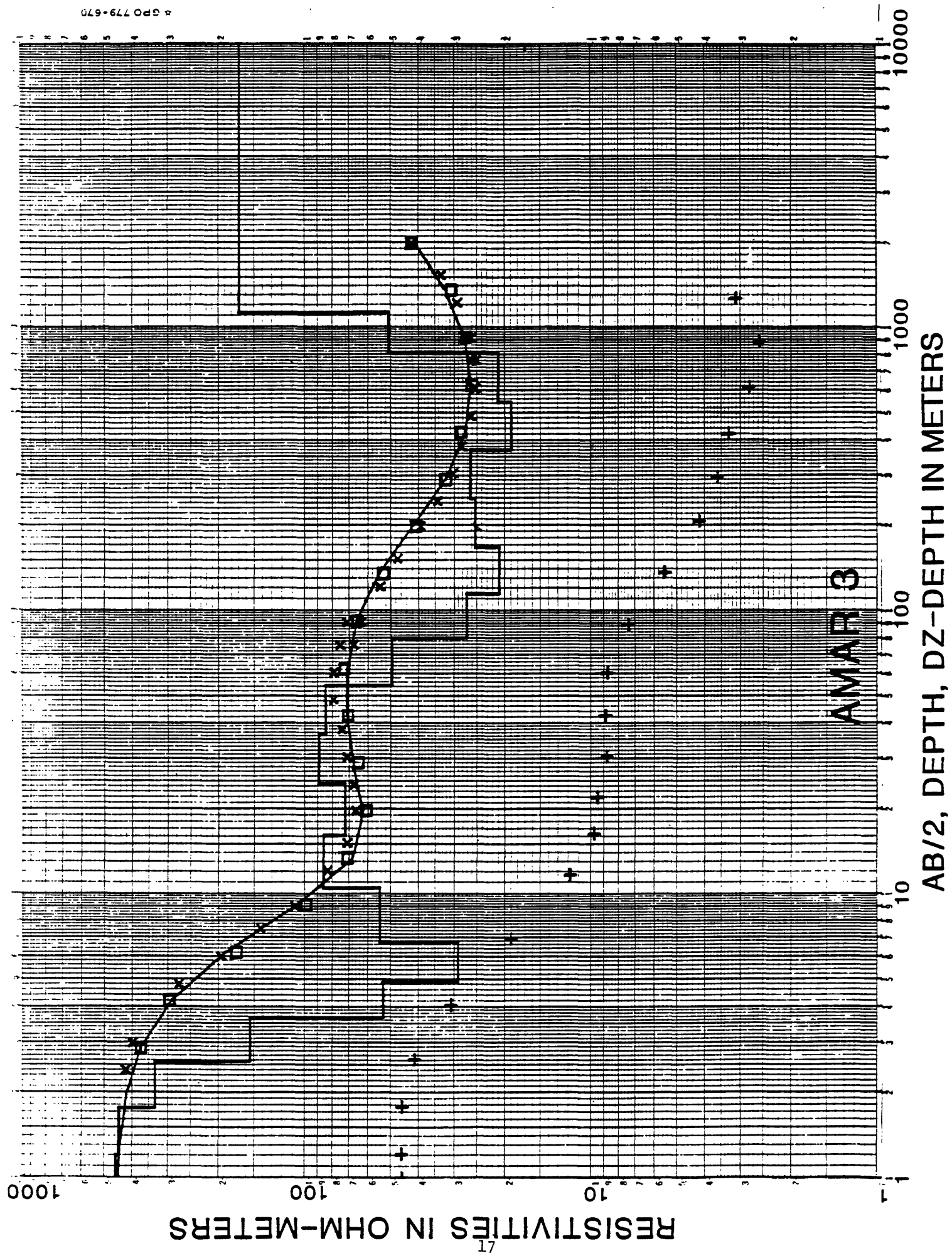
RESISTIVITIES IN OHM-METERS

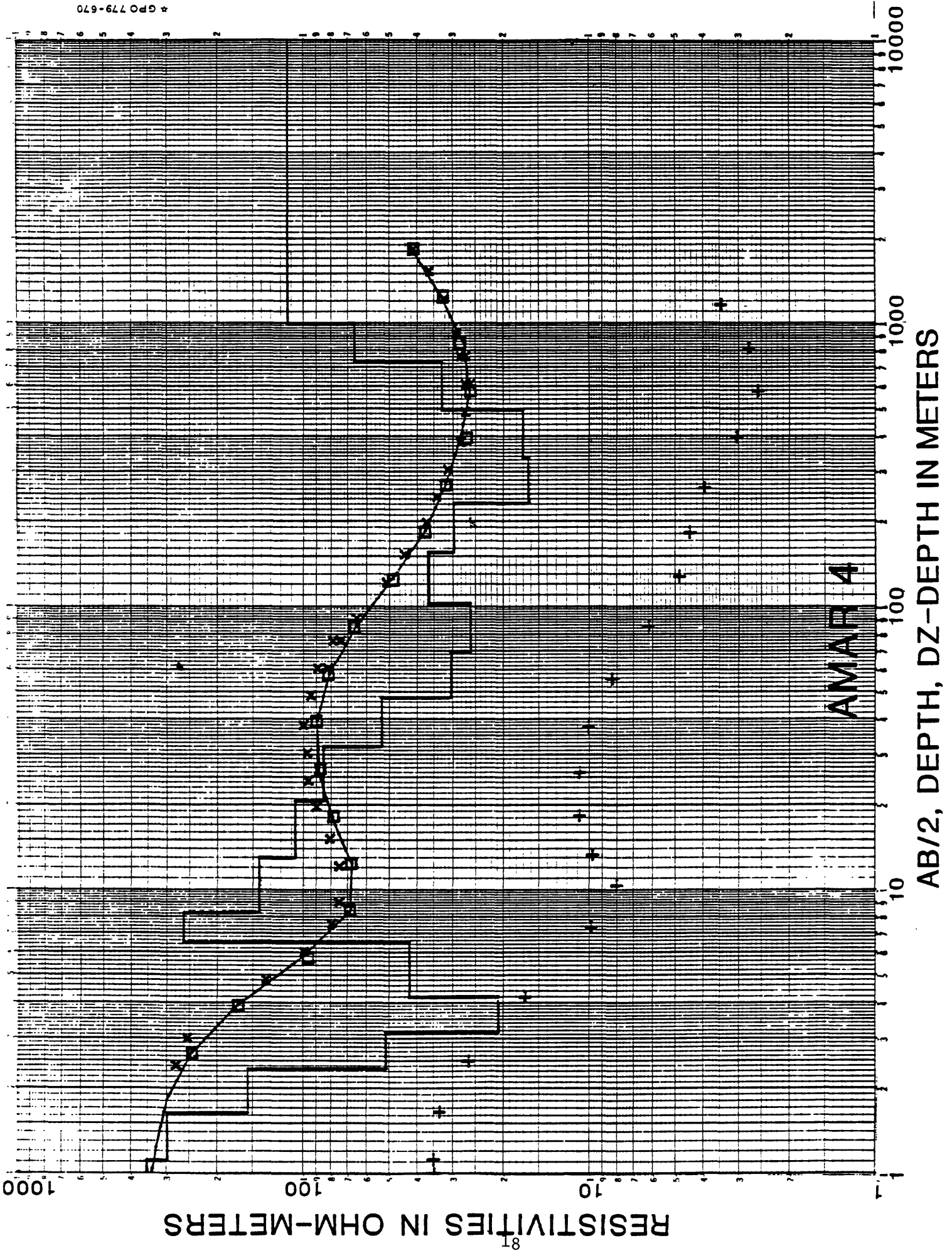
16

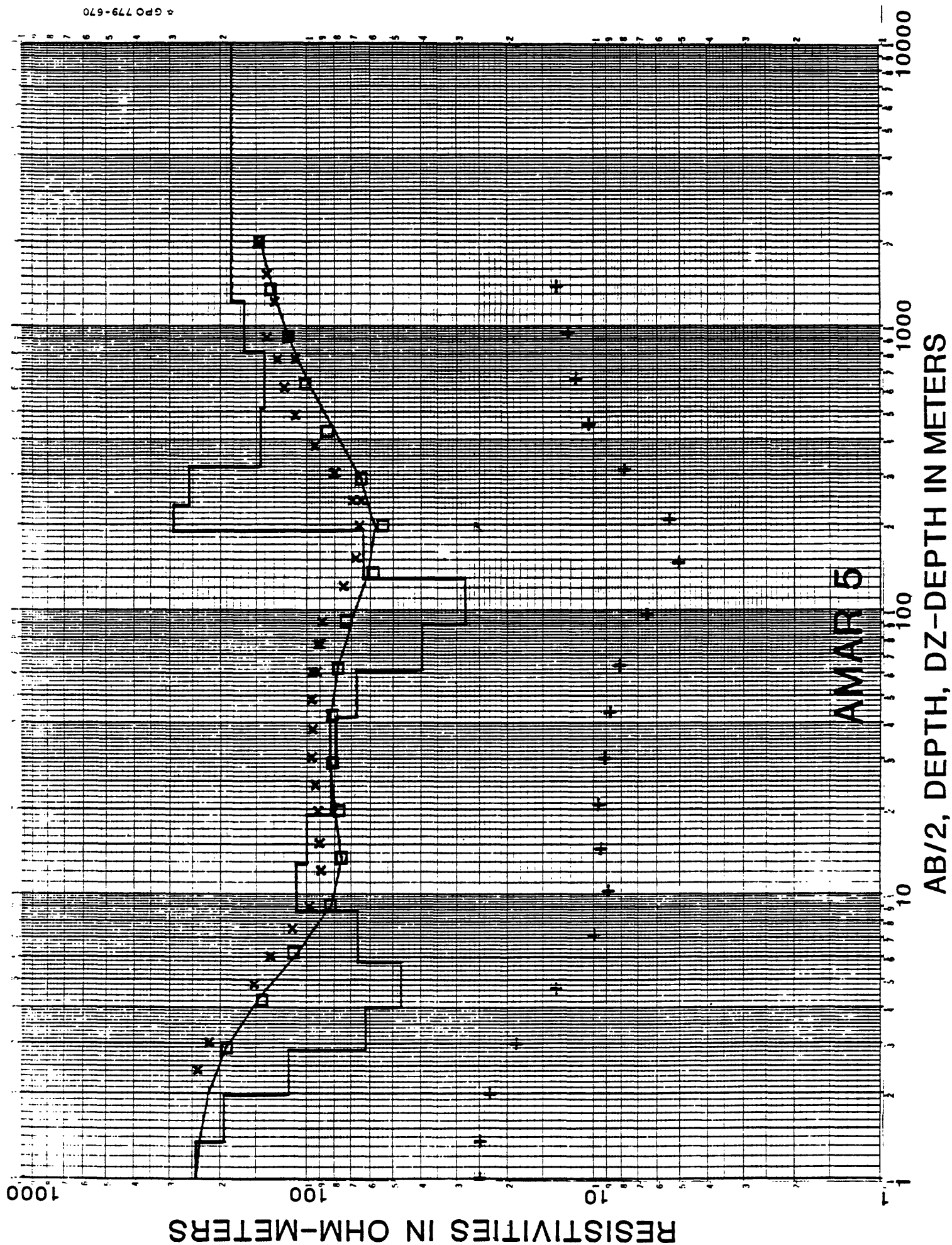
AMAR 2

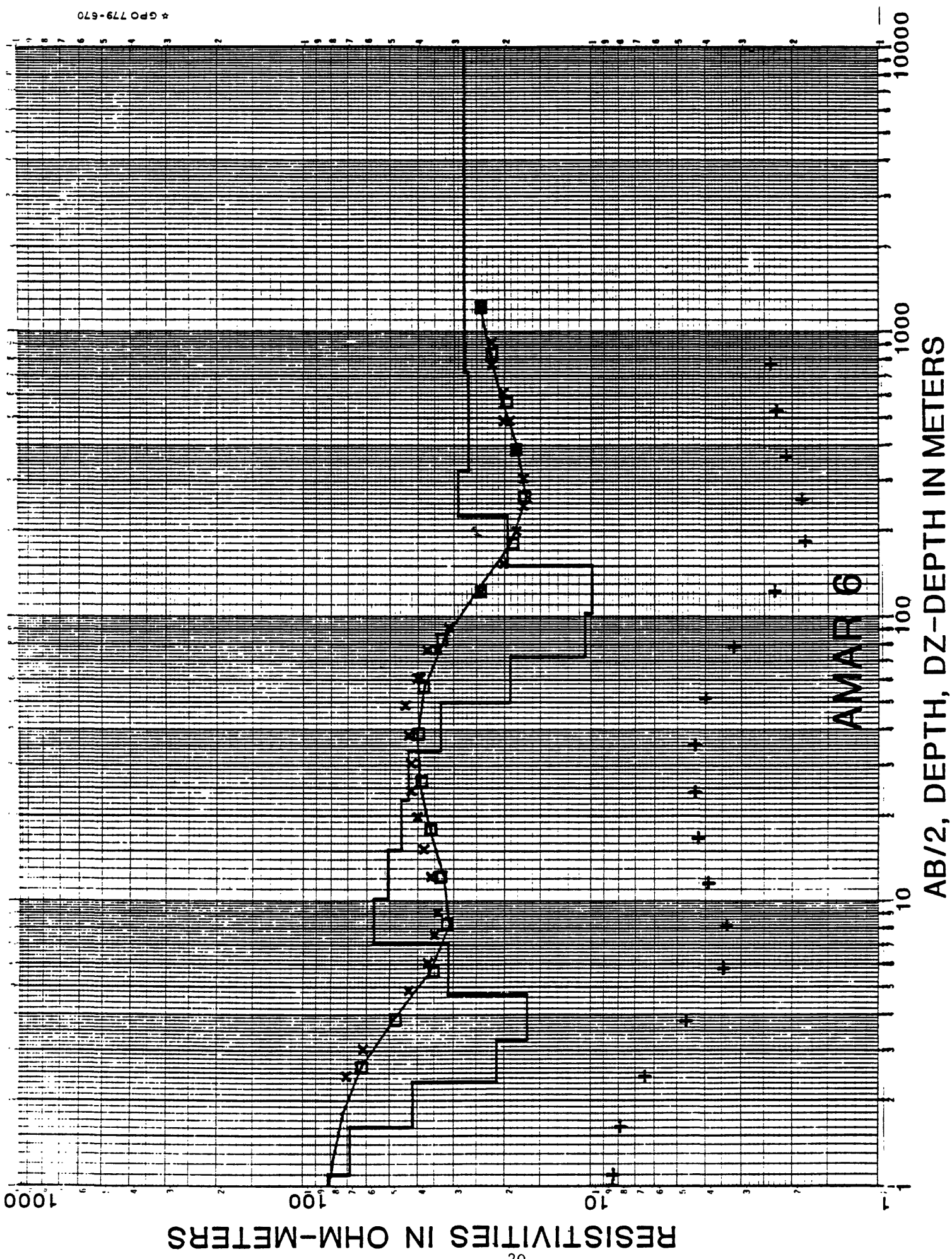
AB/2, DEPTH, DZ-DEPTH IN METERS



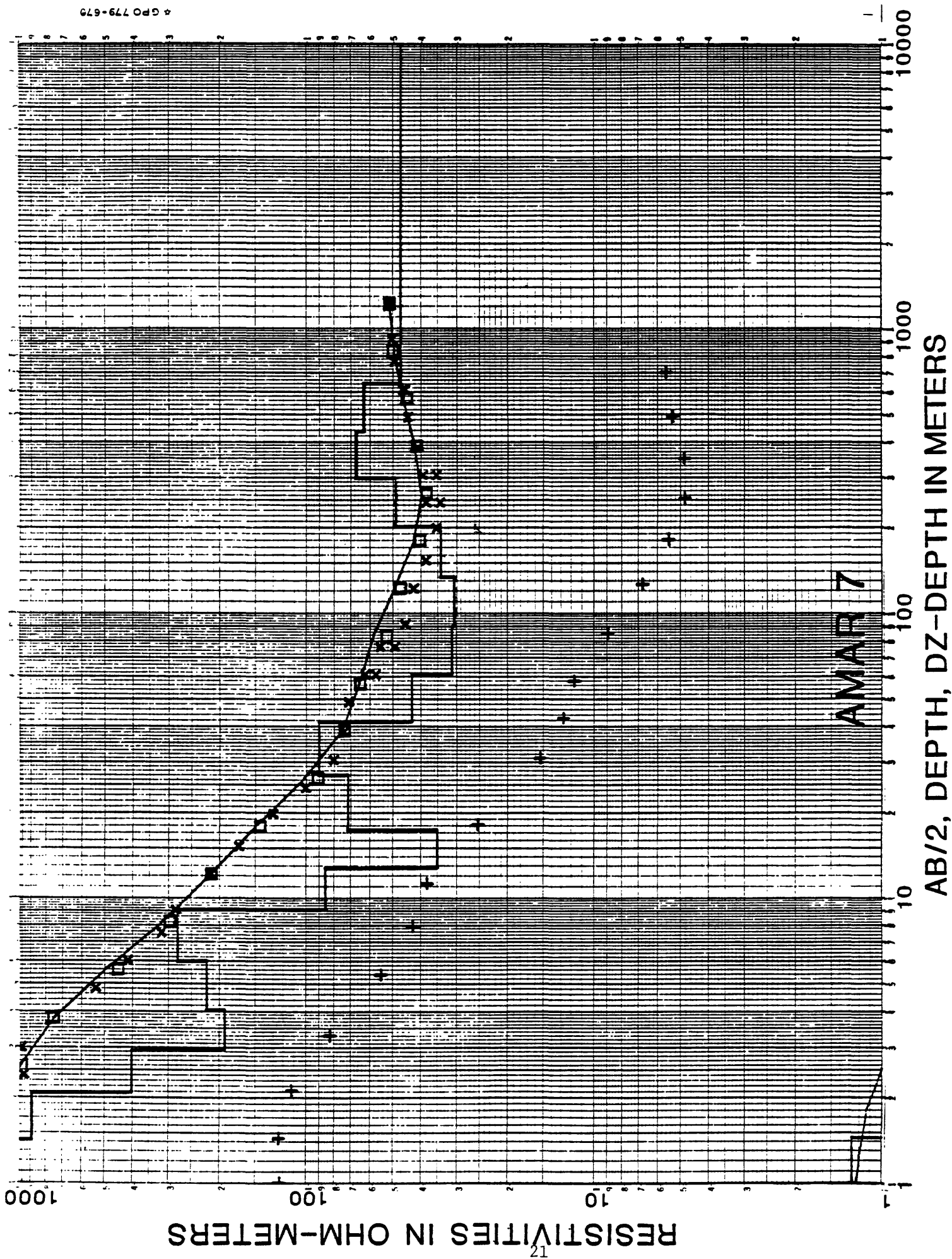








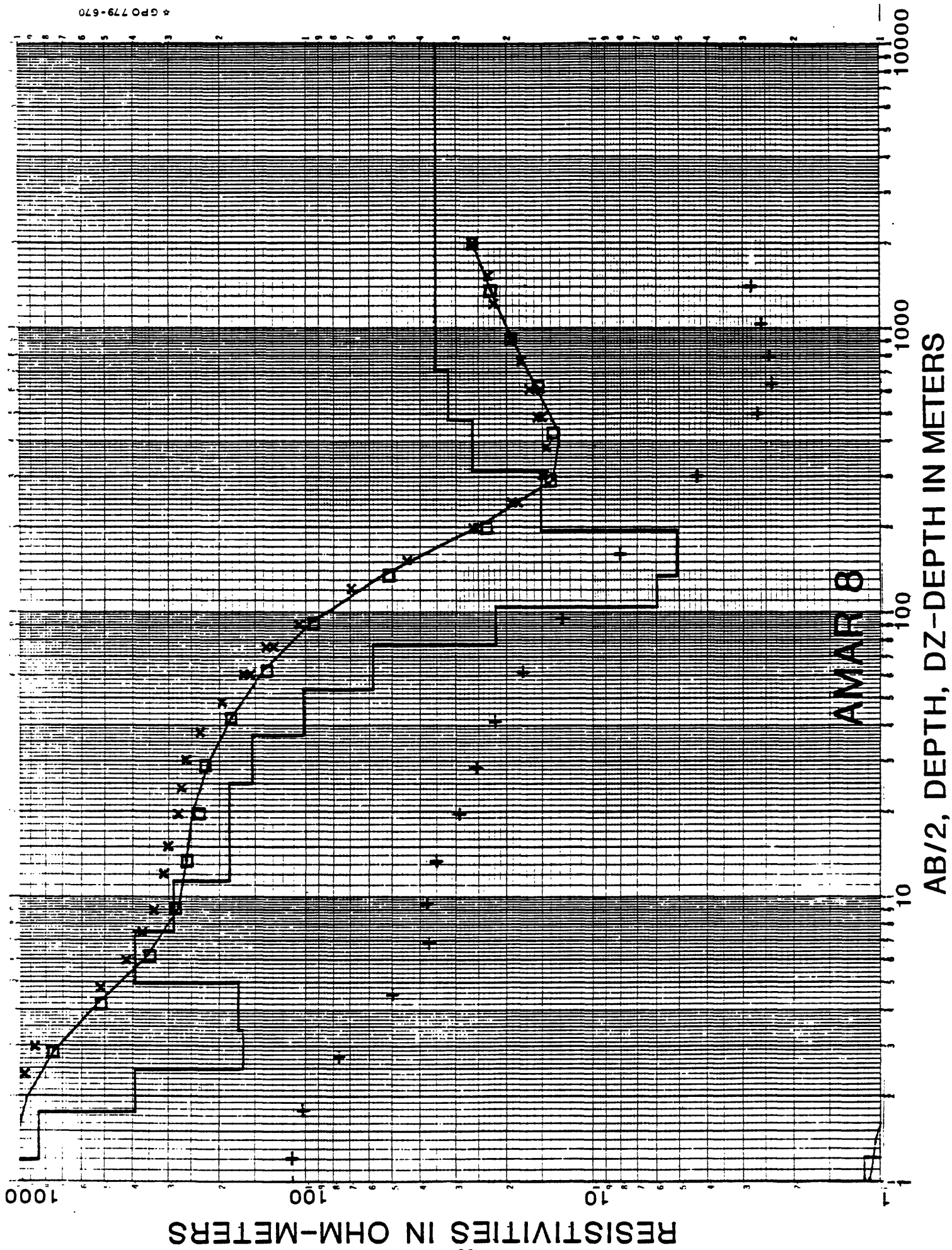
* GPO 779-670

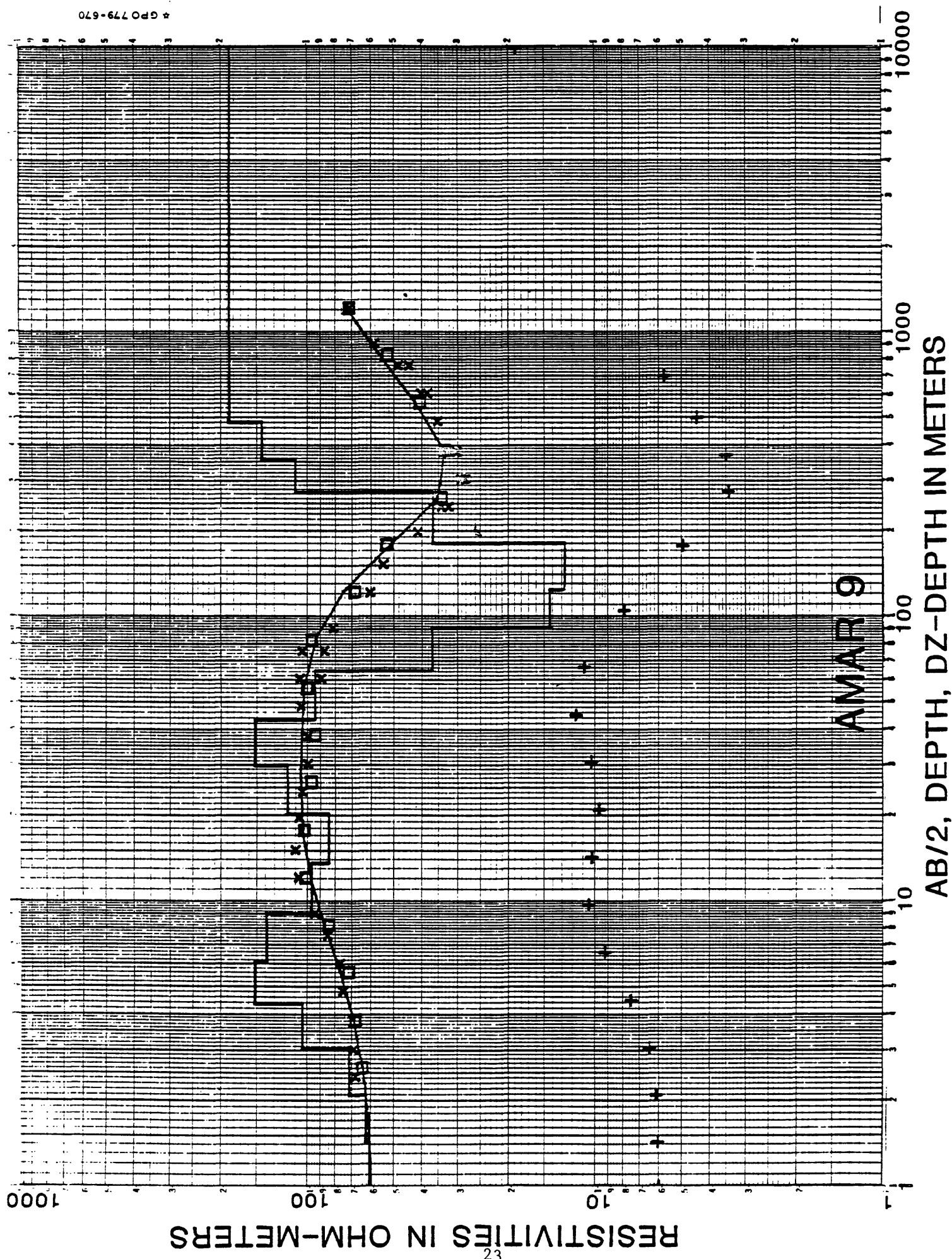


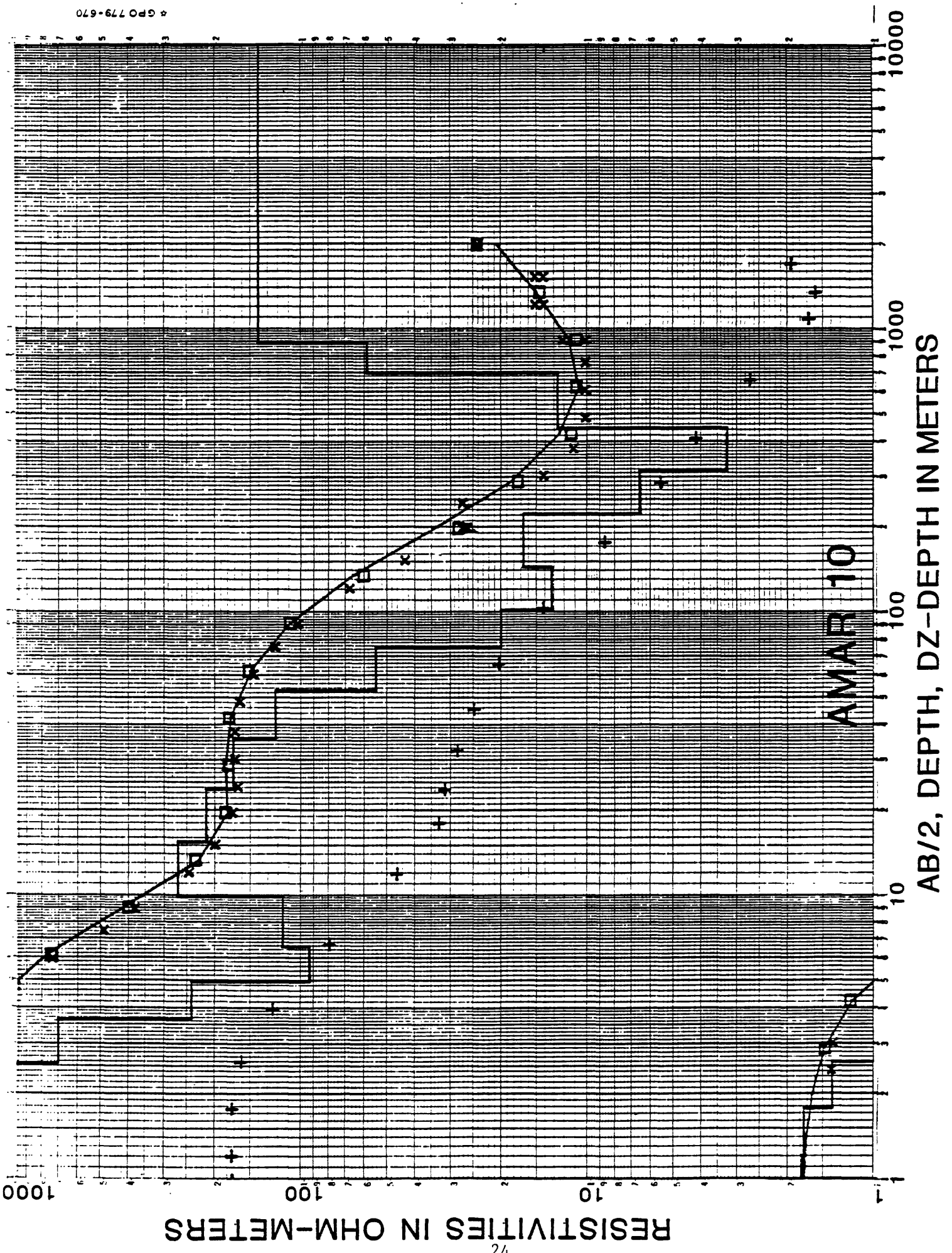
AMAR 7

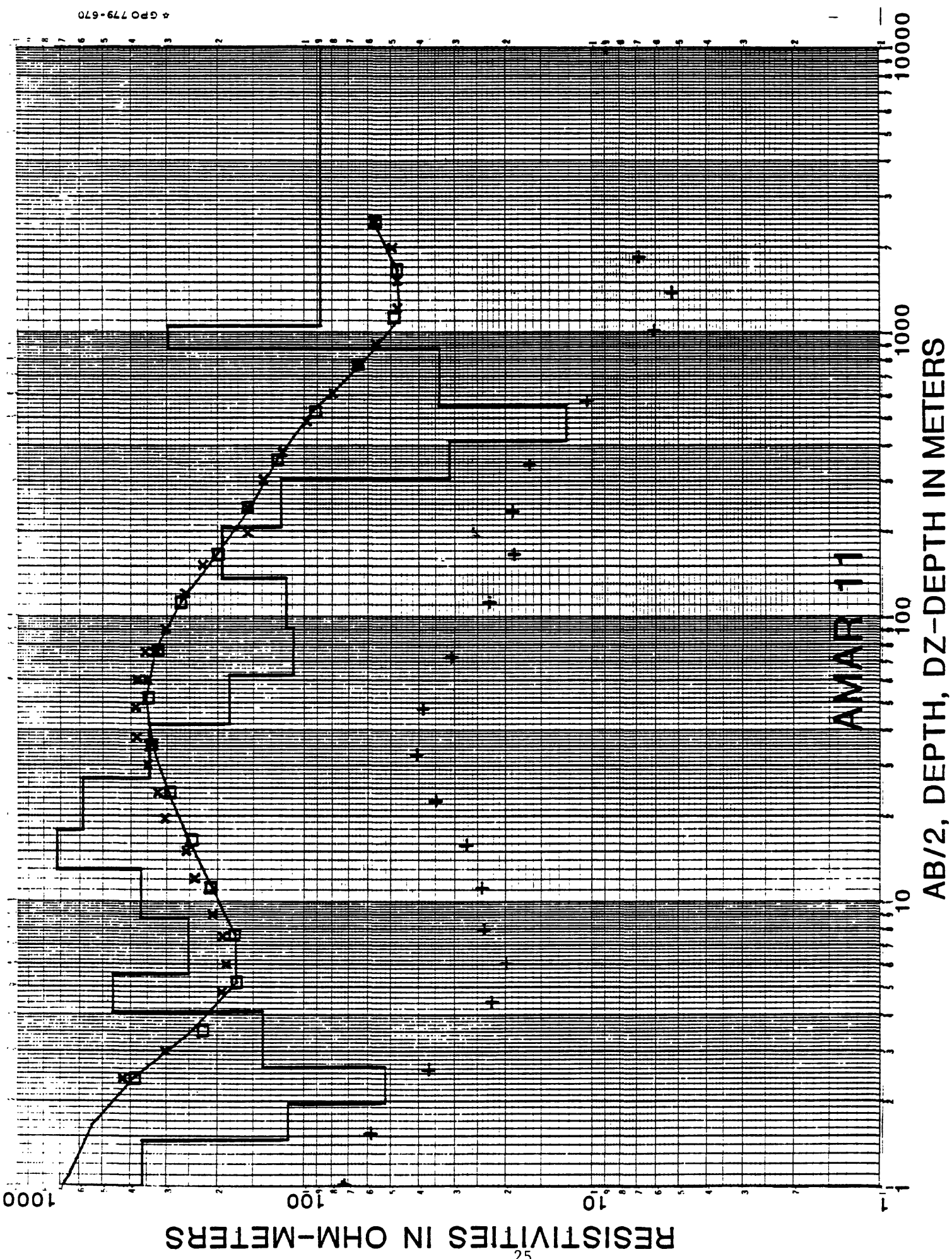
AB/2, DEPTH, DZ-DEPTH IN METERS

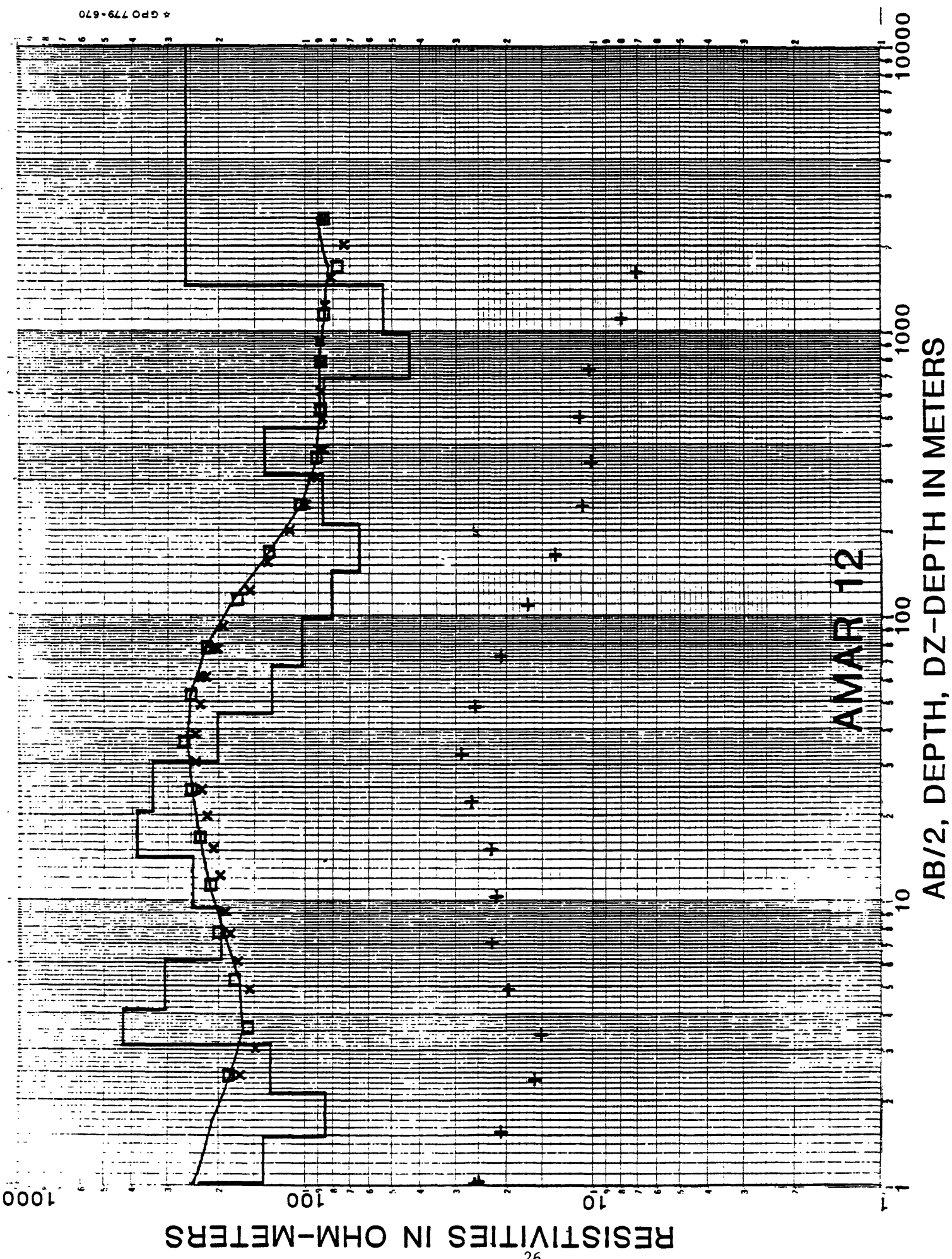
RESISTIVITIES IN OHM-METERS



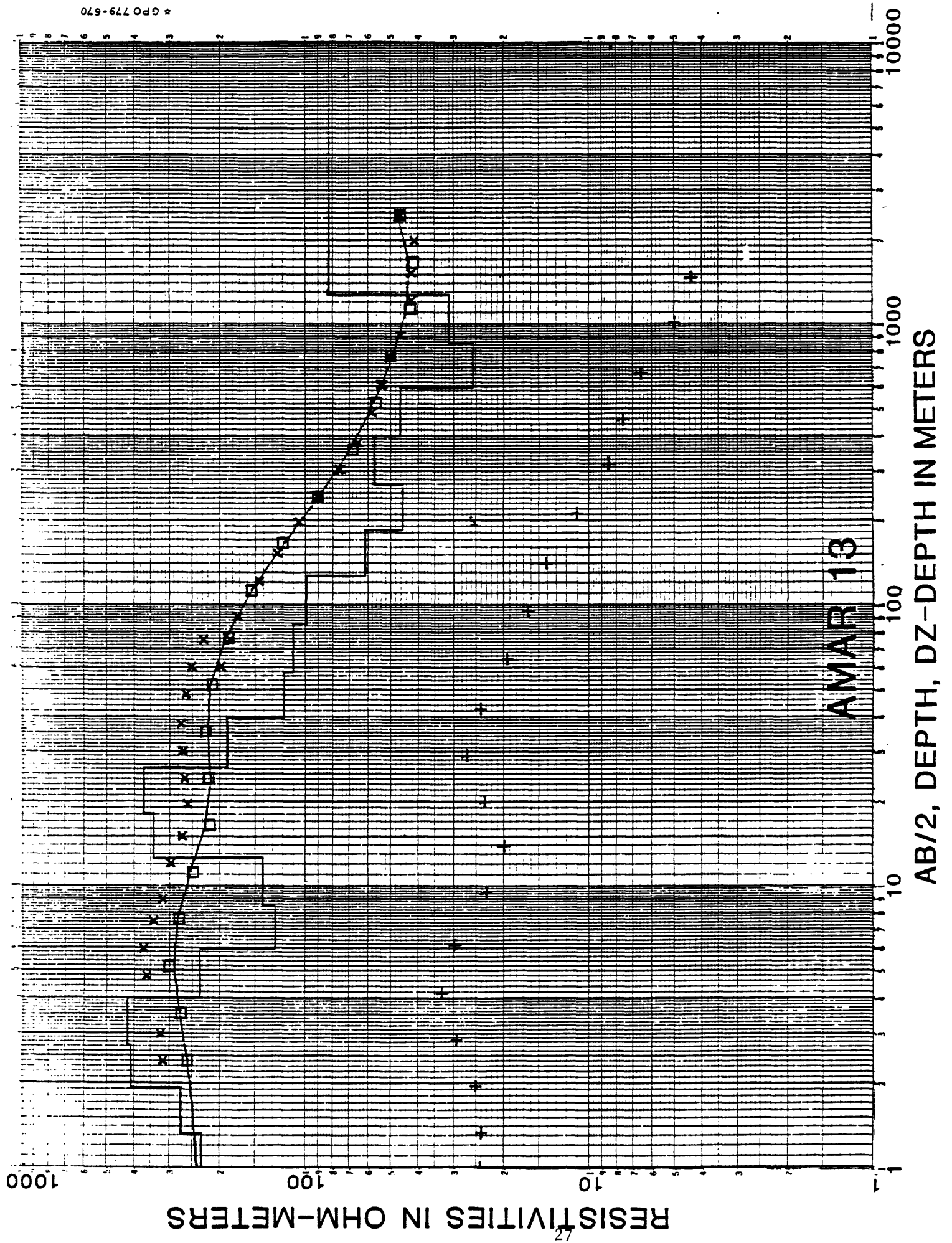


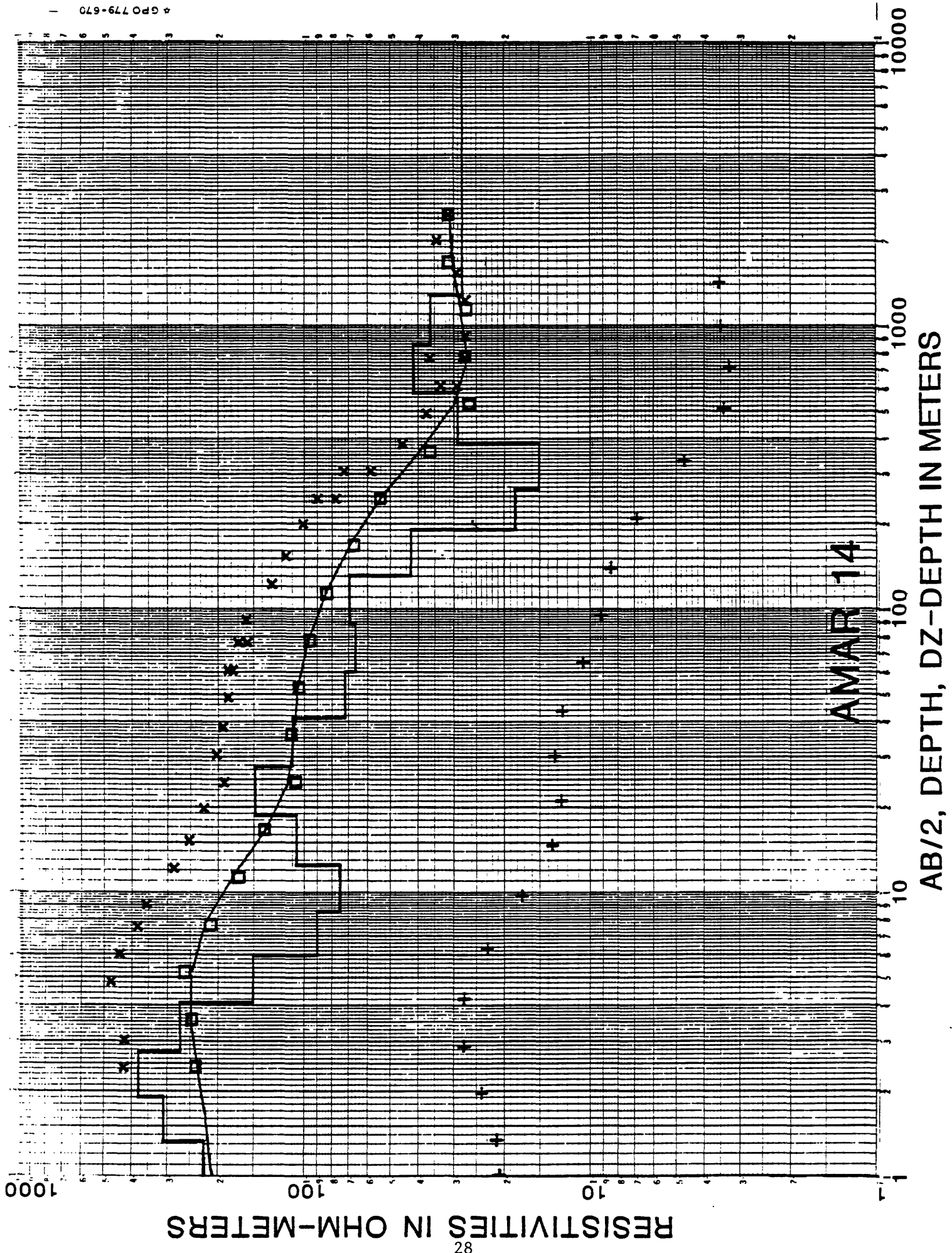


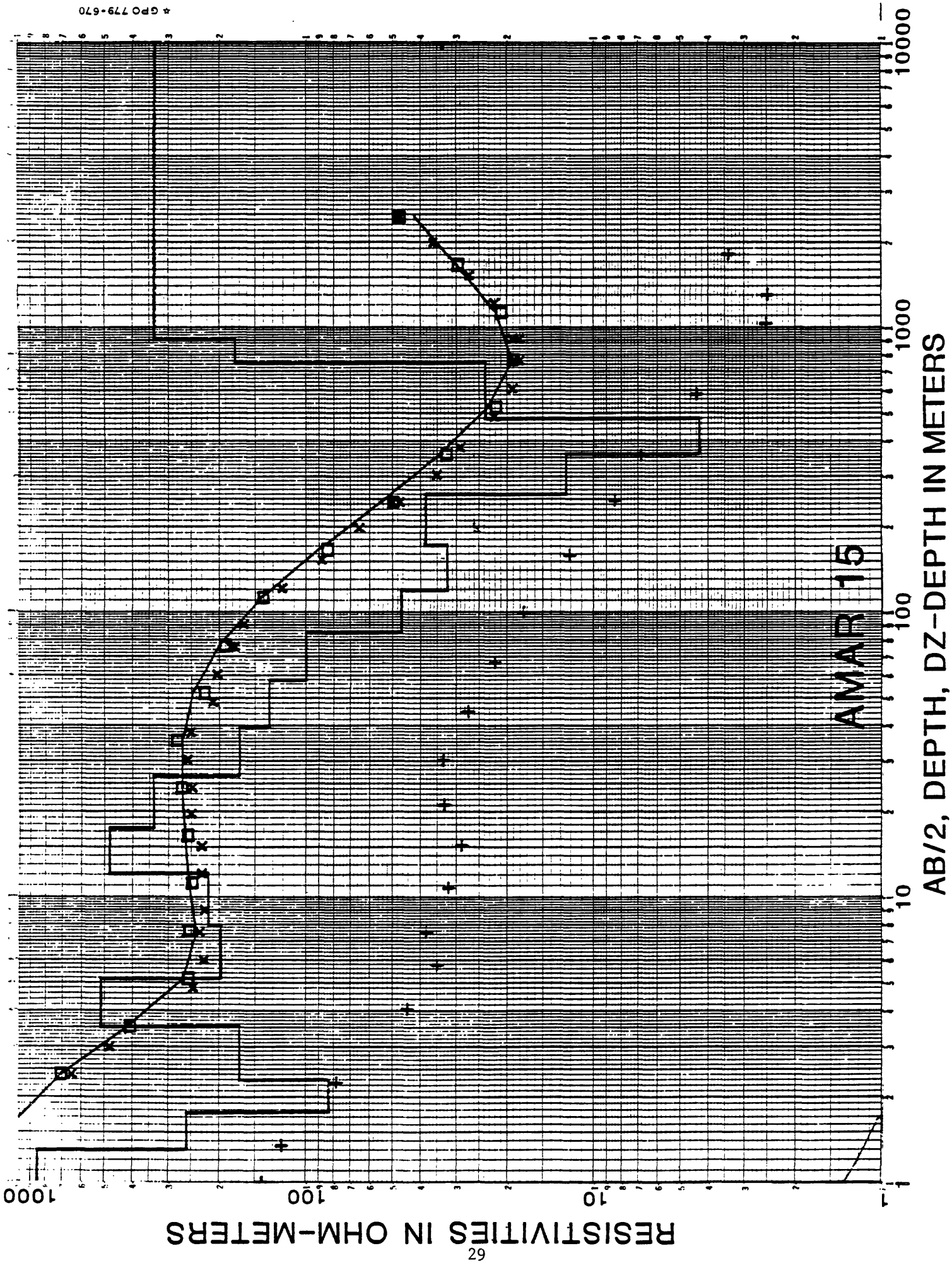


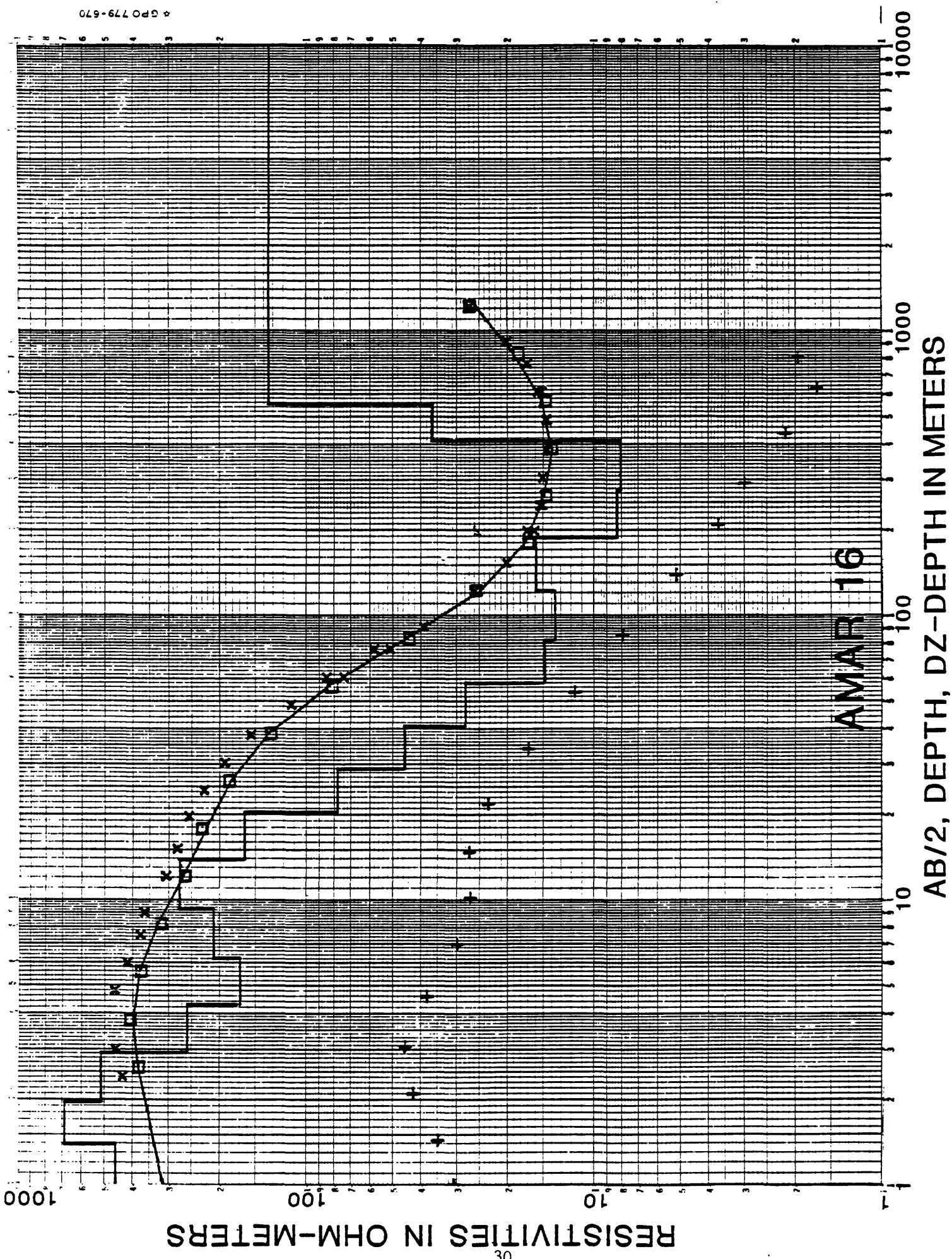


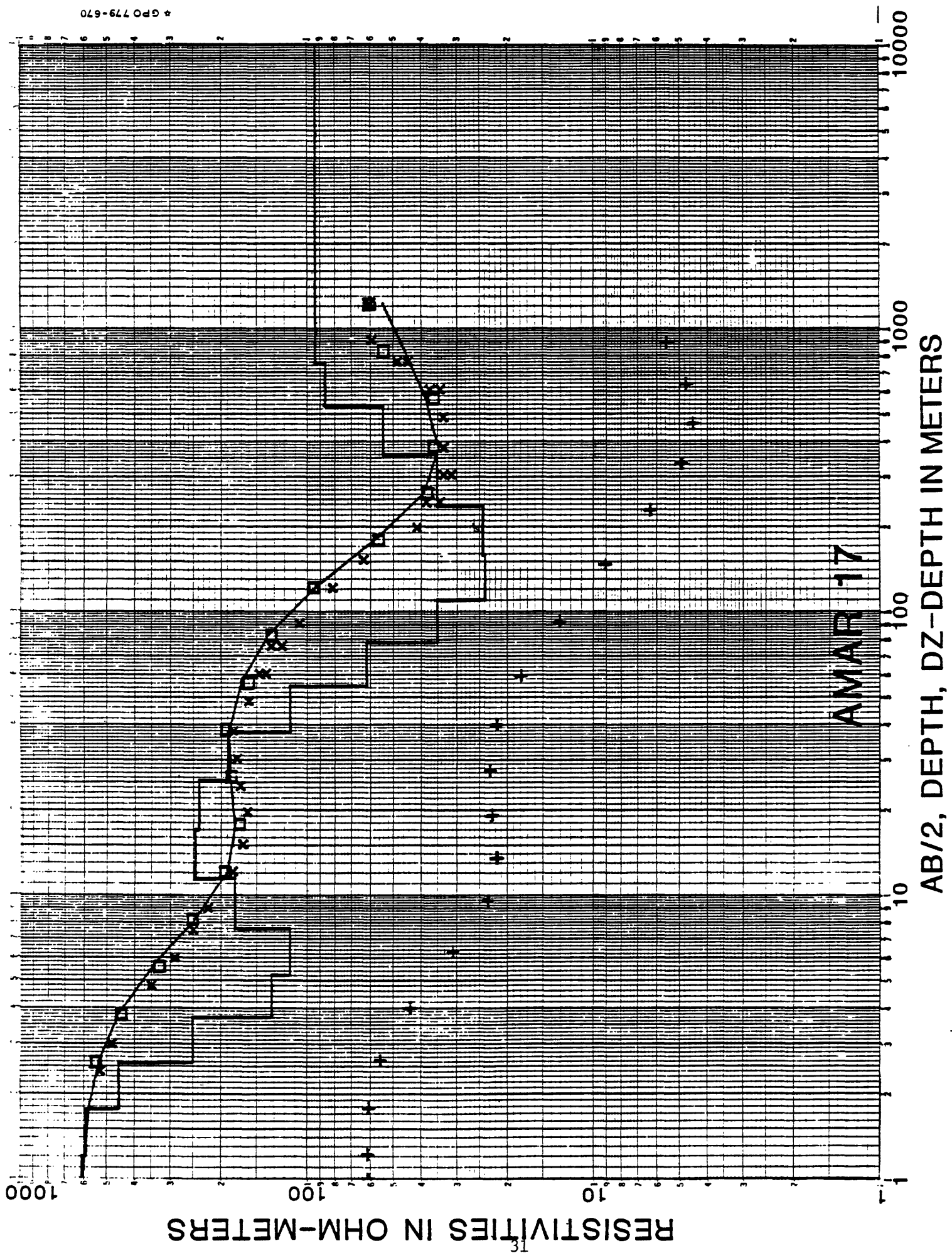
AMAR 12

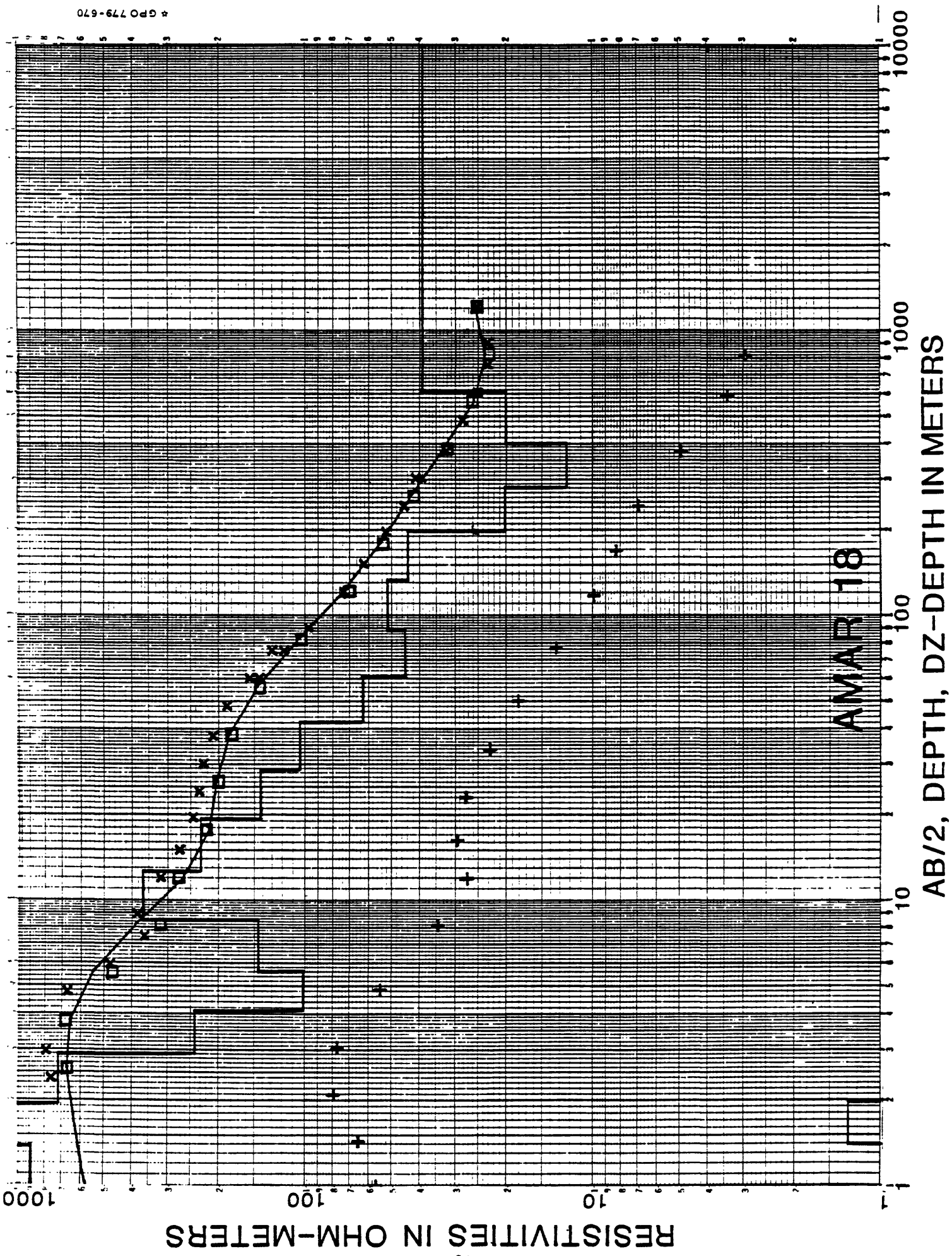




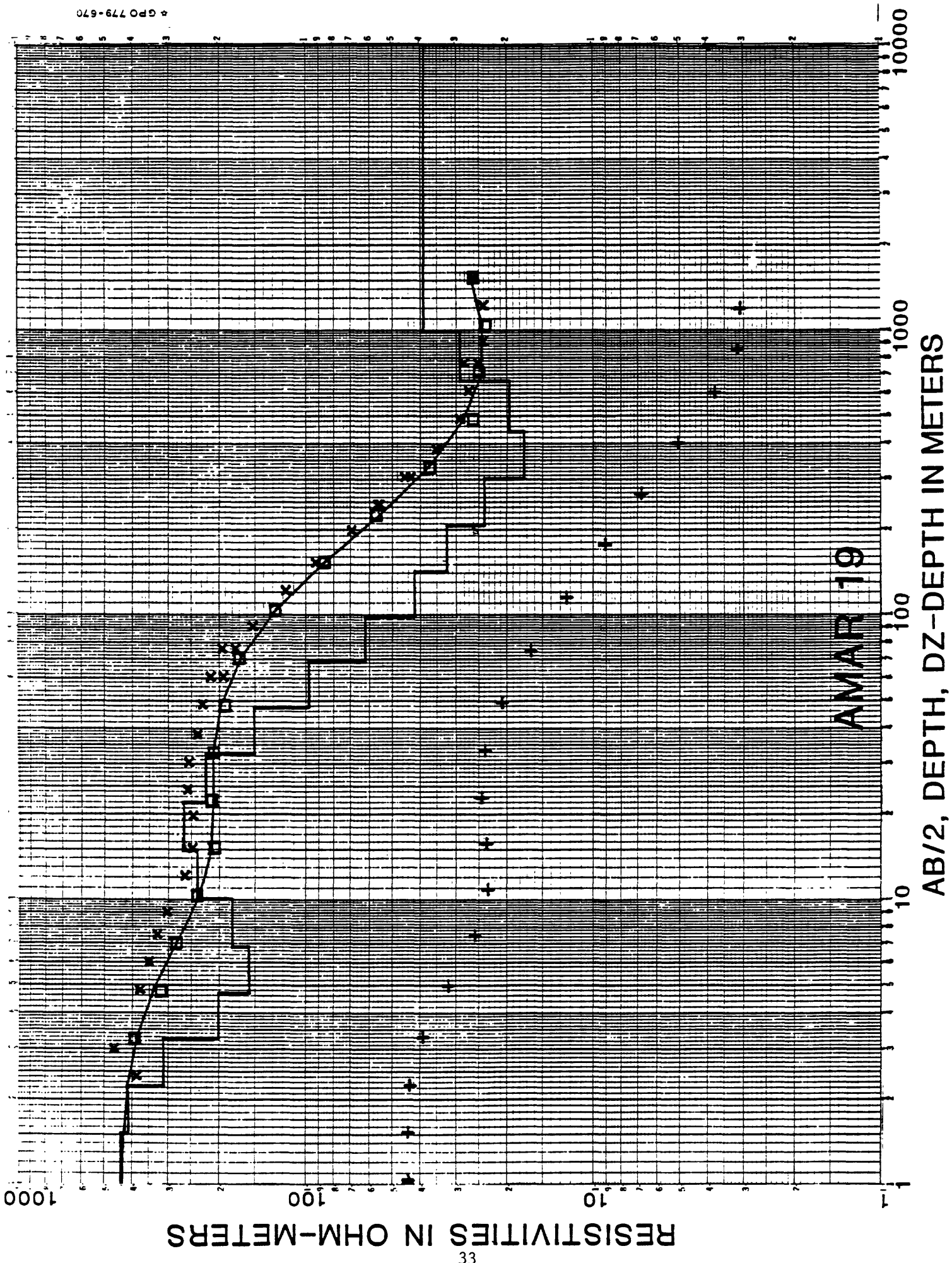


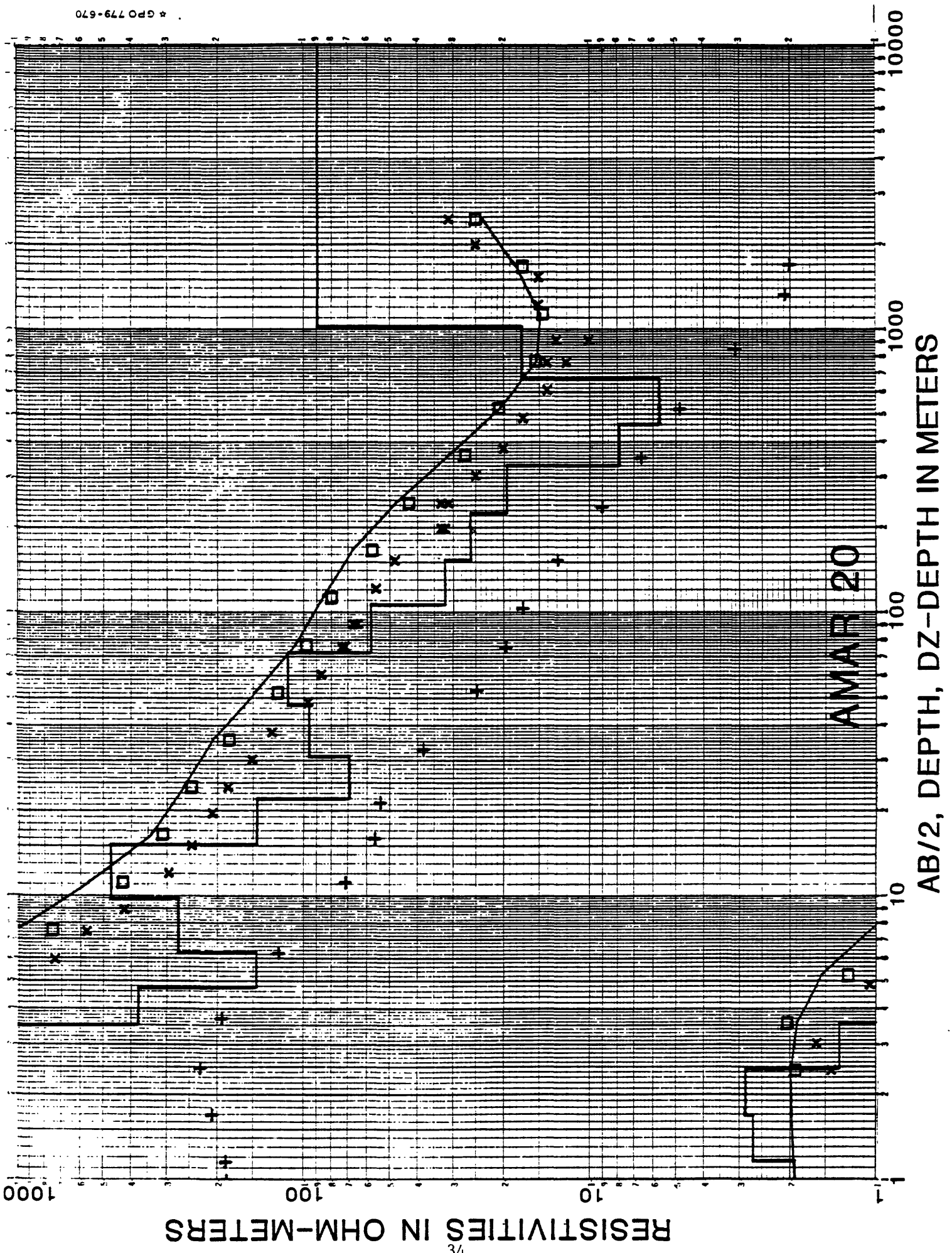






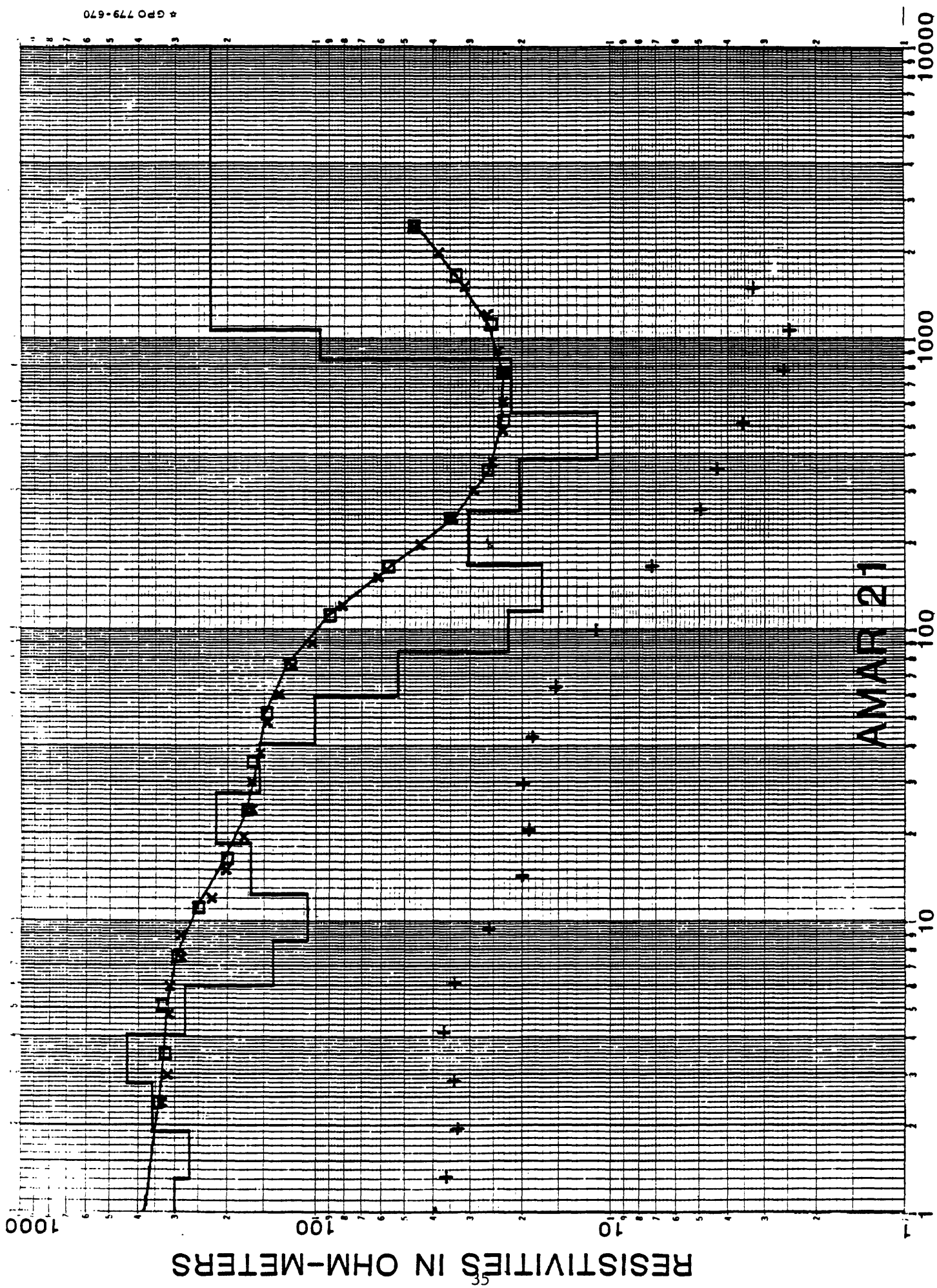
* GPO 779-670

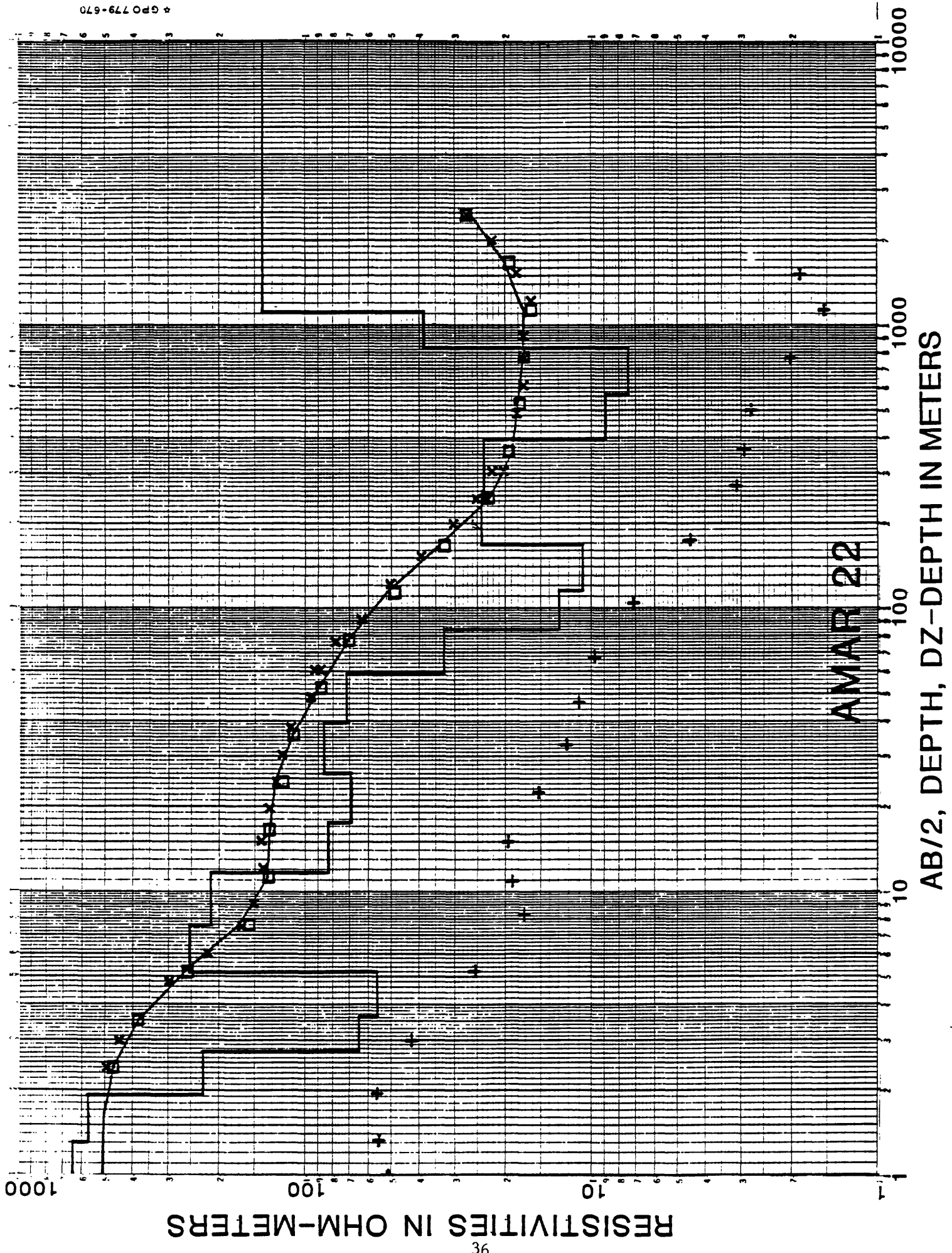


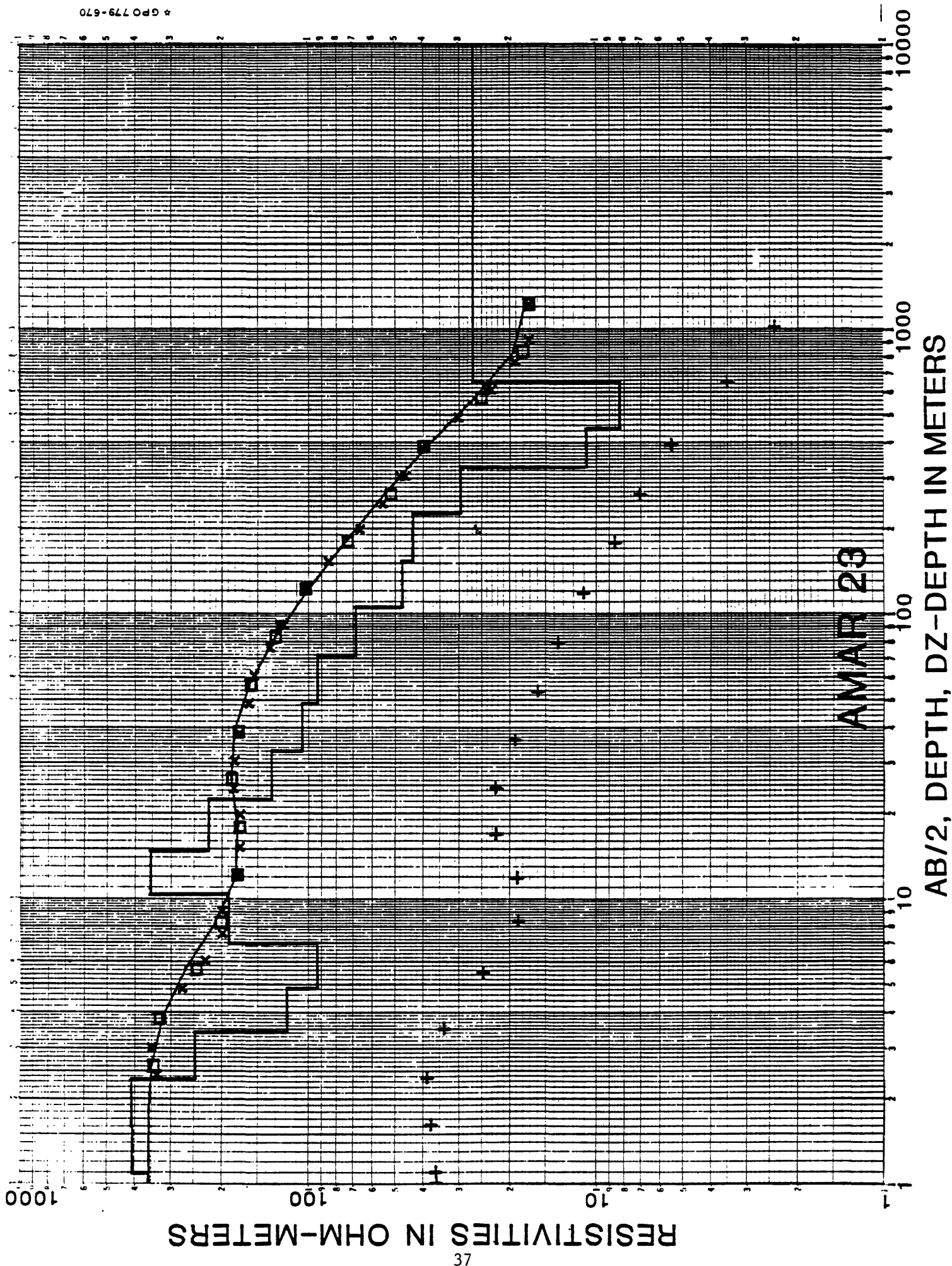


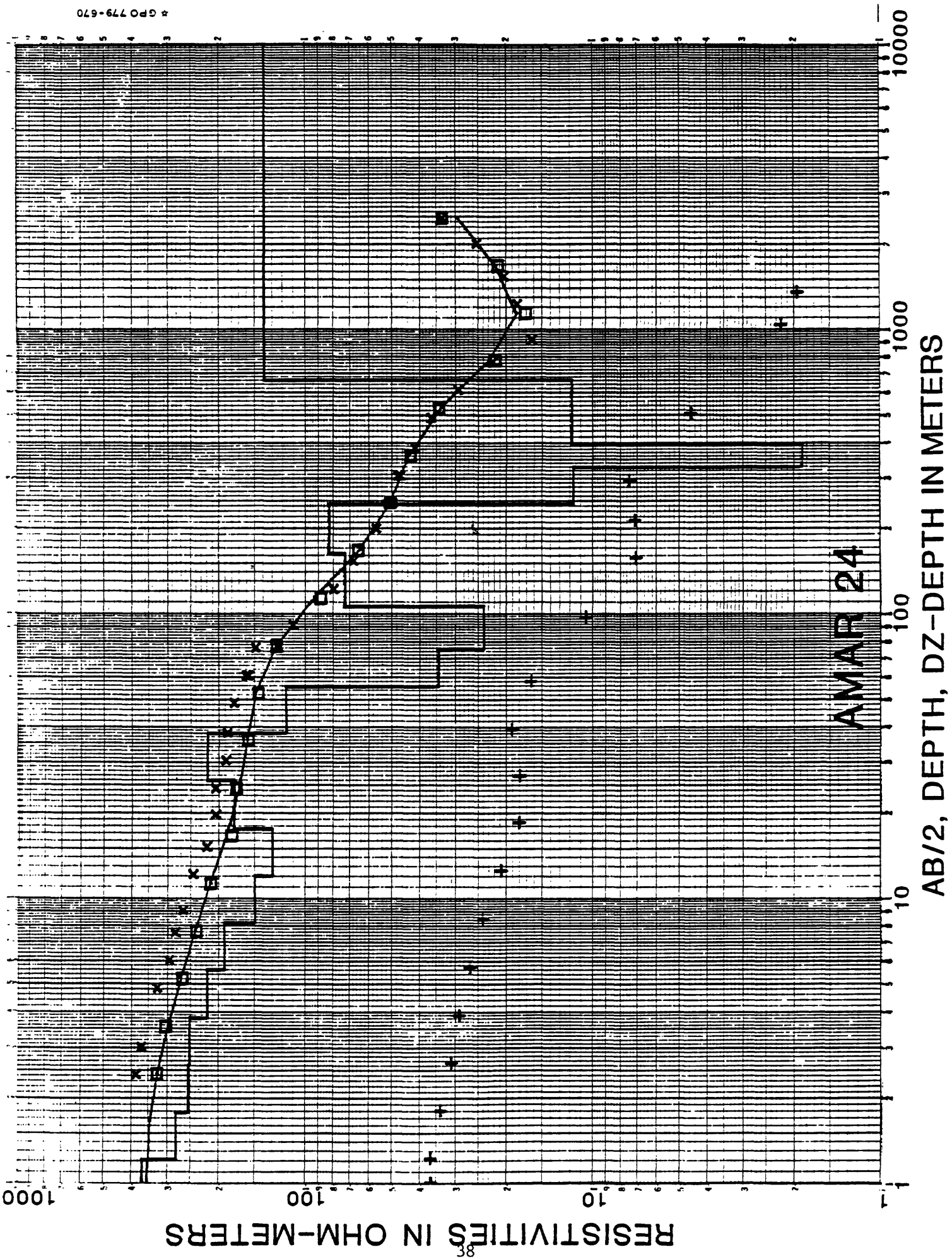
AMAR 21

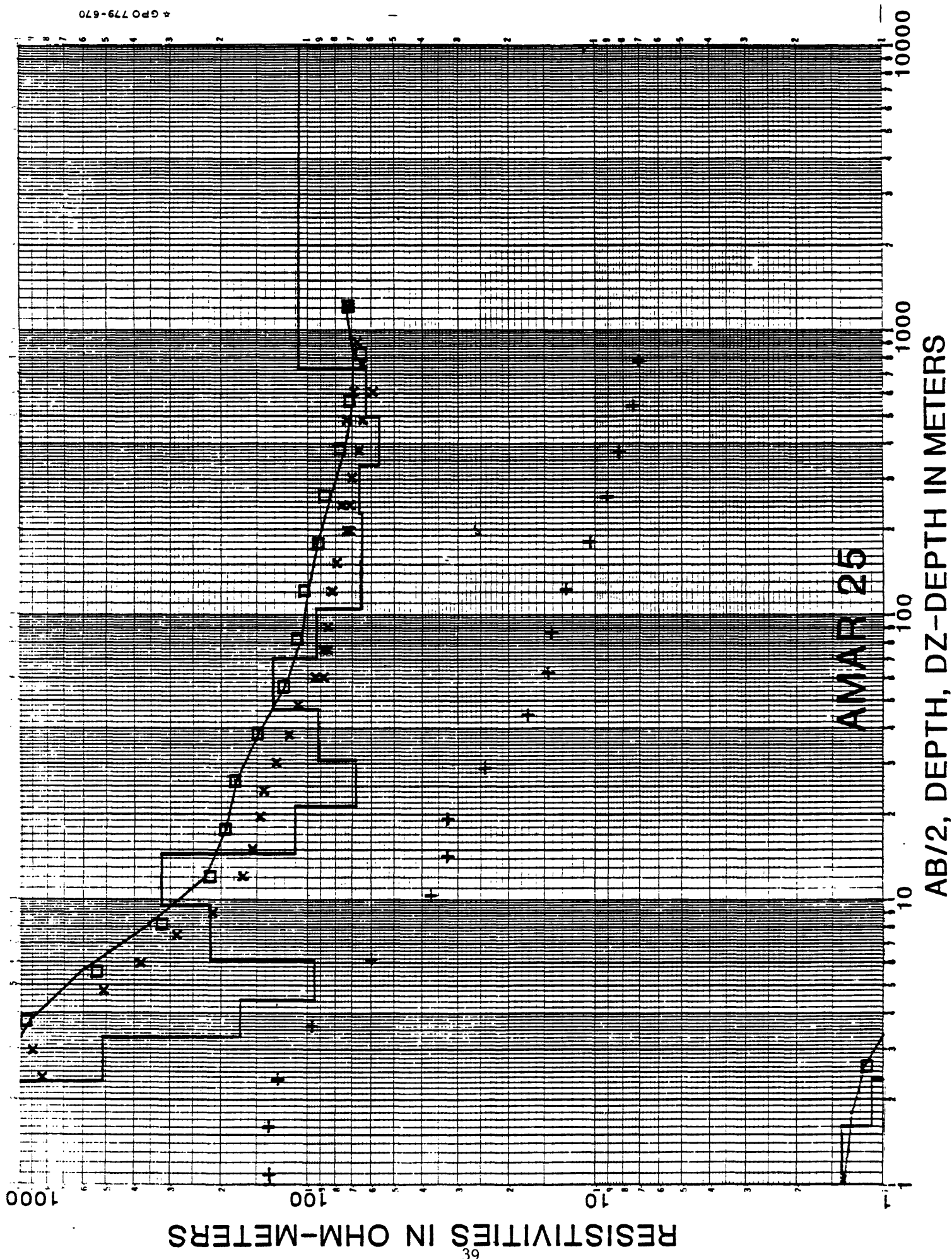
AB/2, DEPTH, DZ-DEPTH IN METERS

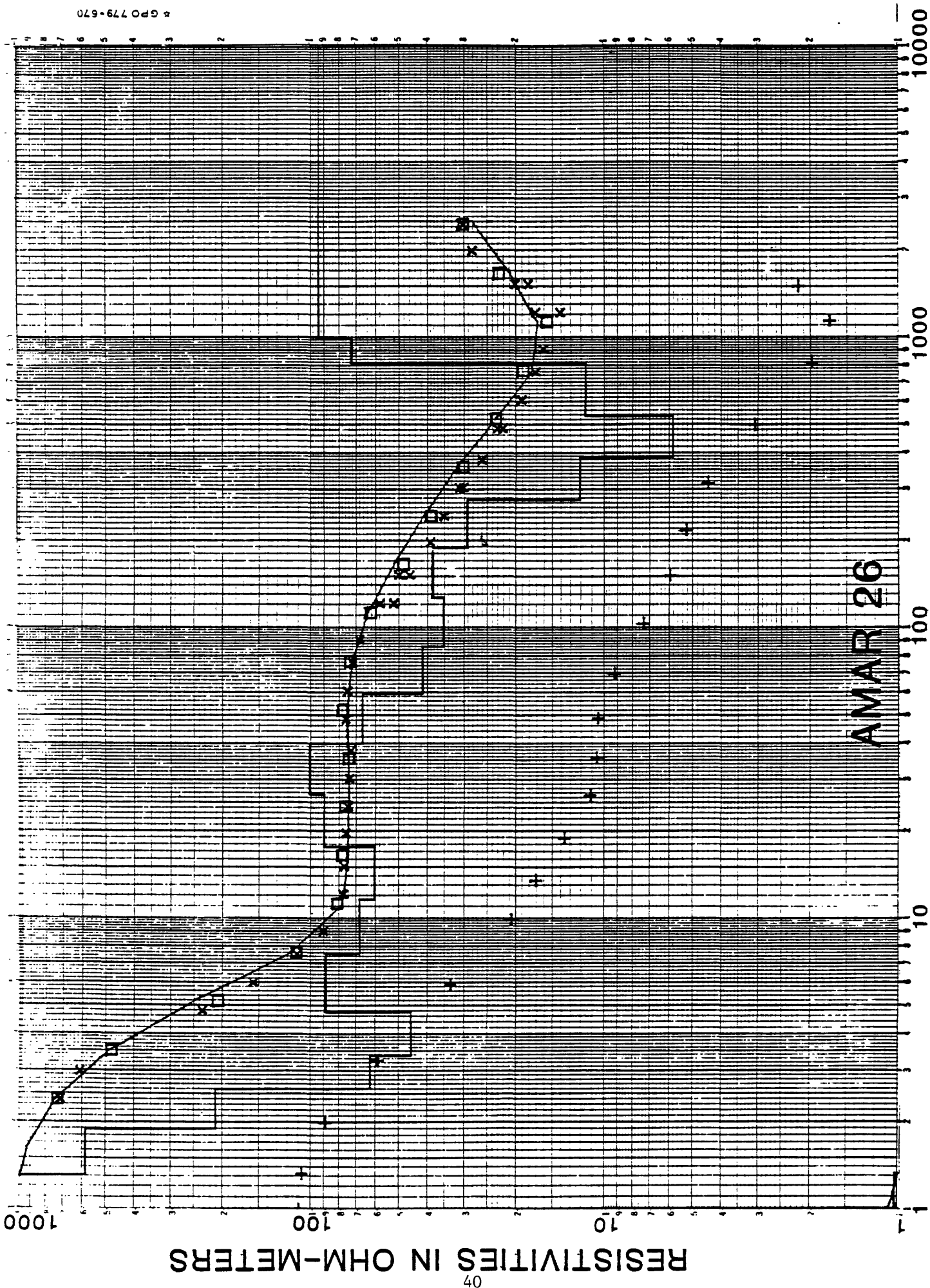


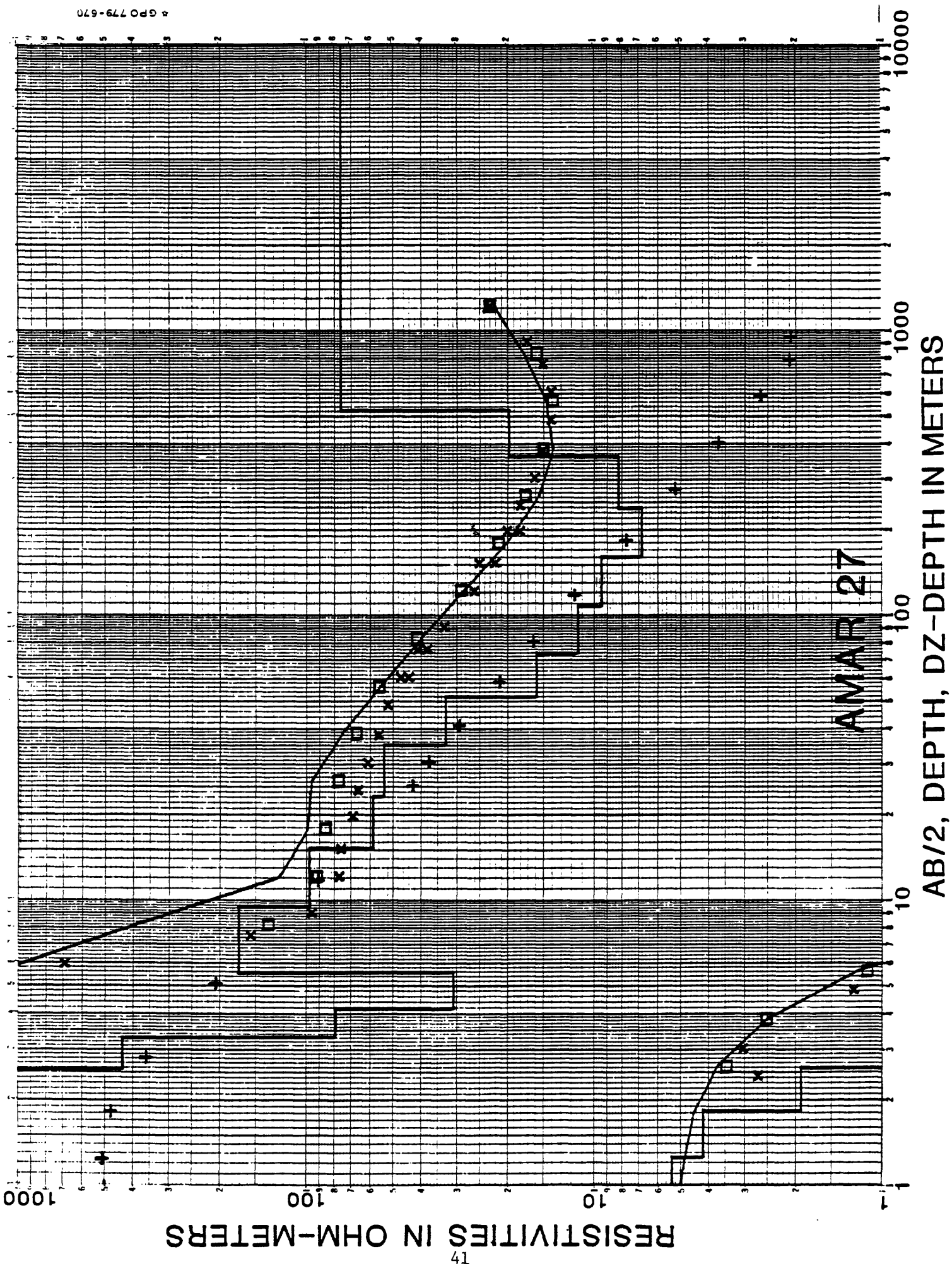


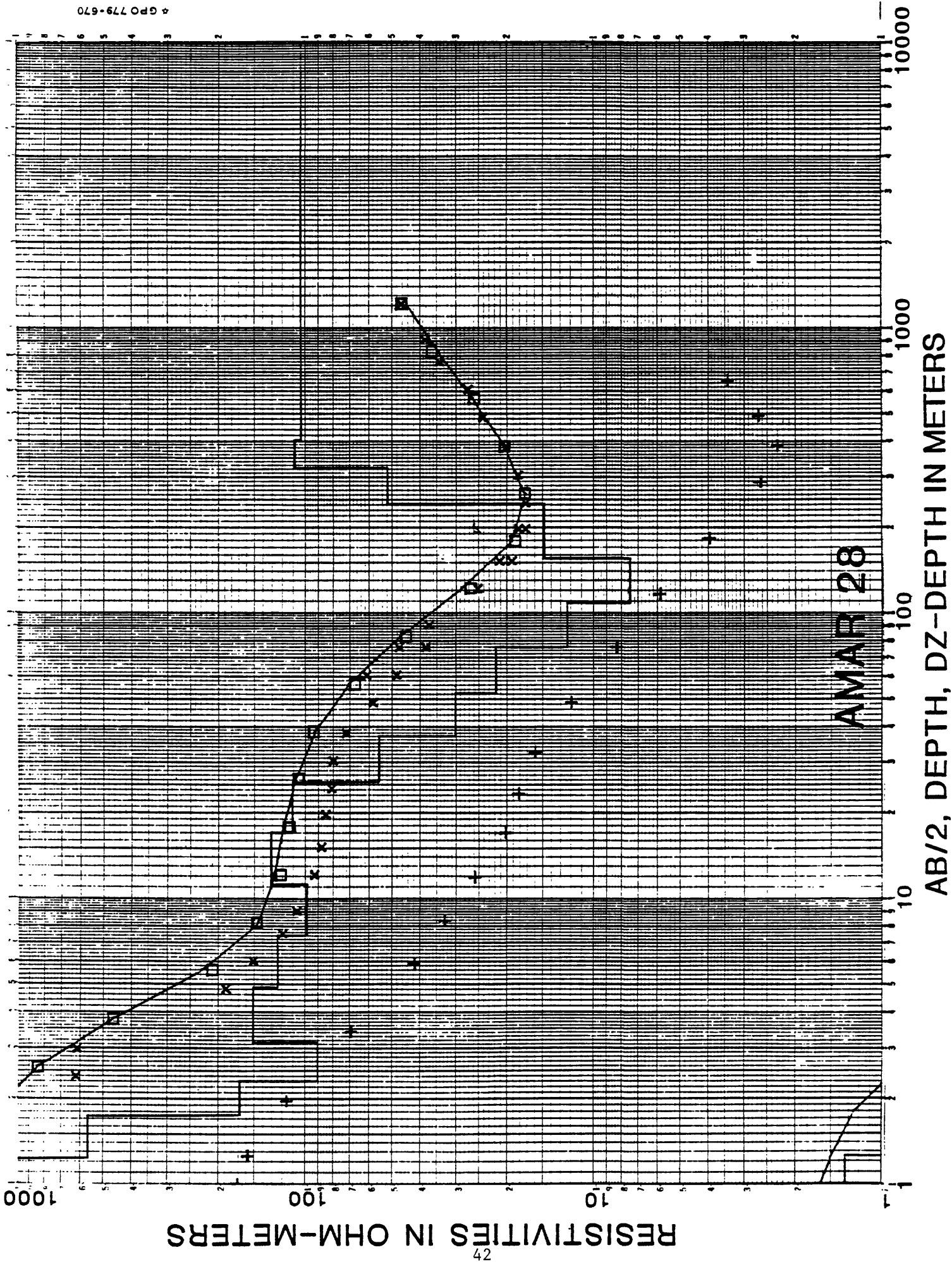


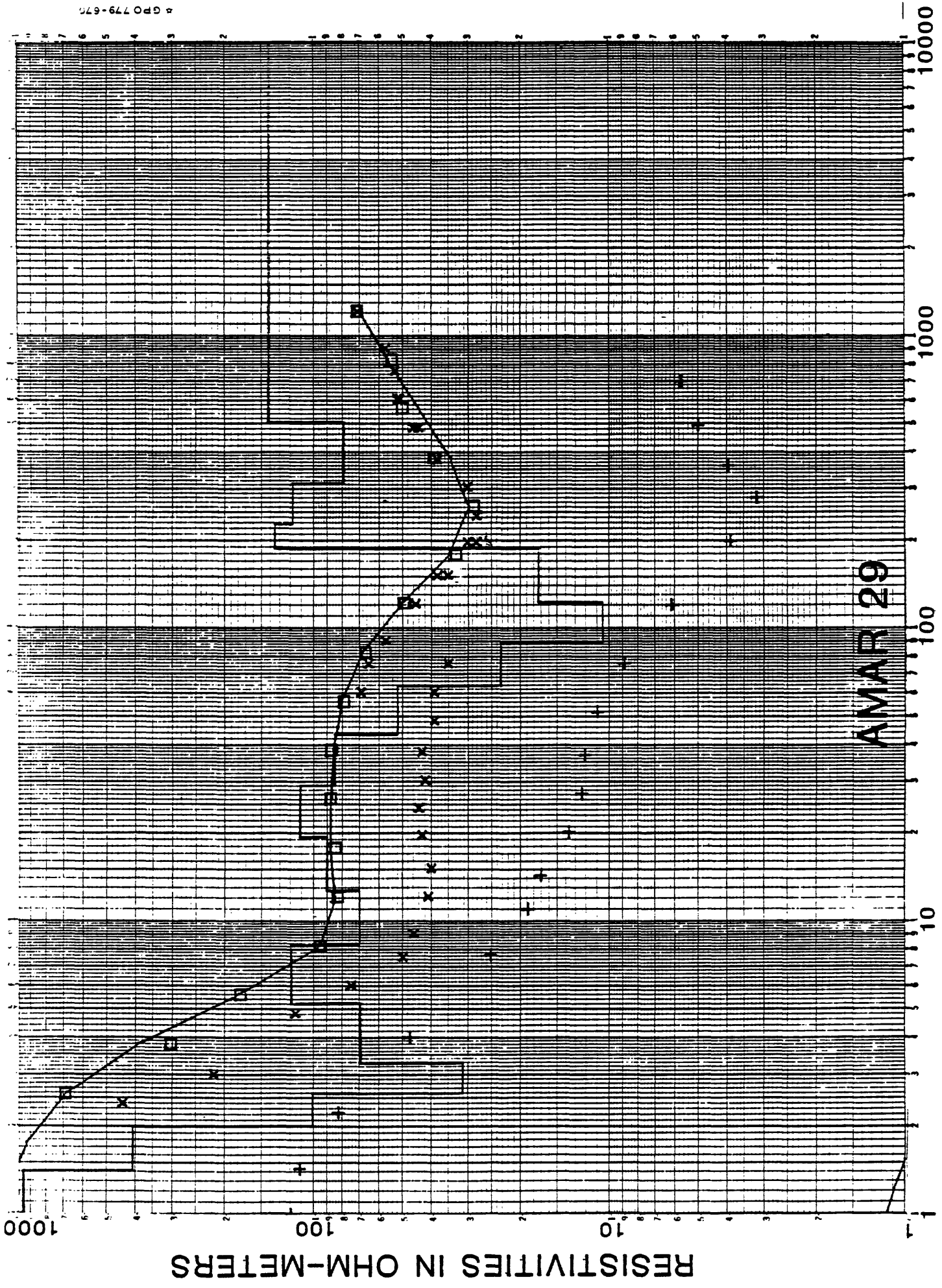




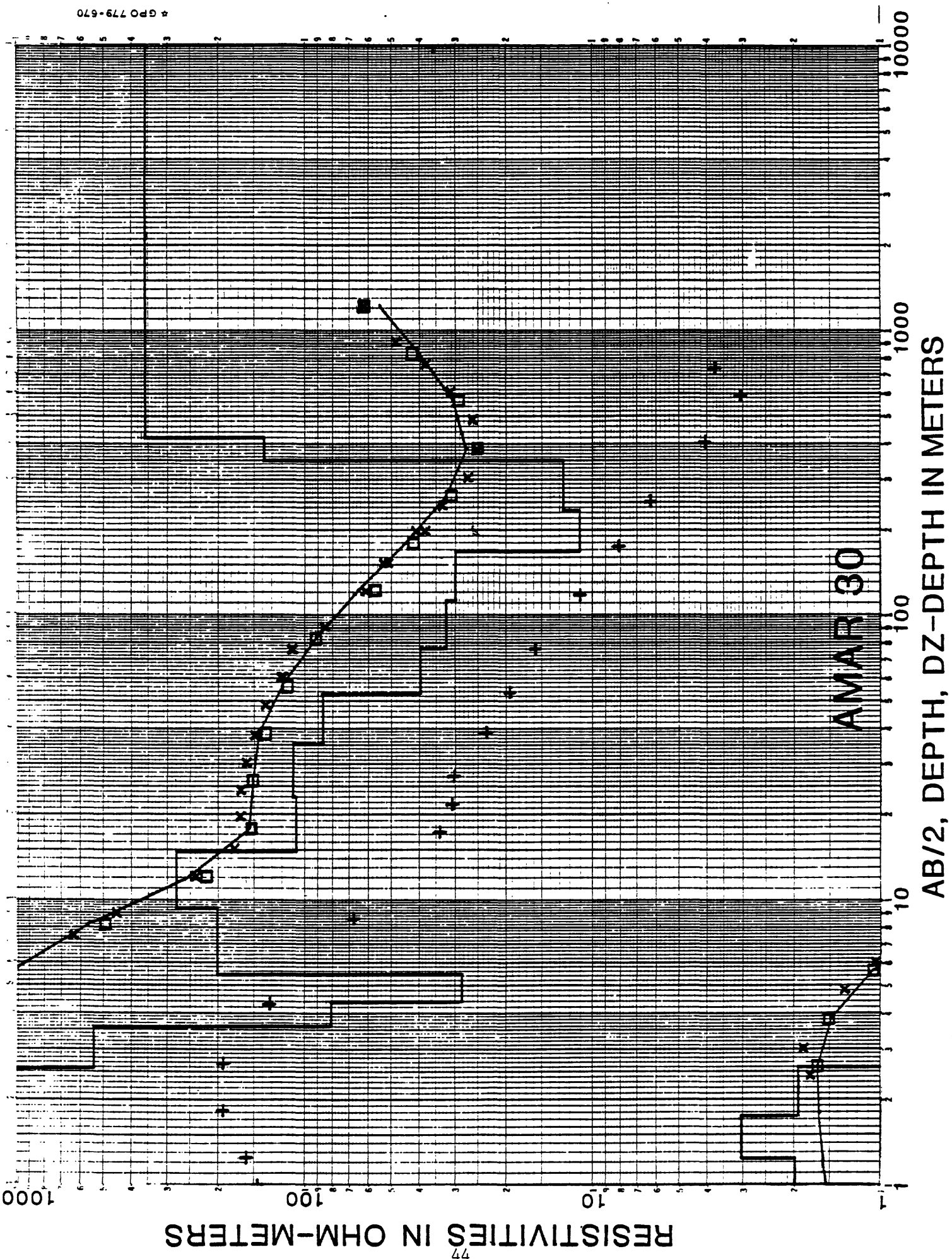


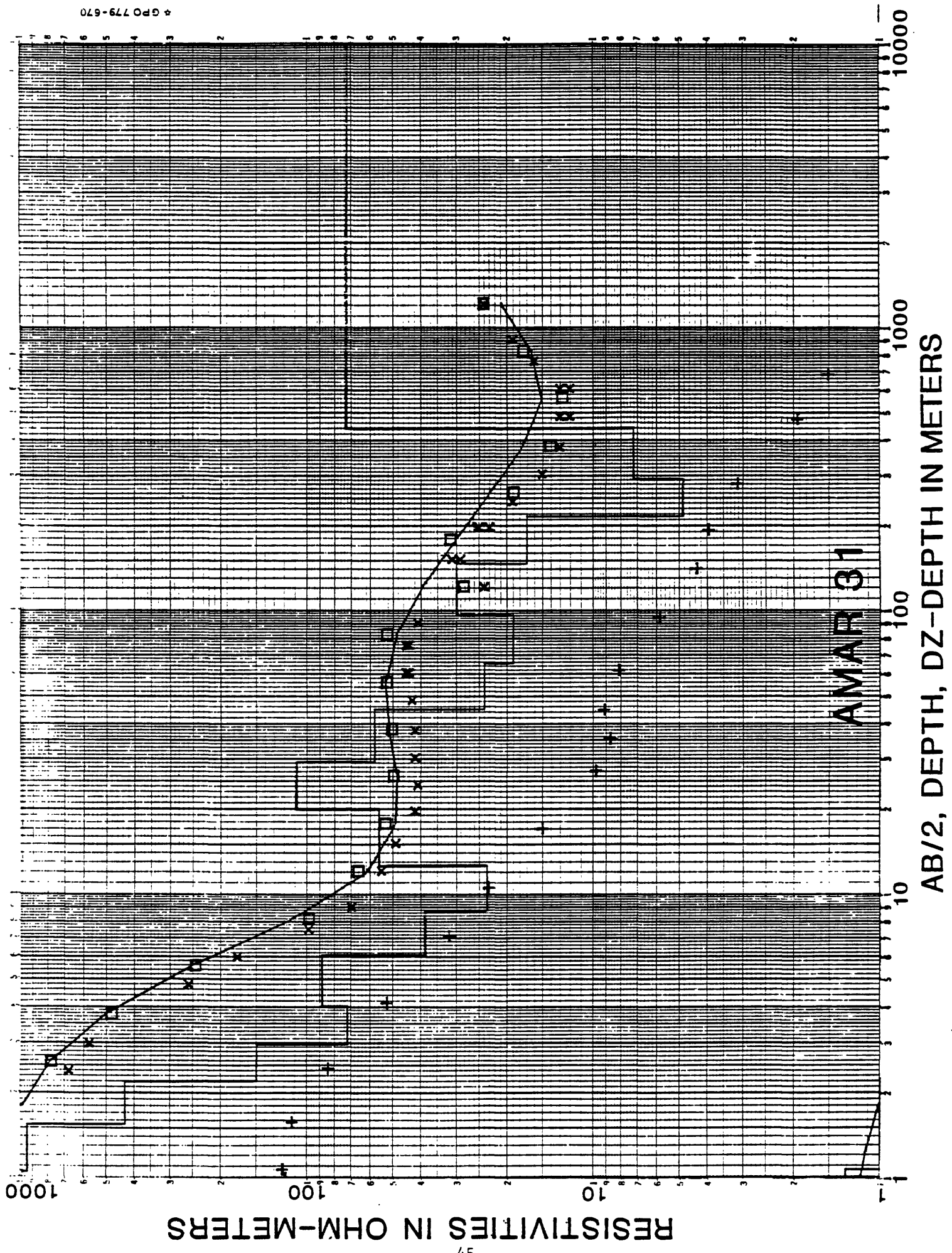




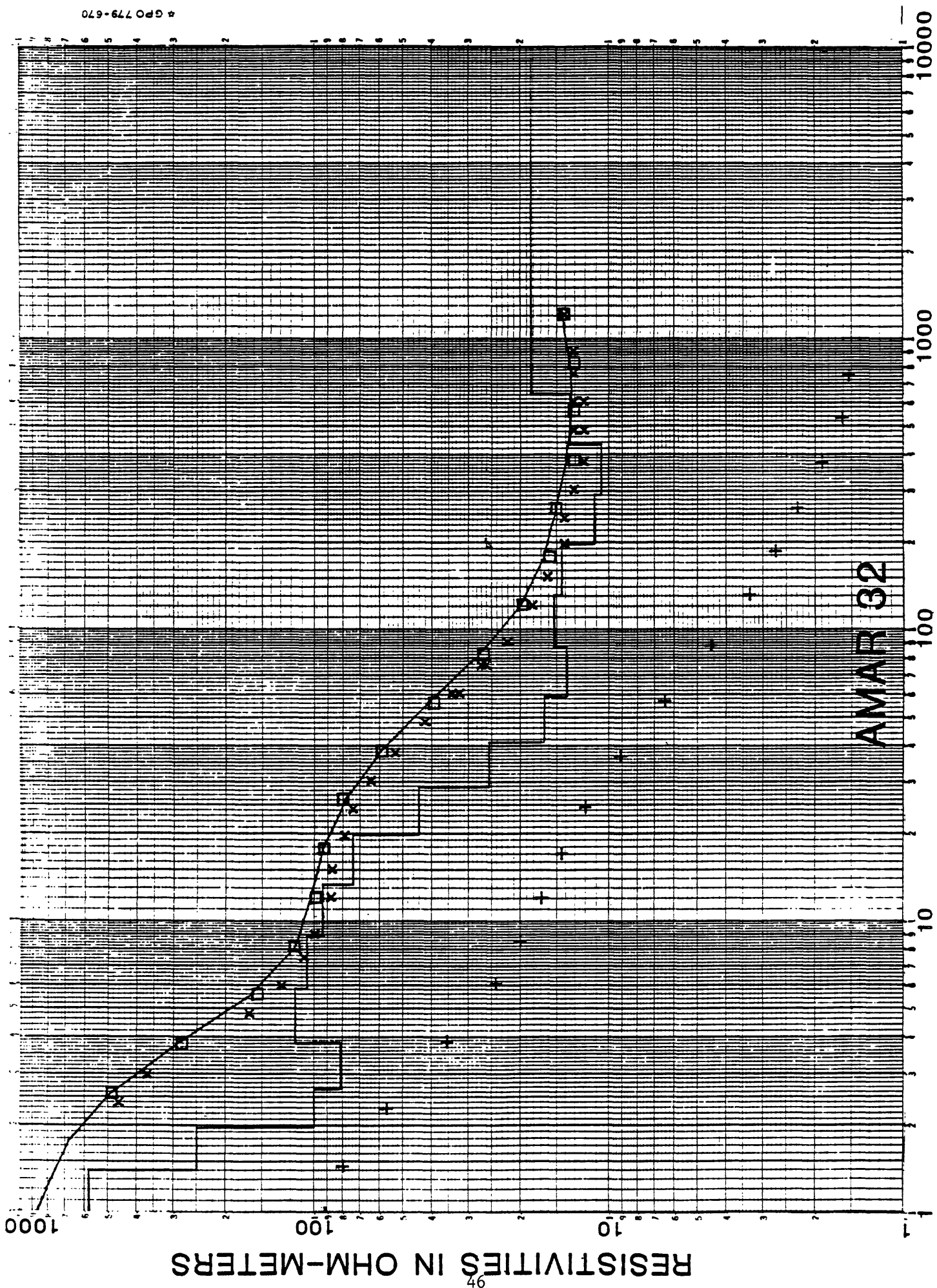


AMAR 29

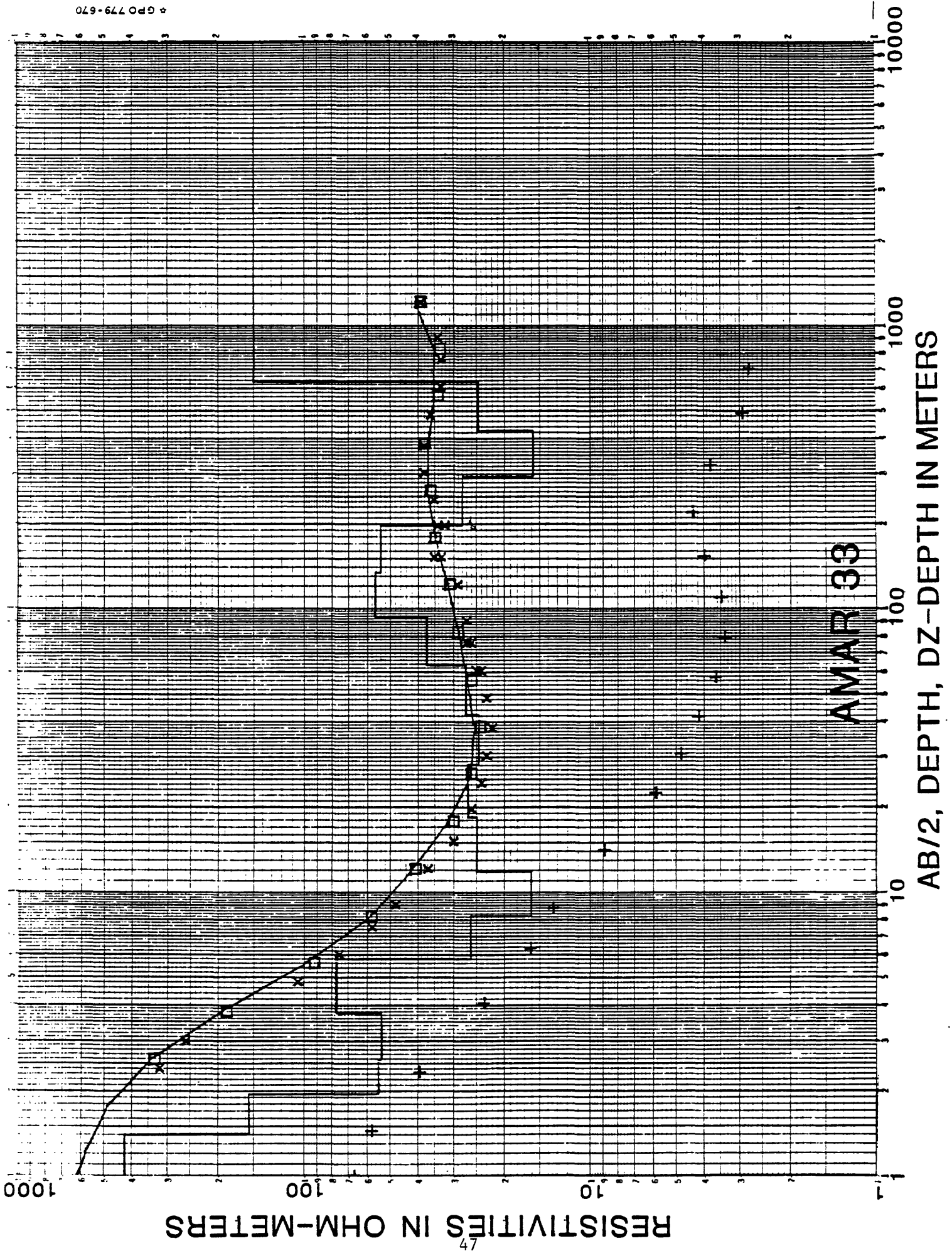


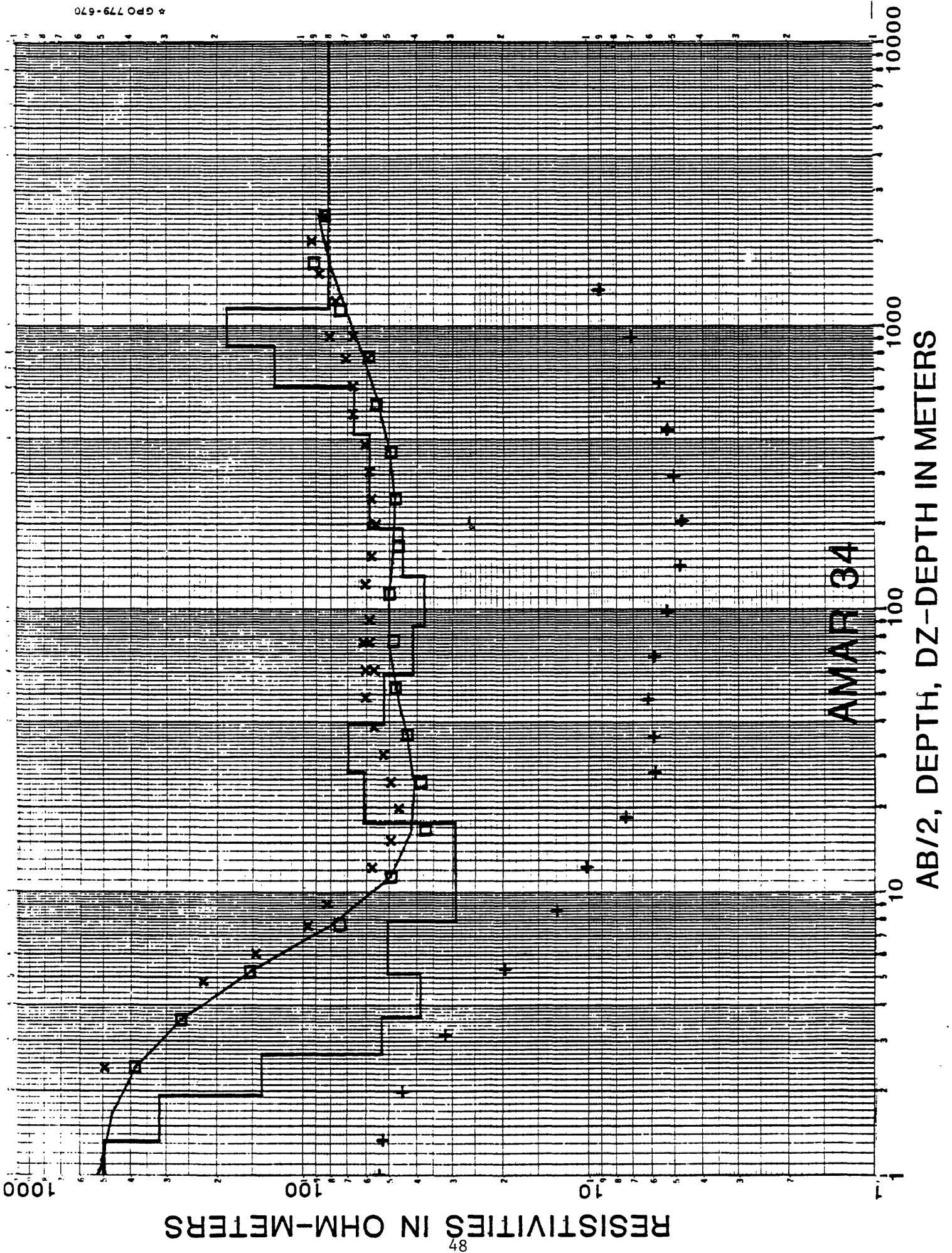


4 GPO 779-670



AB/2, DEPTH, DZ-DEPTH IN METERS



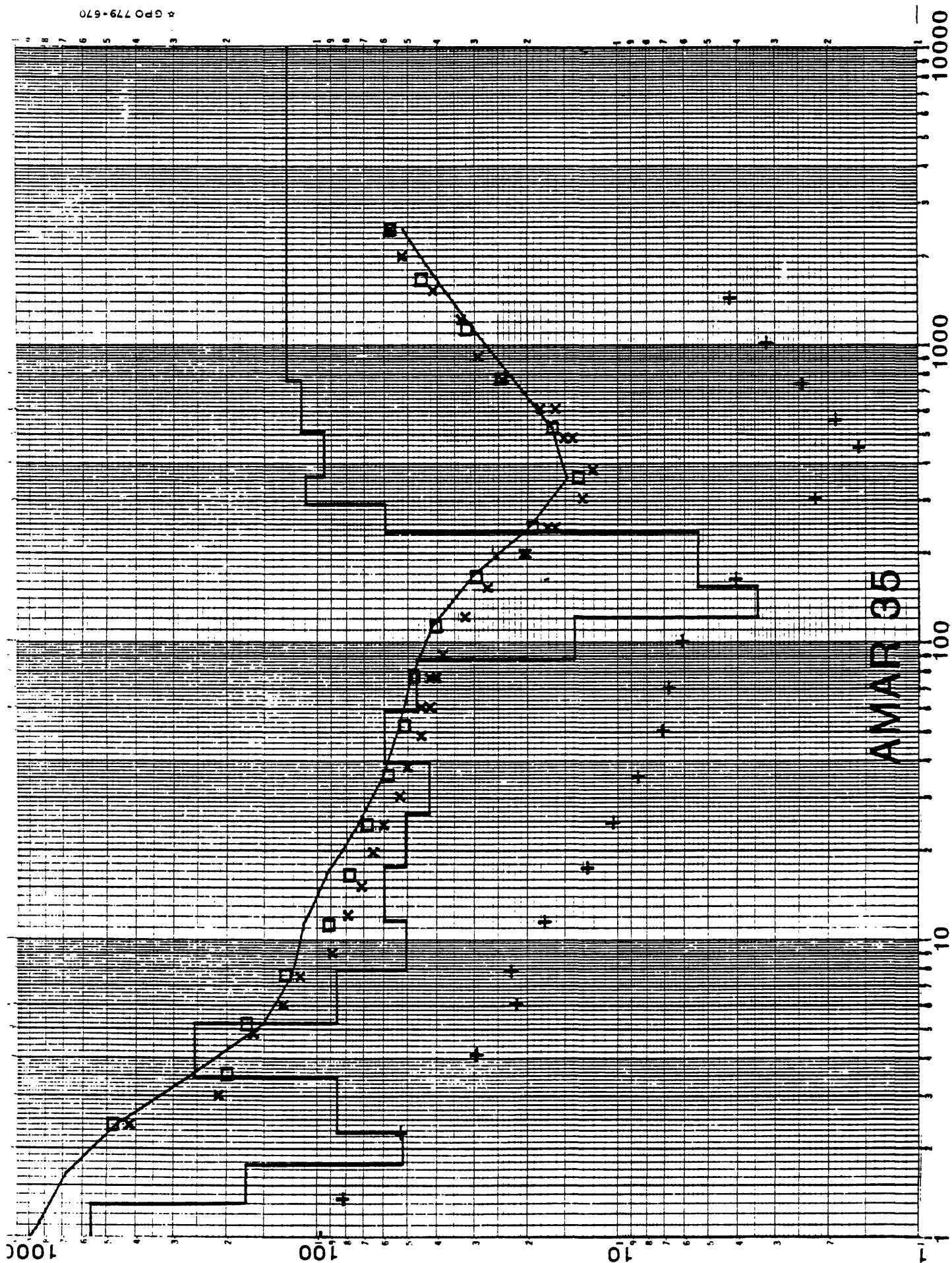


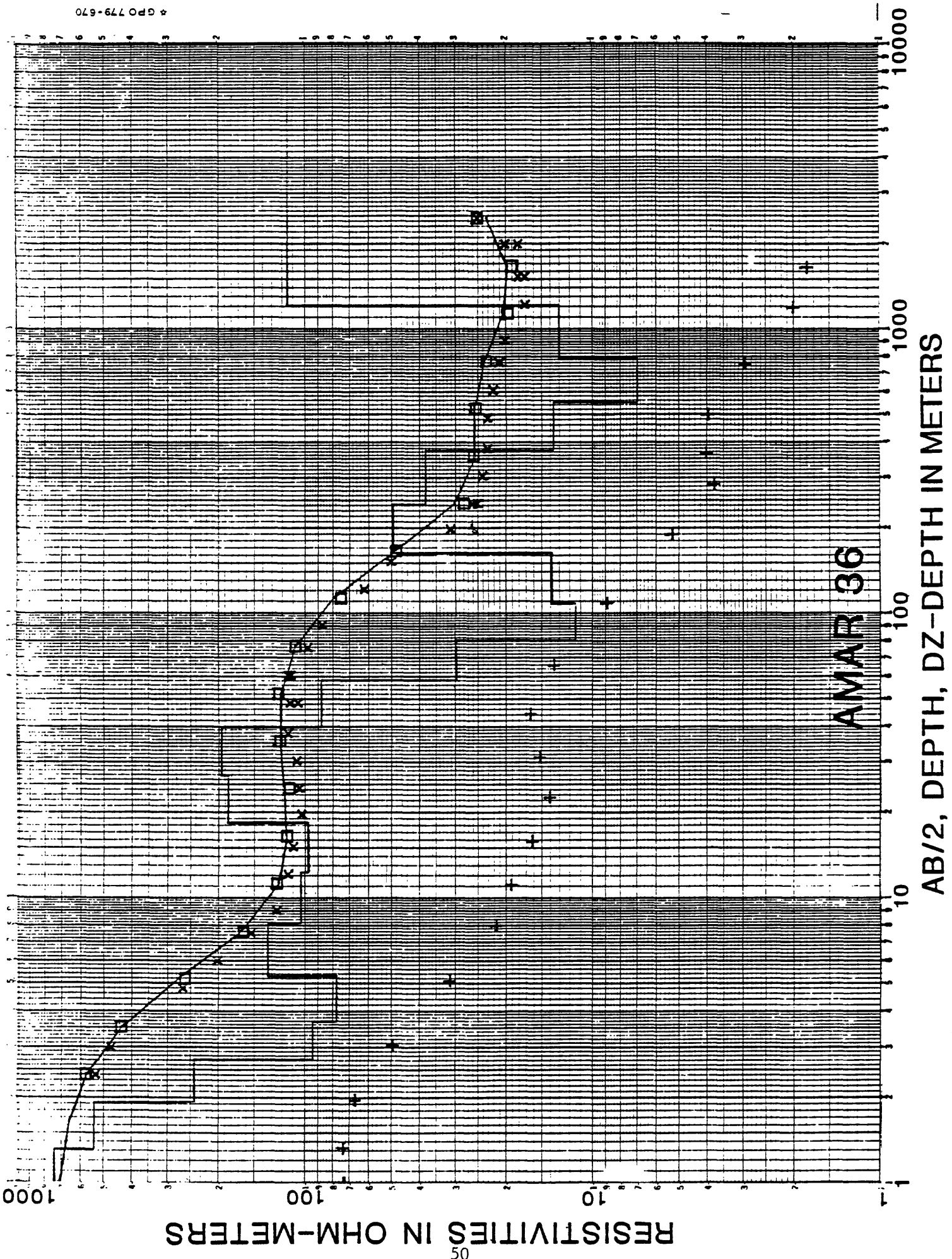
RESISTIVITIES IN OHM-METERS

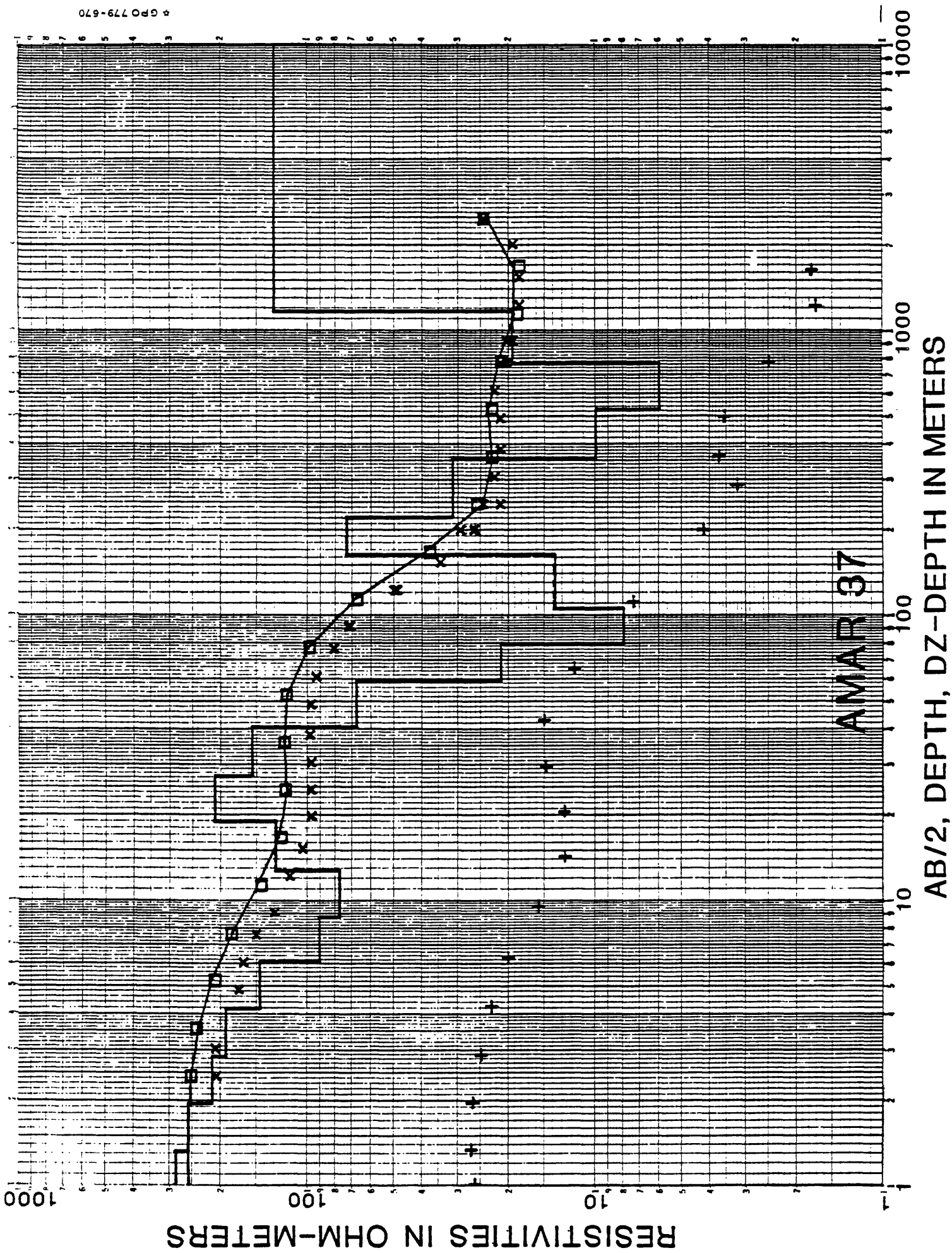
49

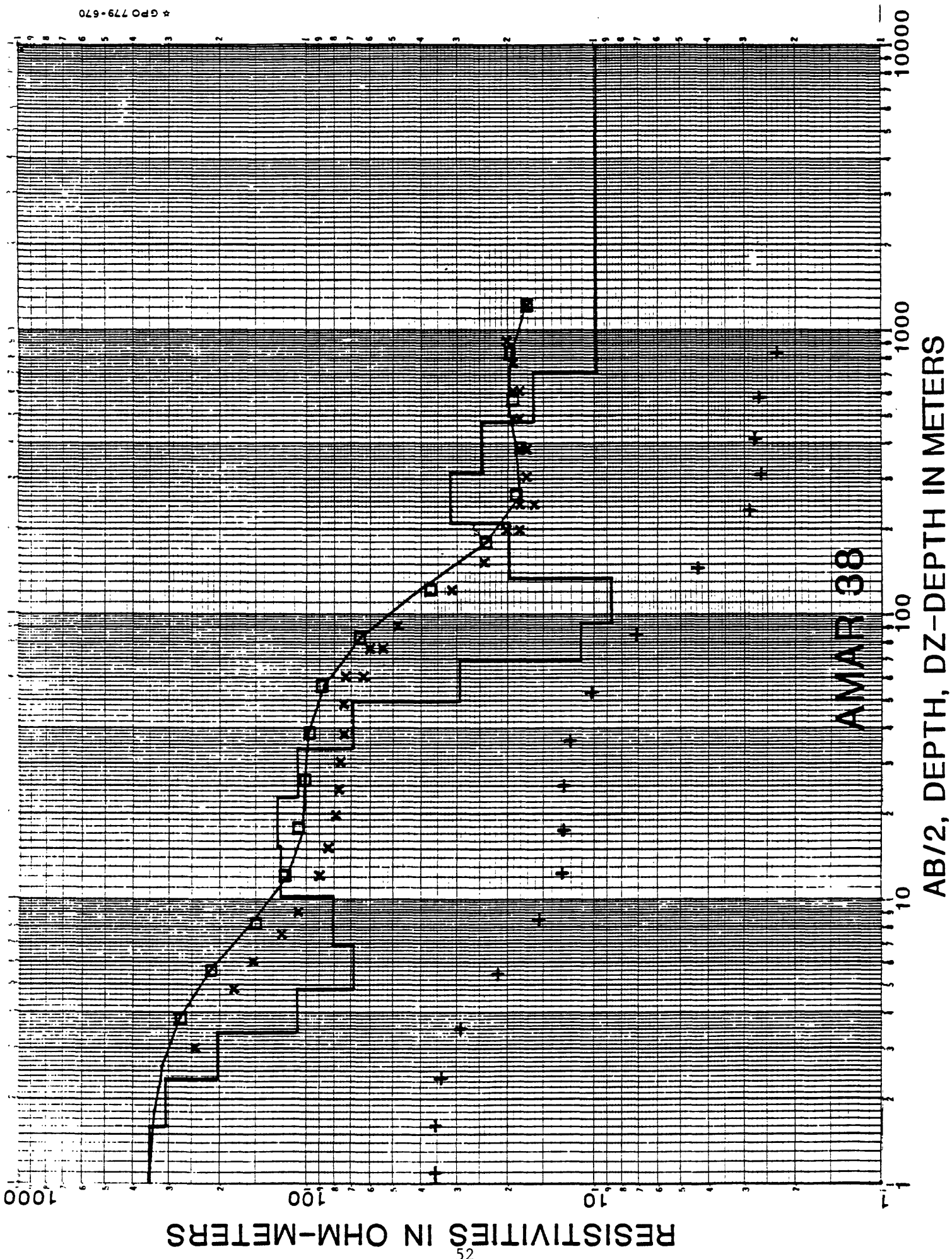
AMAR 35

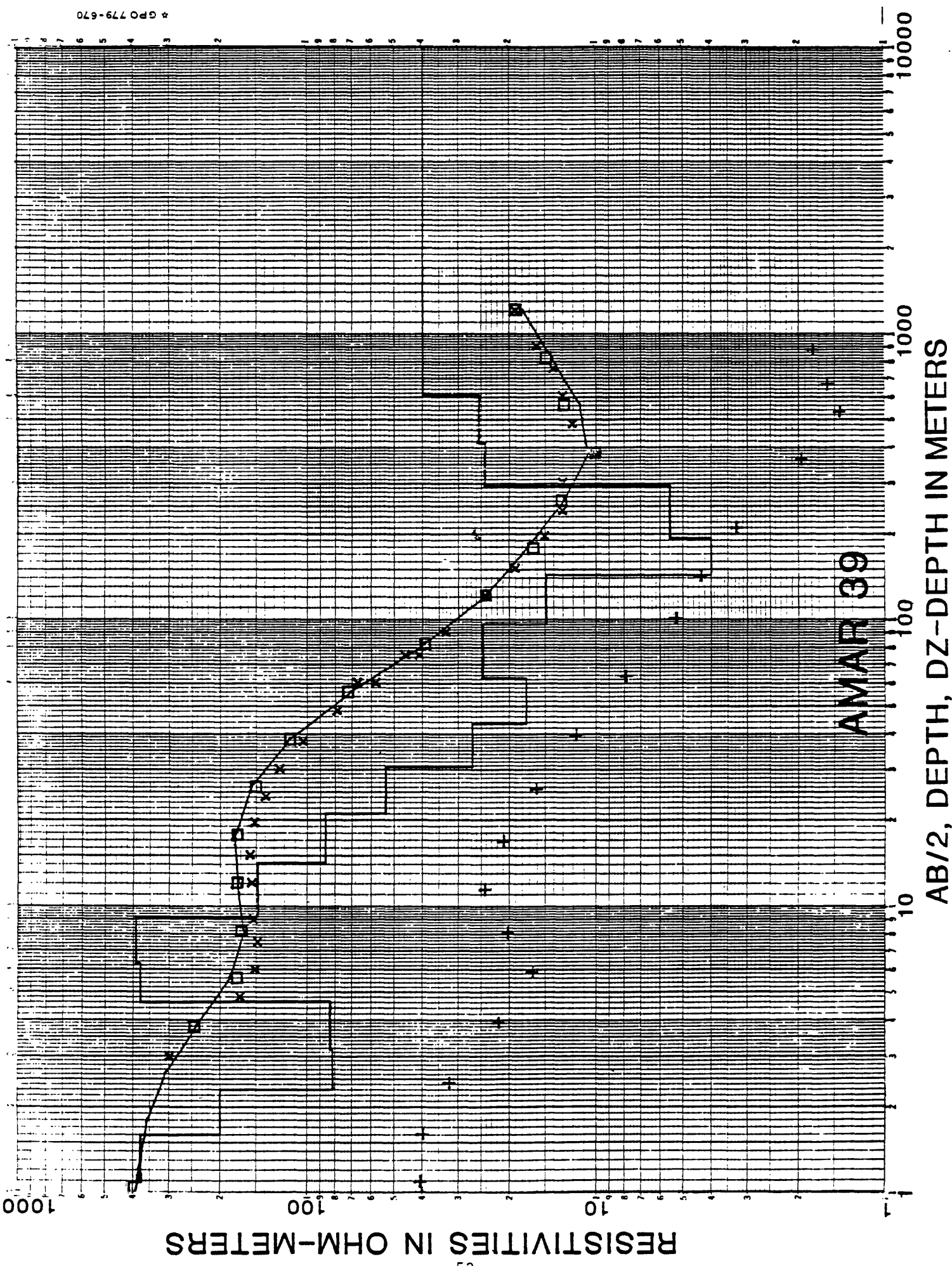
AB/2, DEPTH, DZ-DEPTH IN METERS



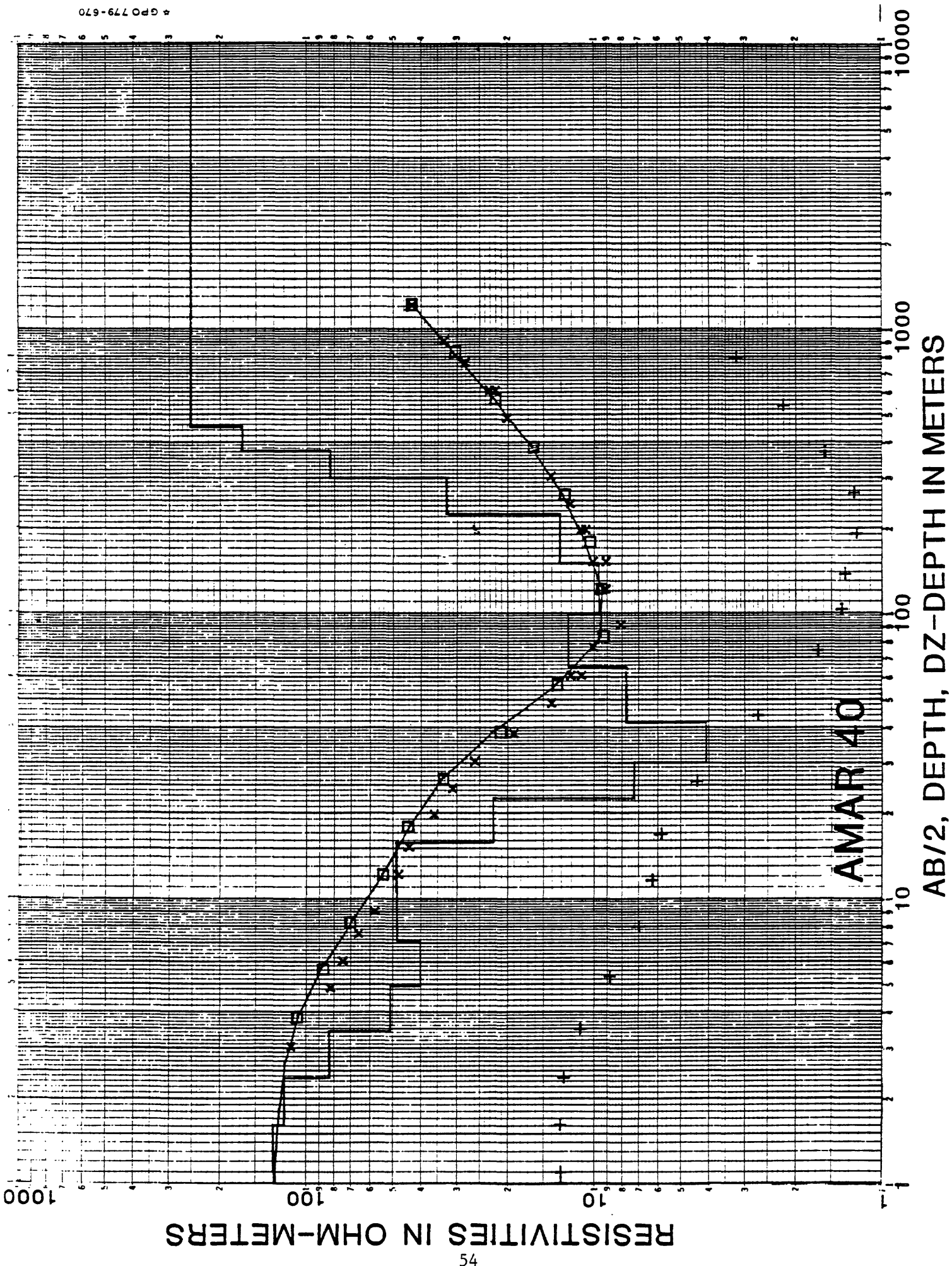


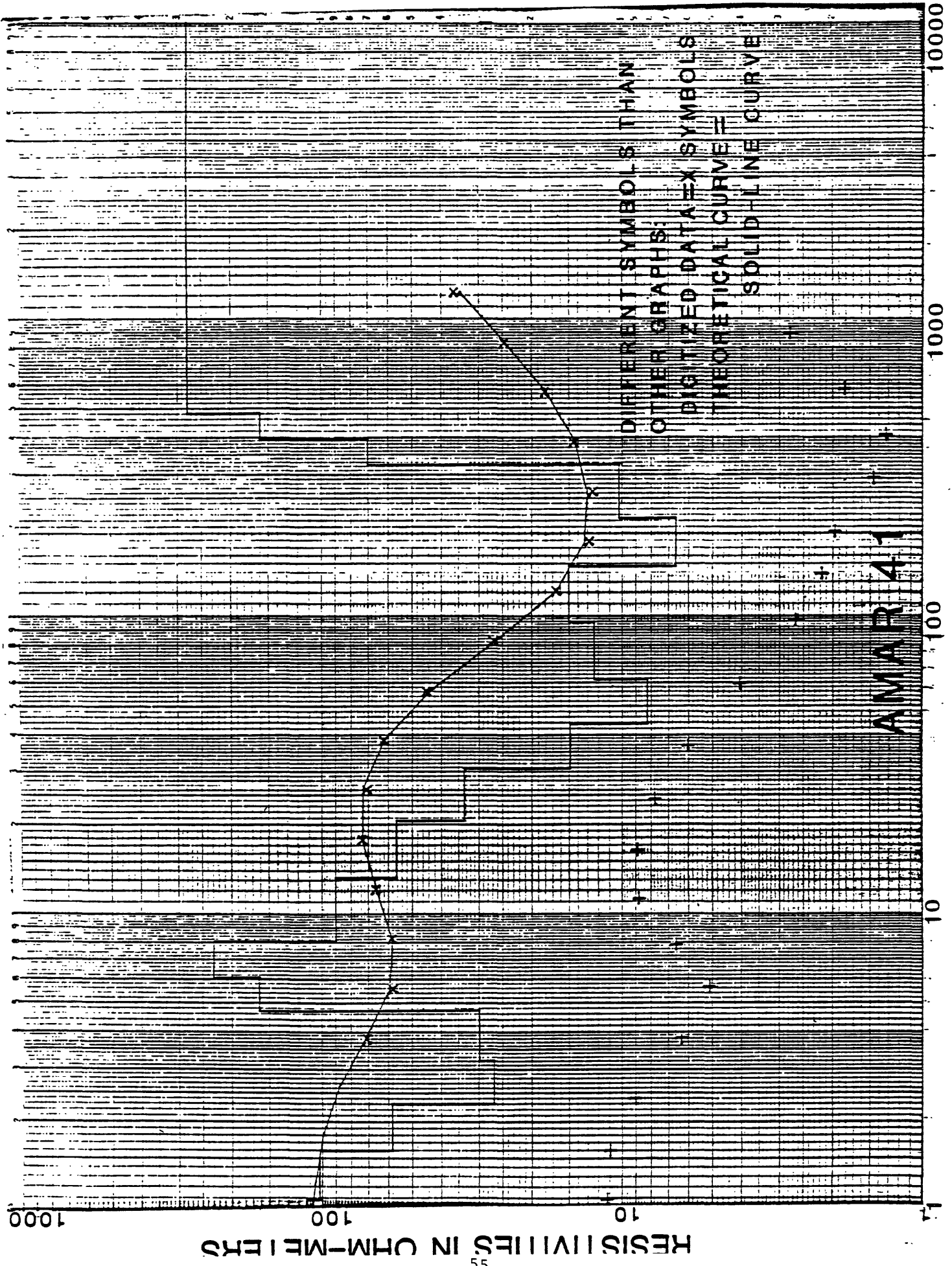


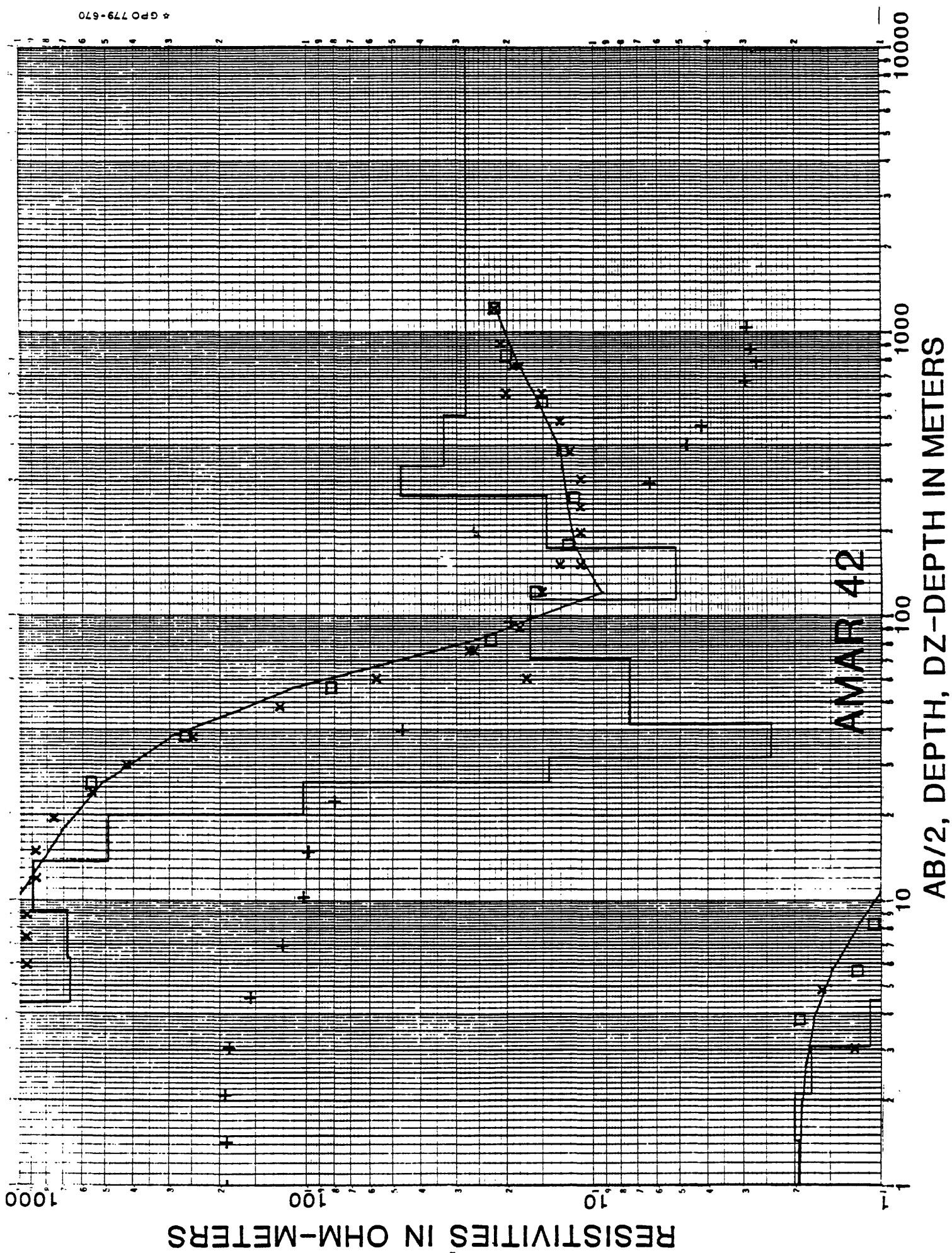




* GPO 779-670





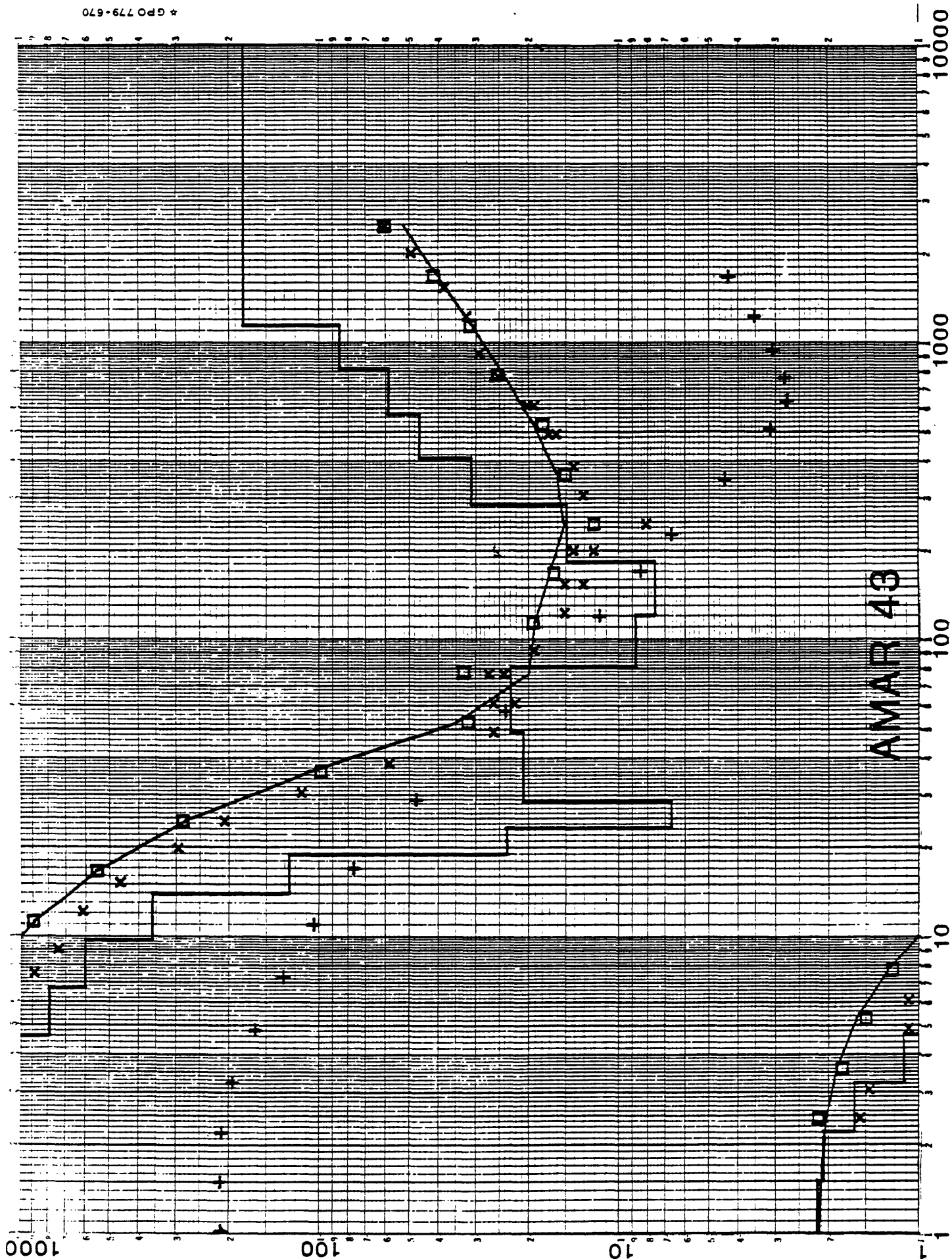


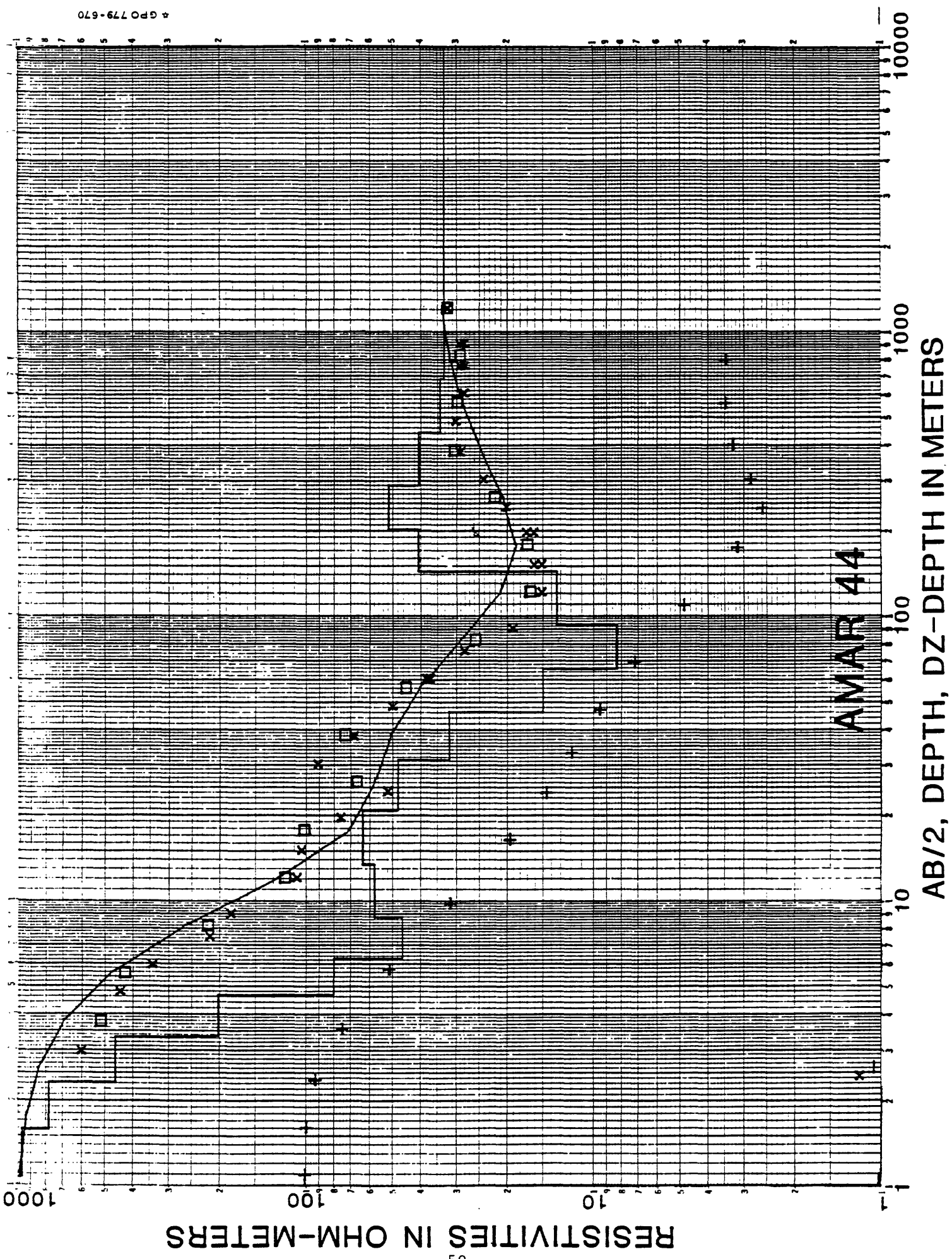
RESISTIVITIES IN OHM-METERS

57

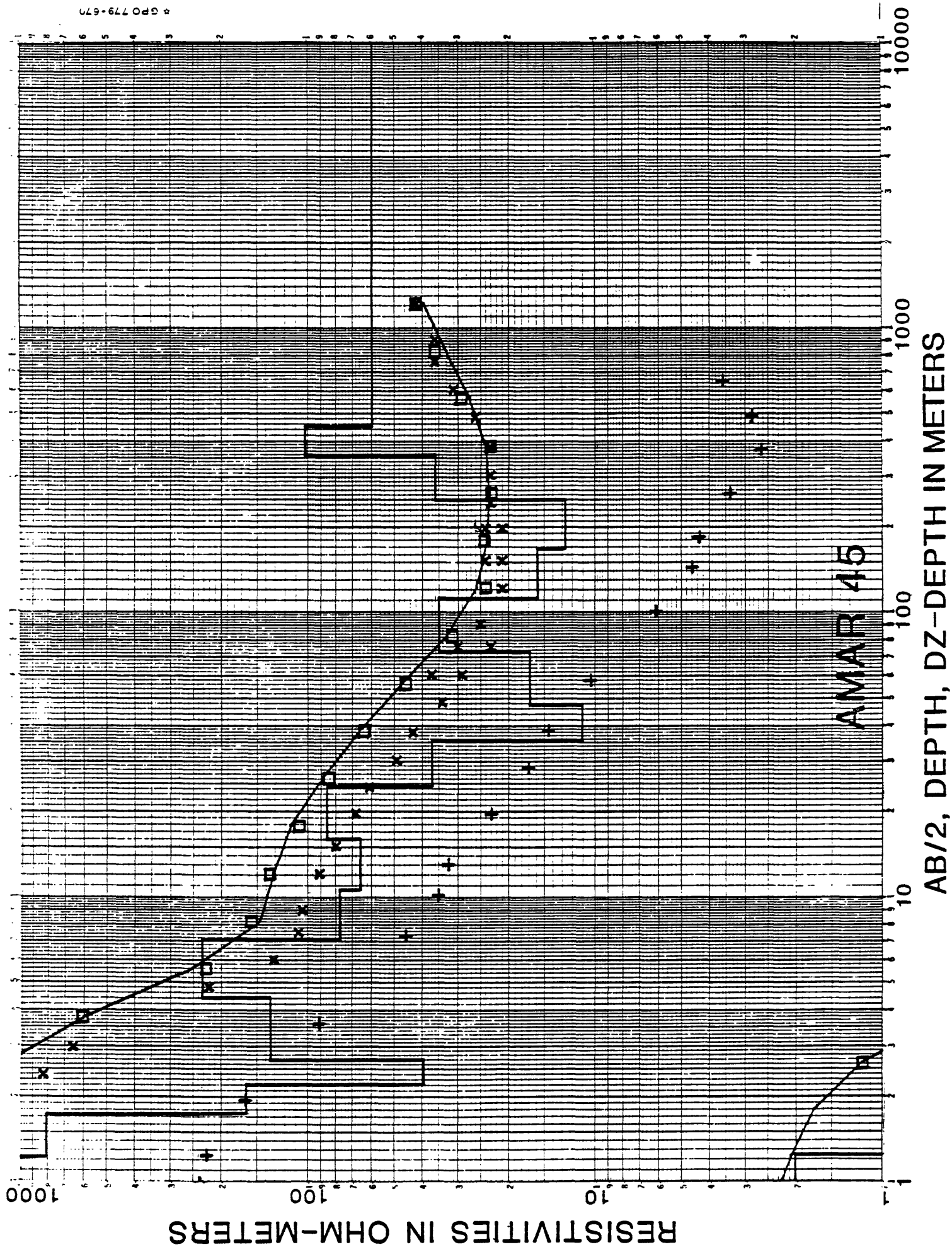
AMAR 43

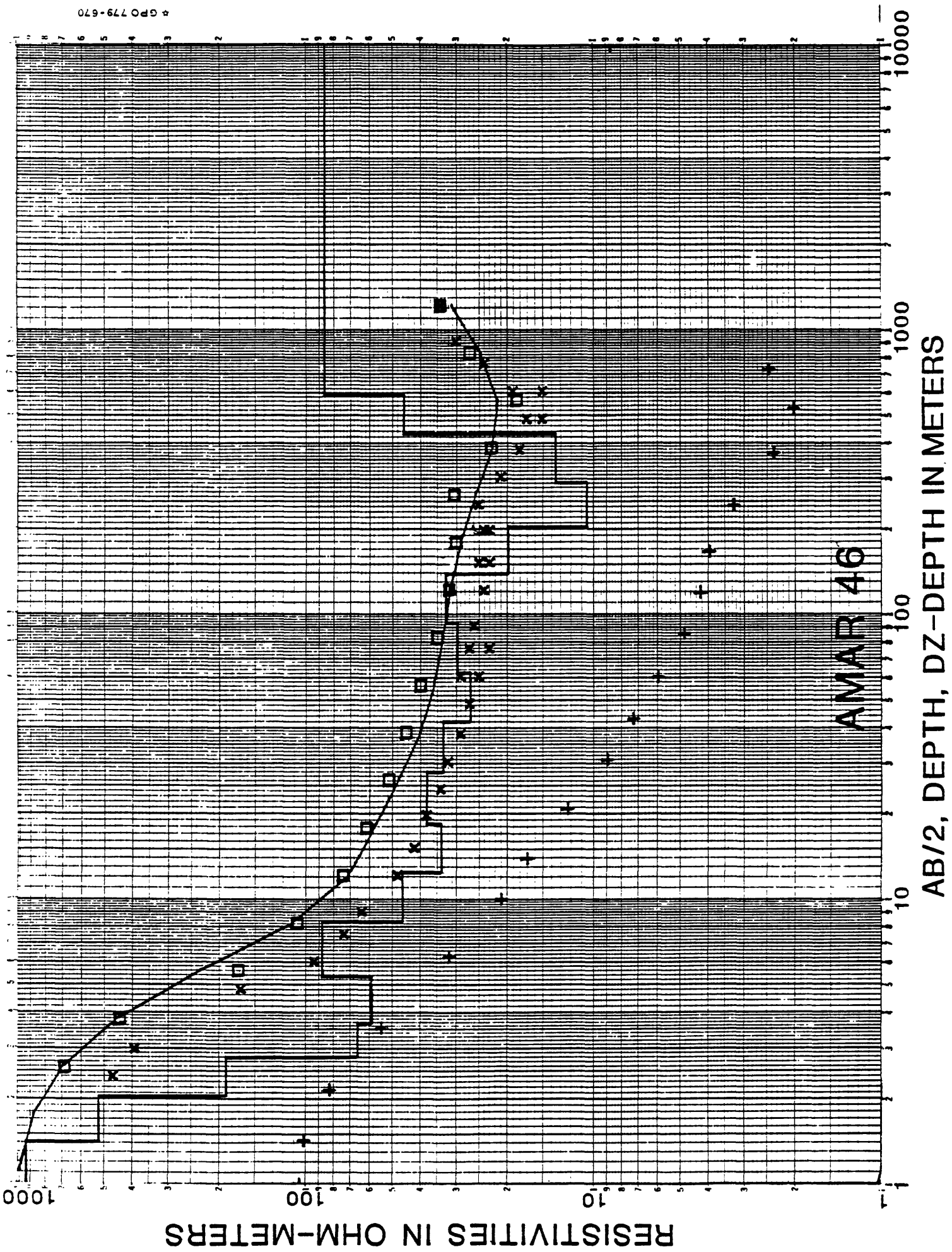
AB/2, DEPTH, DZ-DEPTH IN METERS



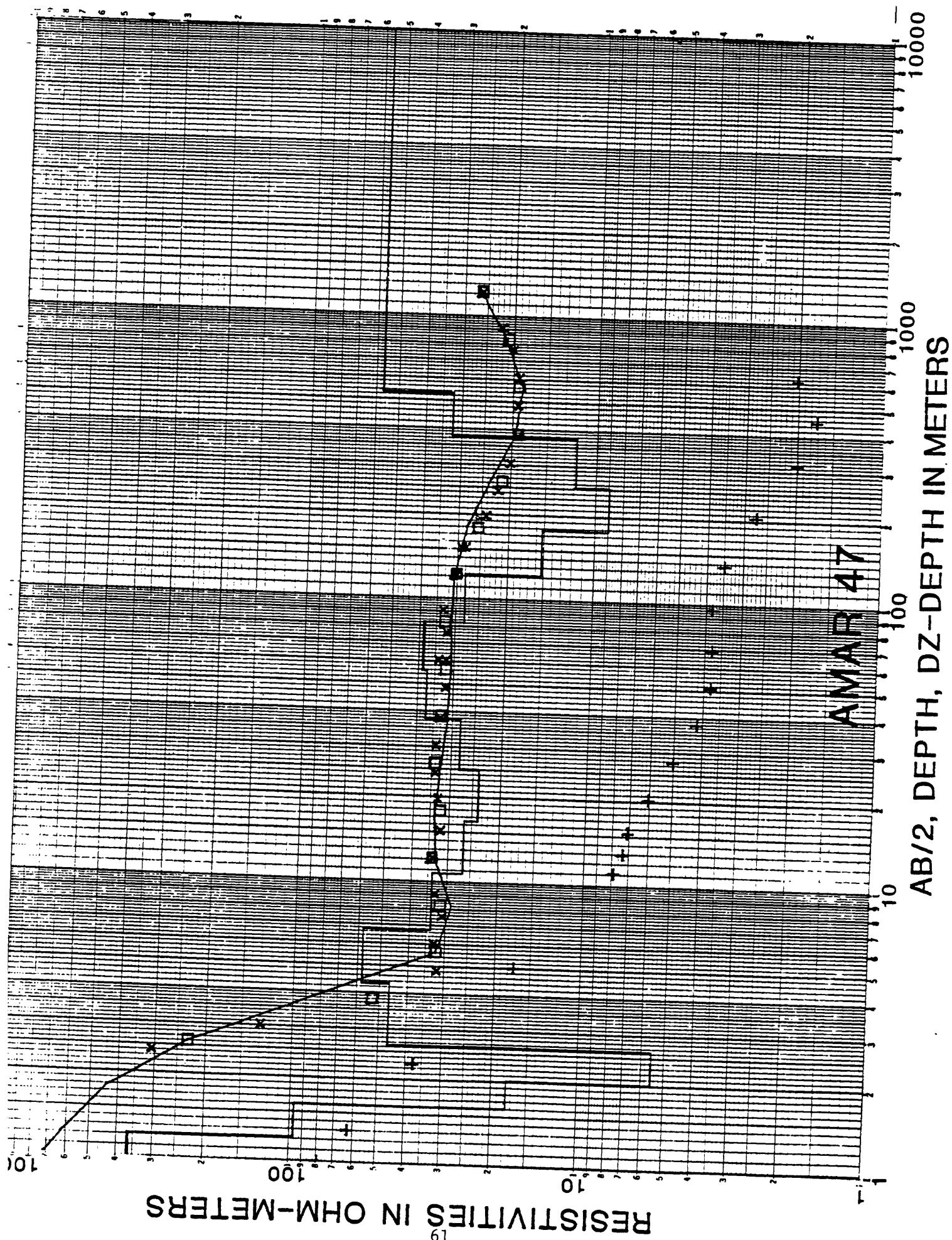


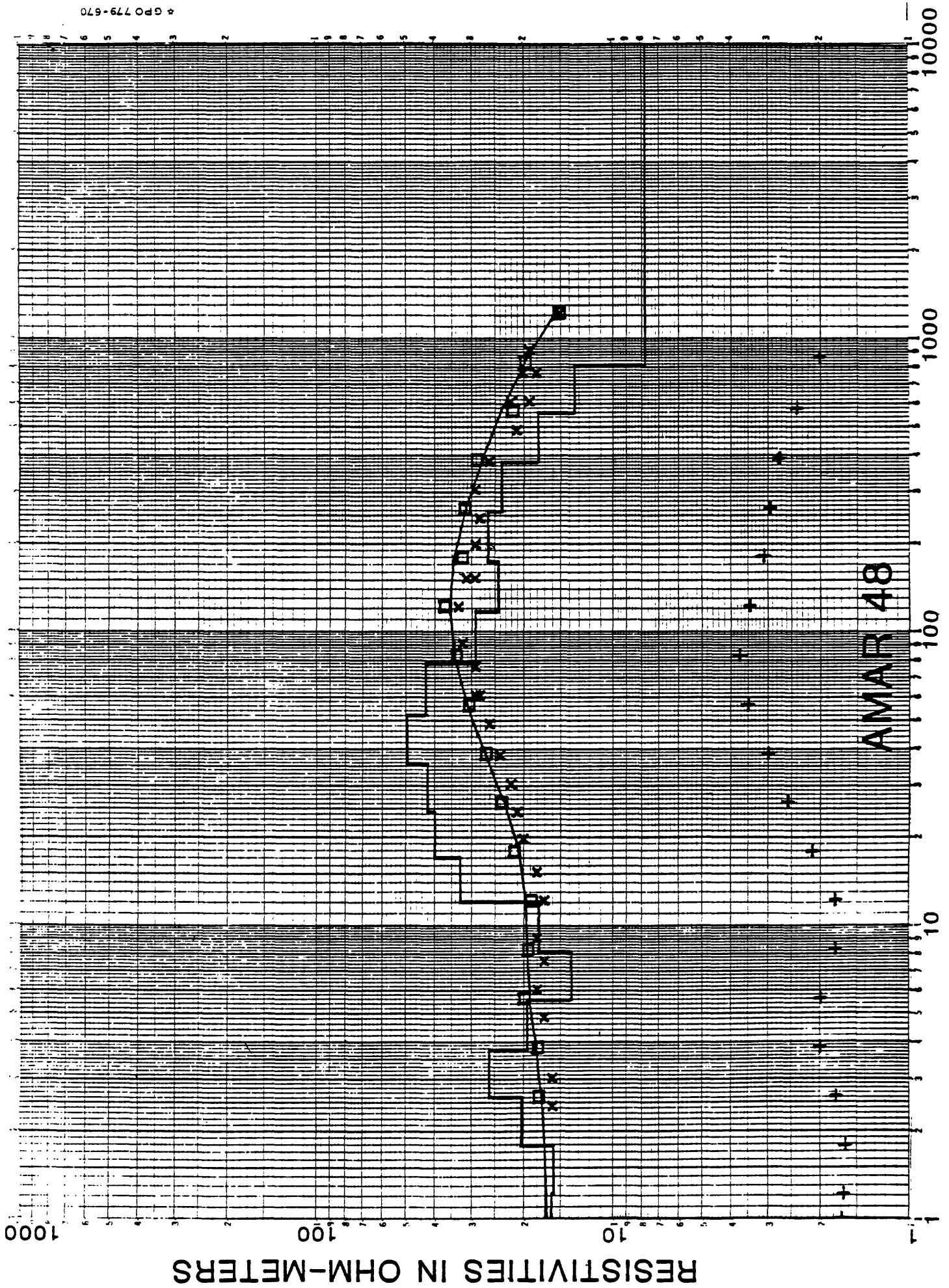
* GPO 779-670





AMAR 46

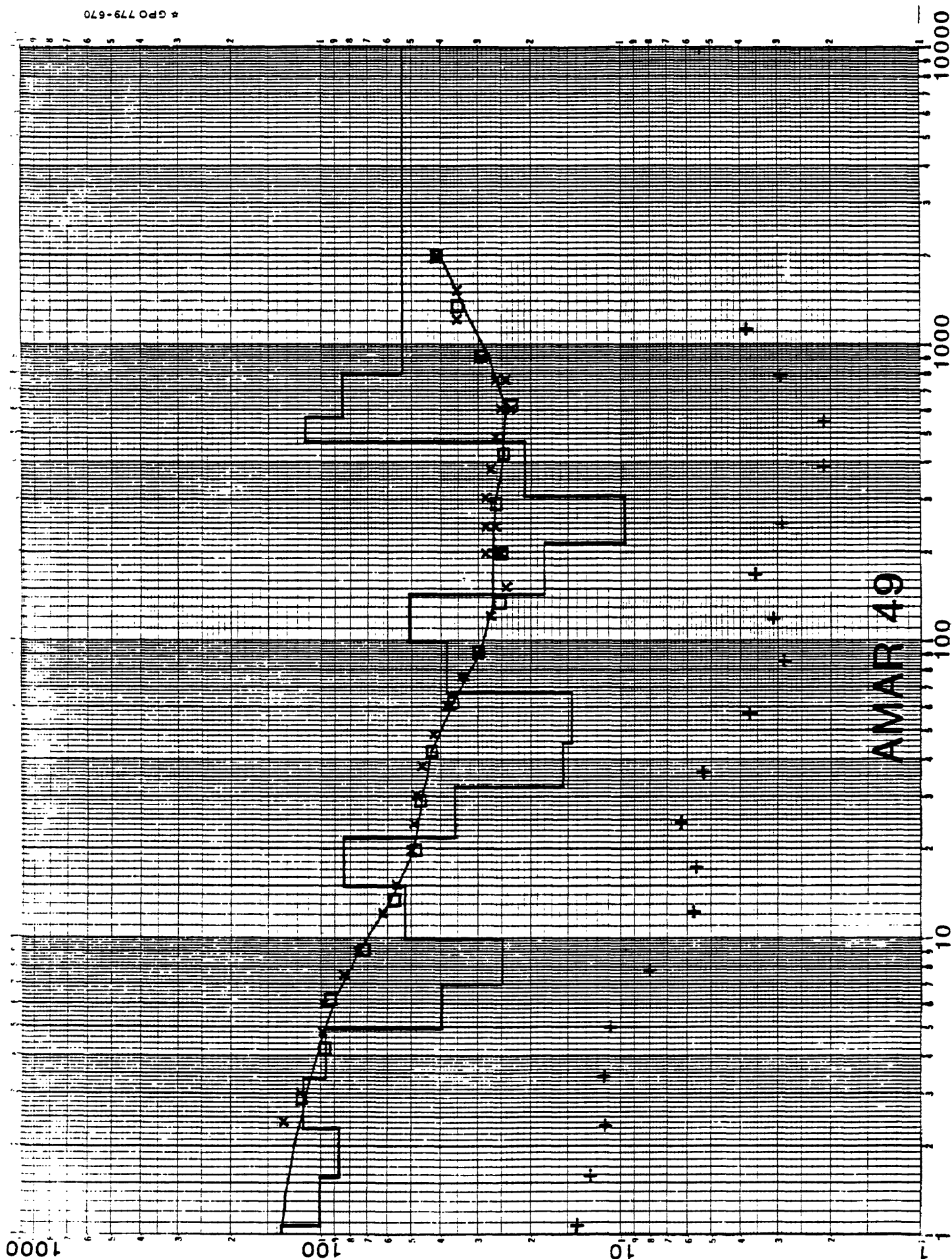


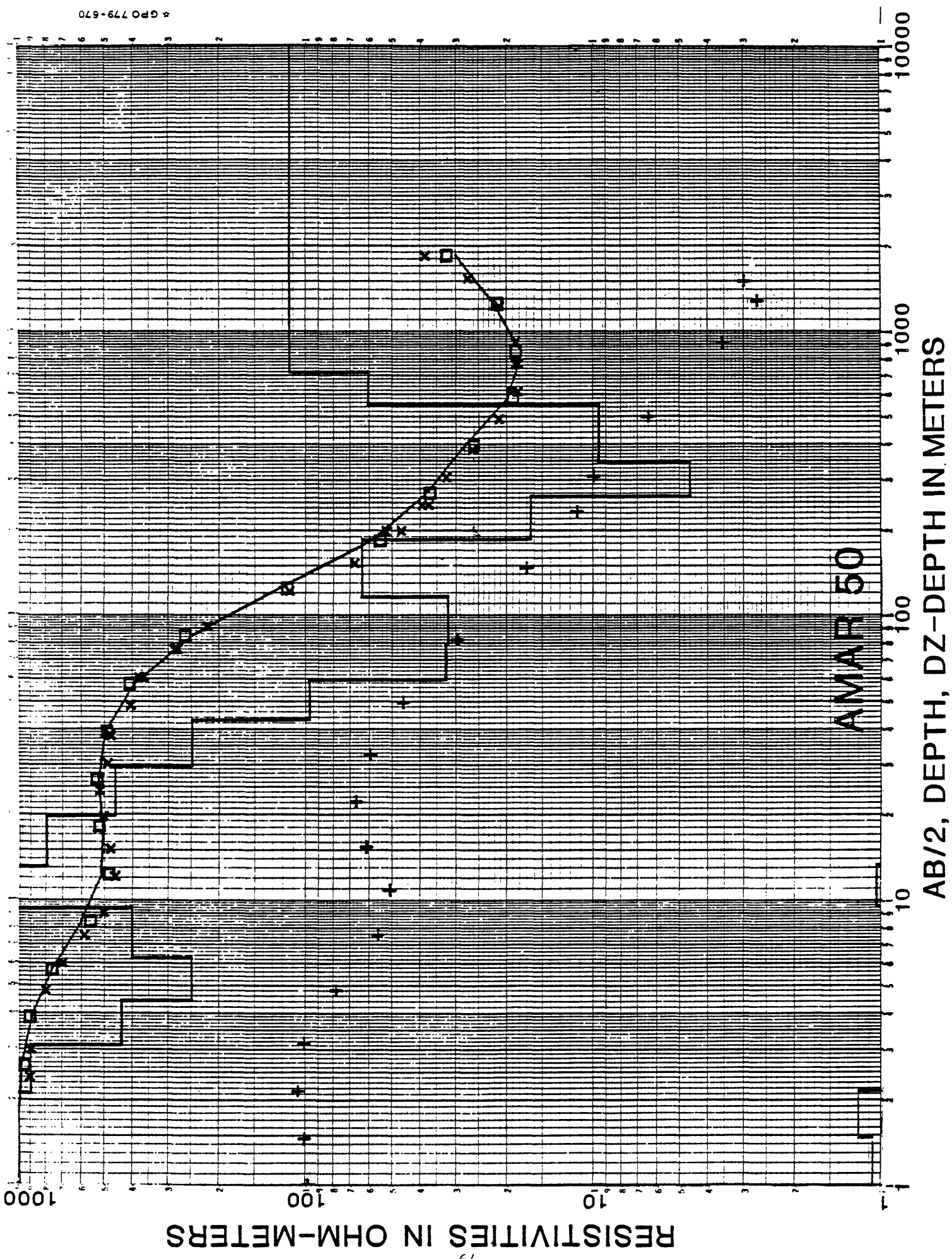


AMAR 49

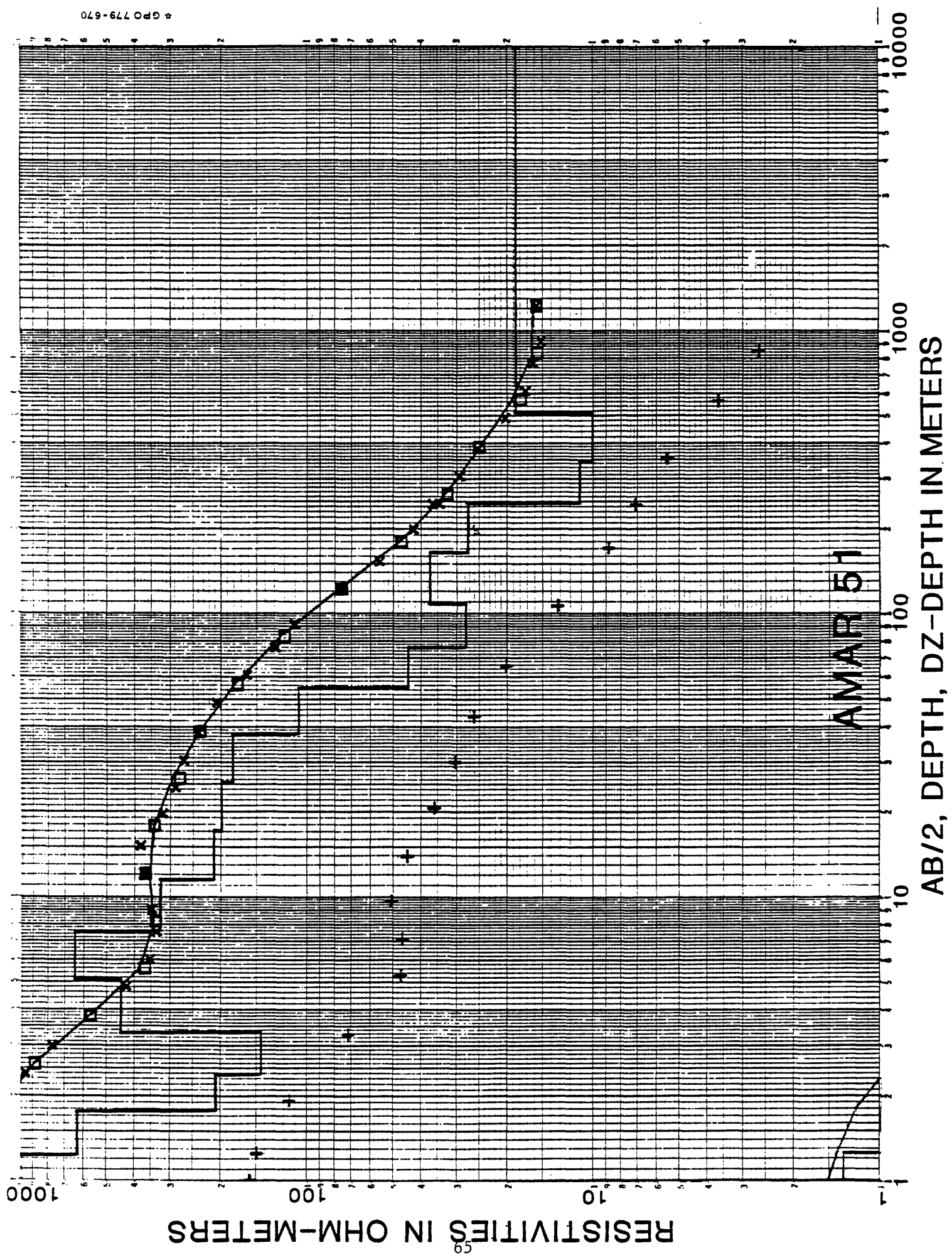
AB/2, DEPTH, DZ-DEPTH IN METERS

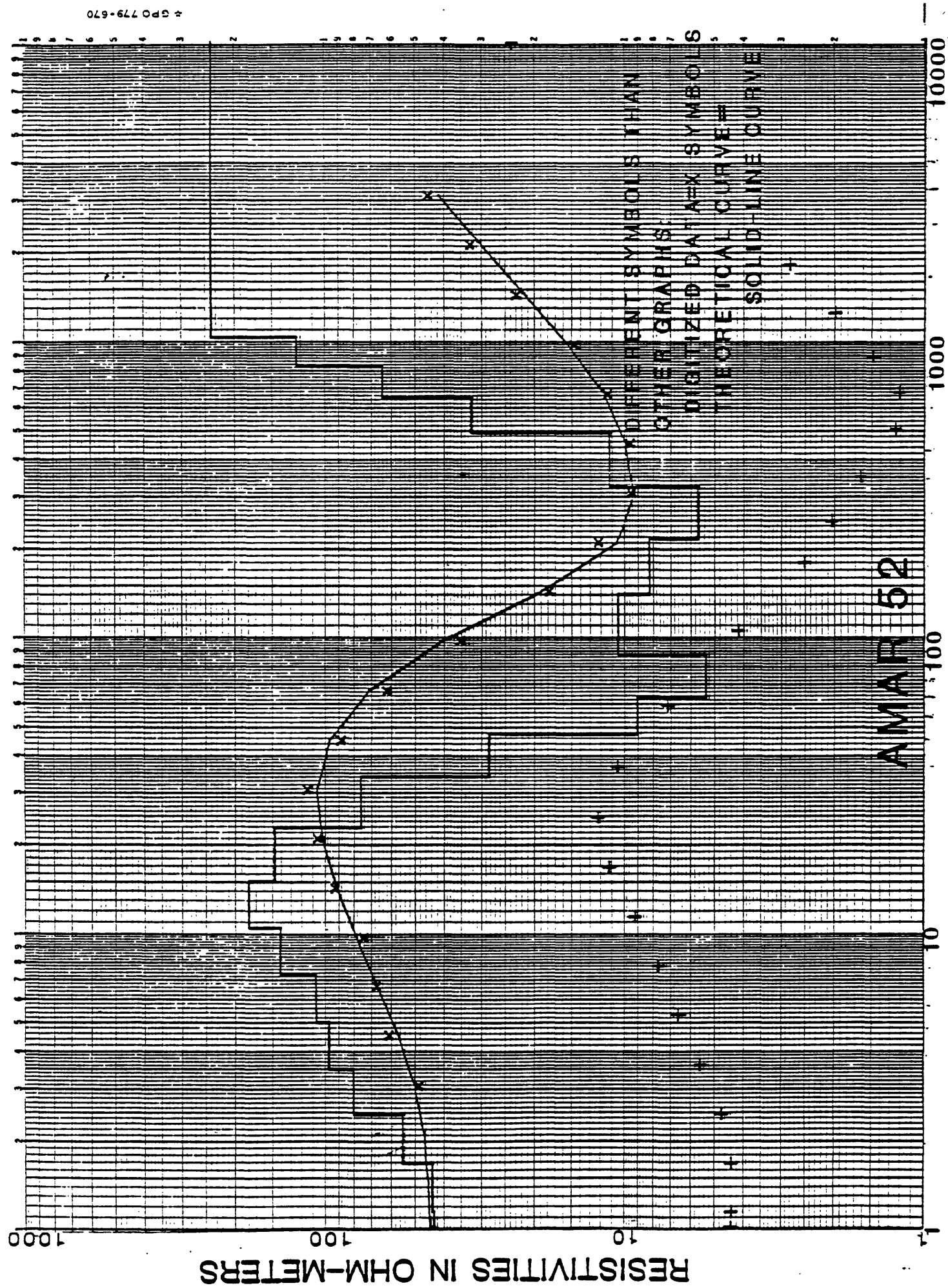
RESISTIVITIES IN OHM-METERS





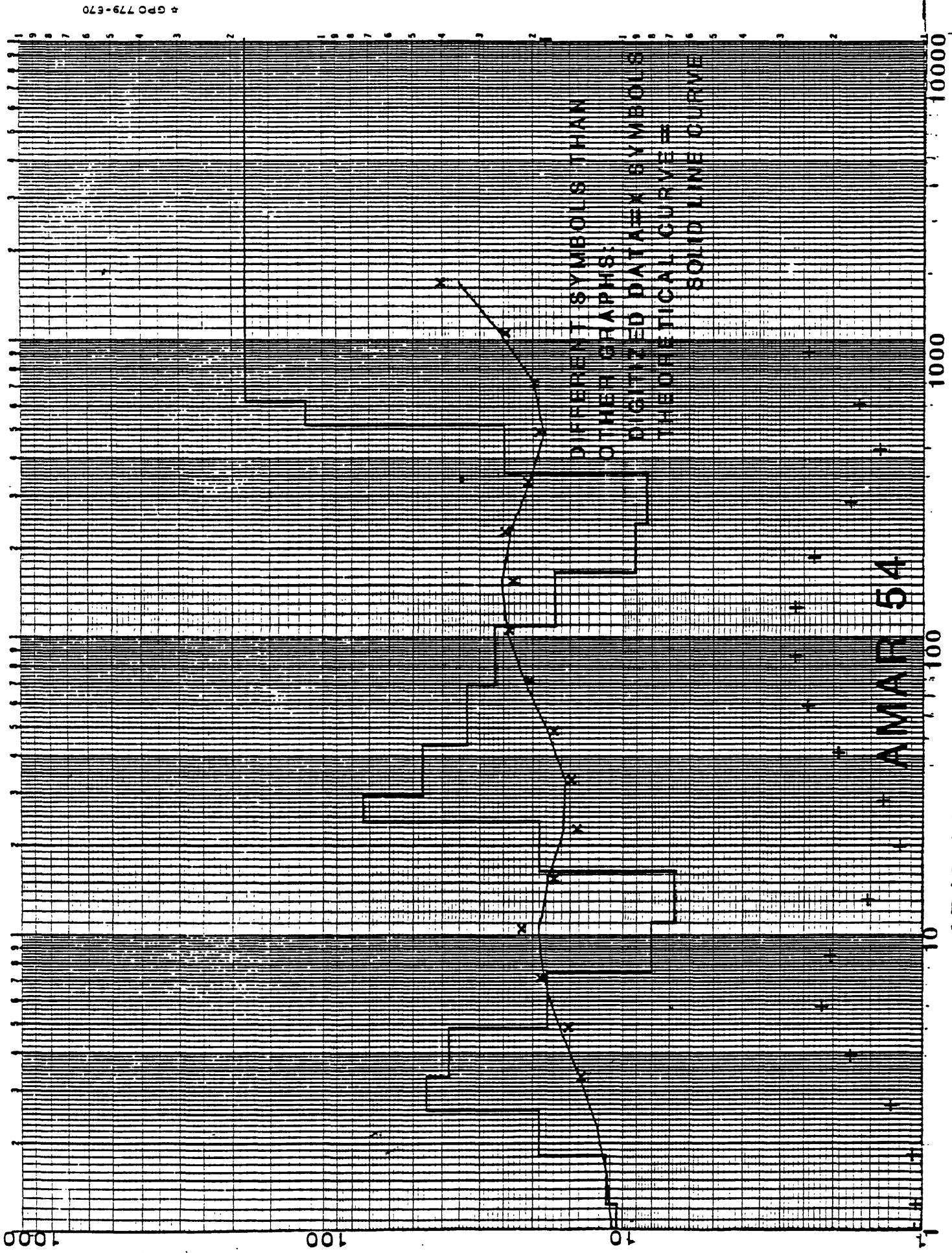
4 GPO 779-670





AB/2, DEPTH, DZ-DEPTH IN METERS

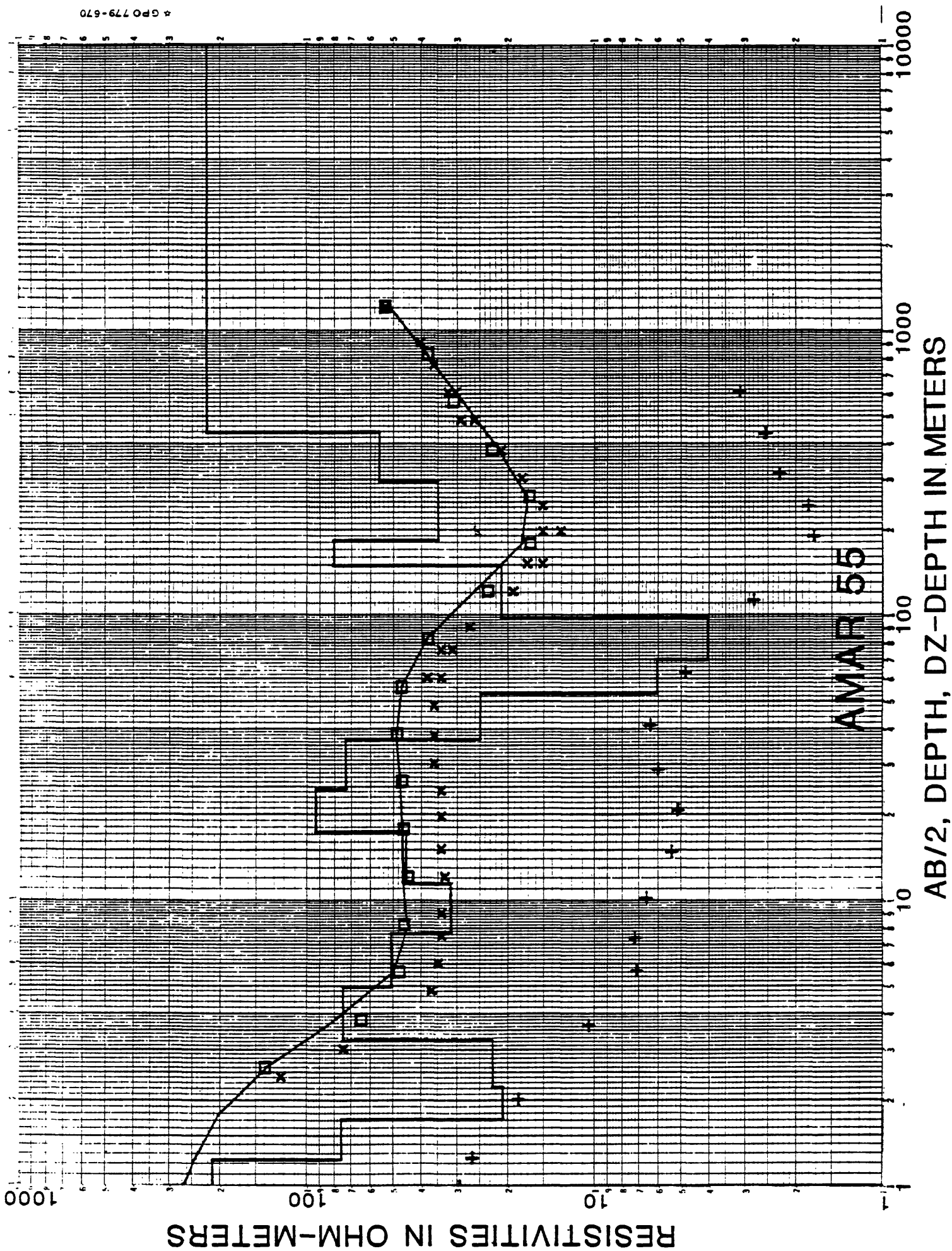
RESISTIVITIES IN OHM-METERS

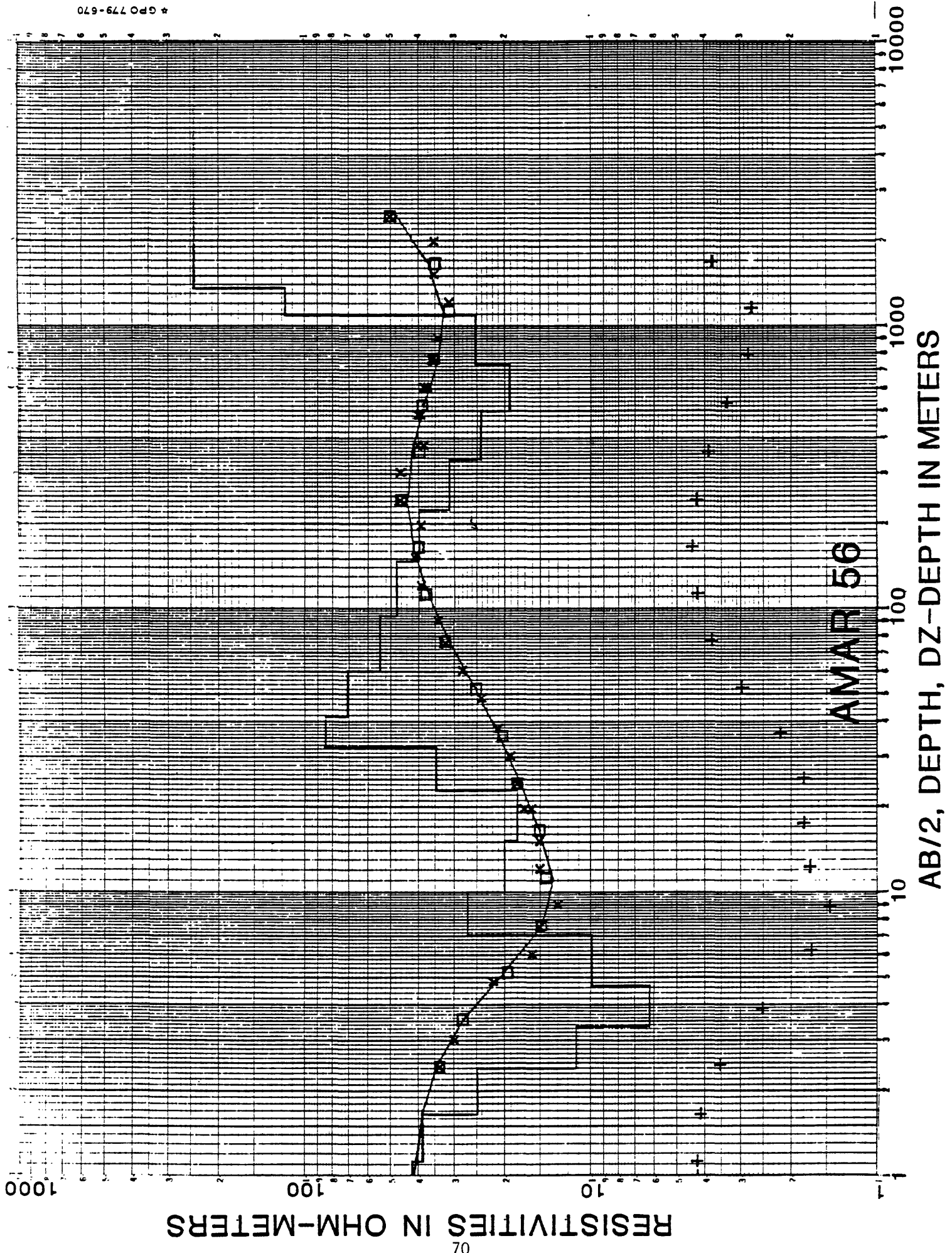


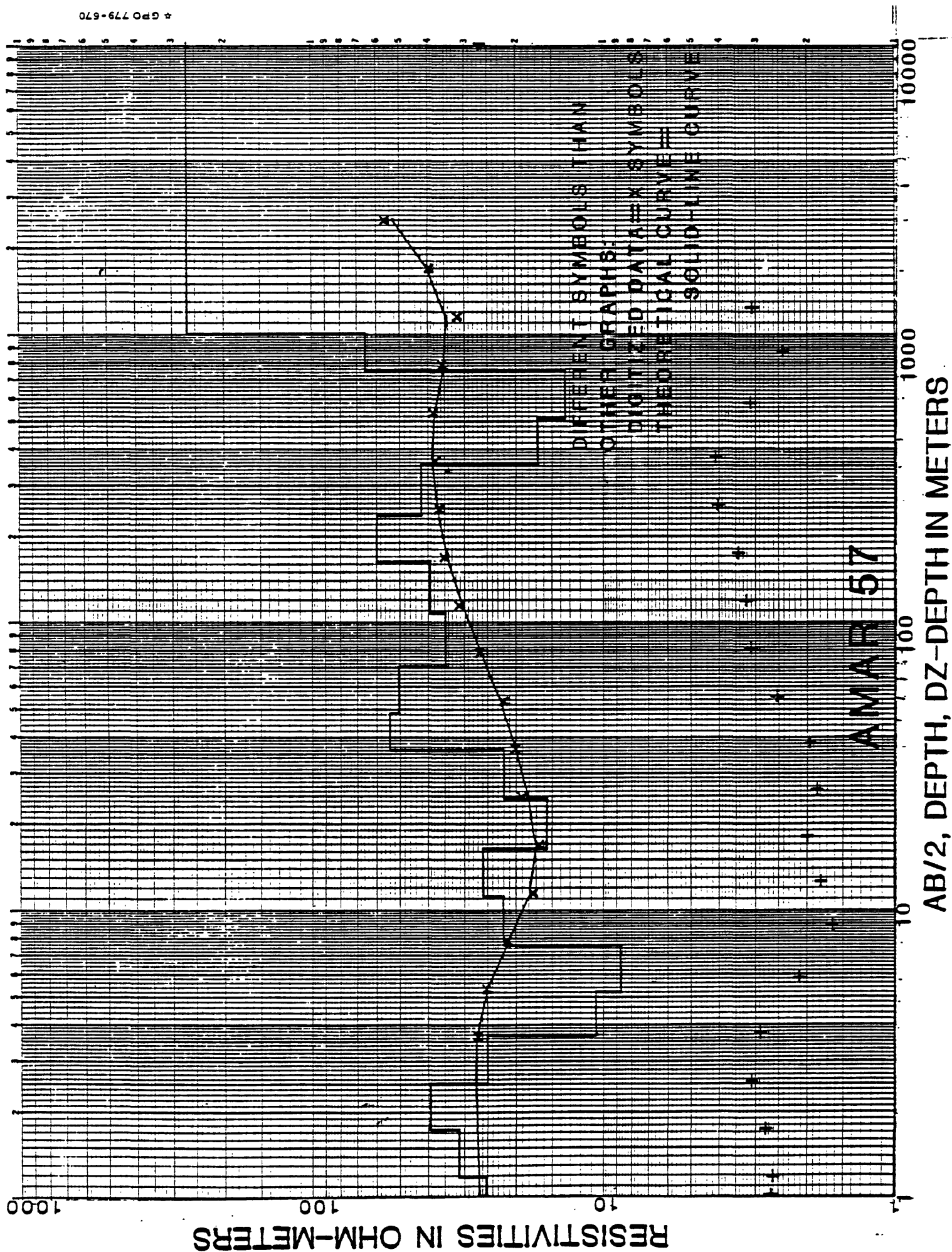
DIFFERENT SYMBOLS THAN
OTHER GRAPHS:
DIGITIZED DATA = X SYMBOLS
THEORETICAL CURVE =
SOLID LINE CURVE

AMAR 54

AB/2, DEPTH, DZ-DEPTH IN METERS







RESISTIVITIES IN OHM-METERS

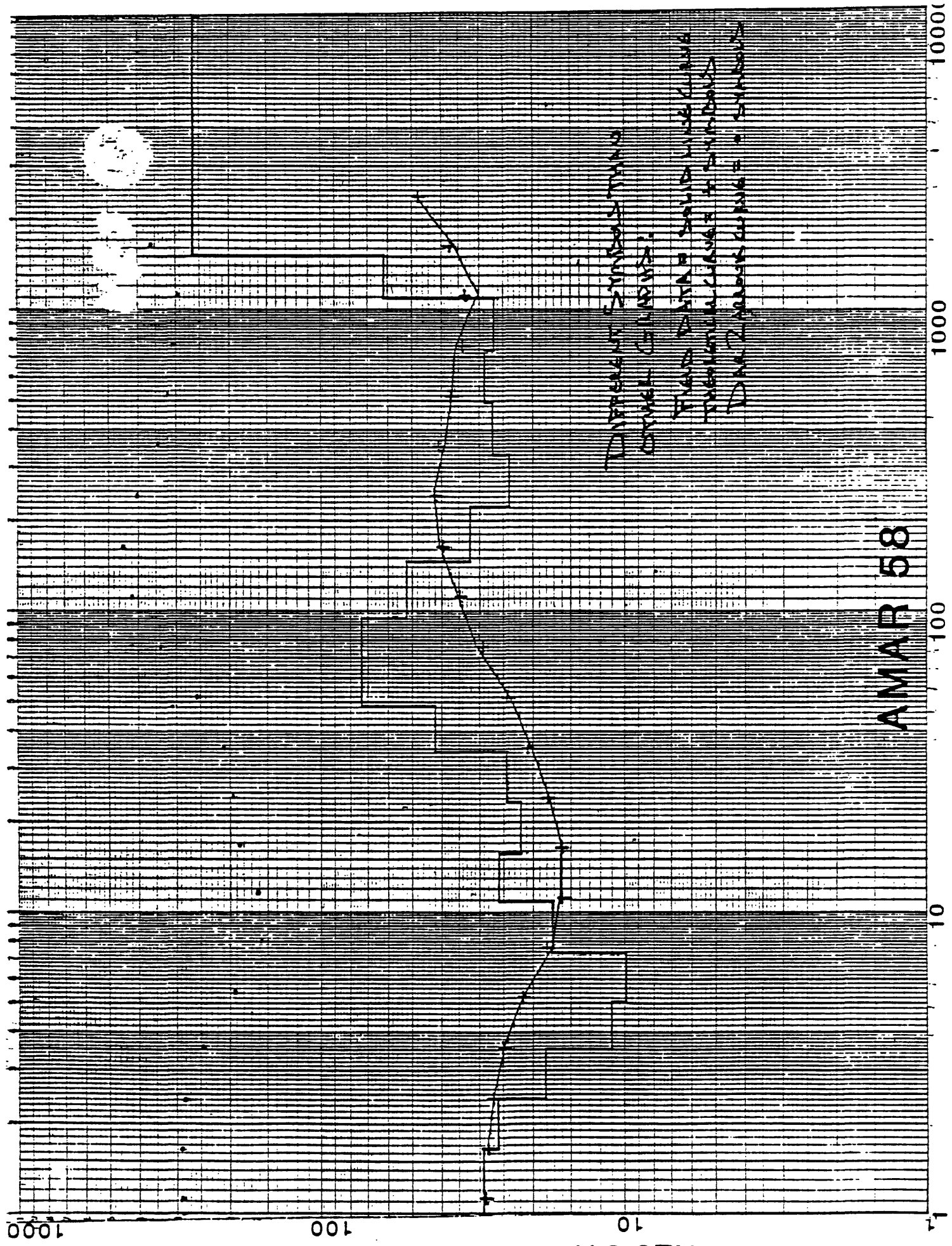
72

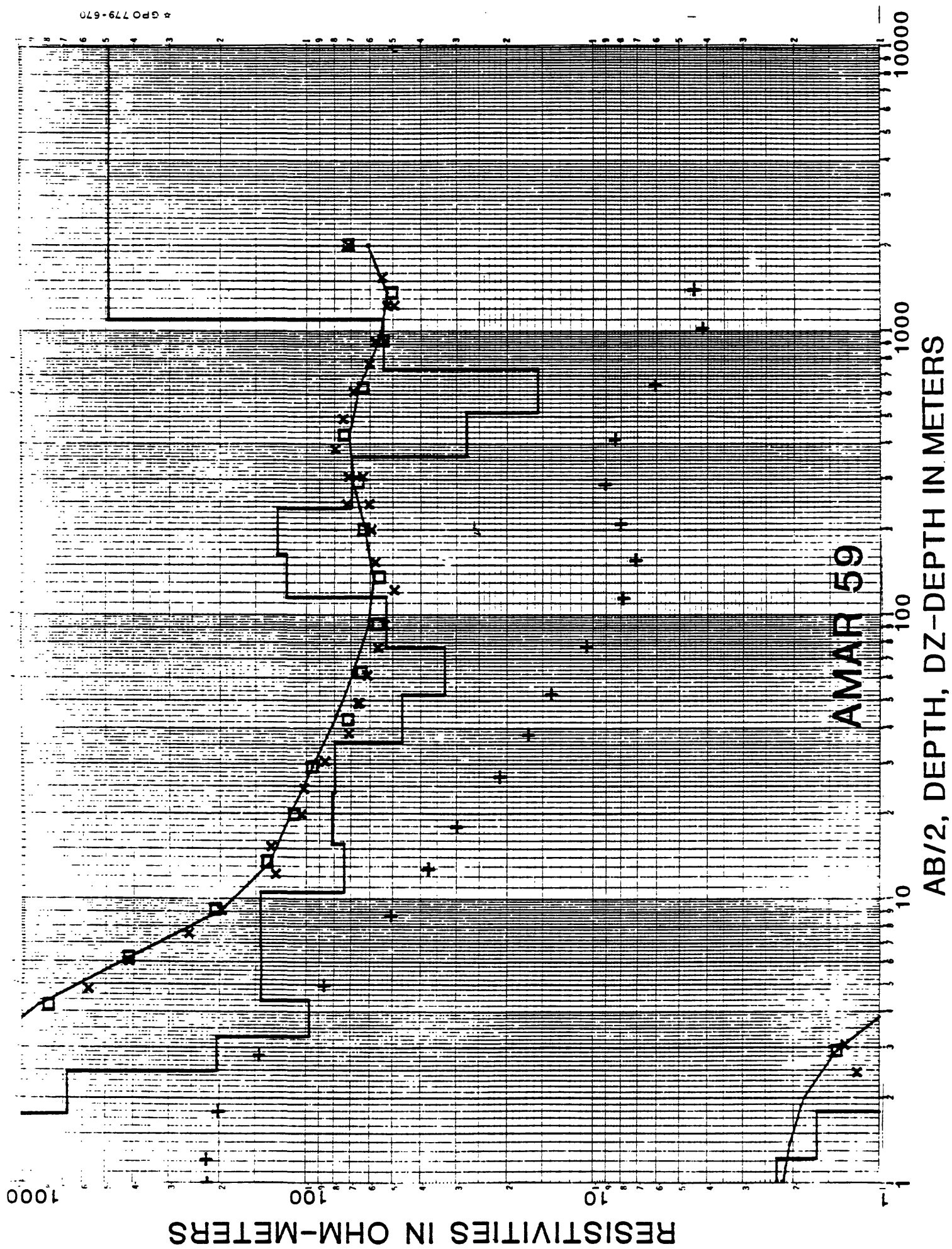
AMAR 58

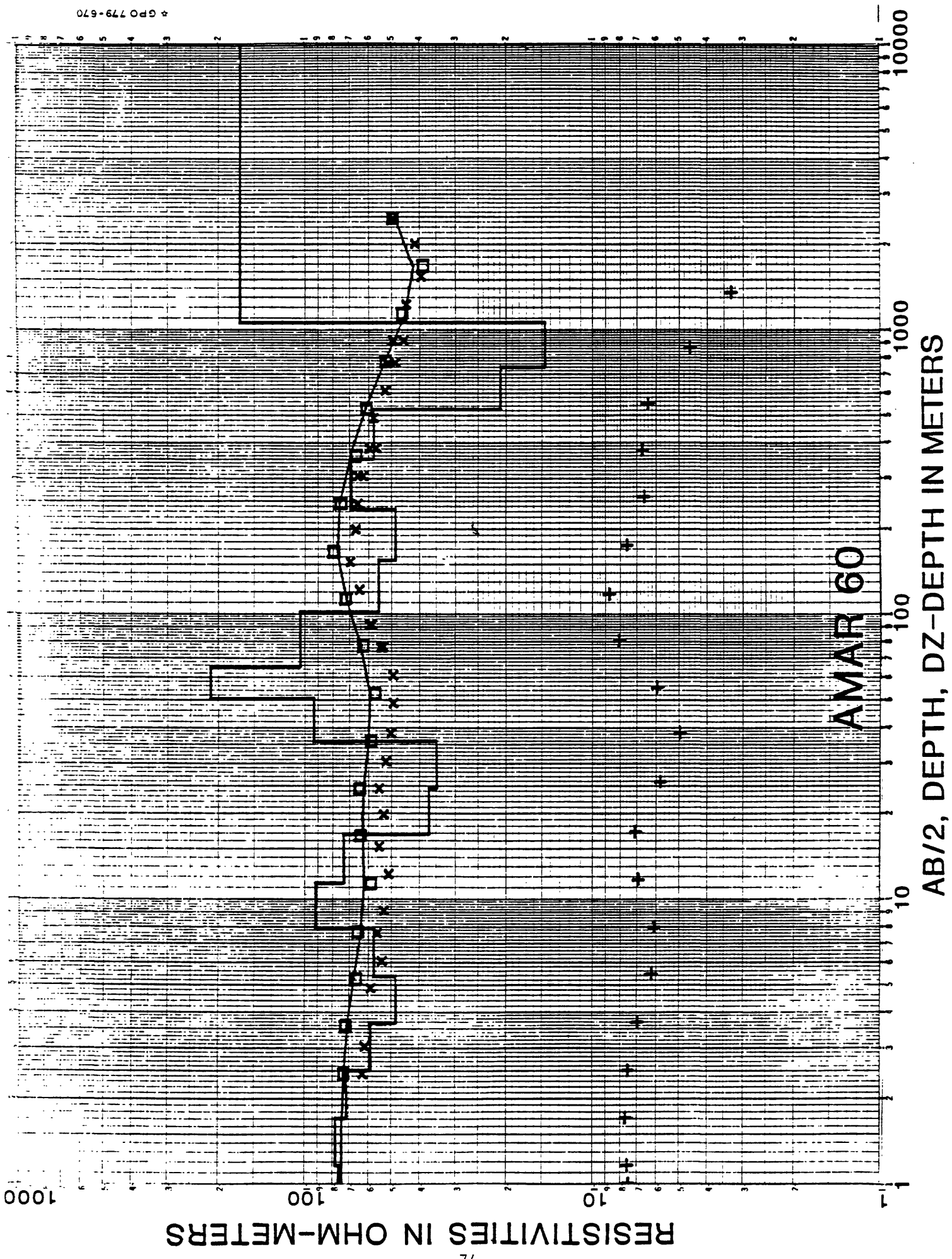
AR/2 DEPTH DZ-DEPTH IN METERS

DIFFERENT SYMBOLS THAN
OTHER CURVES!

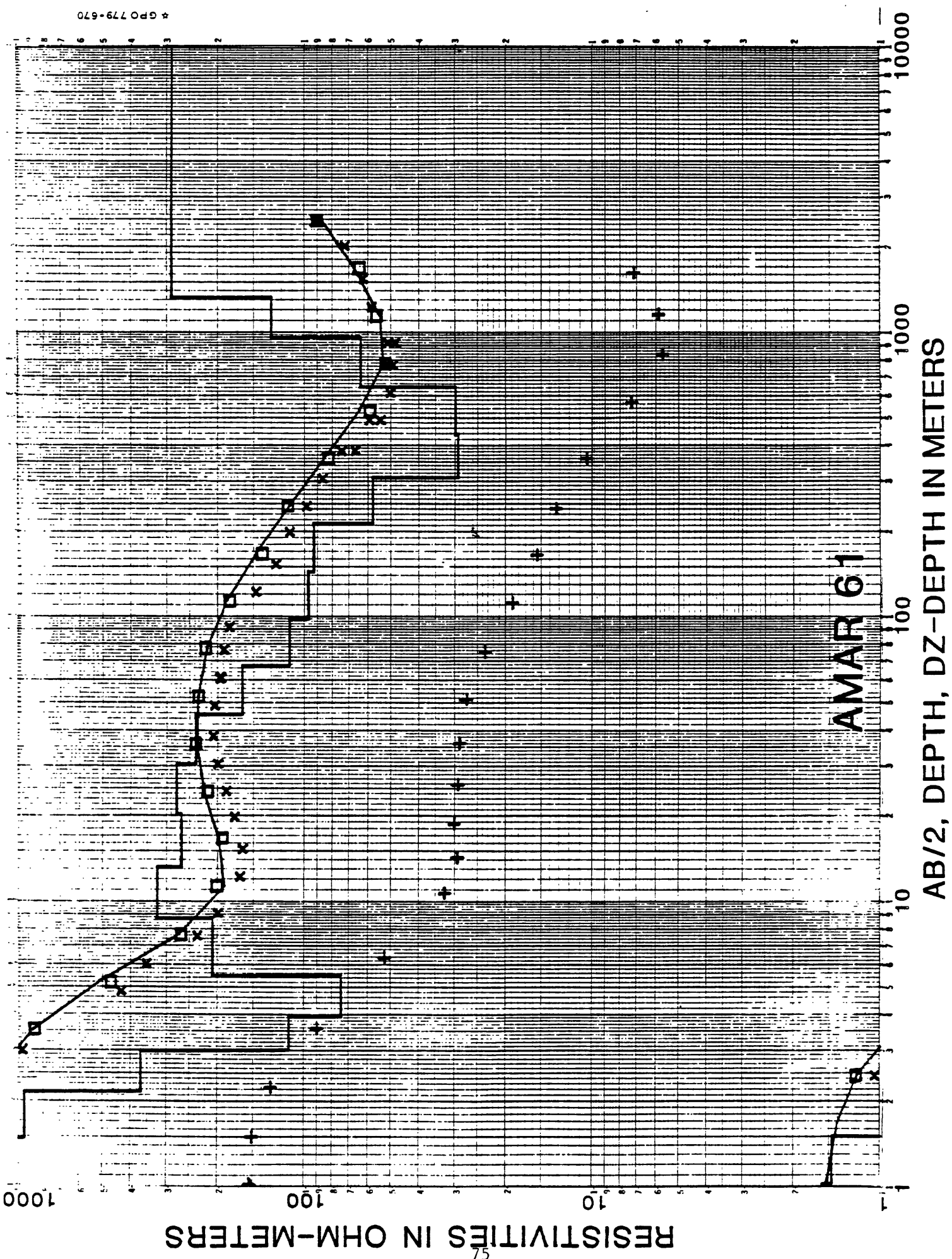
FIELD DATA = SOLID LINE CURVE
THEORETICAL CURVES = SYMBOLS
DATA 2 APPROXIMATELY = SYMBOLS



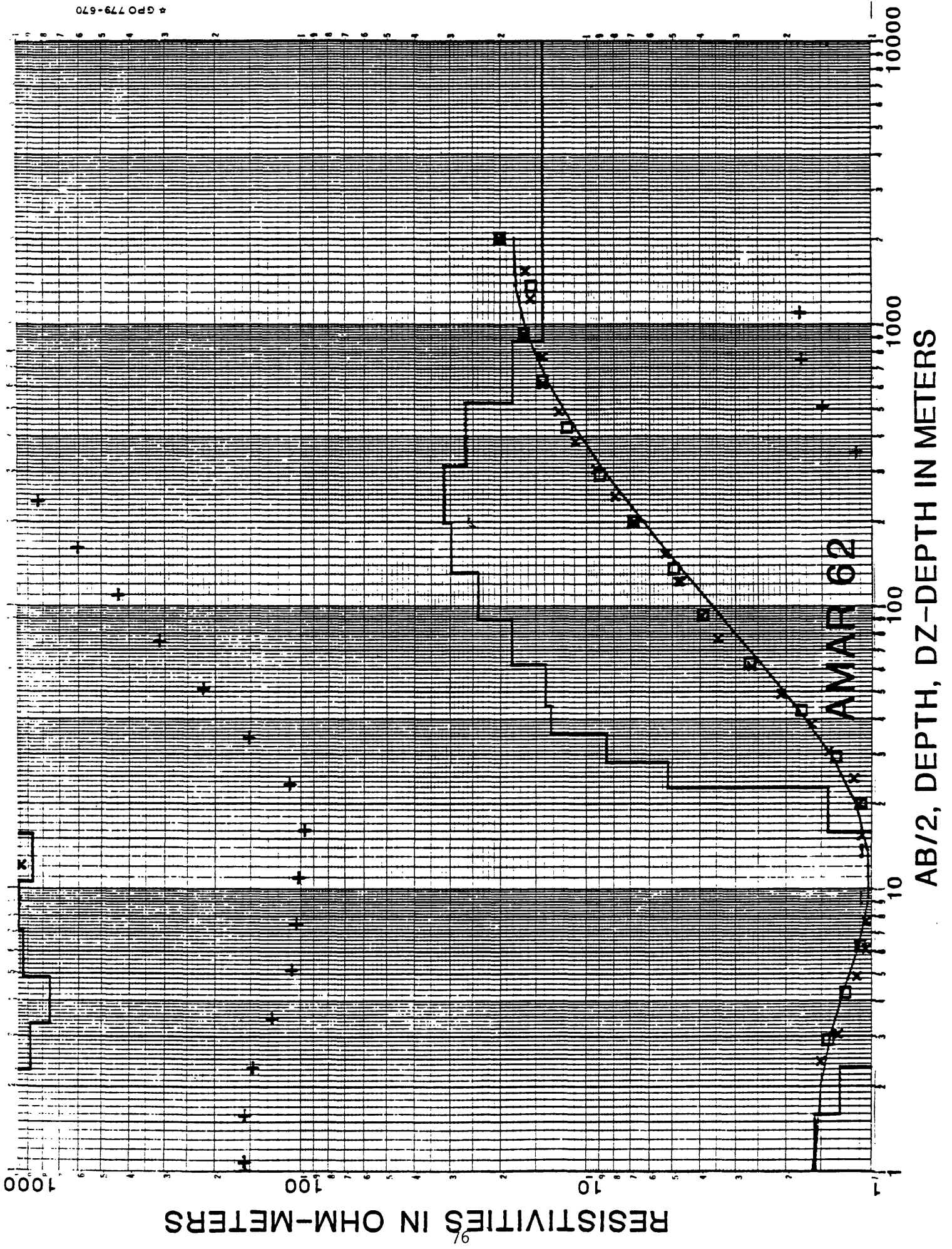




* GPO 779-670



* GPO 779-670

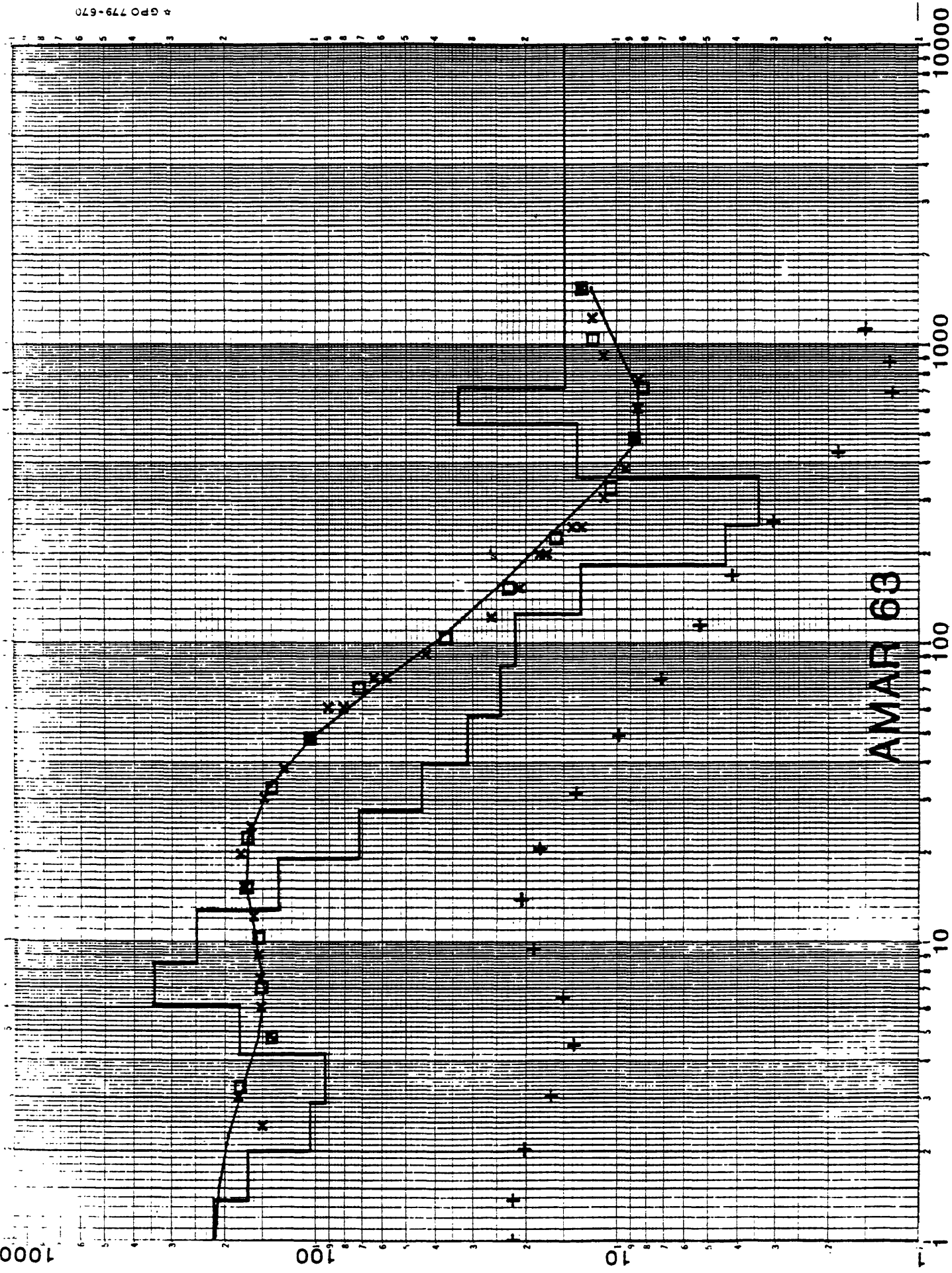


RESISTIVITIES IN OHM-METERS

77

AMAR 63

AB/2, DEPTH, DZ-DEPTH IN METERS

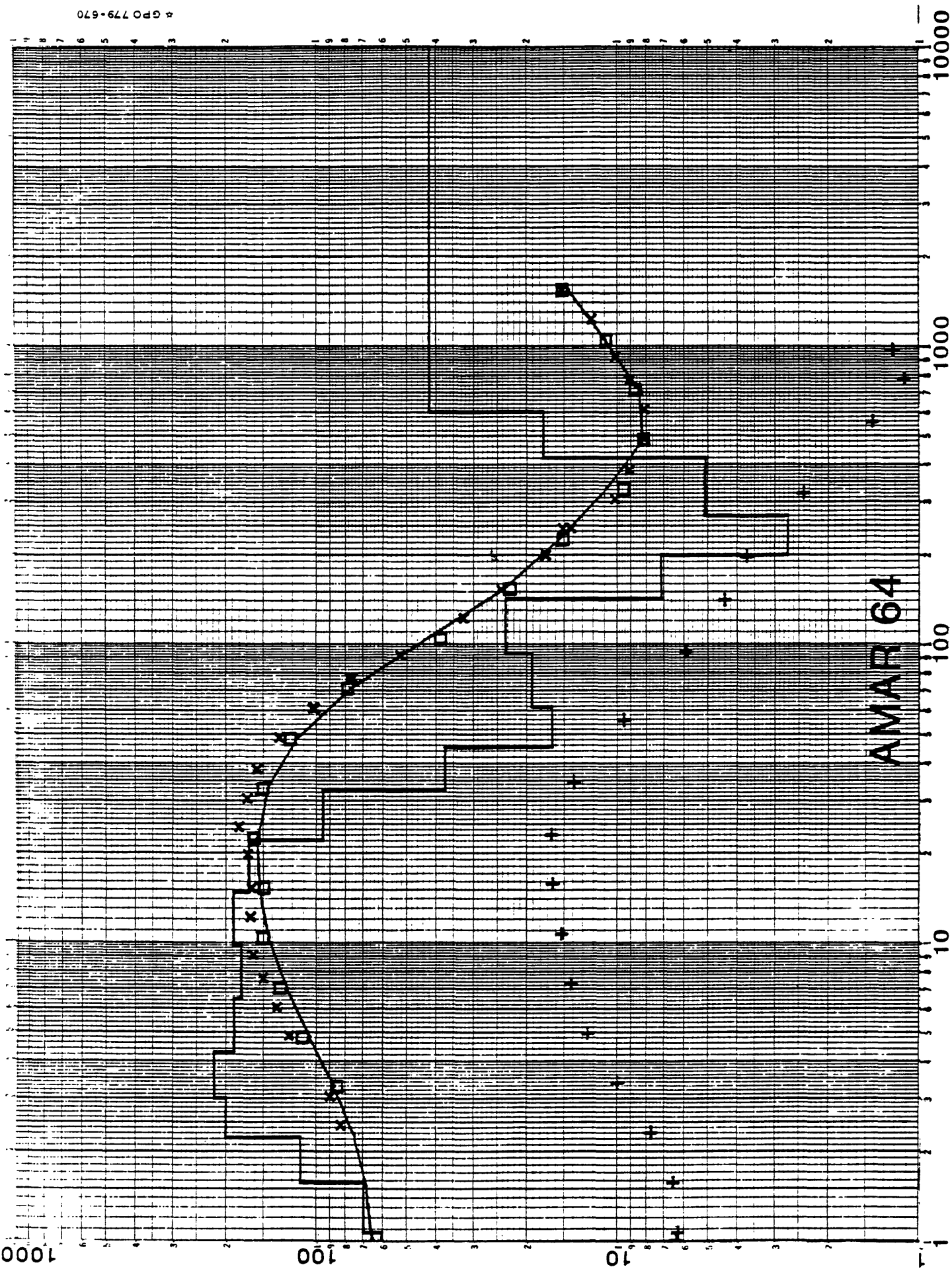


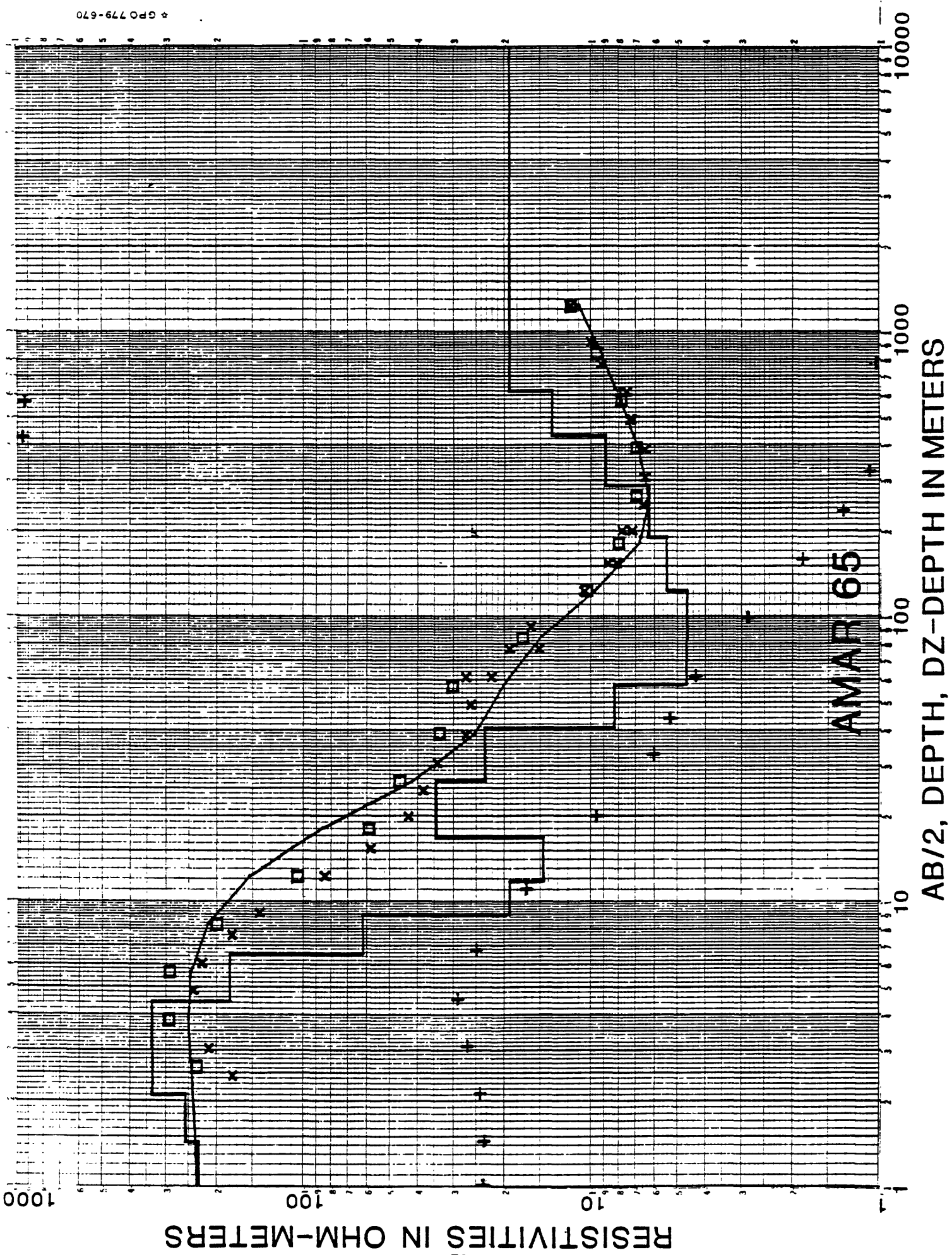
RESISTIVITIES IN OHM-METERS

8

AMAR 64

AB/2, DEPTH, DZ-DEPTH IN METERS

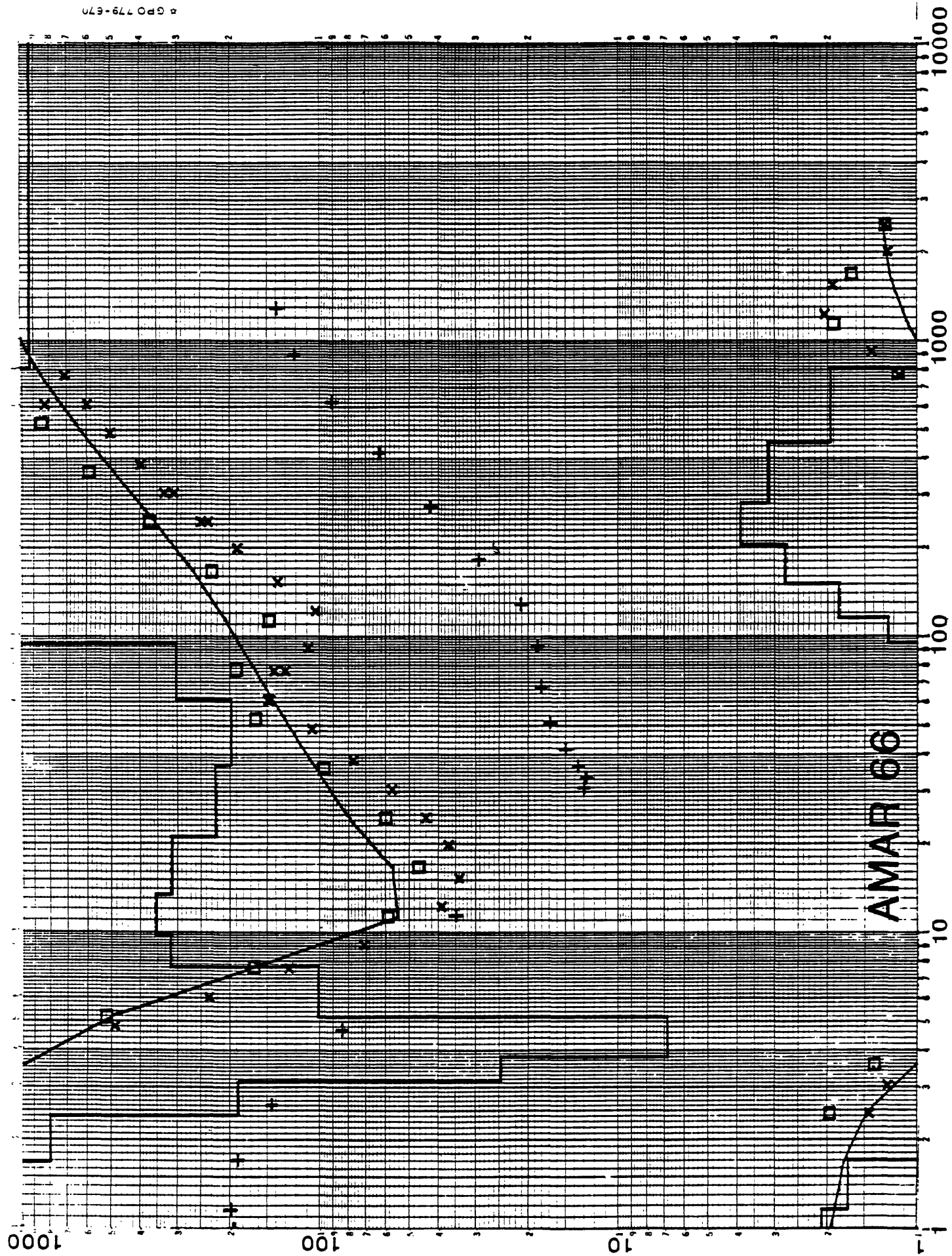




RESISTIVITIES IN OHM-METERS

AMAR 66

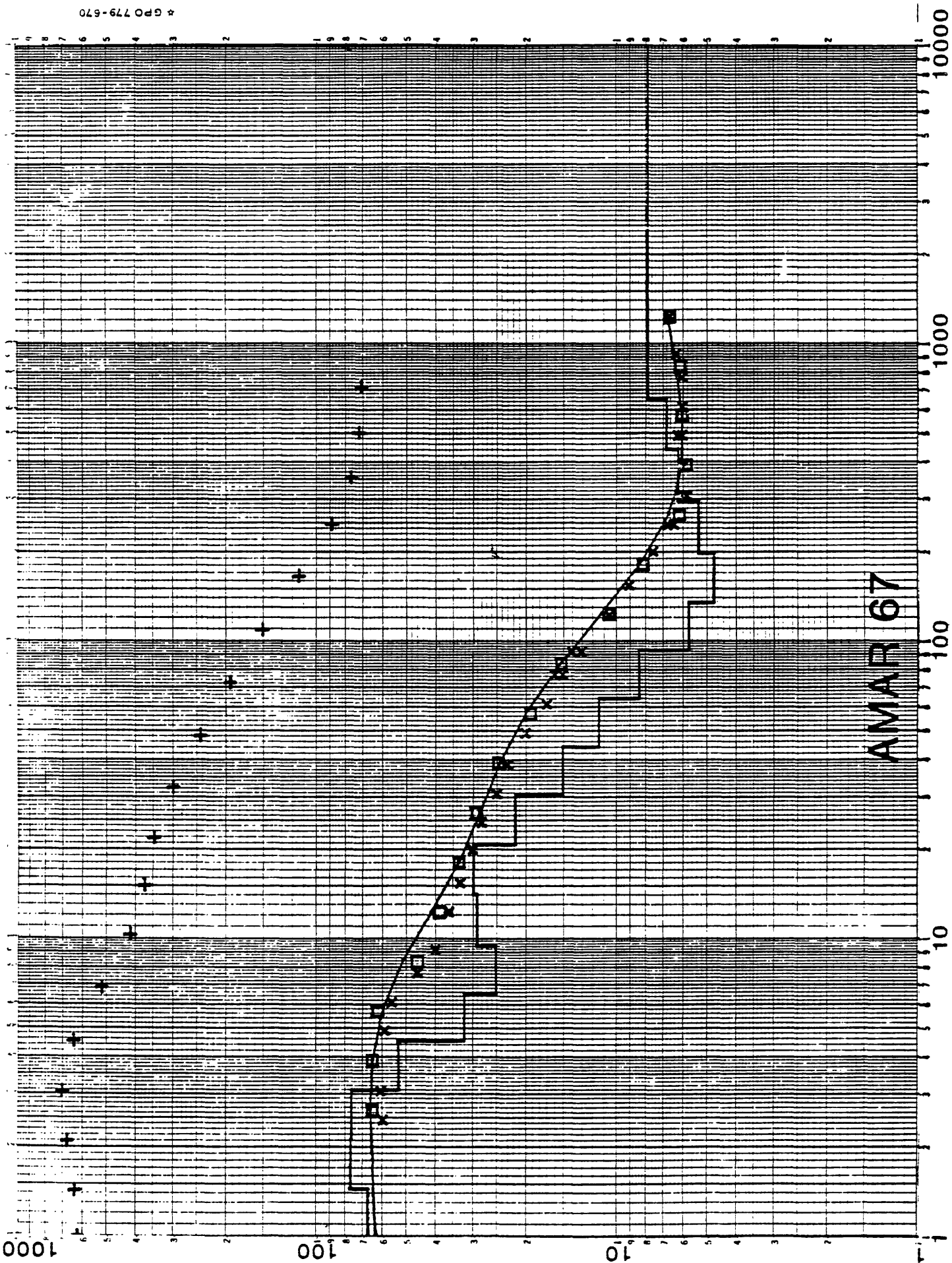
AB/2, DEPTH, DZ-DEPTH IN METERS



AMAR 67

AB/2, DEPTH, DZ-DEPTH IN METERS

RESISTIVITIES IN OHM-METERS



RESISTIVITIES IN OHM-METERS

AB/2, DEPTH, DZ-DEPTH IN METERS

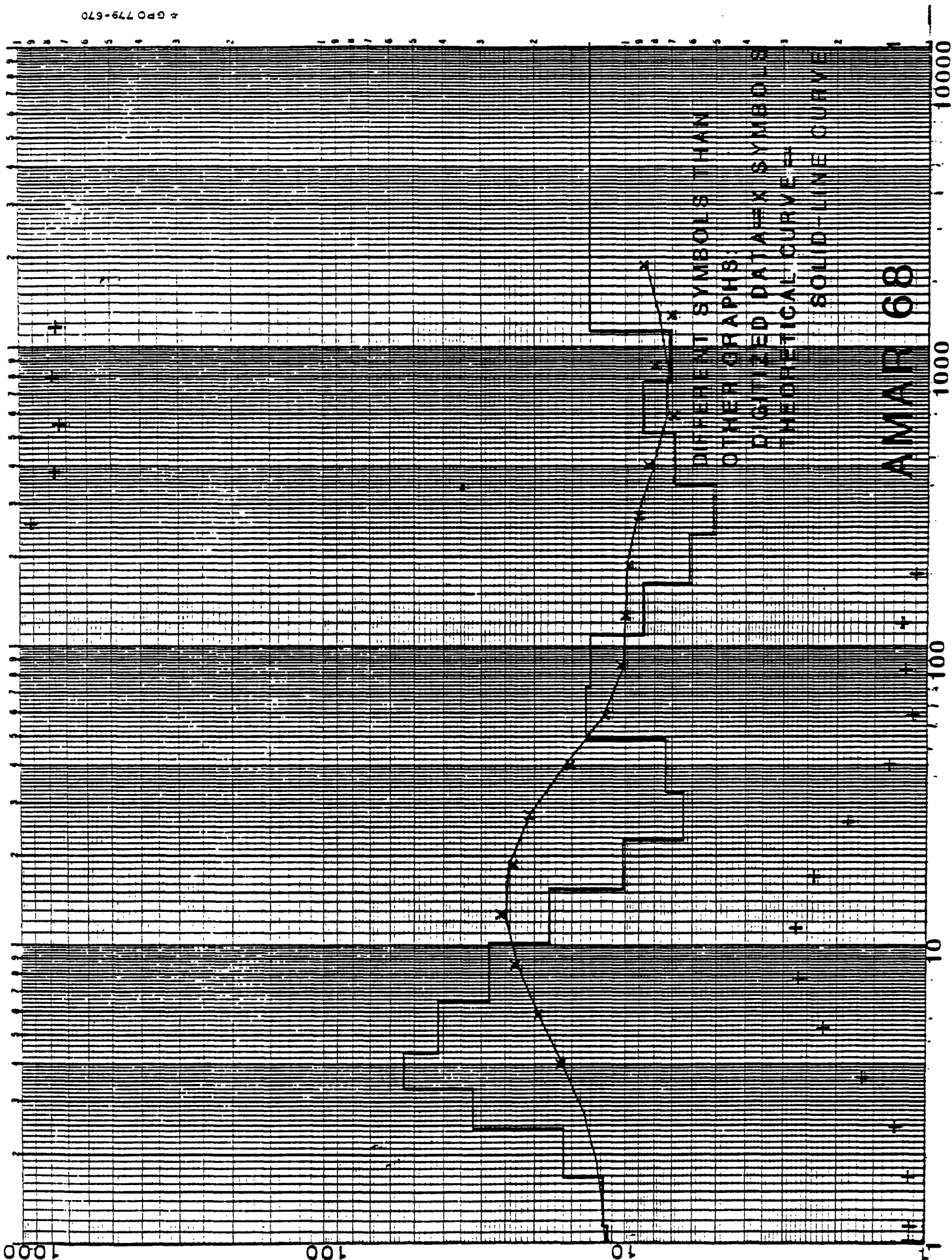
AMAR 68

DIFFERENT SYMBOLS THAN
OTHER GRAPHS:

DIGITIZED DATA = X SYMBOLS

THEORETICAL CURVE =

SOLID-LINE CURVE

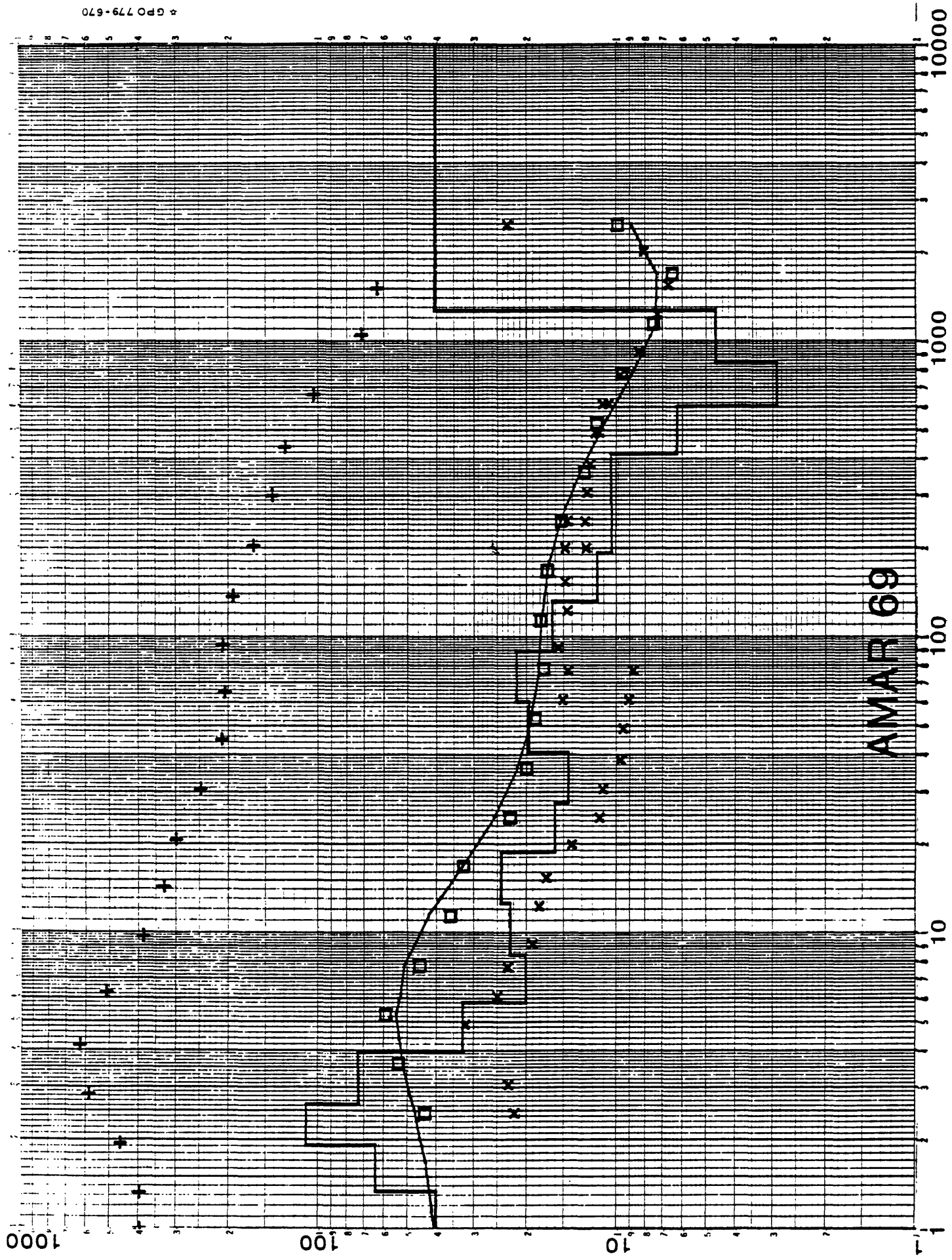


RESISTIVITIES IN OHM-METERS

83

AMAR 69

AB/2, DEPTH, DZ-DEPTH IN METERS

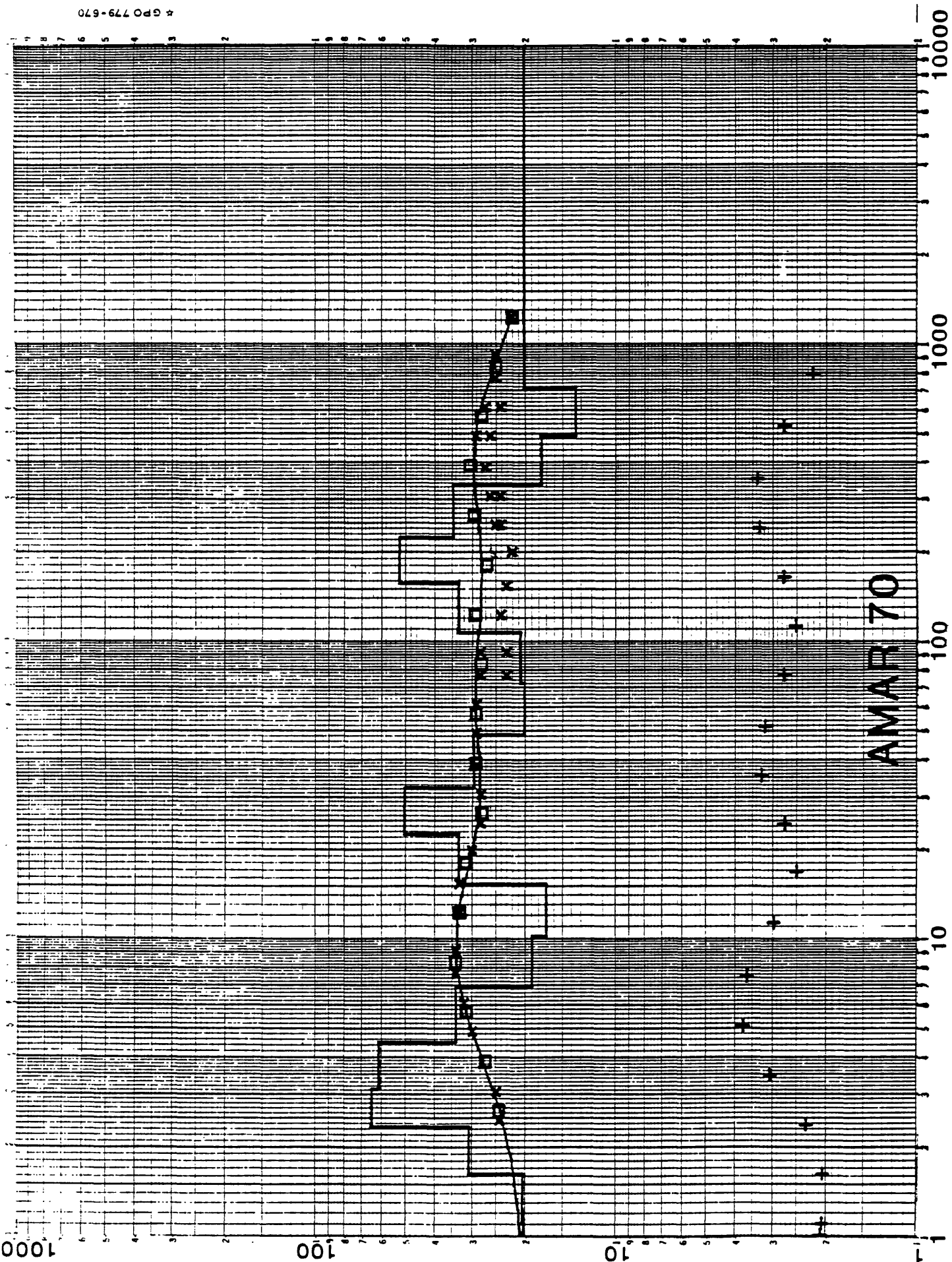


RESISTIVITIES IN OHM-METERS

84

AMAR 70

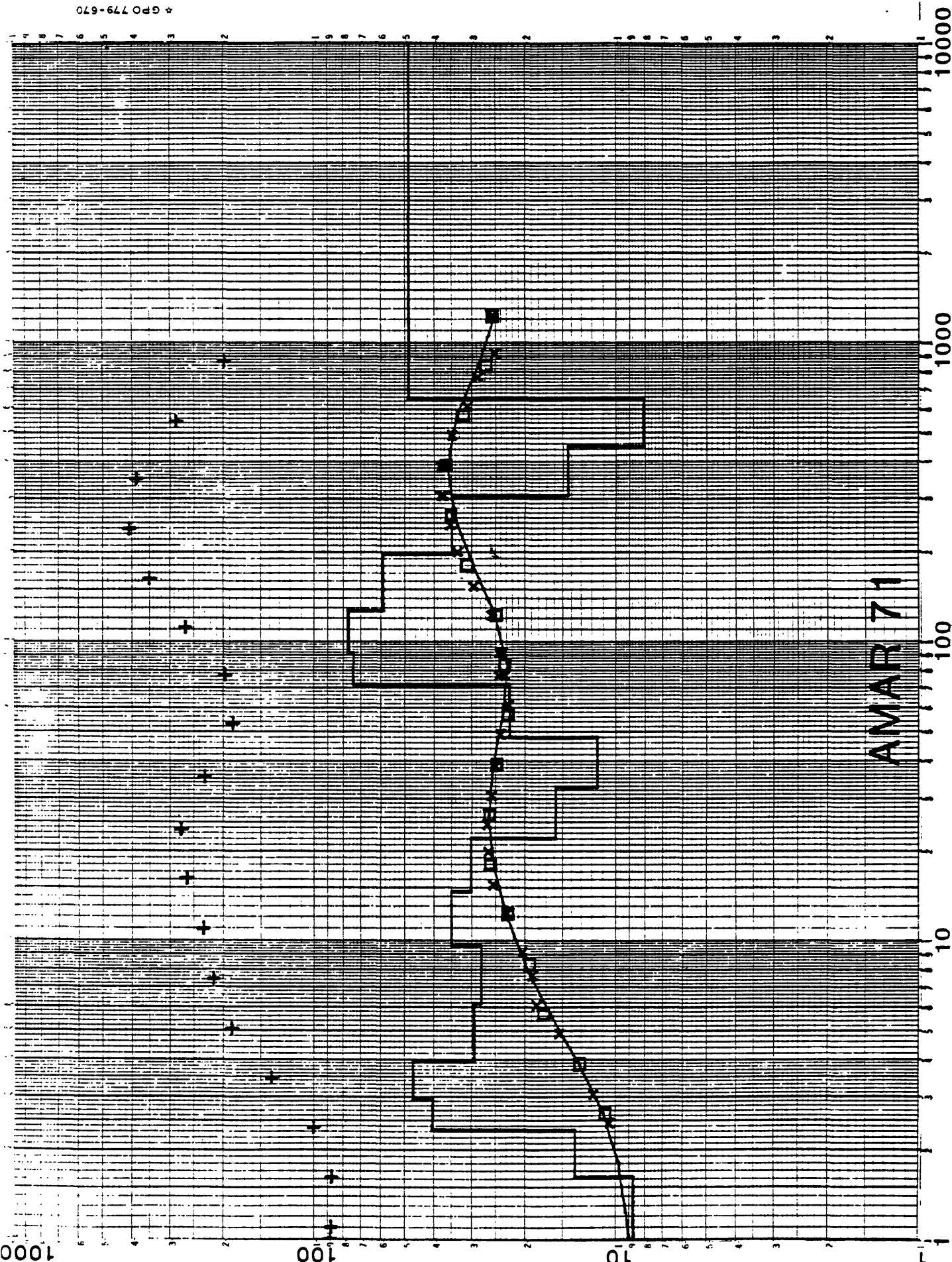
AB/2, DEPTH, DZ-DEPTH IN METERS



AMAR 71

AB/2, DEPTH, DZ-DEPTH IN METERS

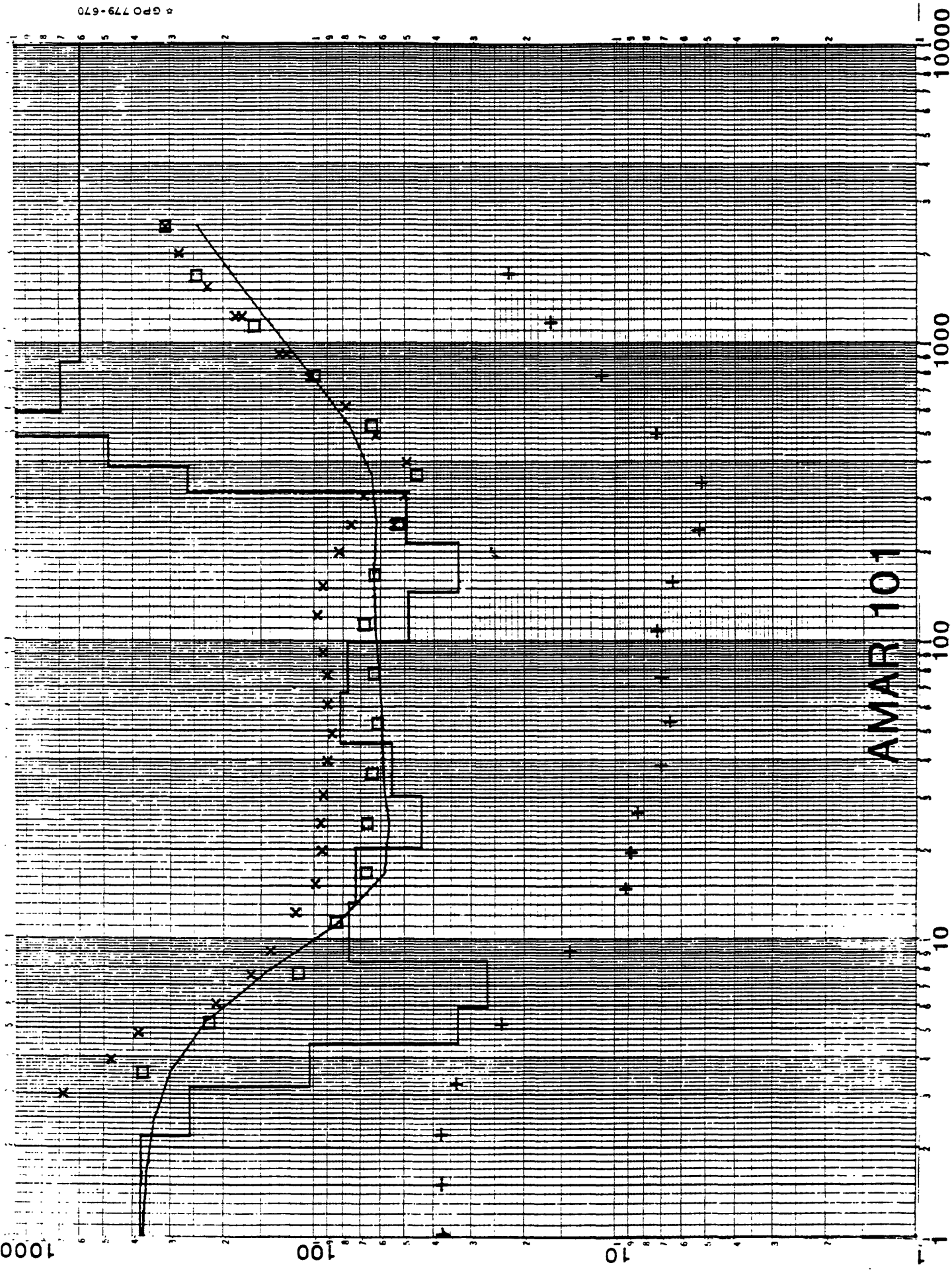
RESISTIVITIES IN OHM-METERS



AMAR 101

AB/2, DEPTH, DZ--DEPTH IN METERS

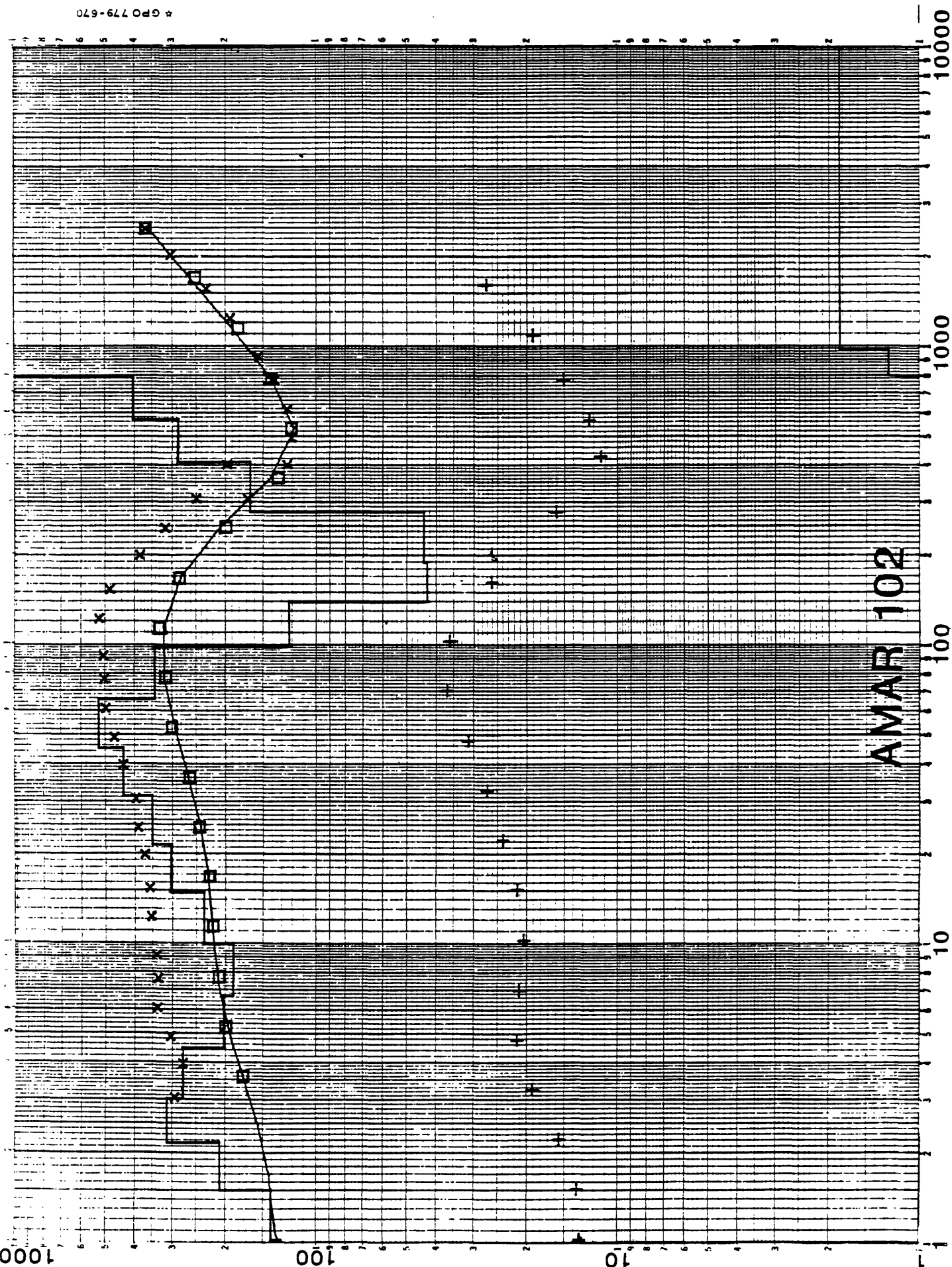
RESISTIVITIES IN OHM-METERS

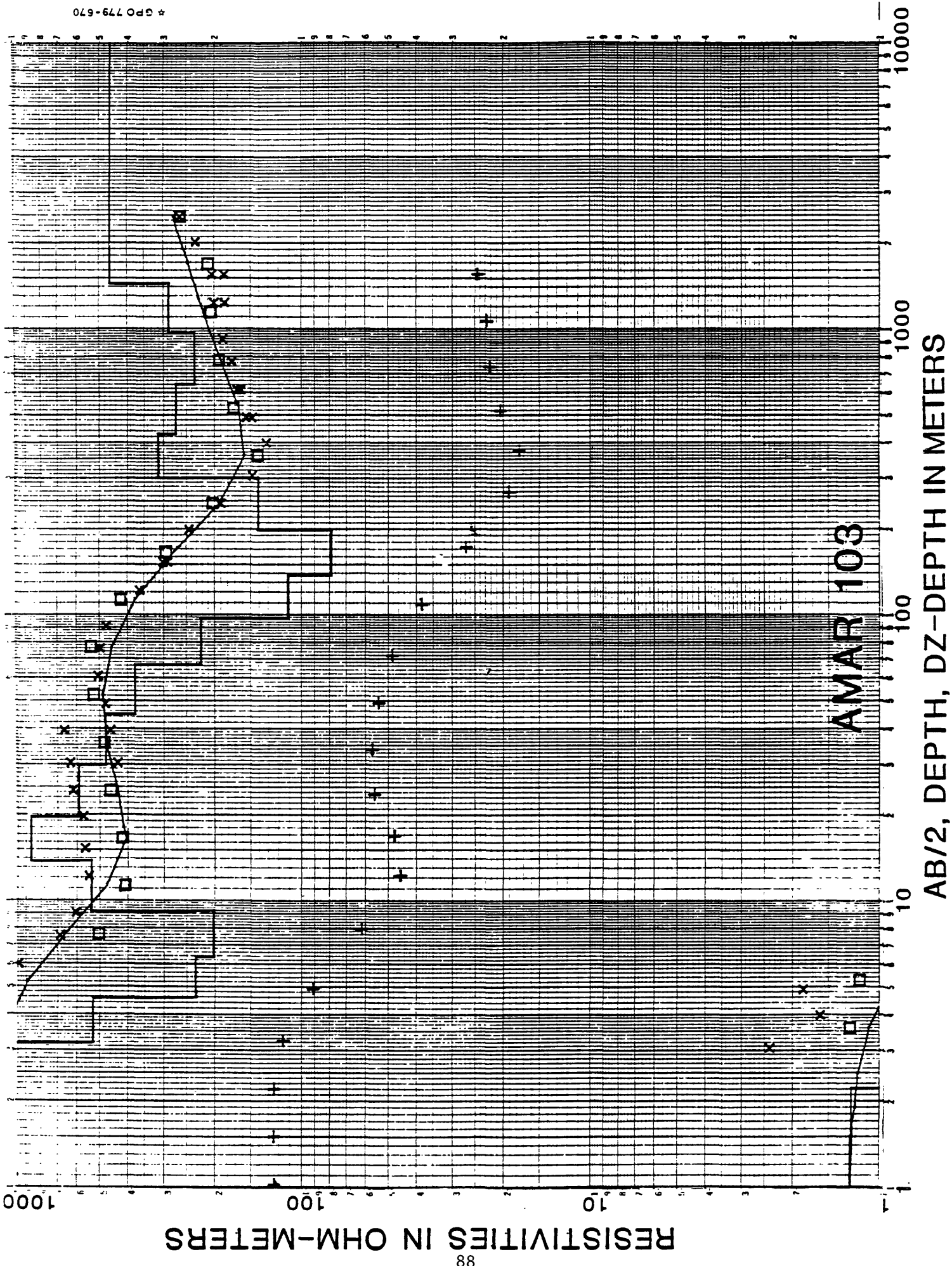


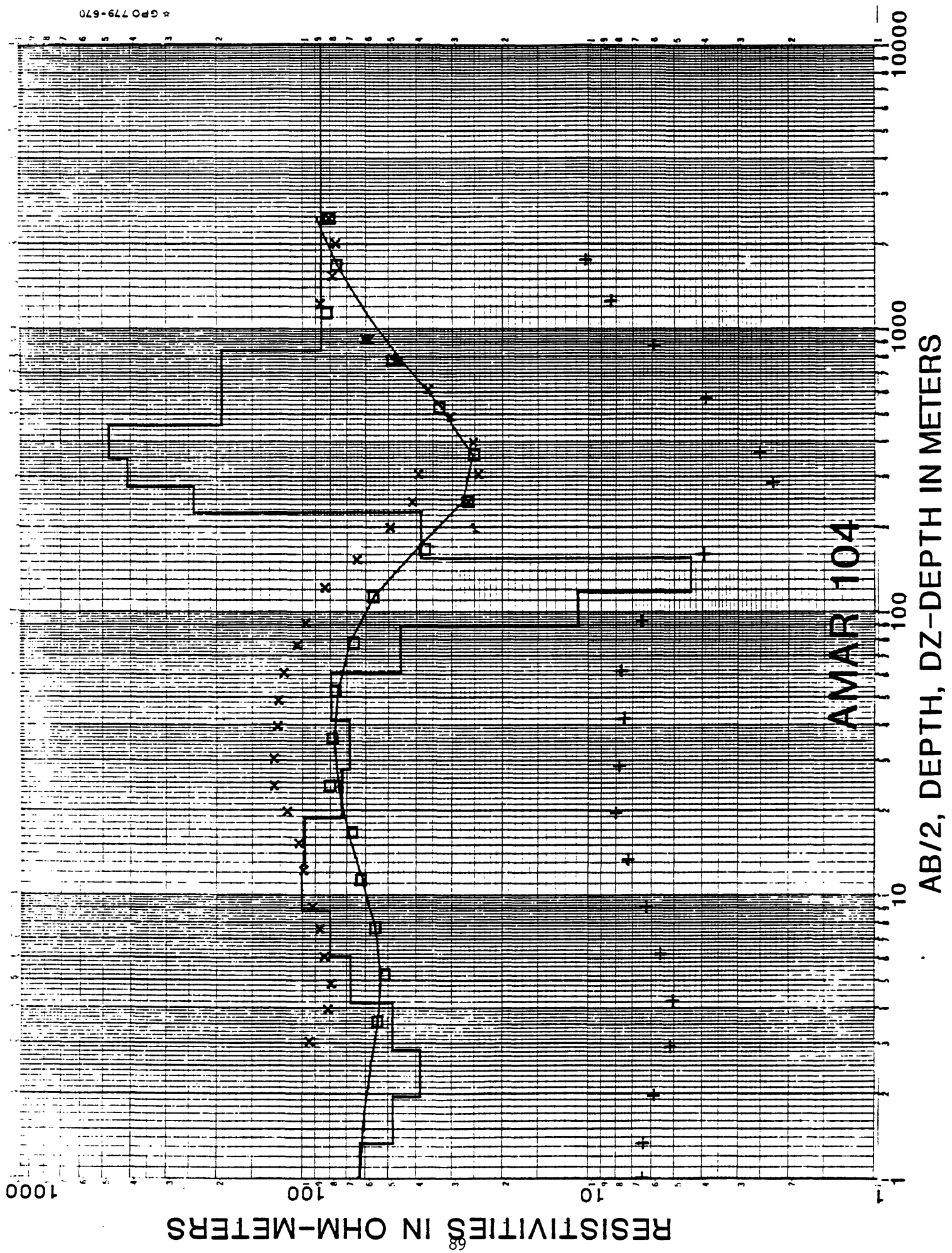
AMAR 102

AB/2, DEPTH, DZ-DEPTH IN METERS

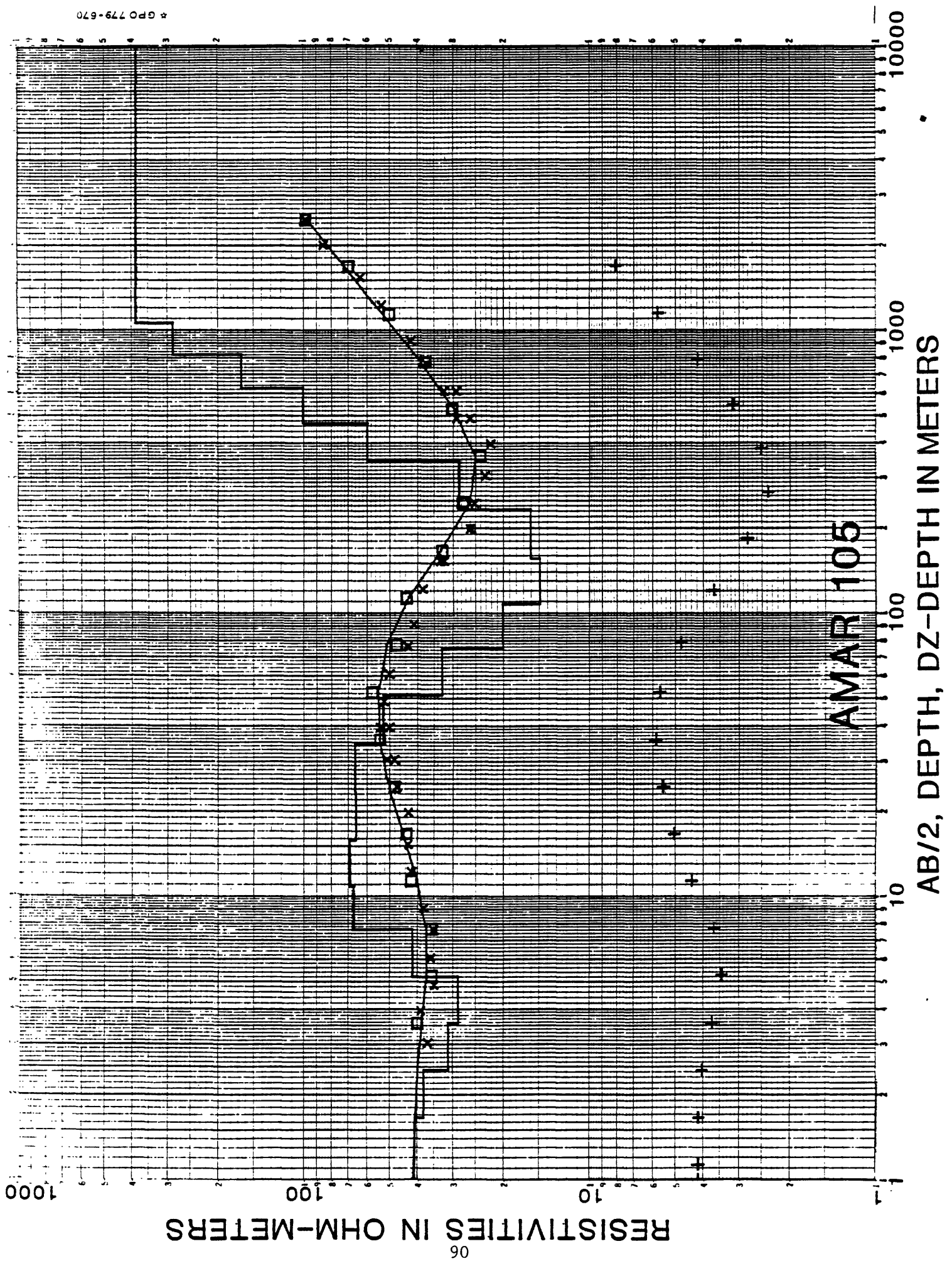
RESISTIVITIES IN OHM-METERS

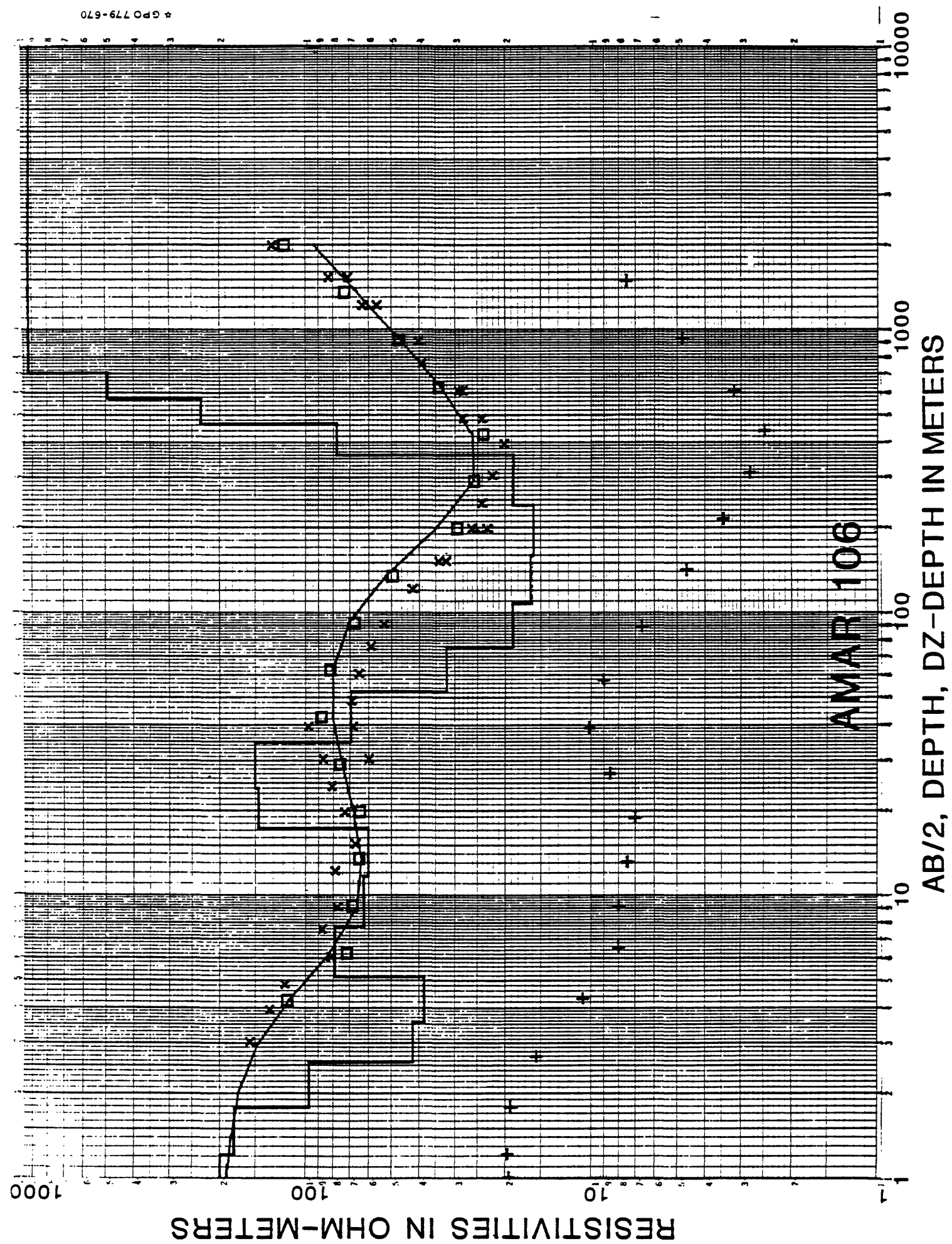






AMAR 104



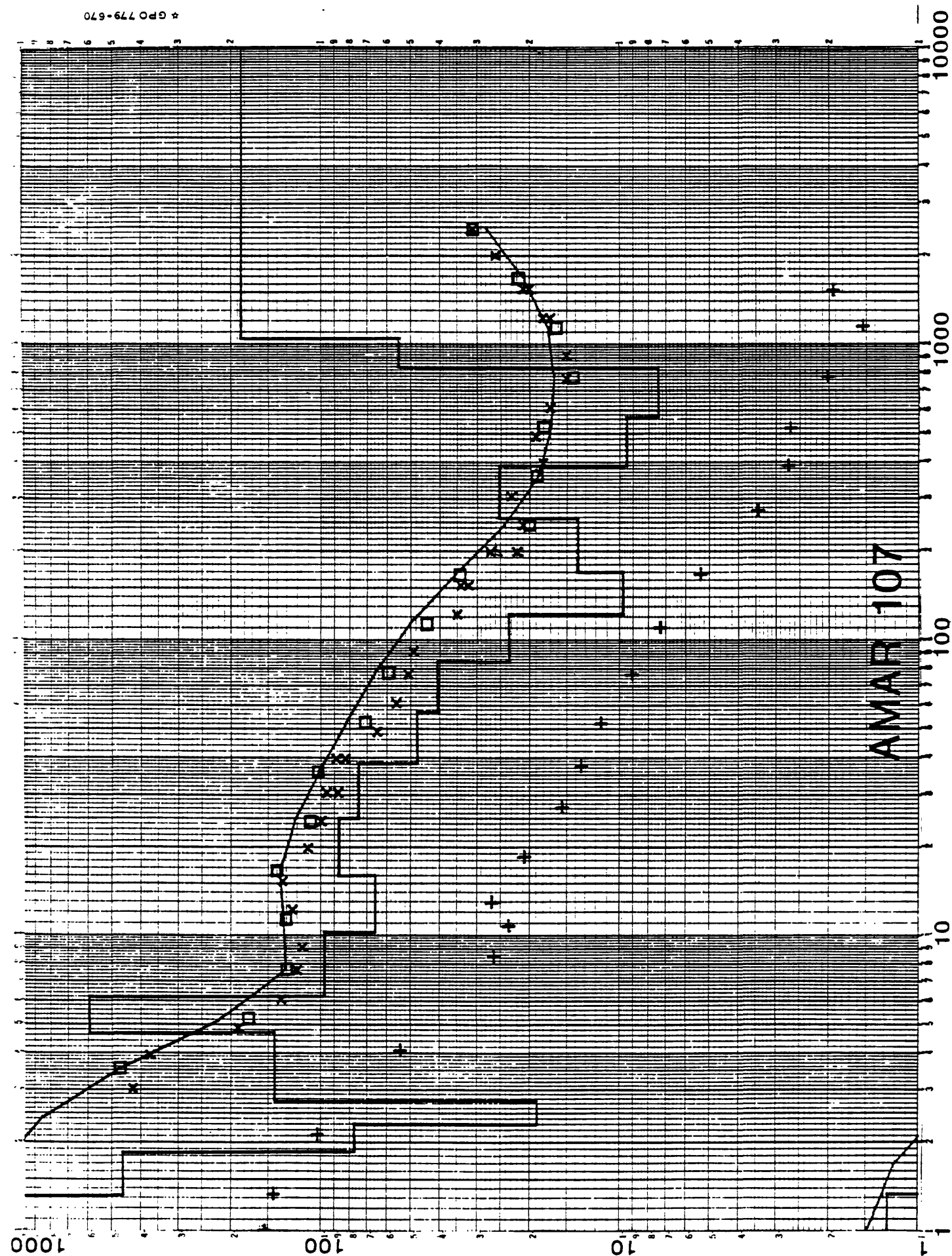


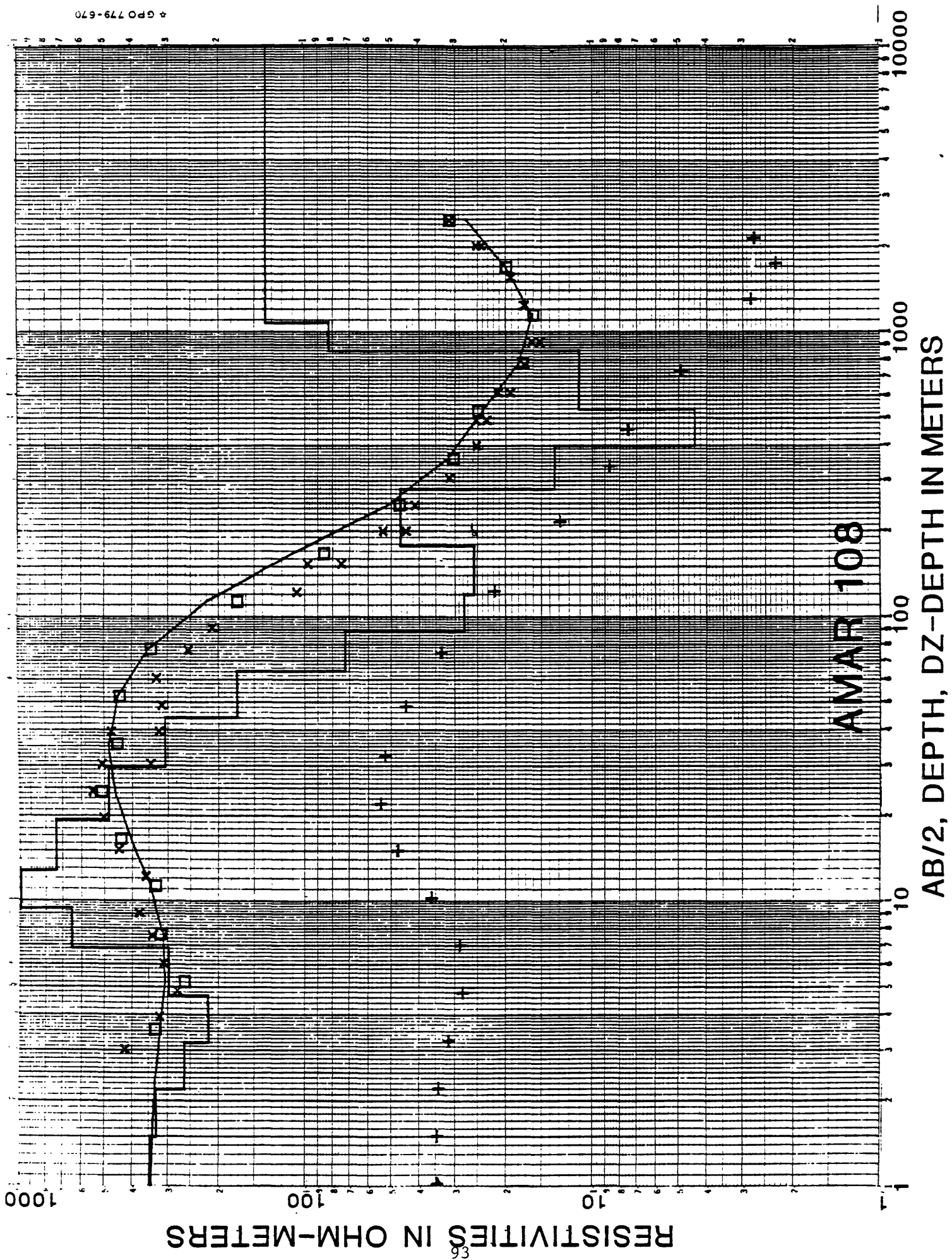
RESISTIVITIES IN OHM-METERS

92

AMAR 107

AB/2, DEPTH, DZ-DEPTH IN METERS

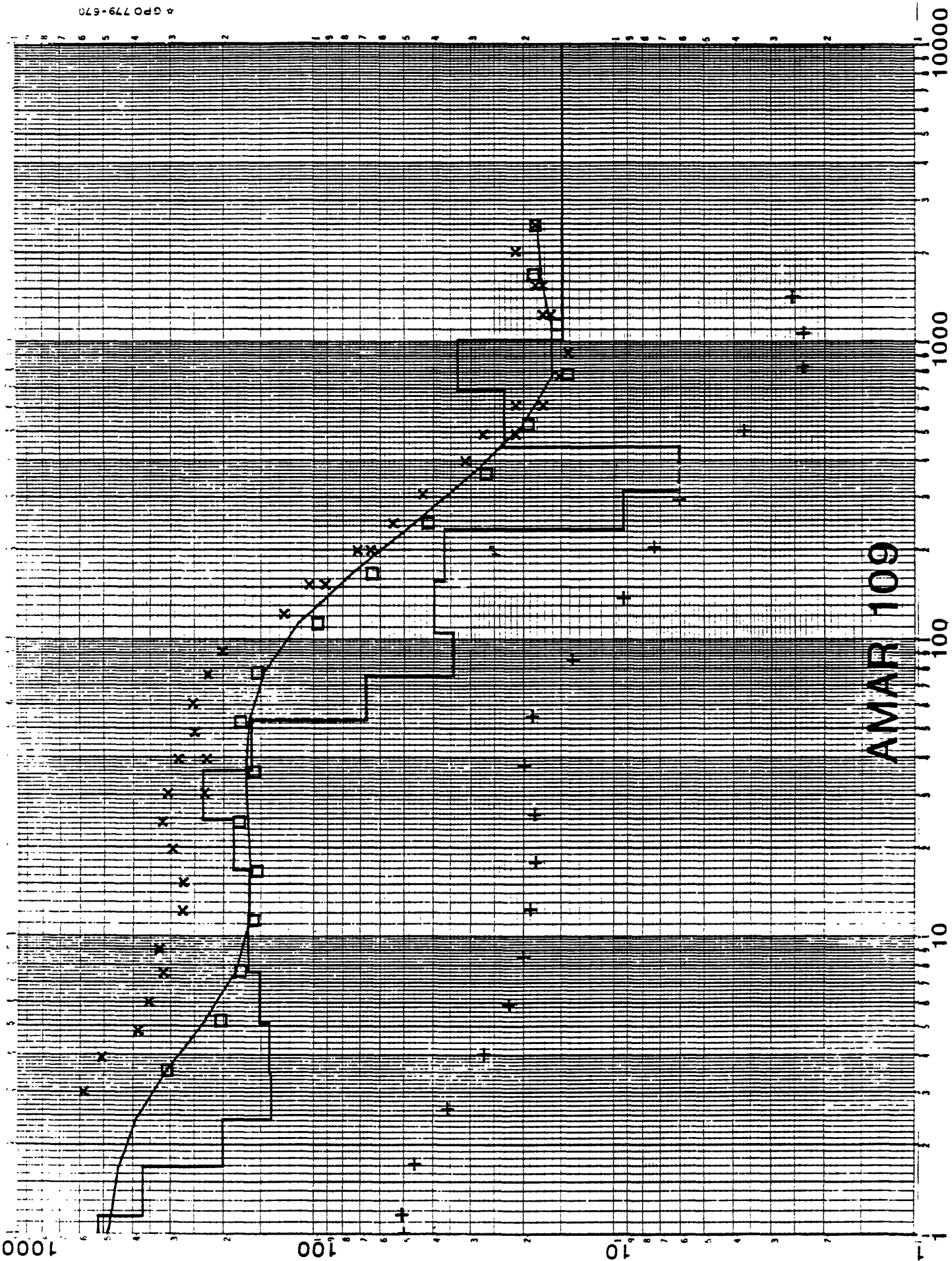


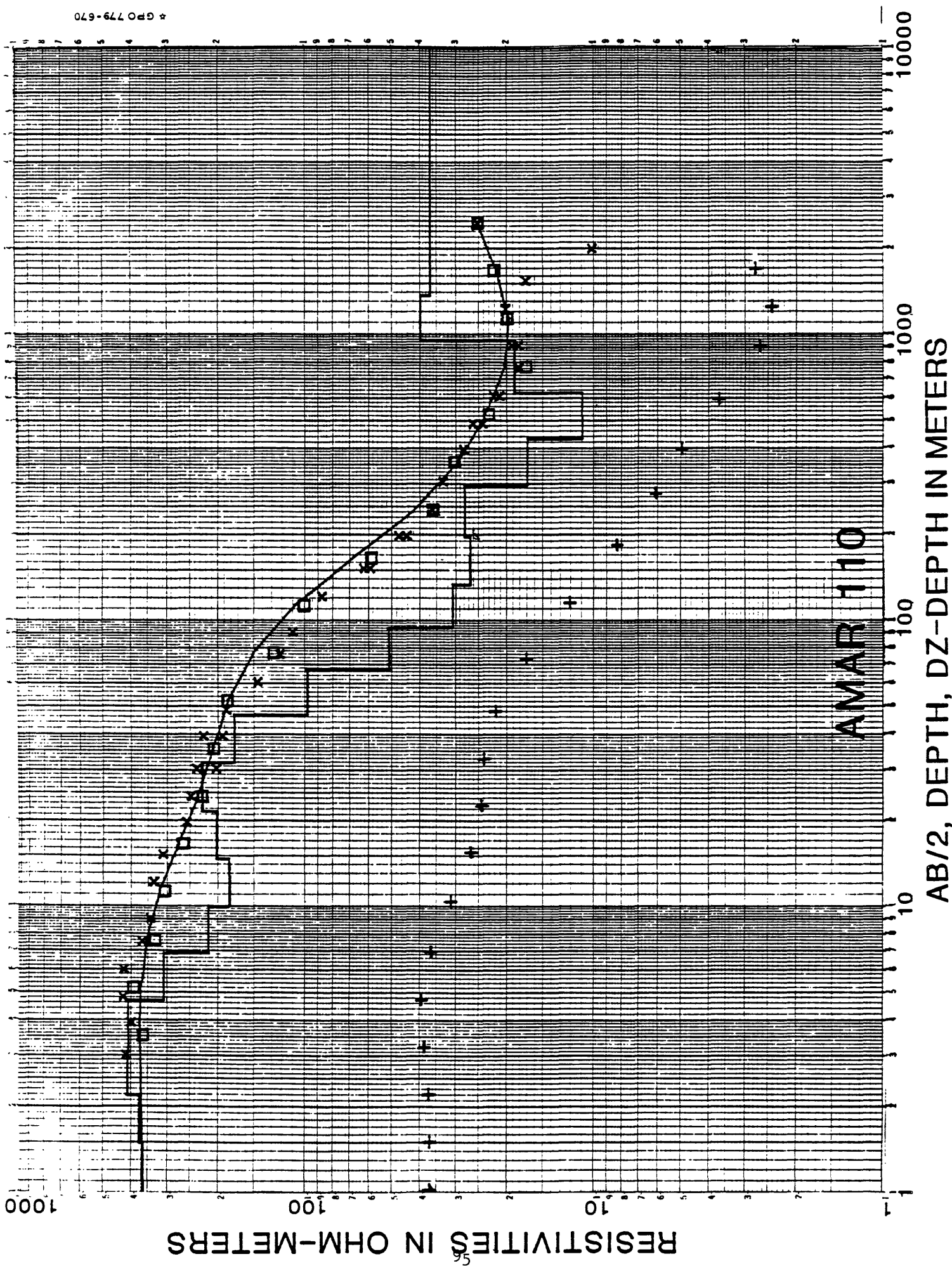


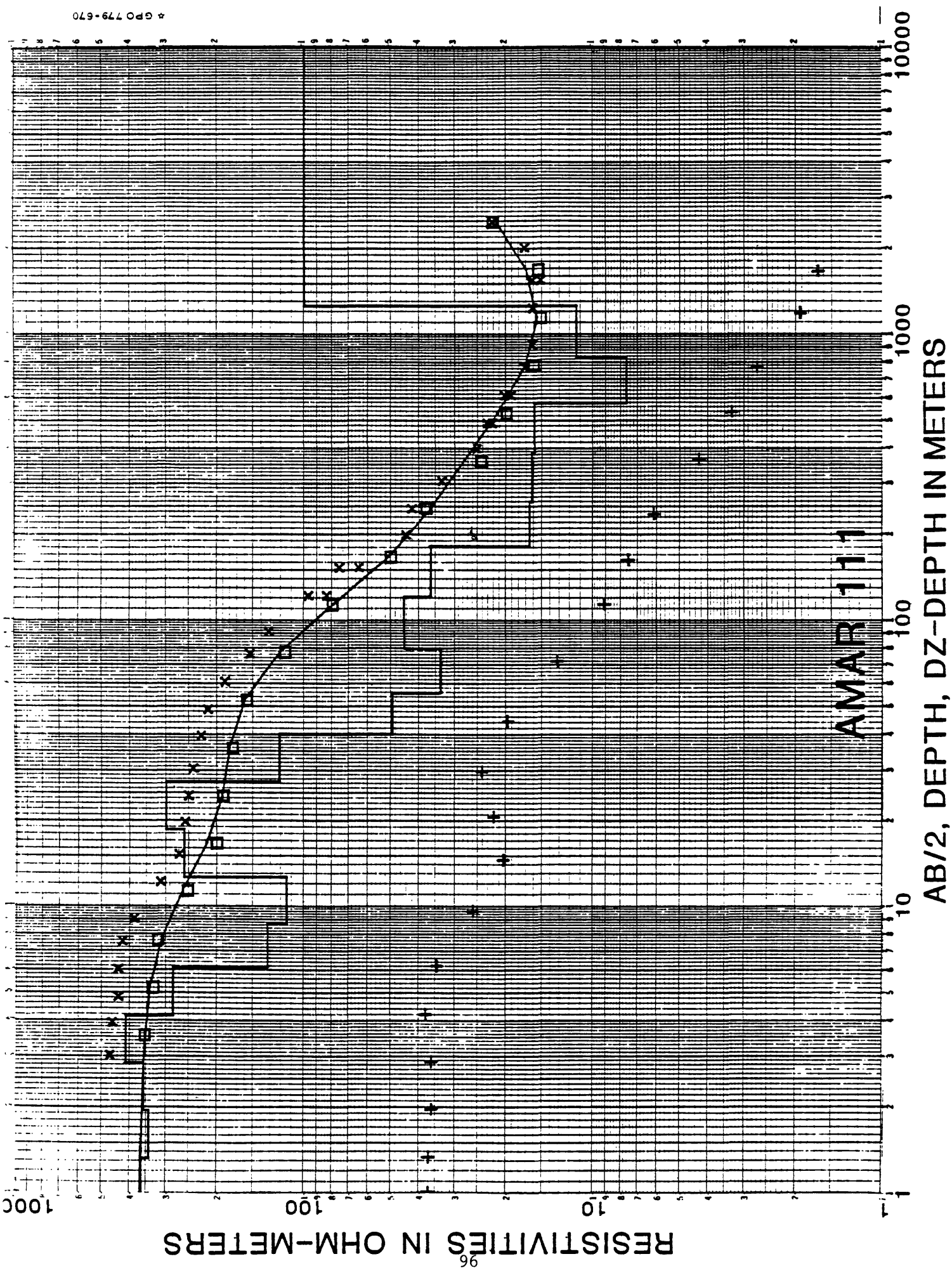
AMAR 109

AB/2, DEPTH, DZ-DEPTH IN METERS

RESISTIVITIES IN OHM-METERS



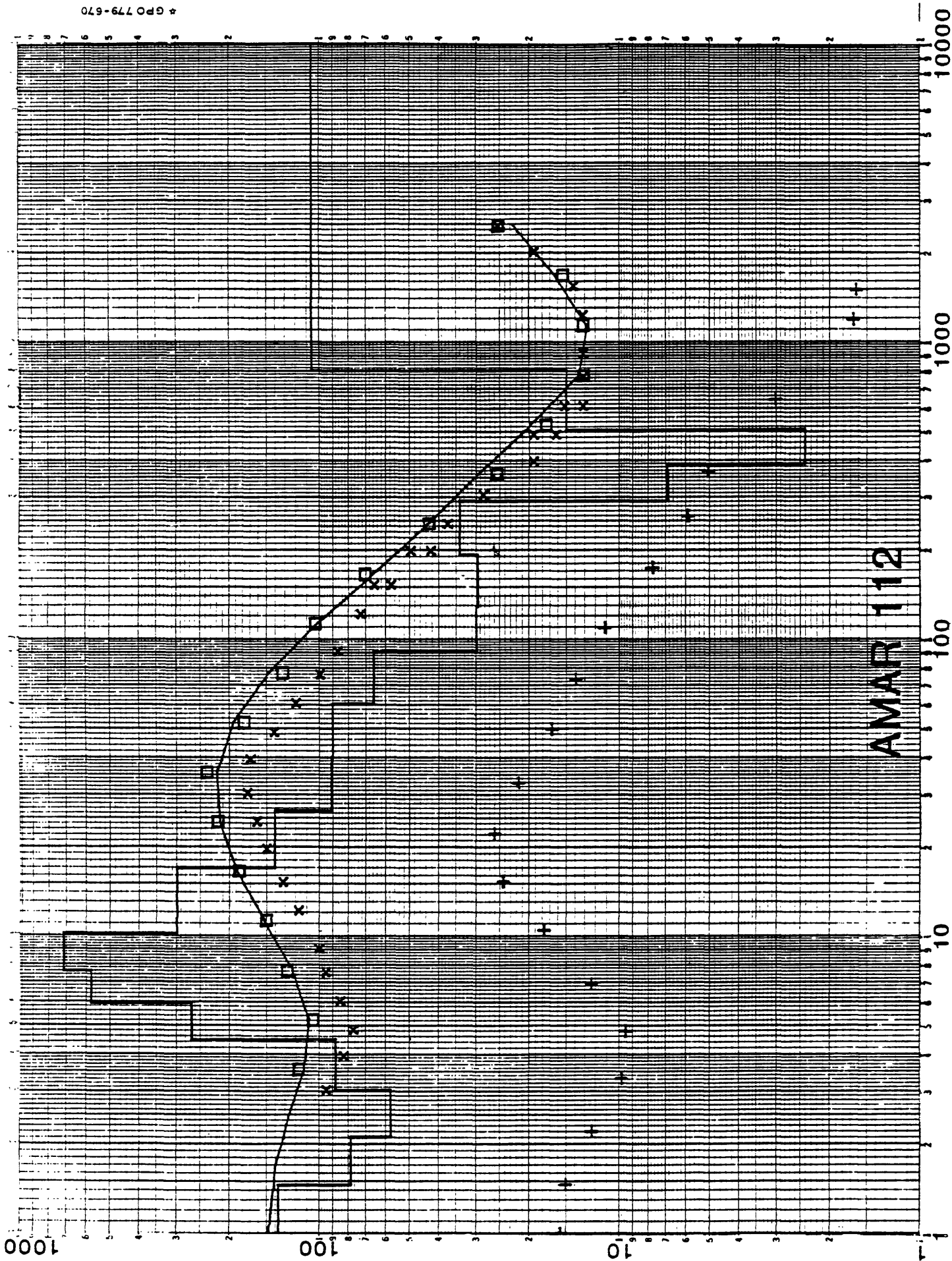




RESISTIVITIES IN OHM-METERS

AB/2, DEPTH, DZ-DEPTH IN METERS

AMAR 112

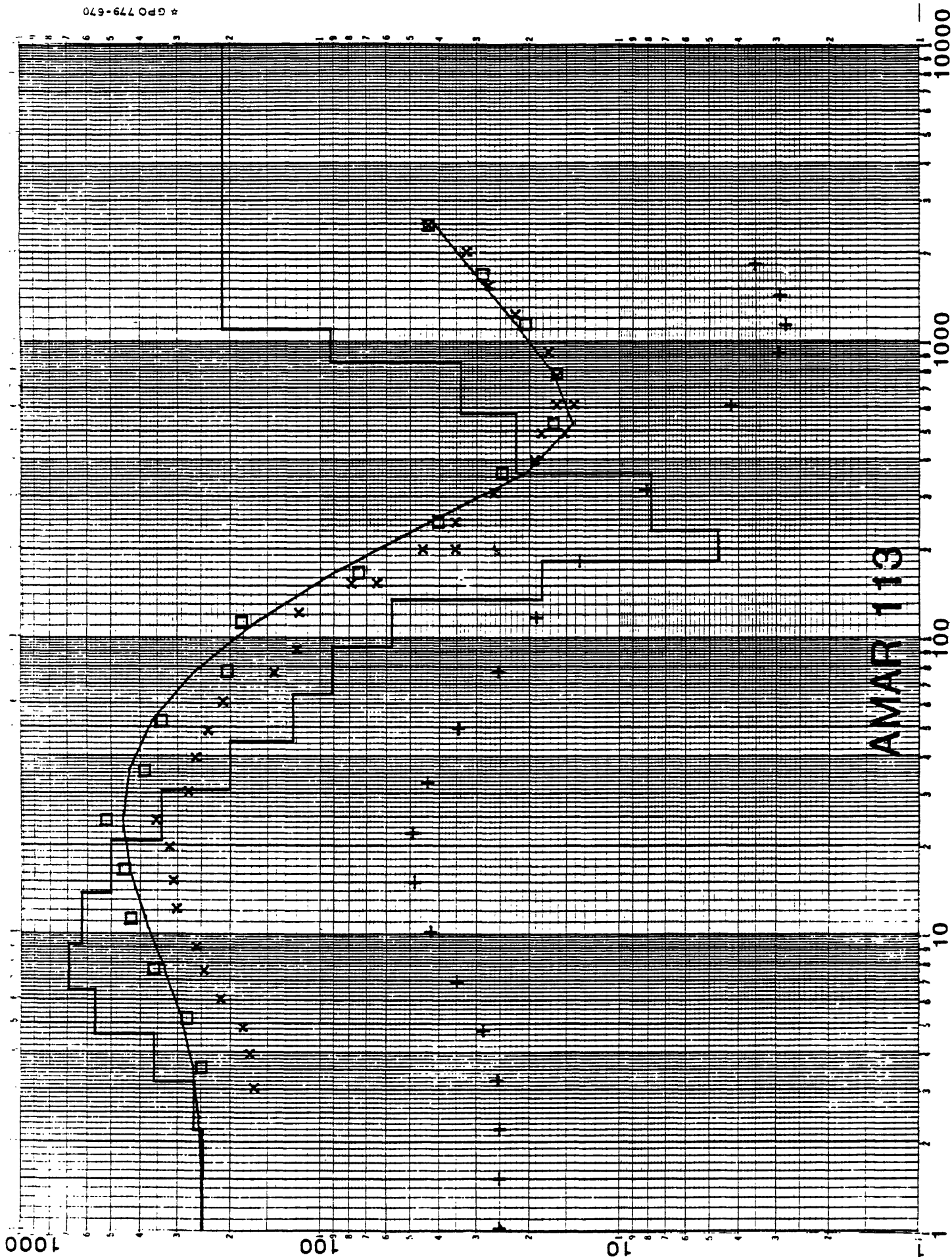


RESISTIVITIES IN OHM-METERS

98

AMAR 113

AB/2, DEPTH, DZ-DEPTH IN METERS

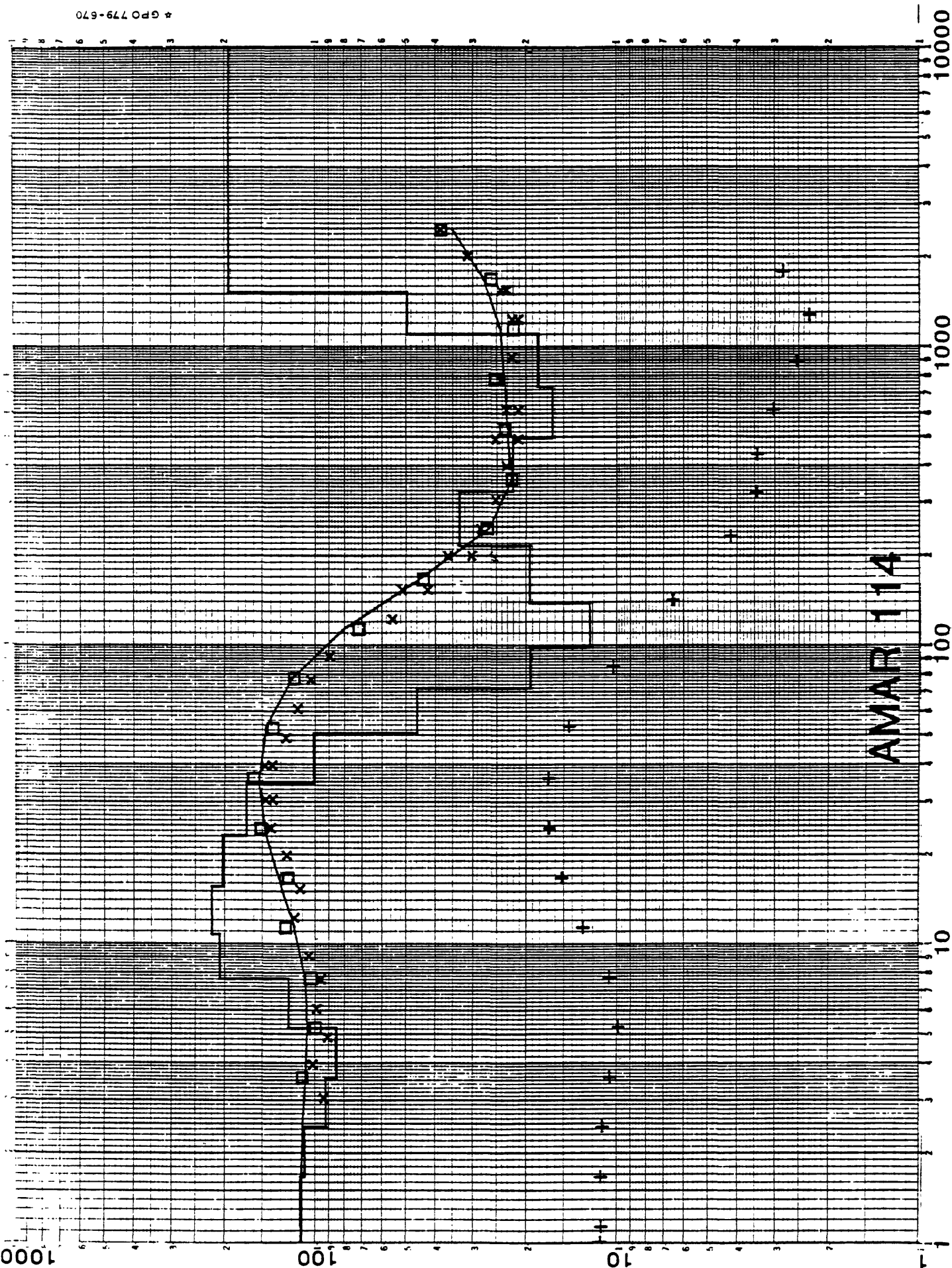


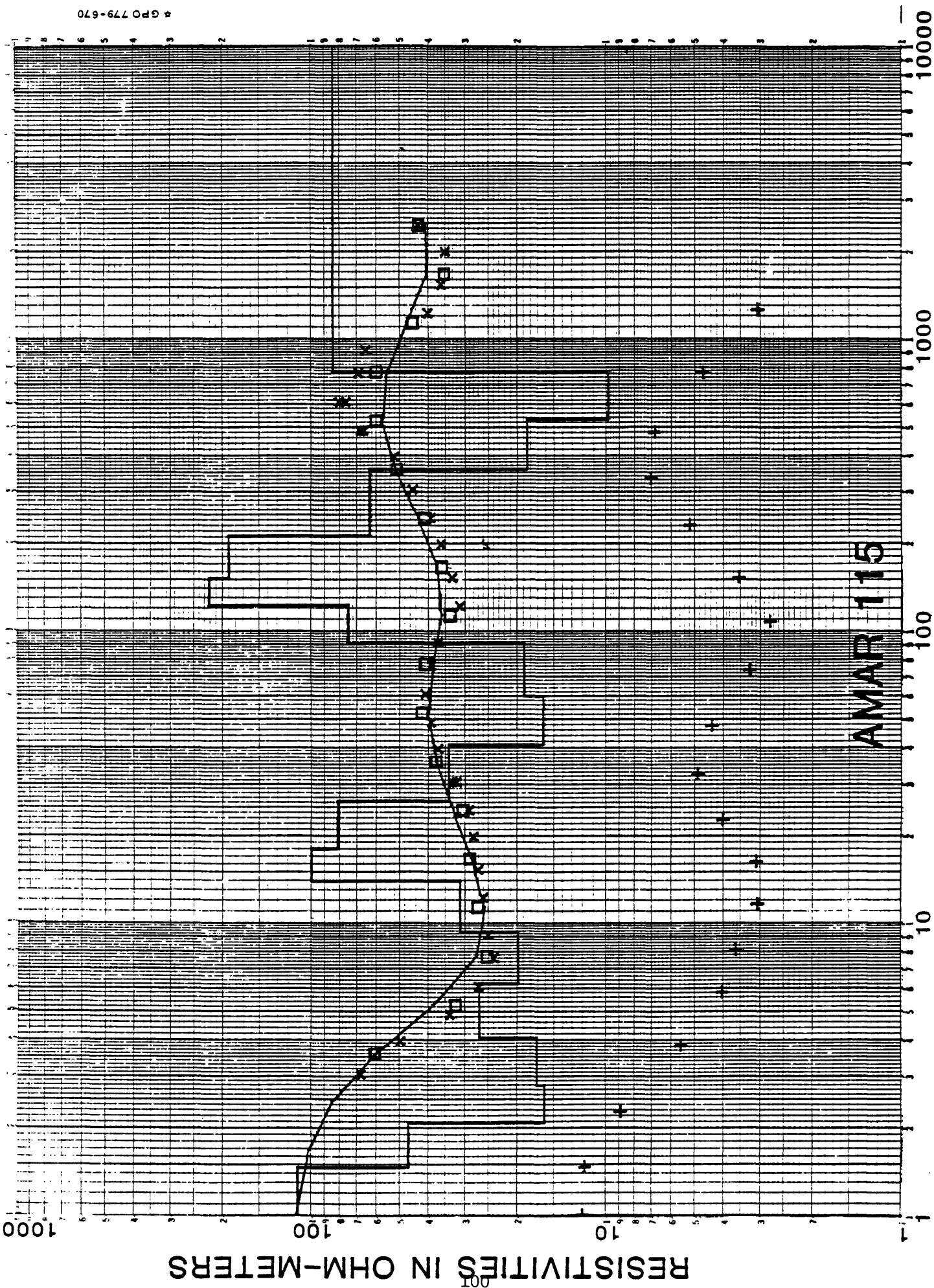
RESISTIVITIES IN OHM-METERS

66

AMAR 114

AB/2, DEPTH, DZ-DEPTH IN METERS



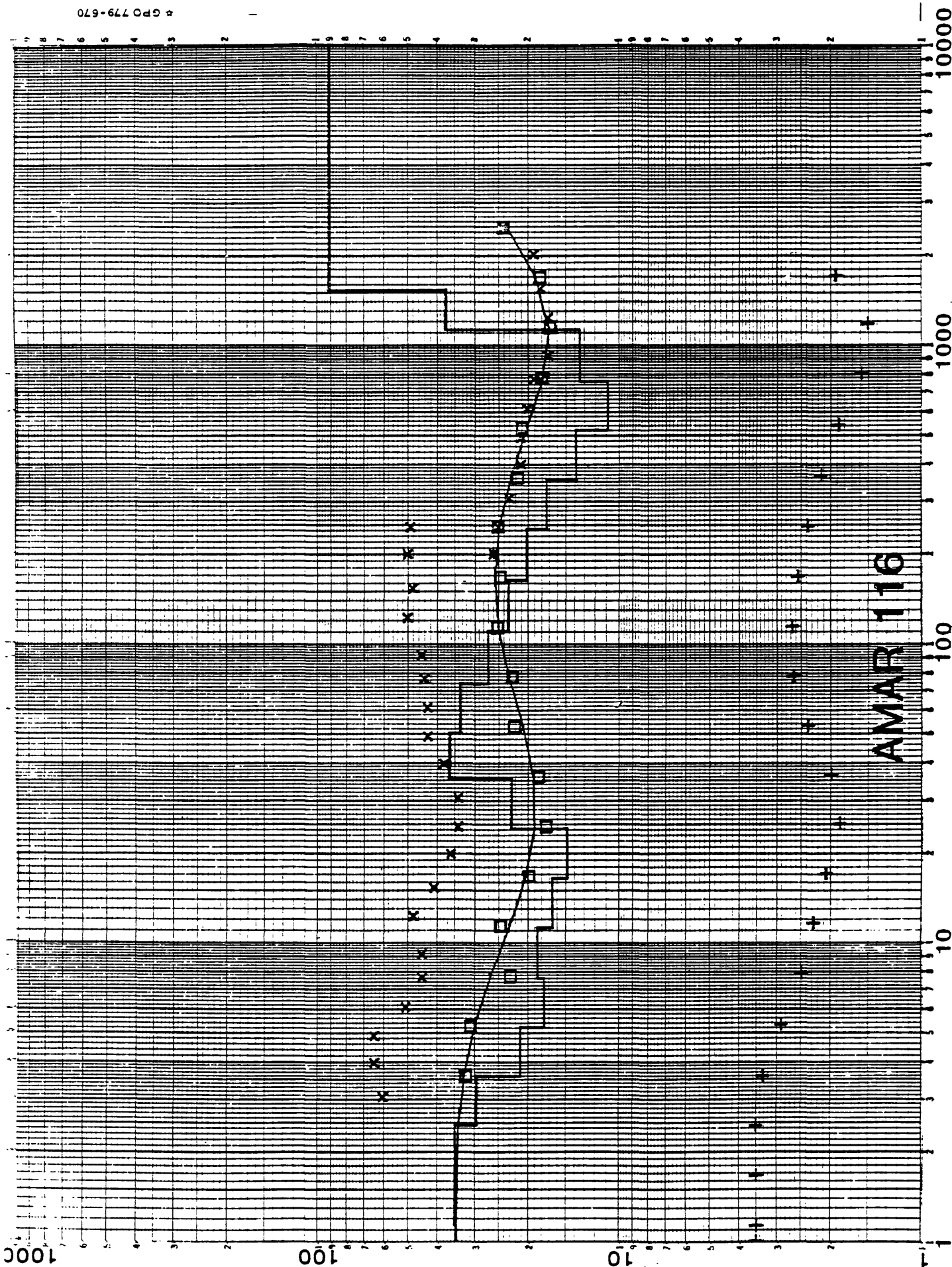


AB/2, DEPTH, DZ-DEPTH IN METERS

RESISTIVITIES IN OHM-METERS

AMAR 116

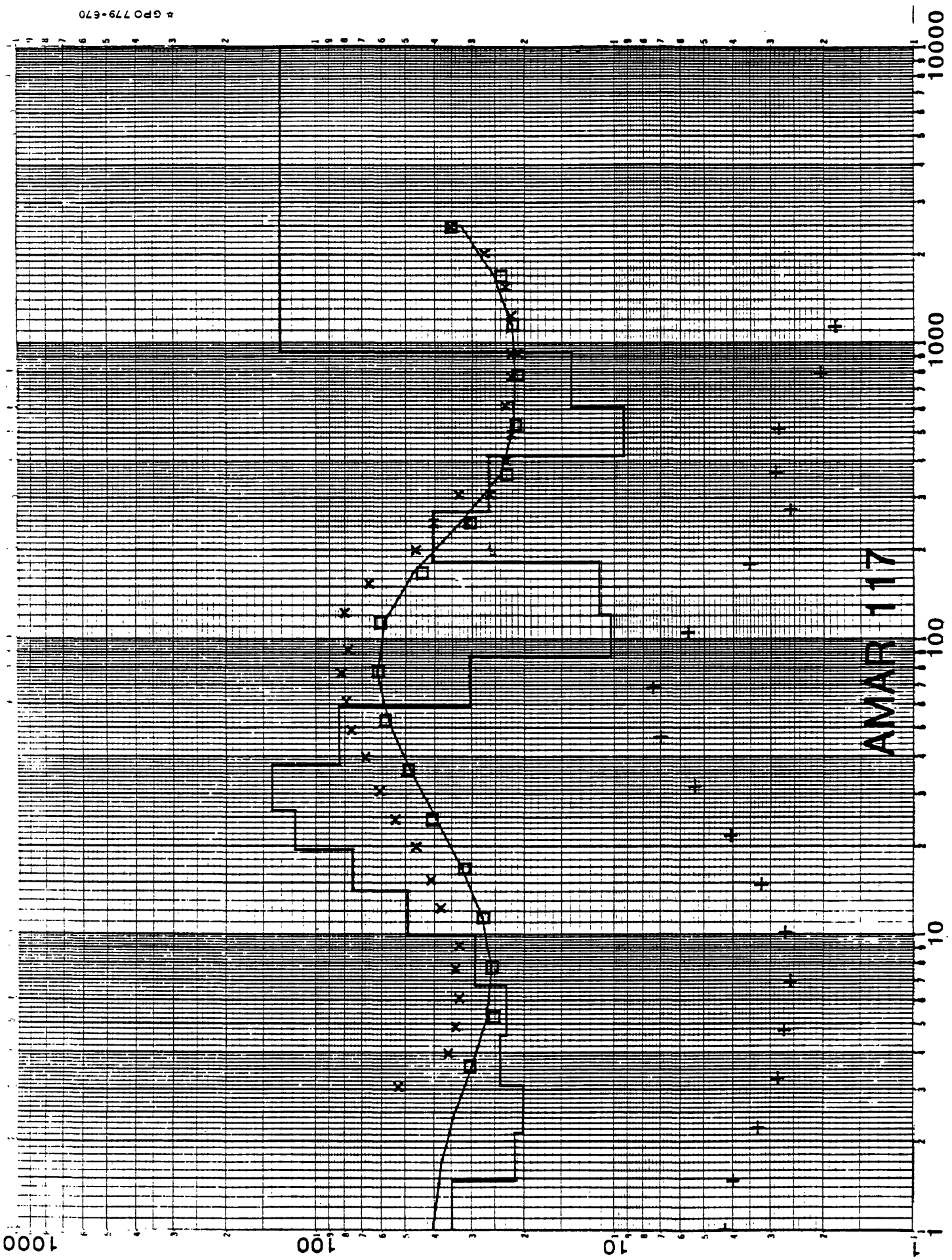
AB/2, DEPTH, DZ-DEPTH IN METERS

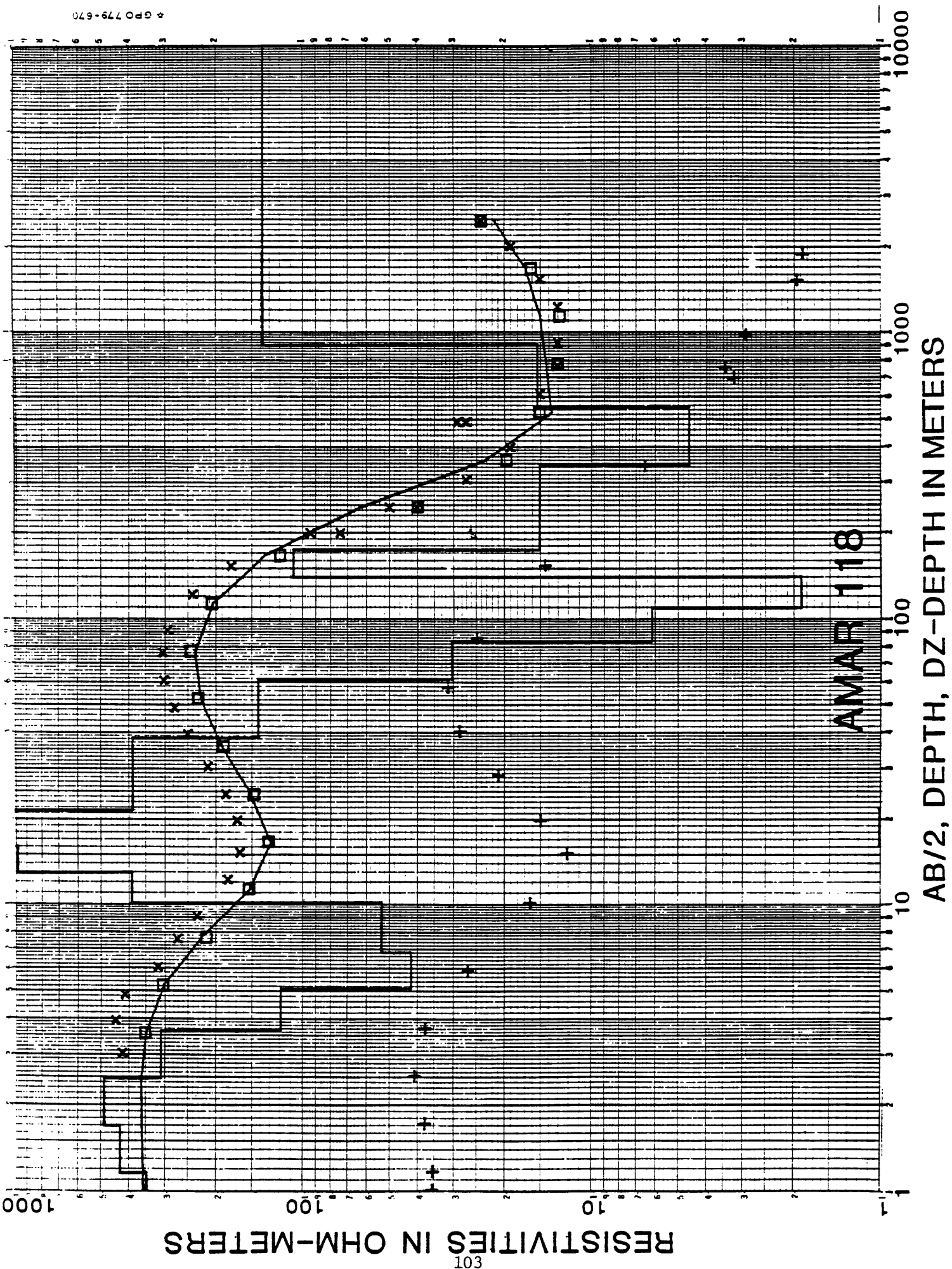


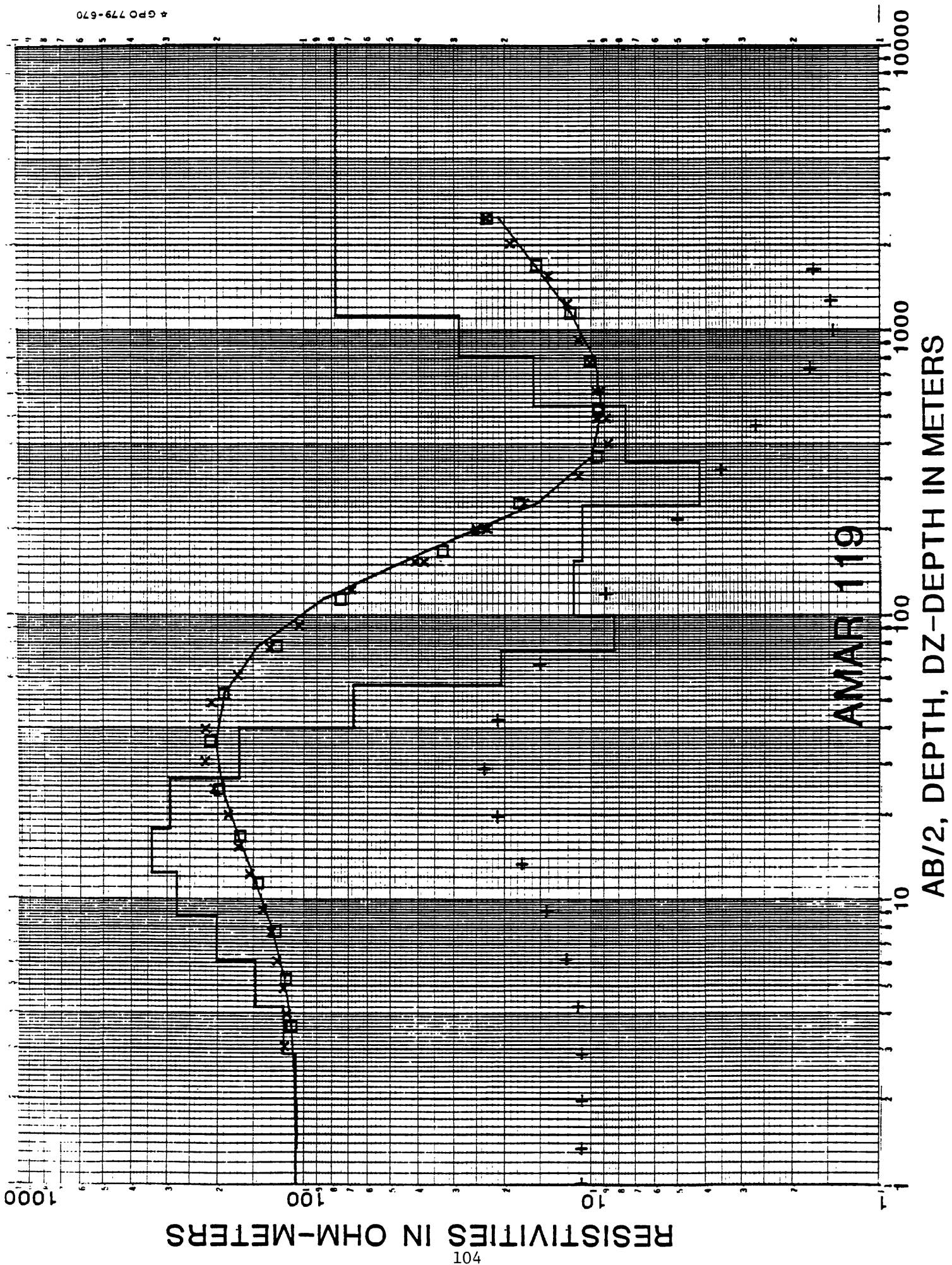
AMAR 117

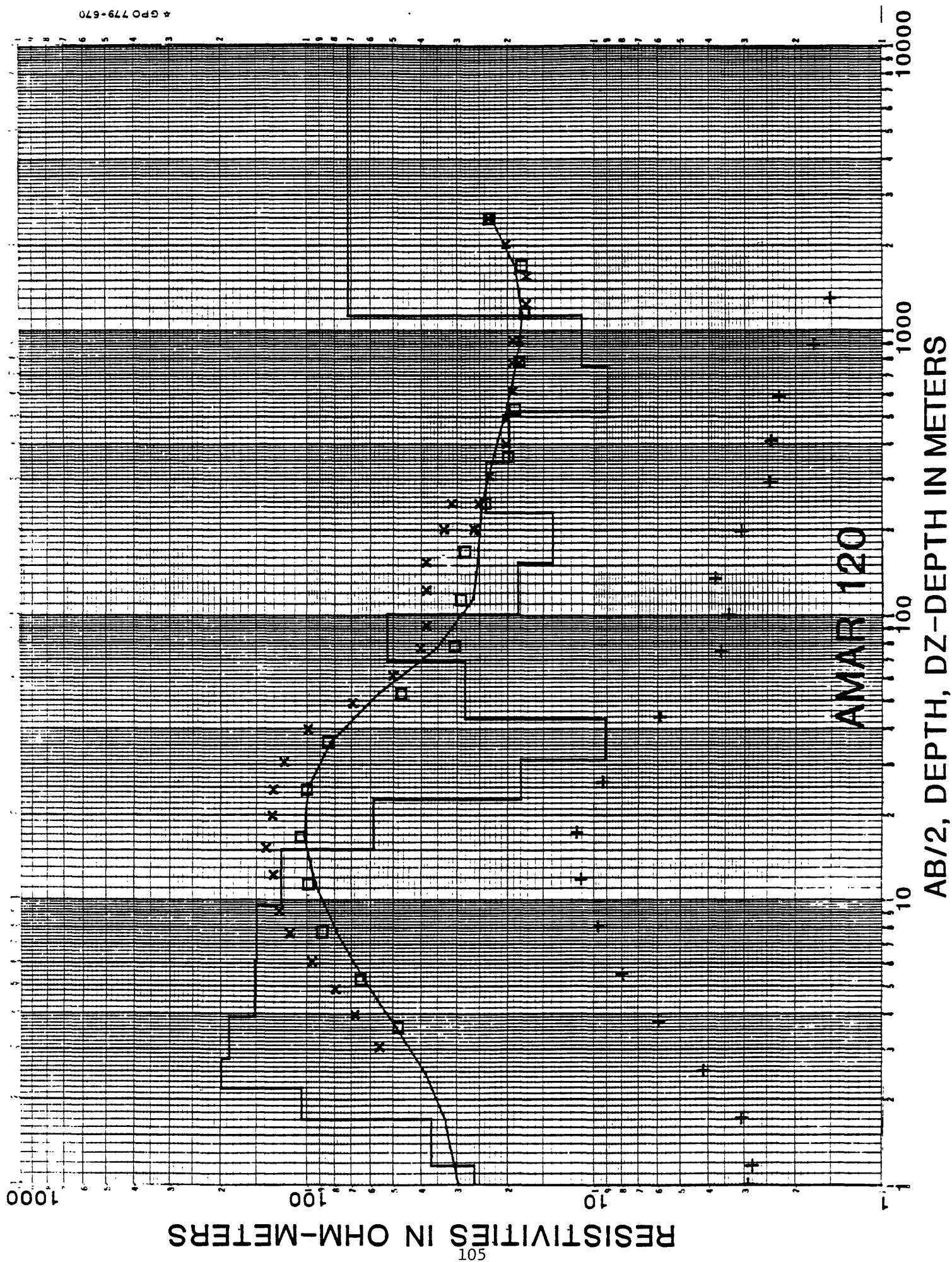
RESISTIVITIES IN OHM-METERS

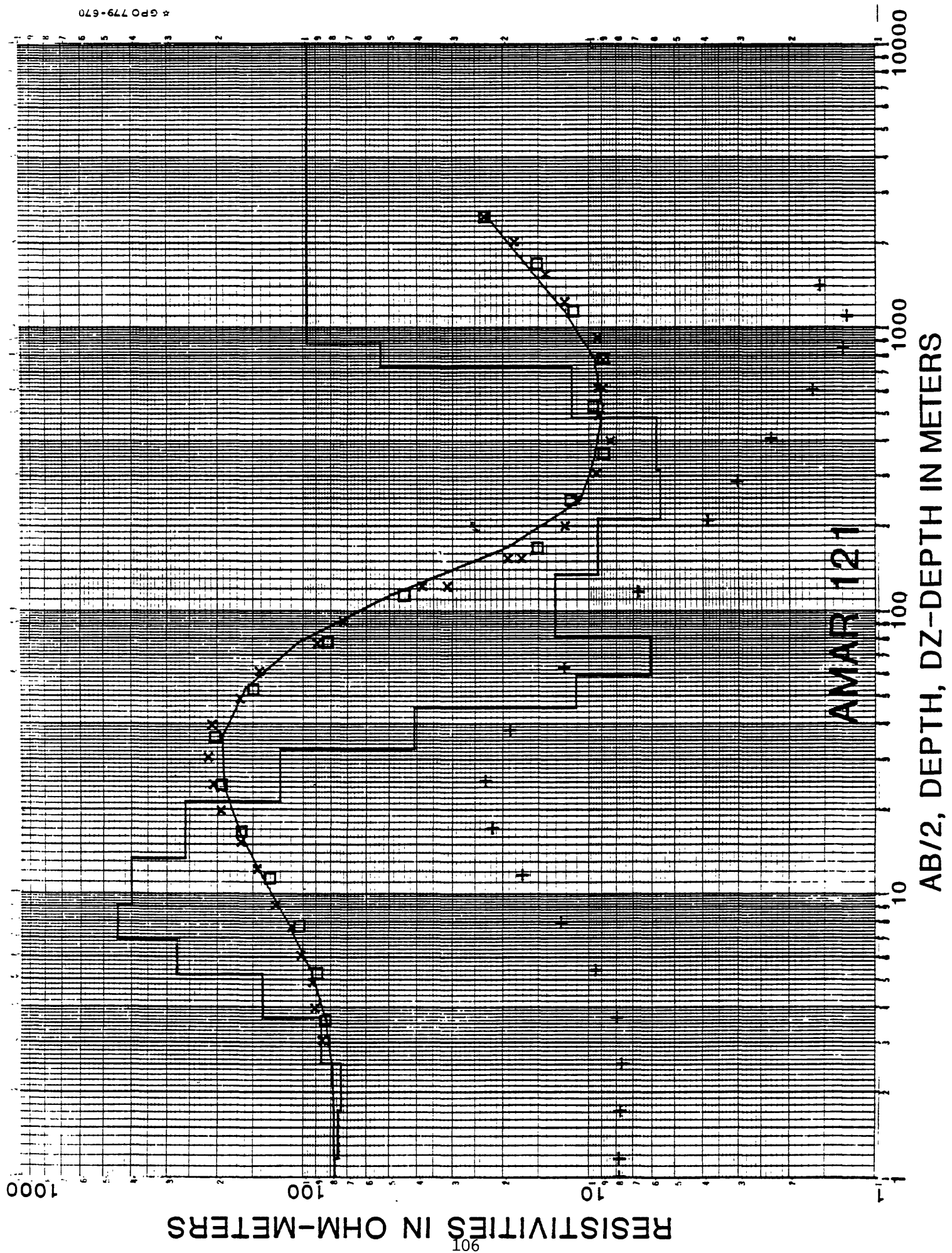
AB/2, DEPTH, DZ-DEPTH IN METERS









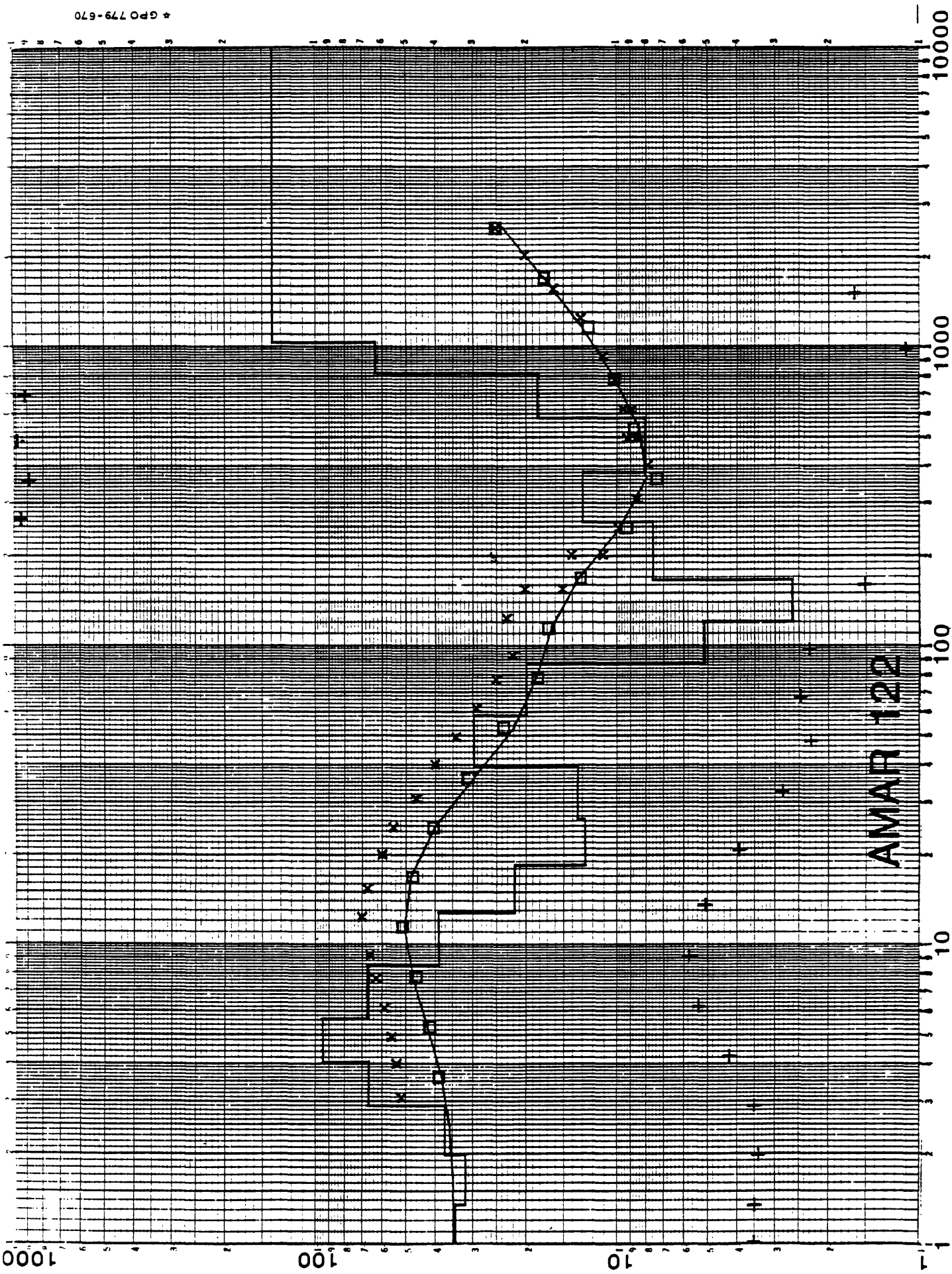


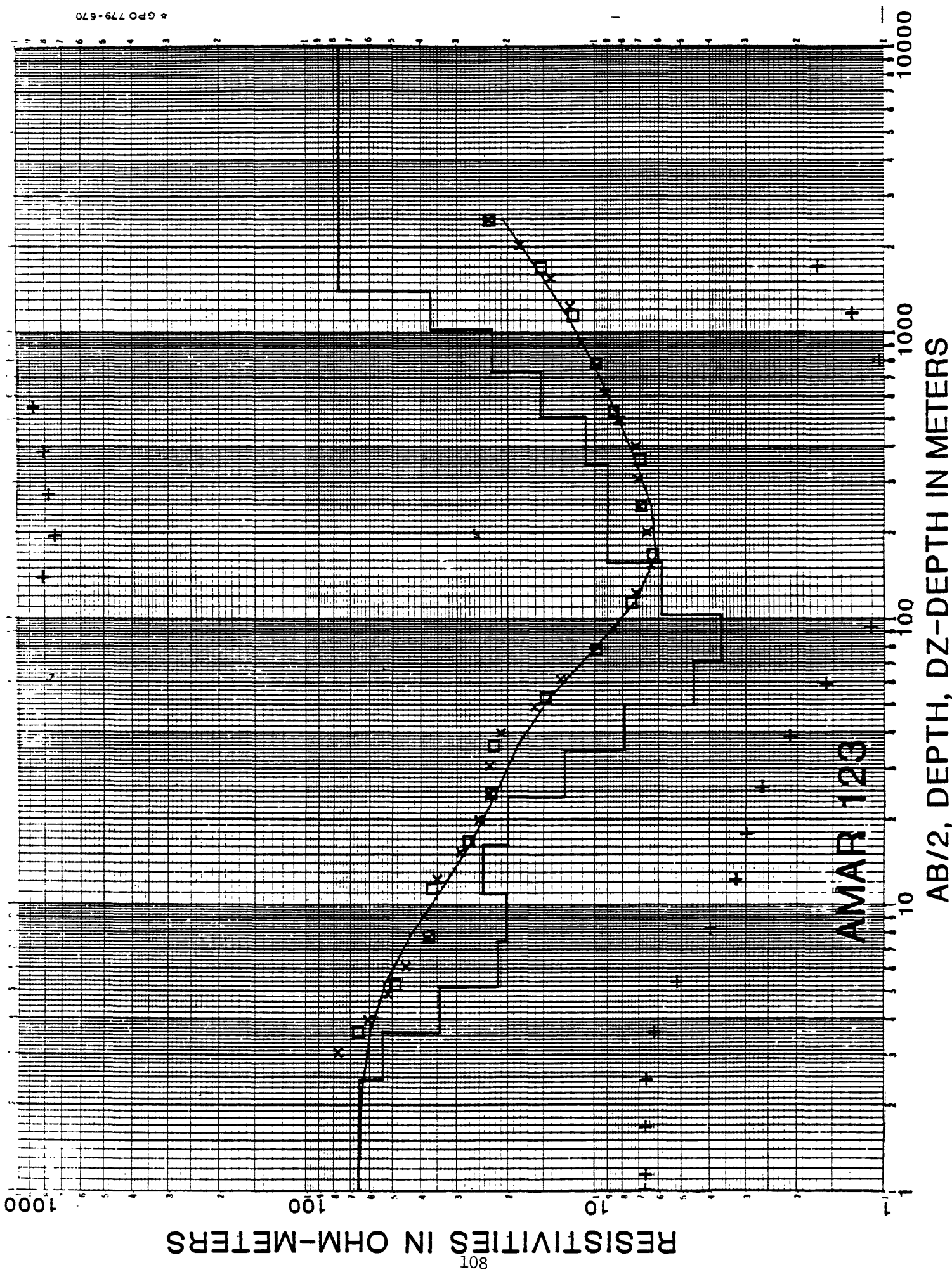
RESISTIVITIES IN OHM-METERS

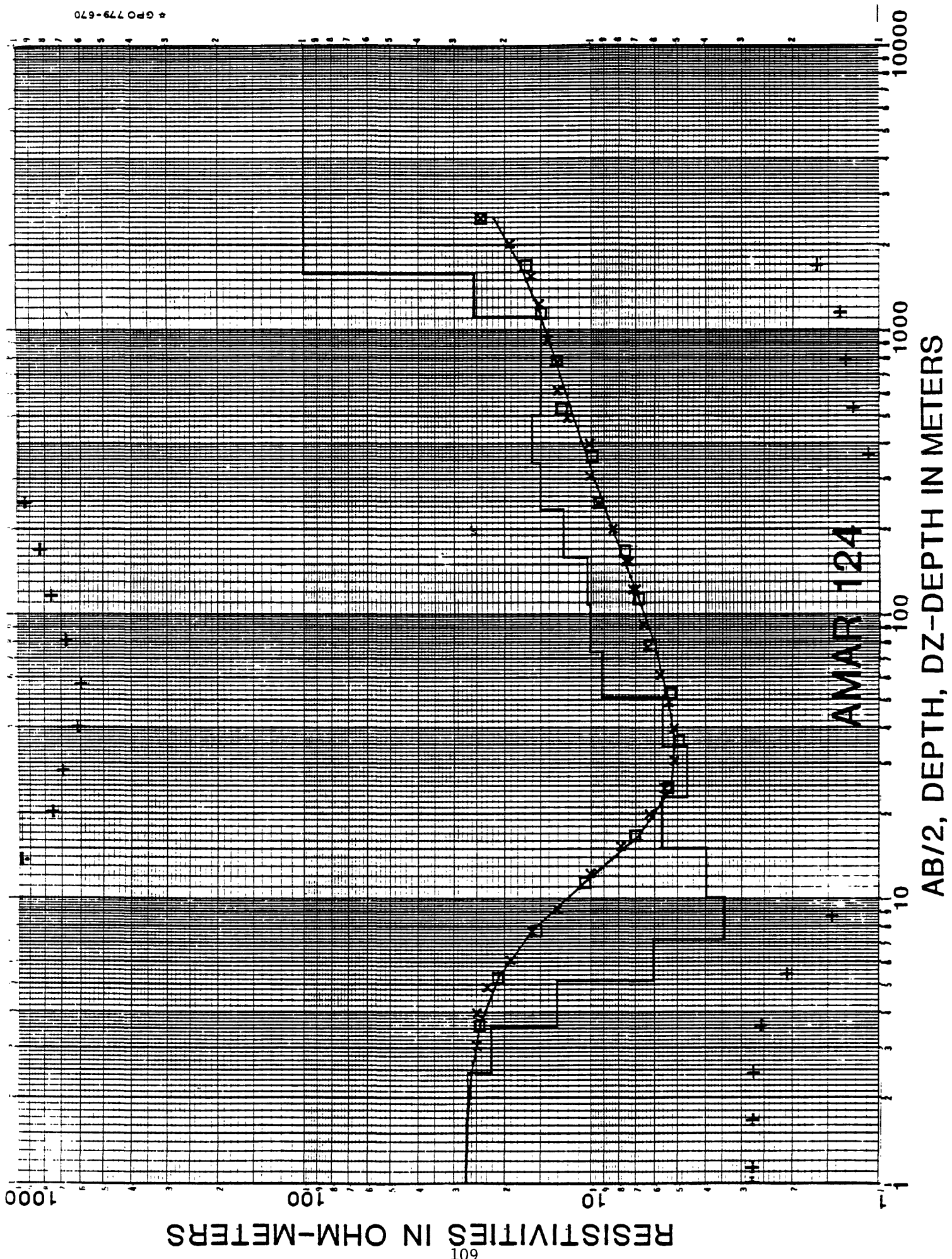
107

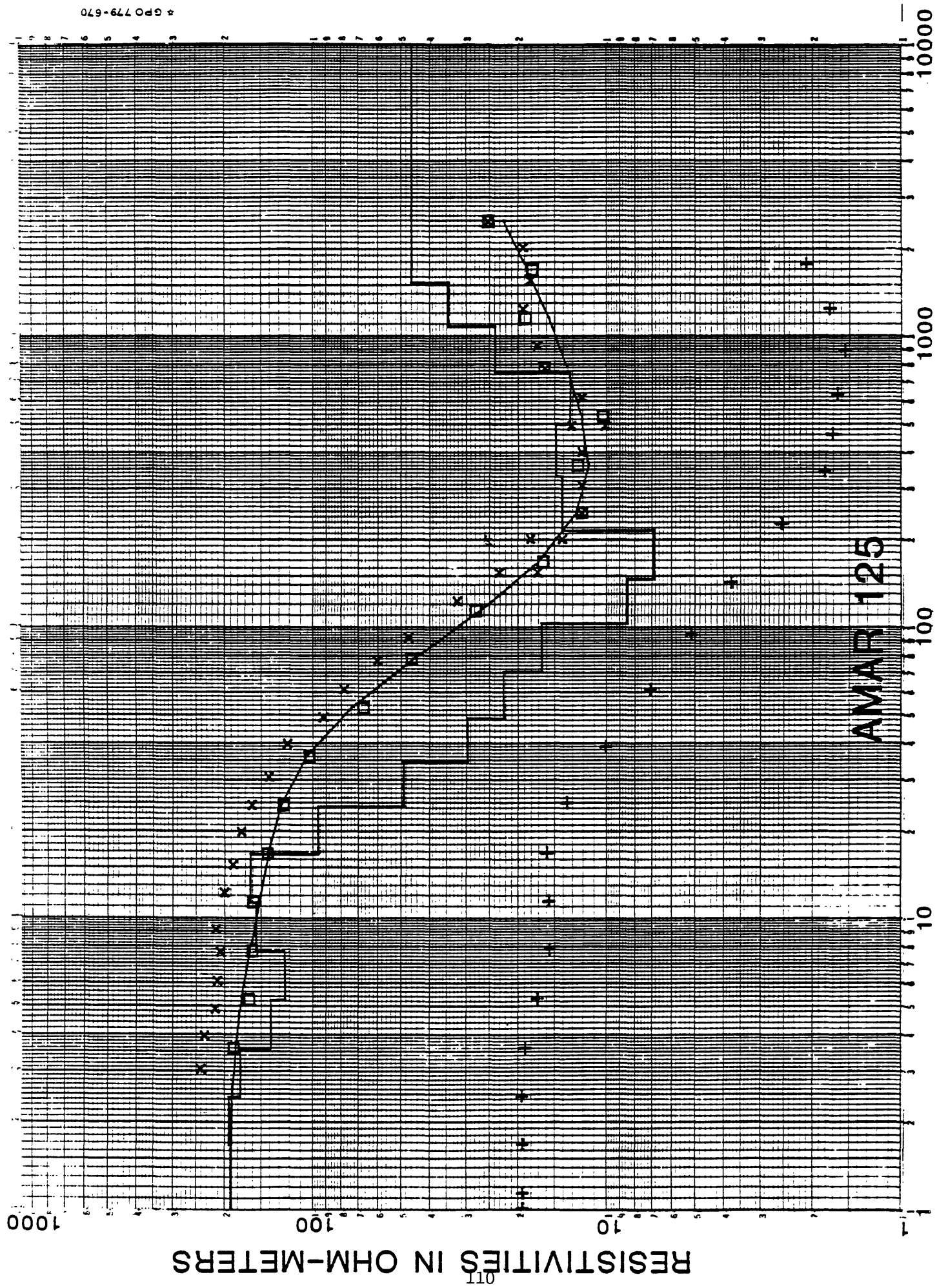
AMAR 122

AB/2, DEPTH, DZ-DEPTH IN METERS









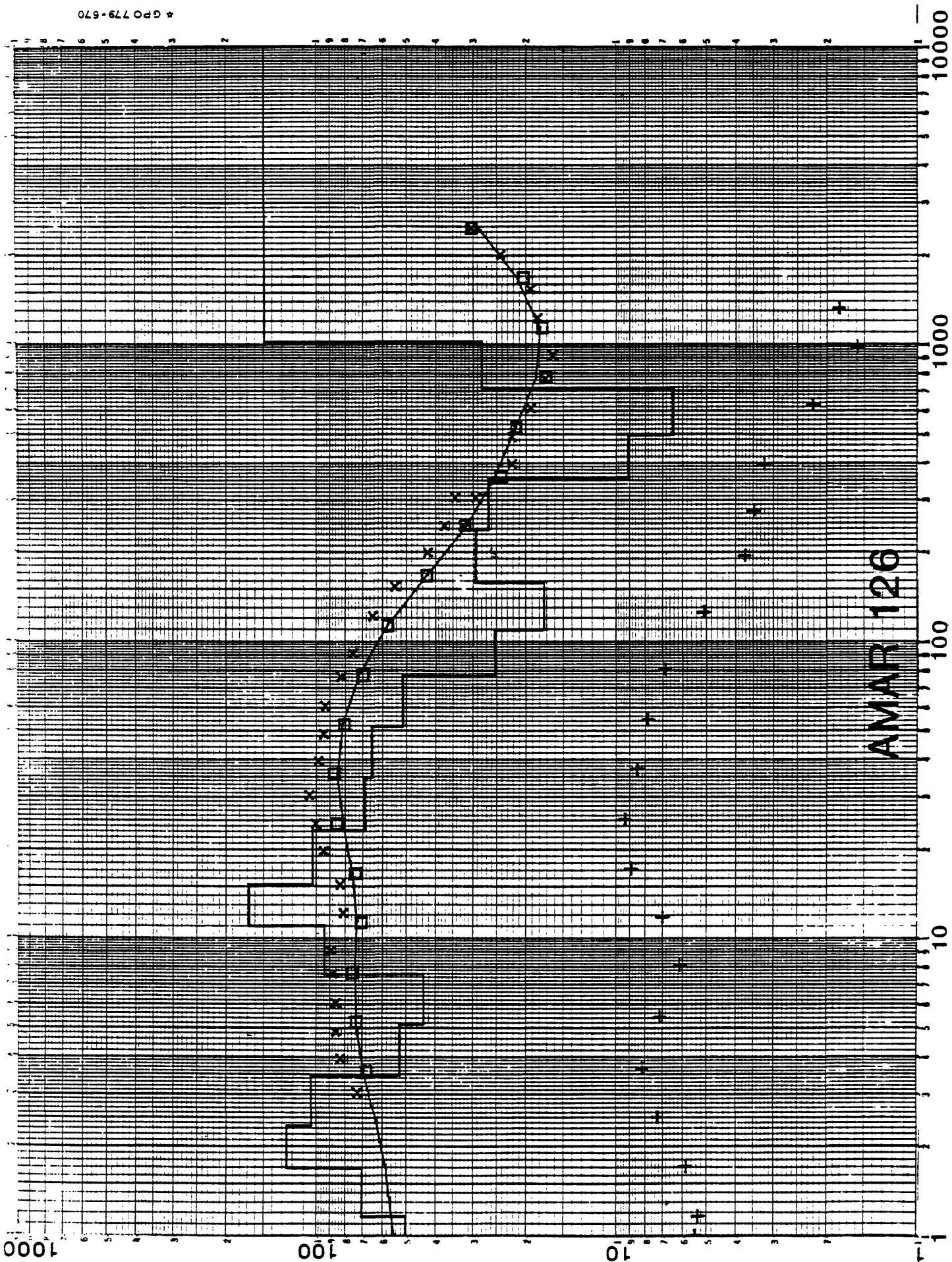
AMAR 125

AB/2, DEPTH, DZ-DEPTH IN METERS

RESISTIVITIES IN OHM-METERS

ANAP 126

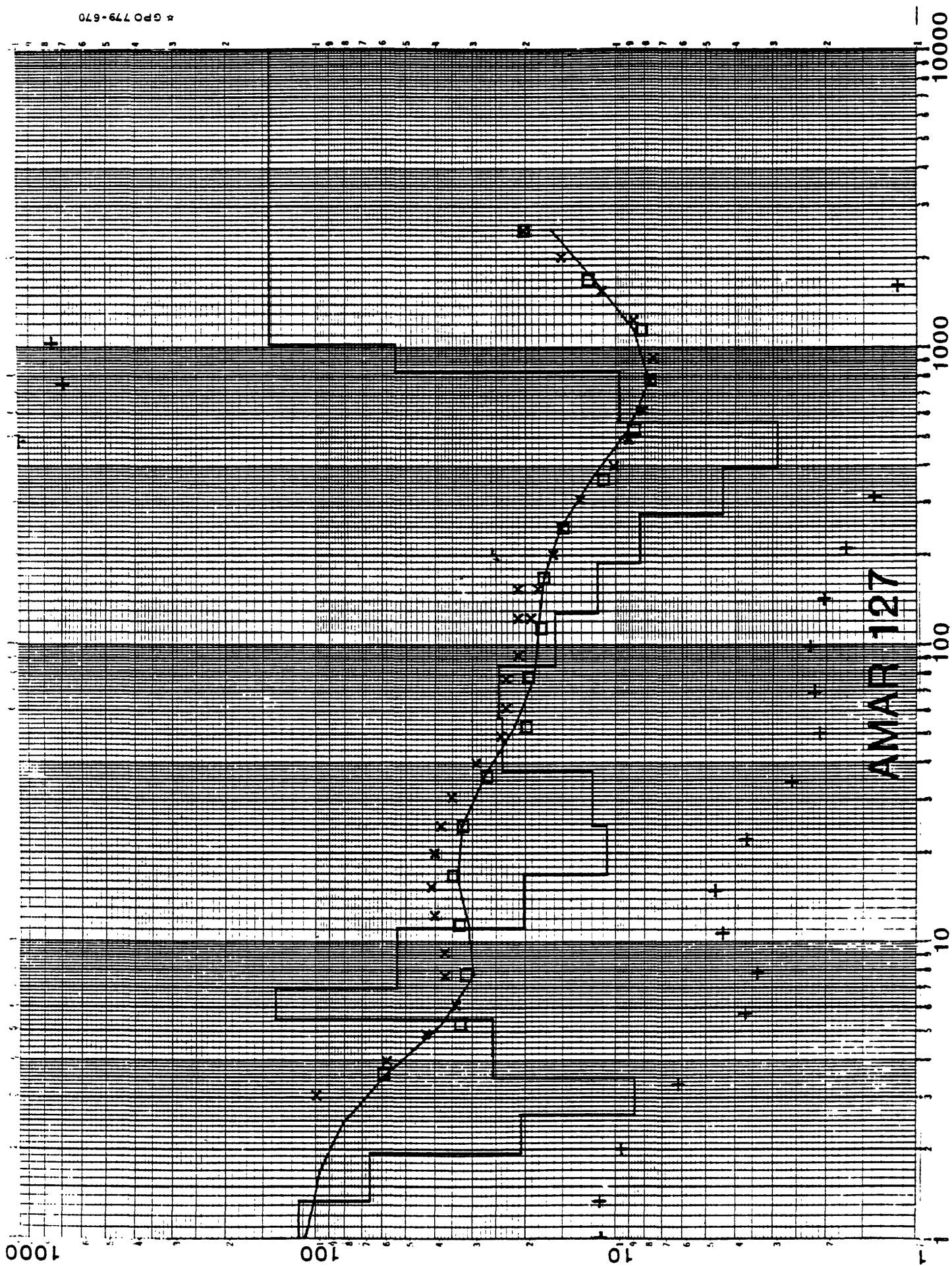
AB/2, DEPTH, DZ-DEPTH IN METERS

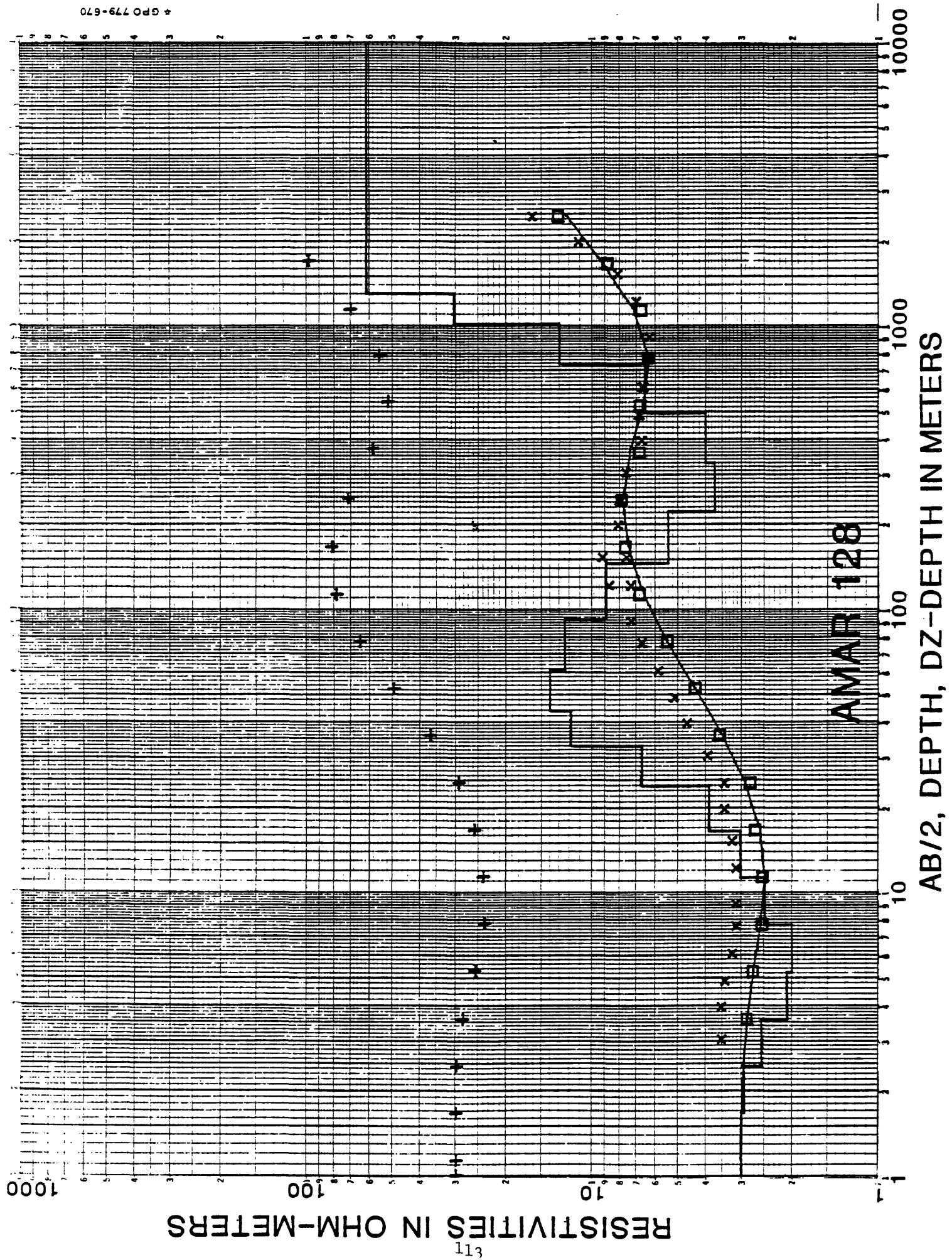


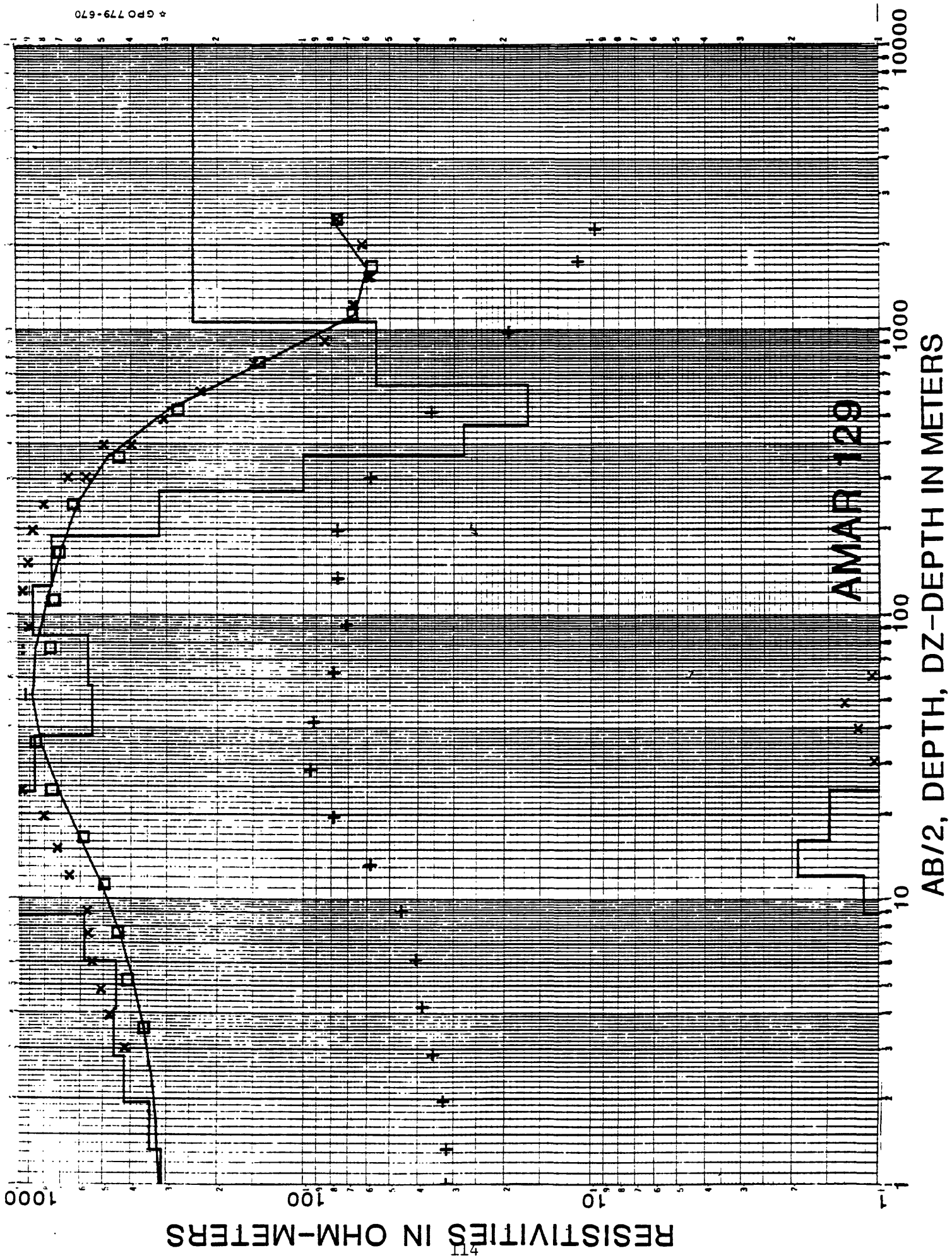
RESISTIVITIES IN OHM-METERS

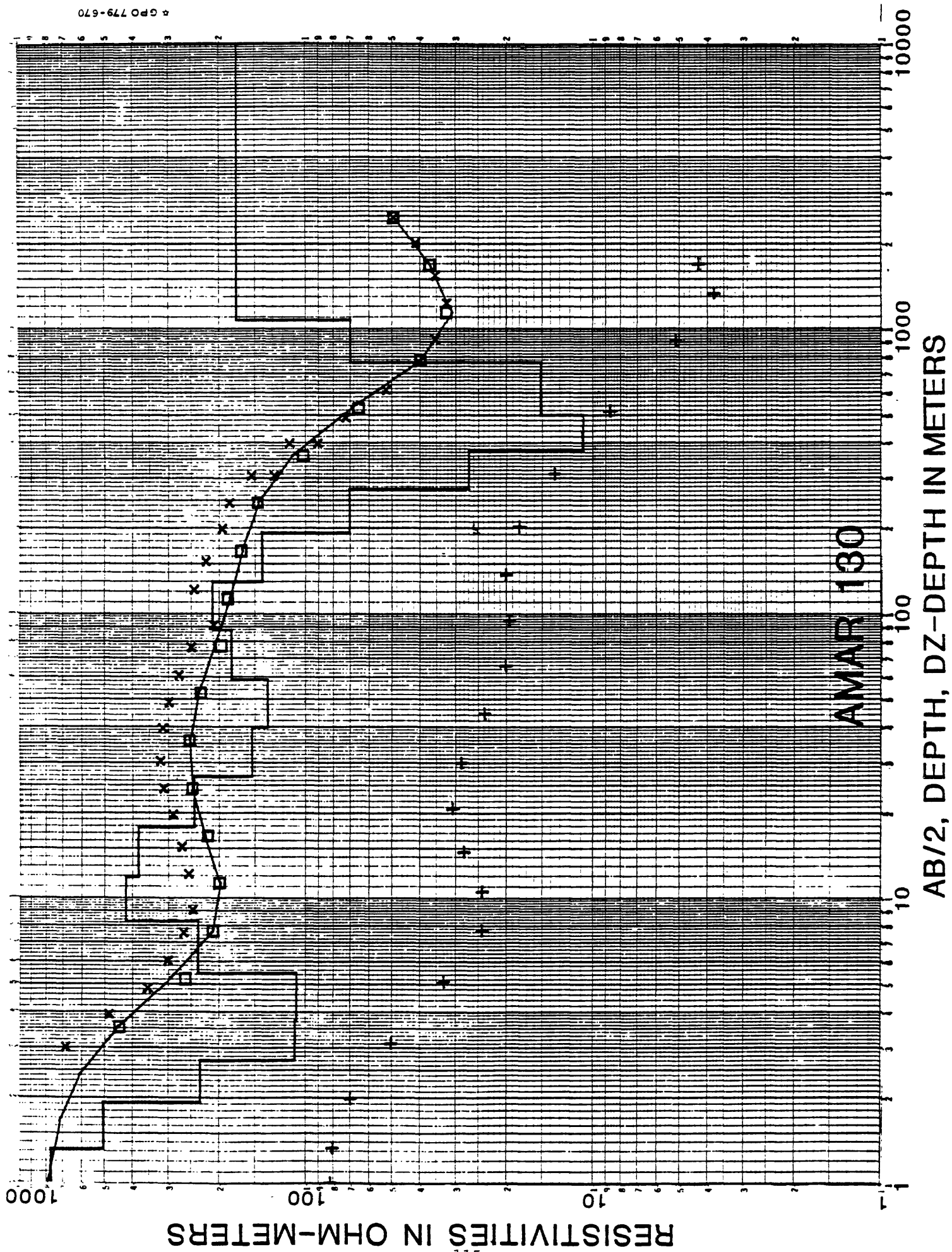
ANAP 127

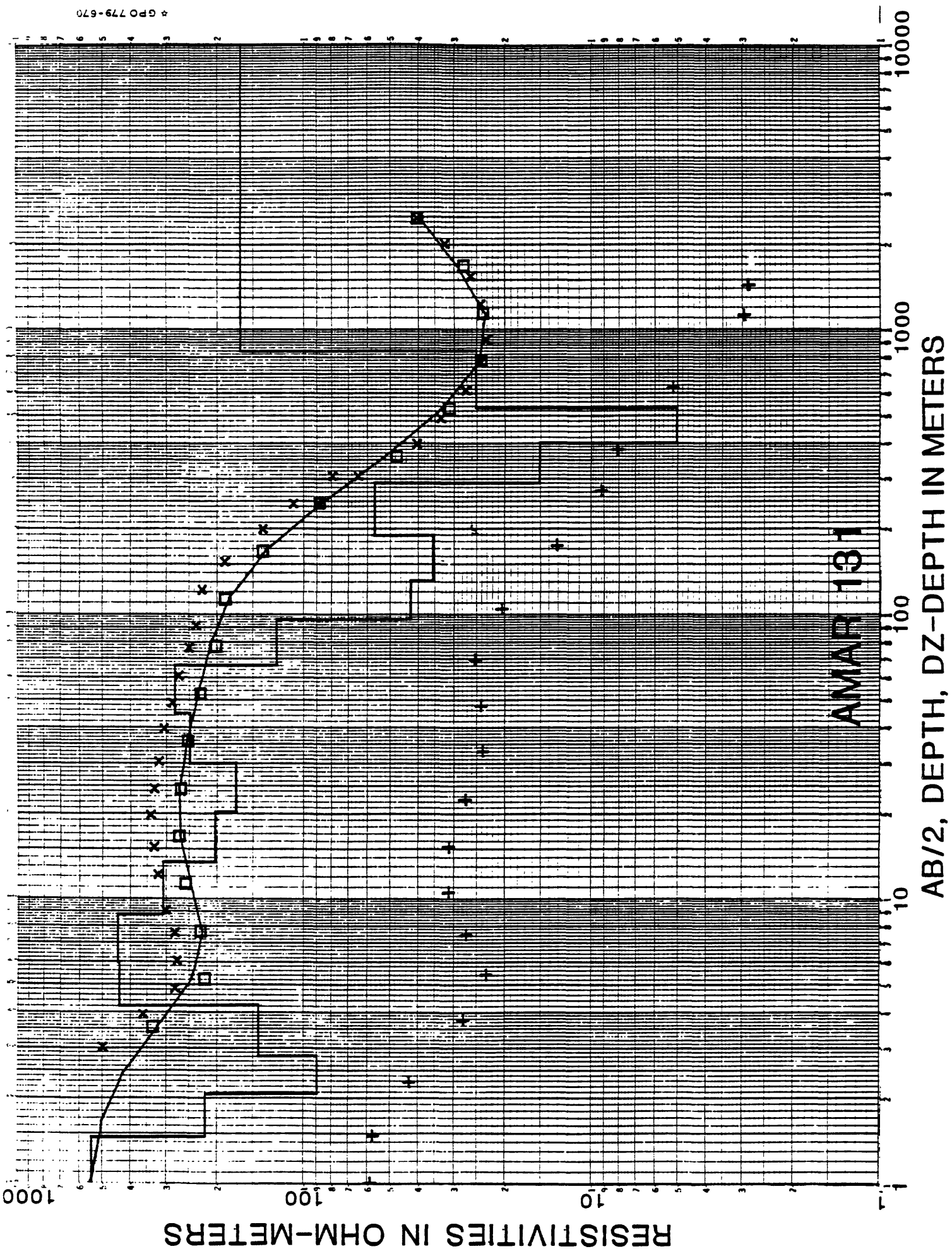
AB/2, DEPTH, DZ-DEPTH IN METERS

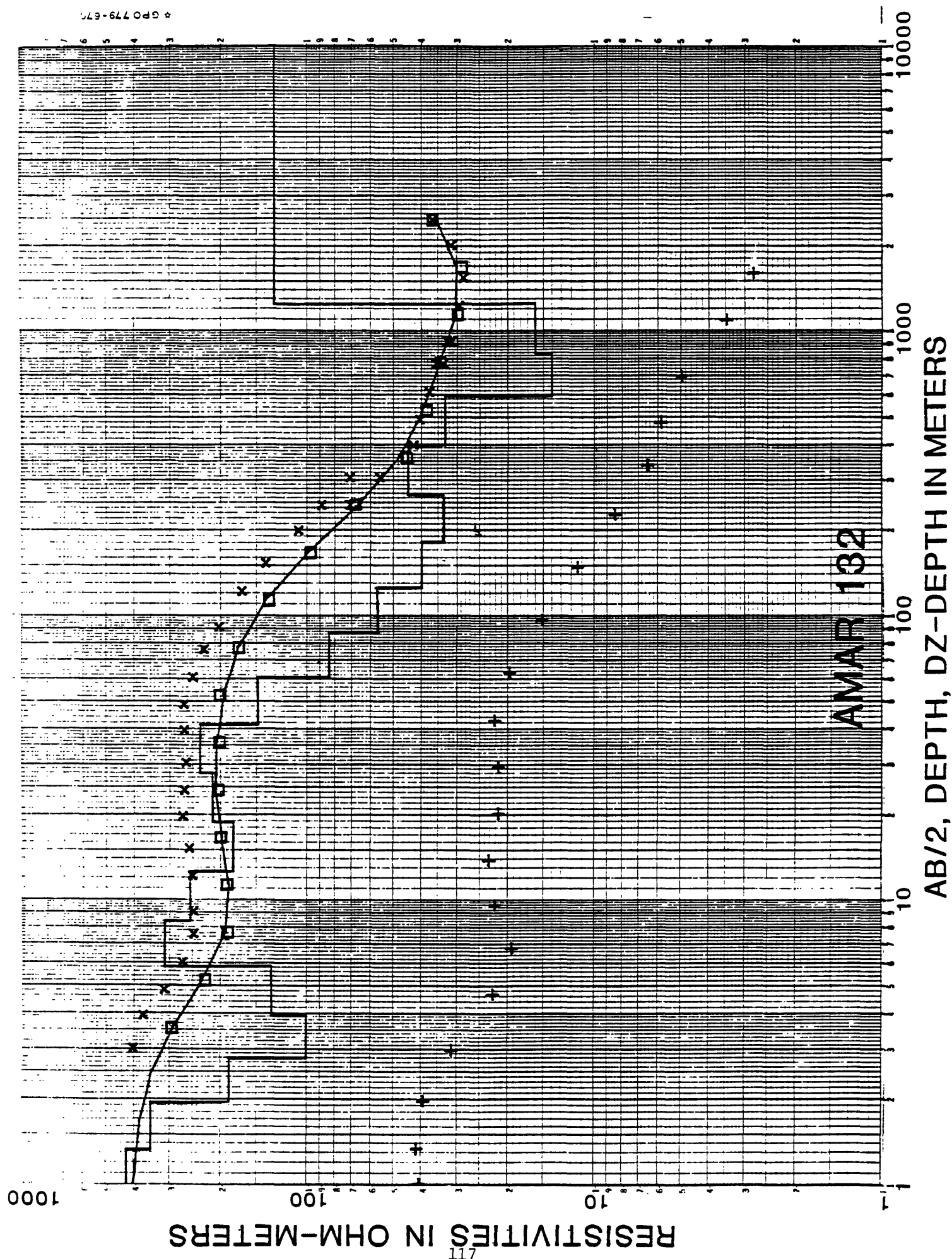


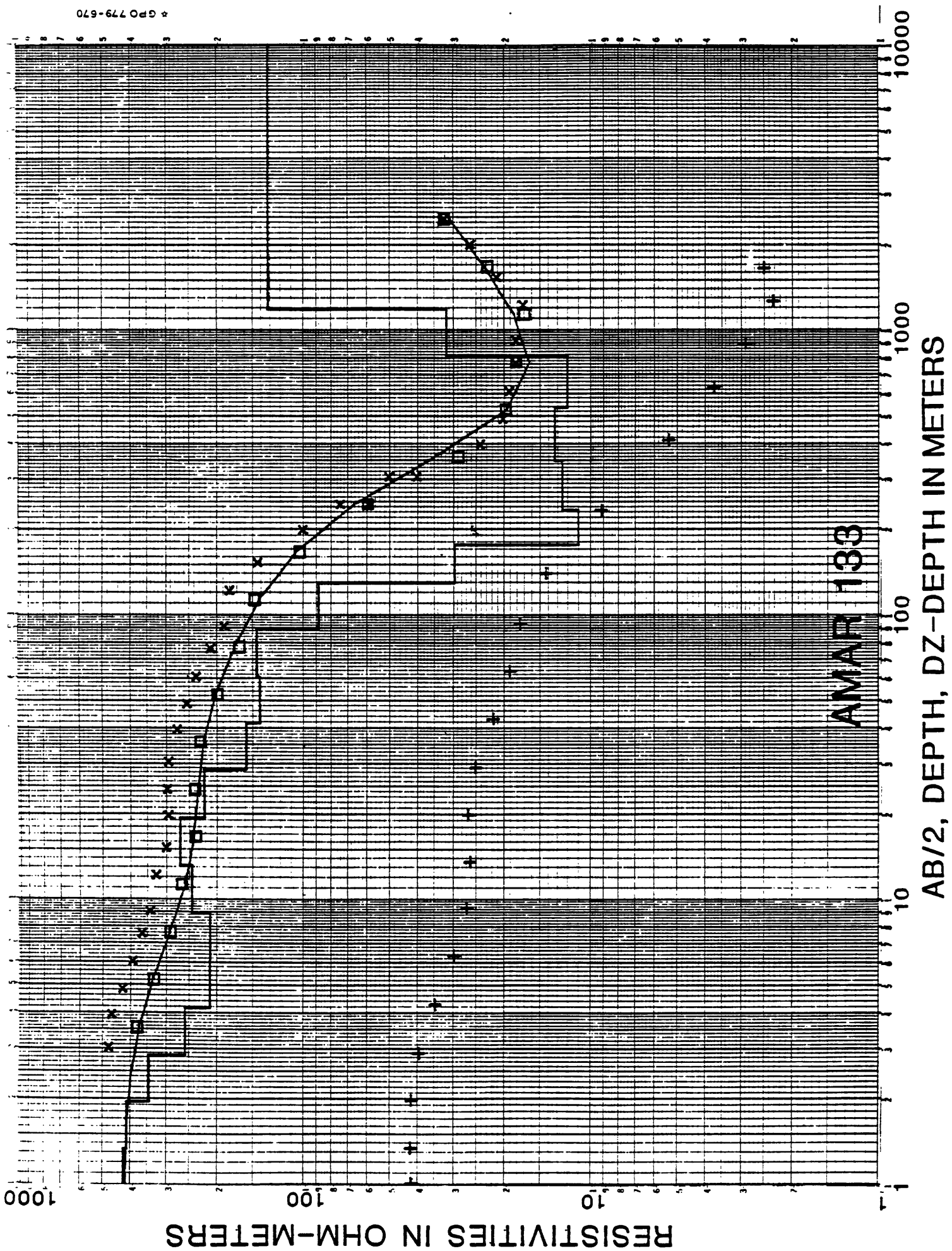


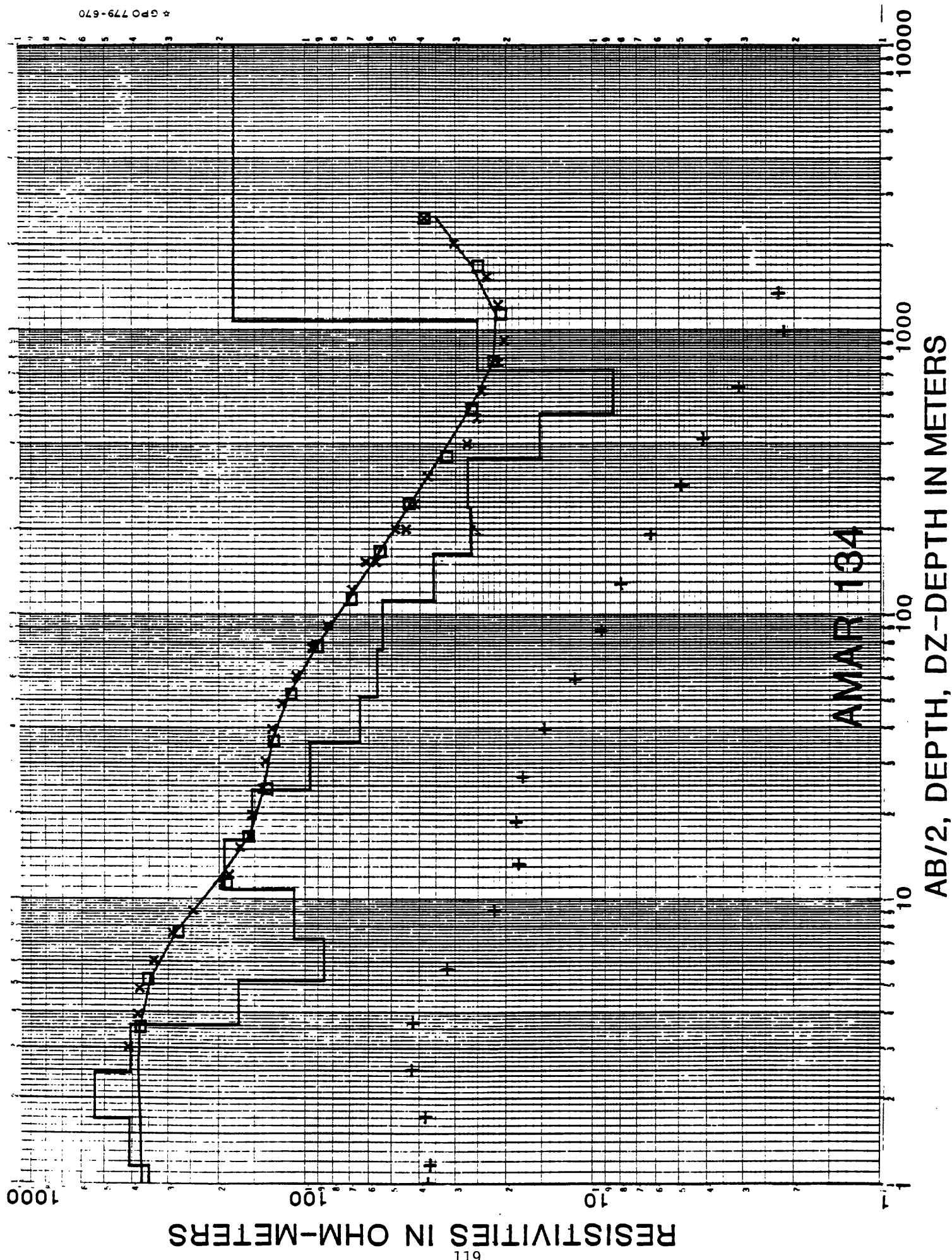


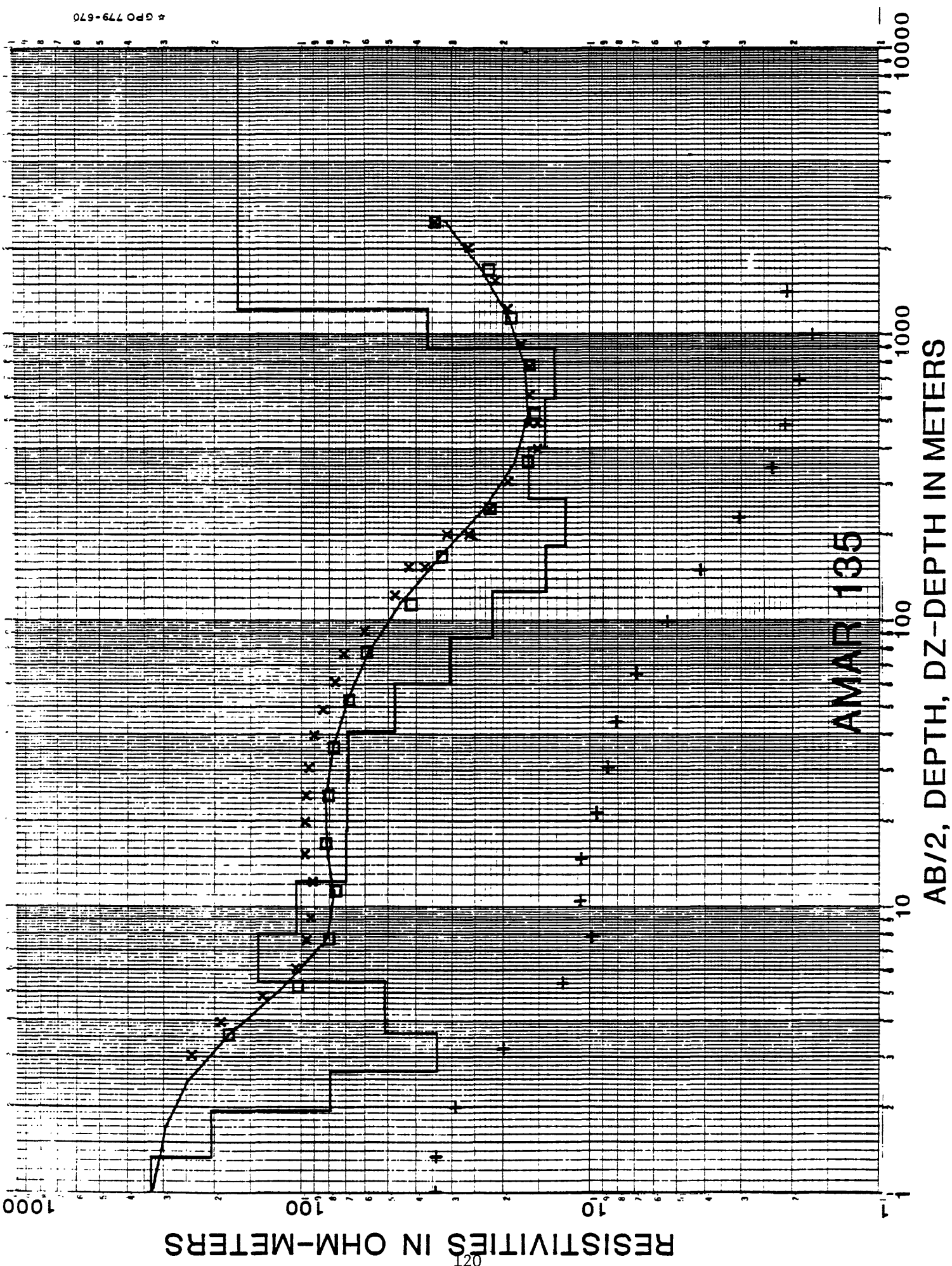






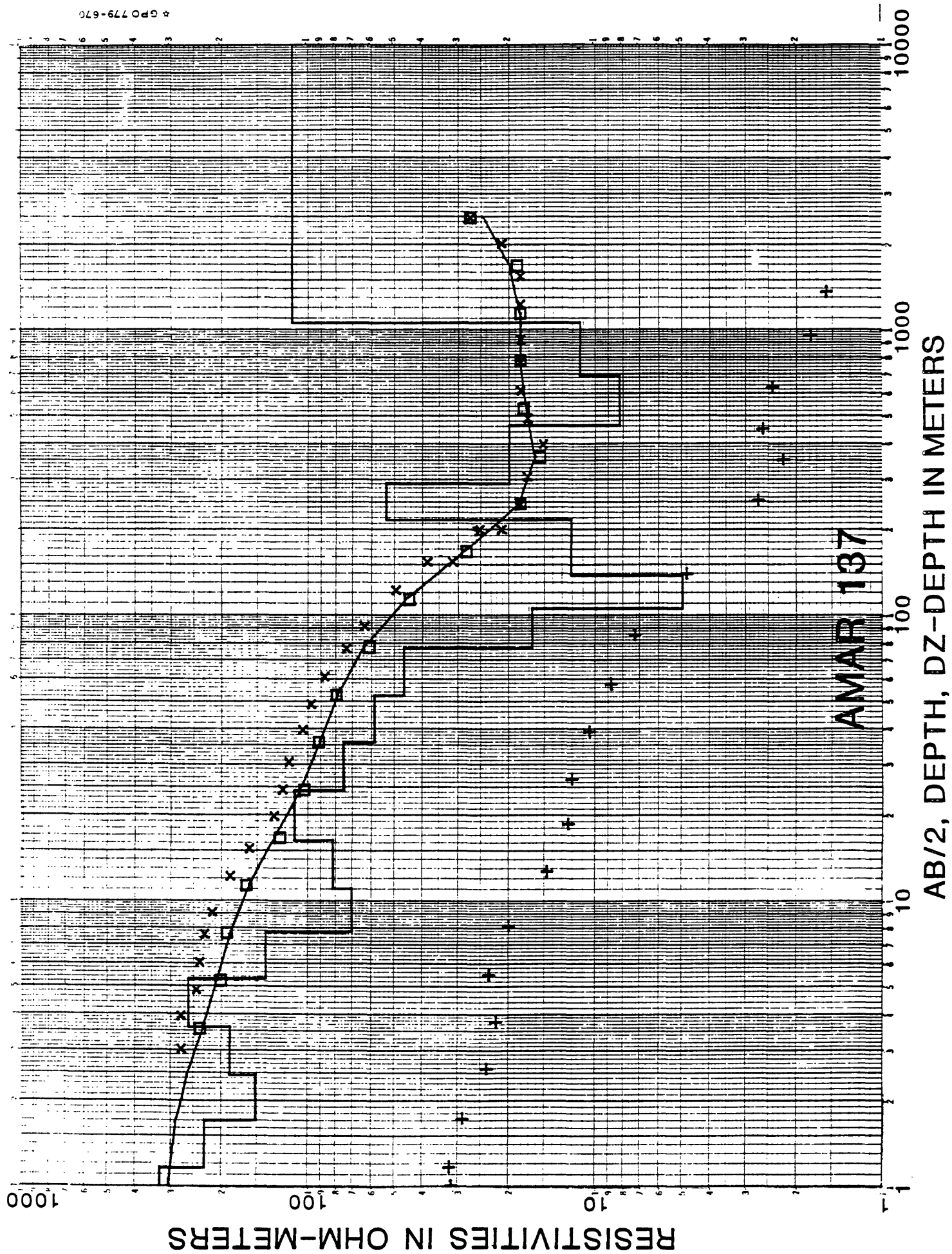


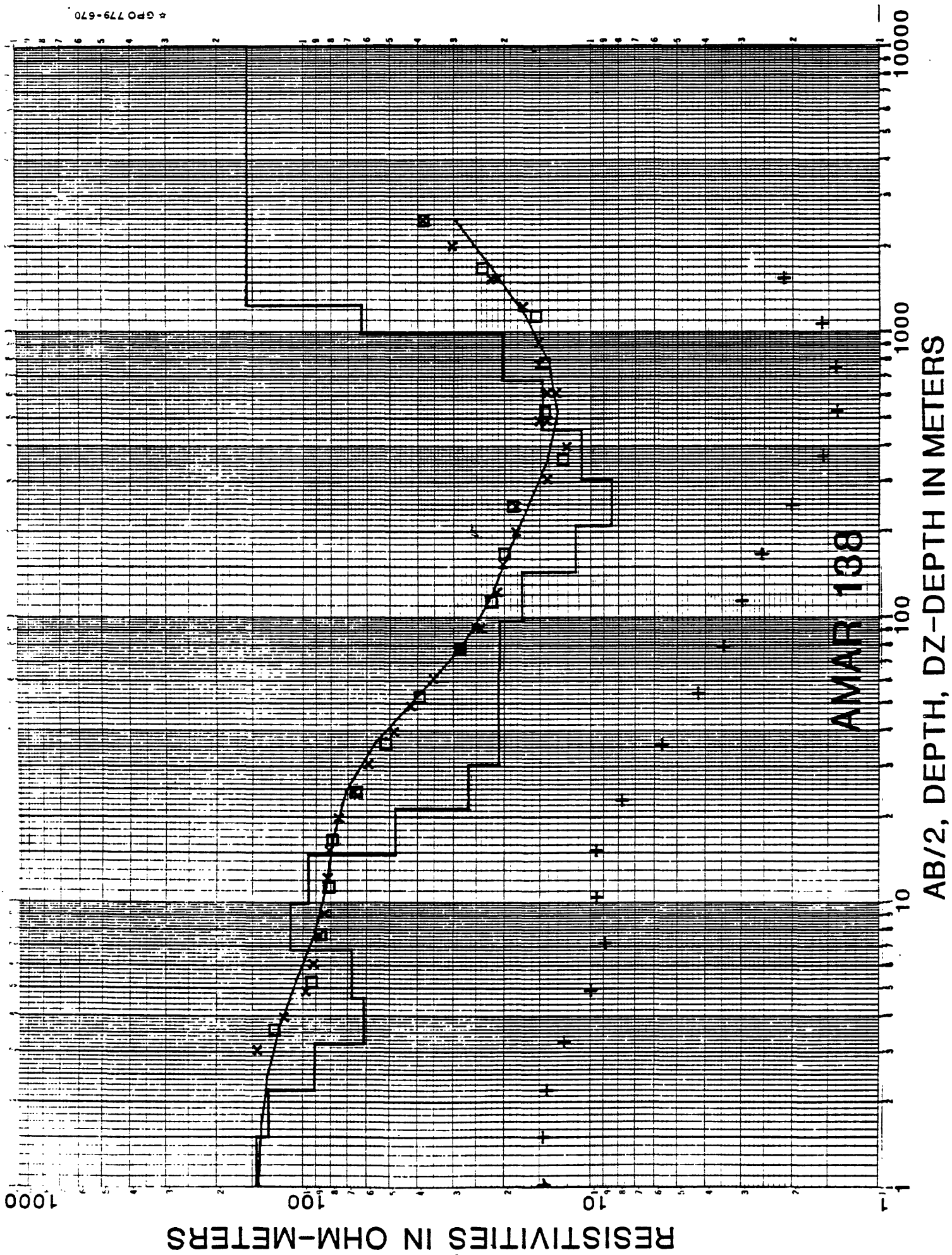




AMAR 136

AB/2, DEPTH, DZ-DEPTH IN METERS

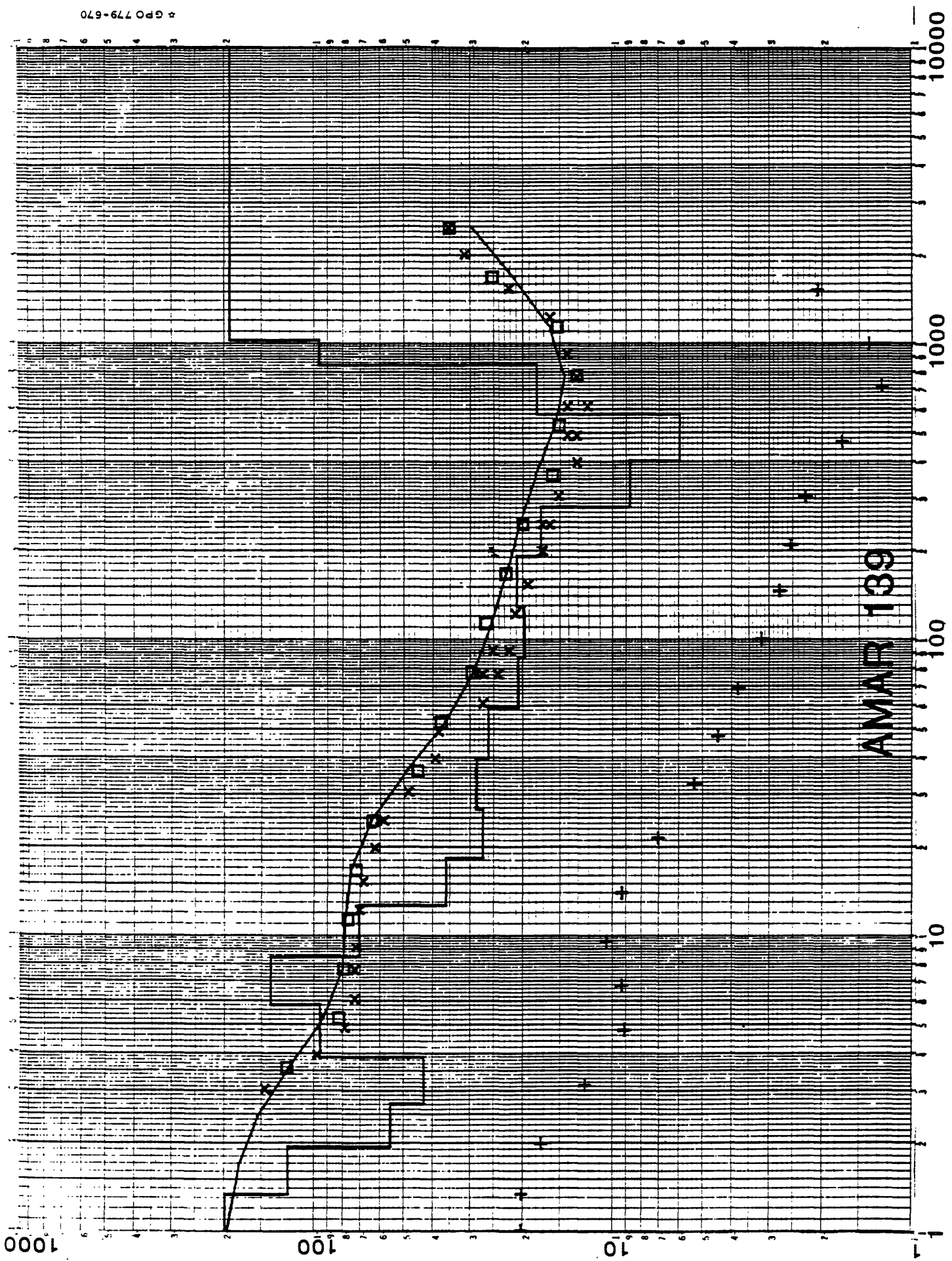


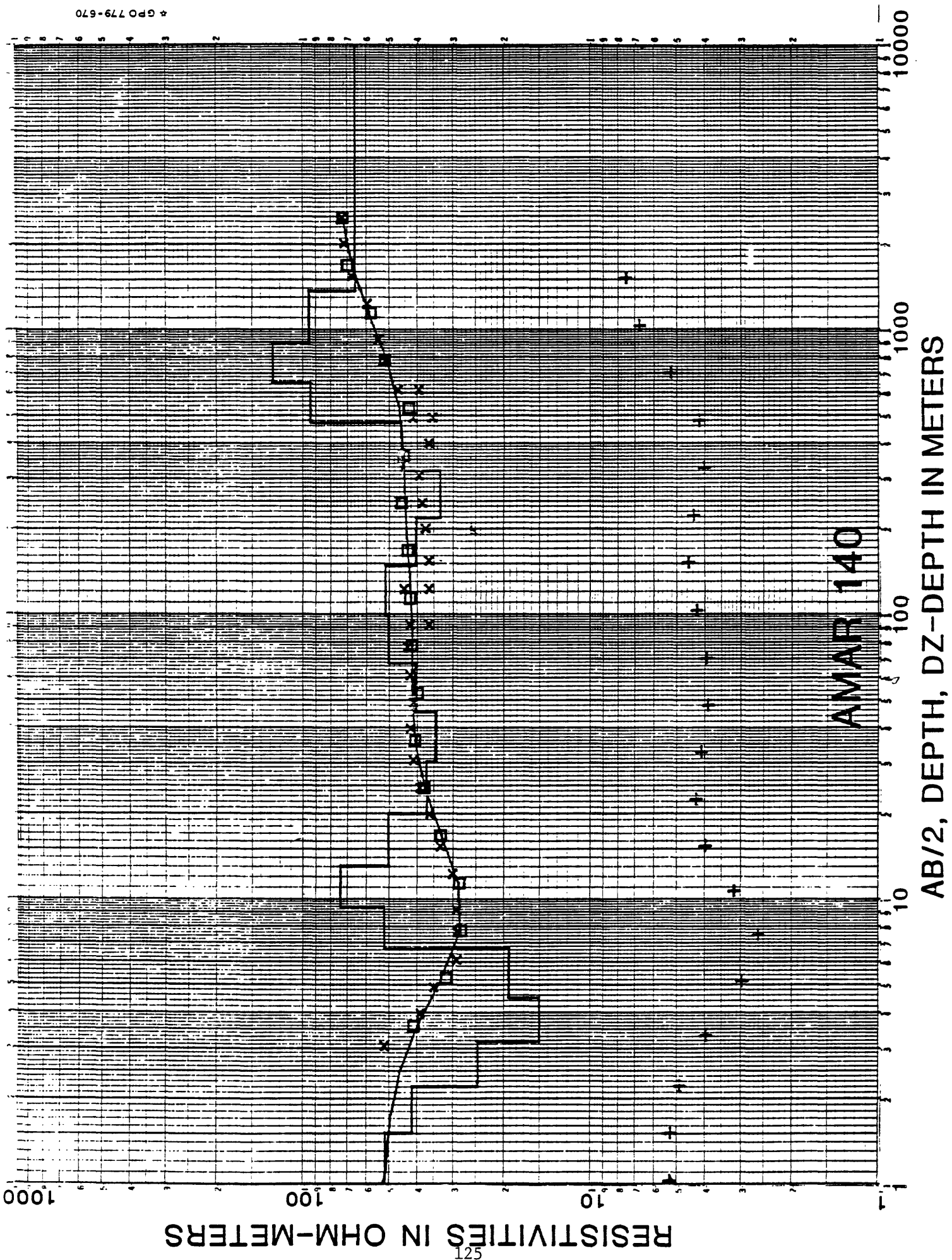


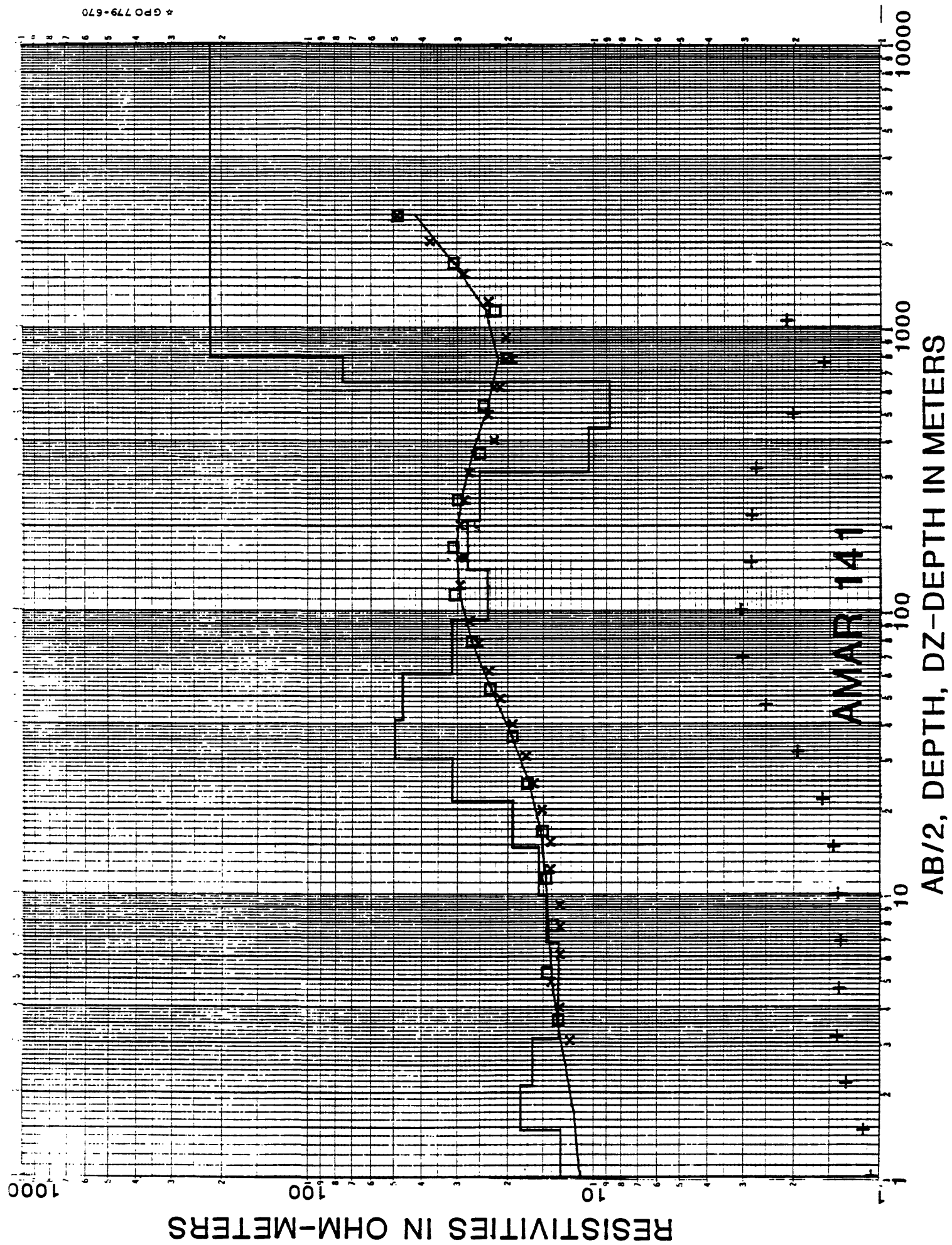
AMAR 139

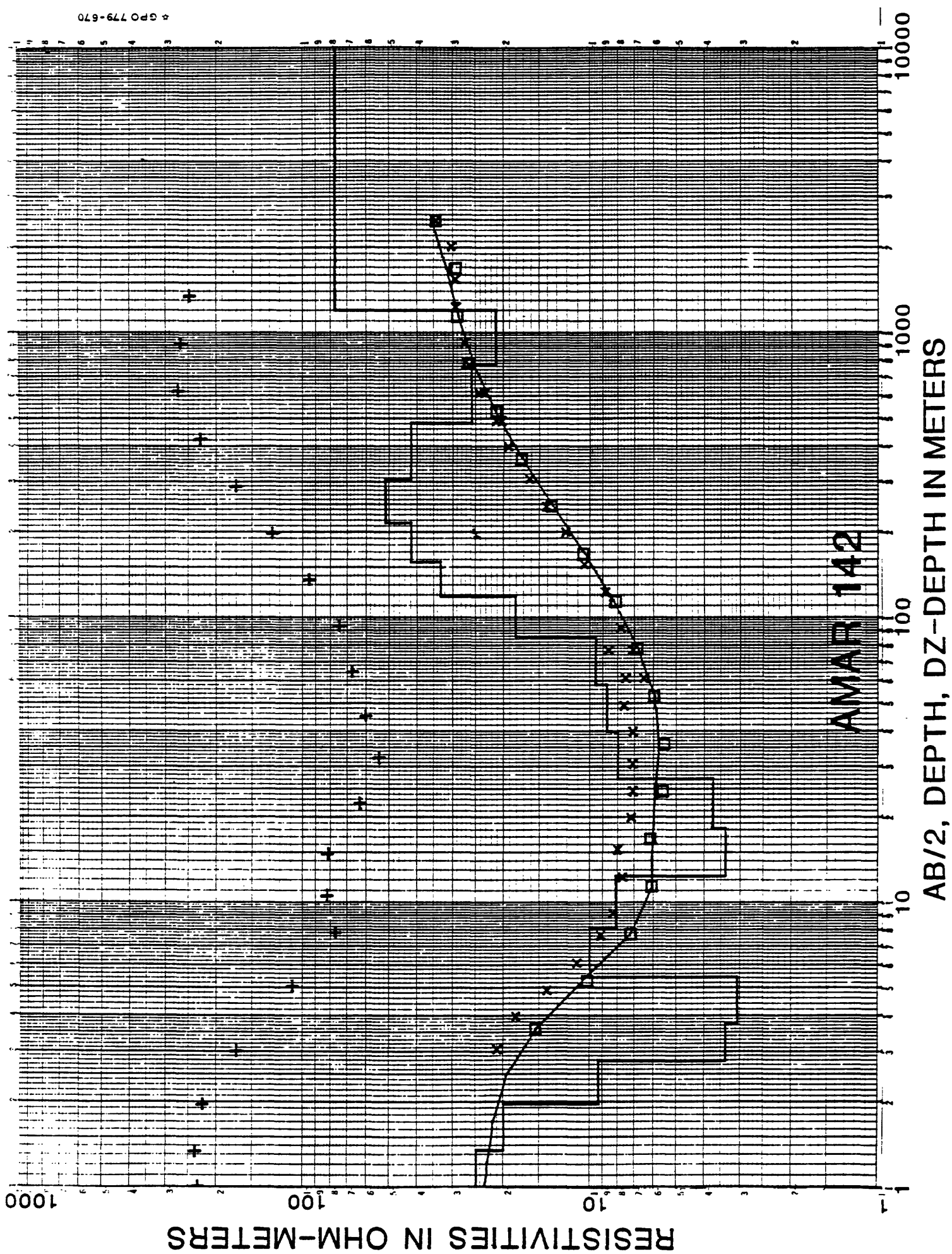
AB/2, DEPTH, DZ-DEPTH IN METERS

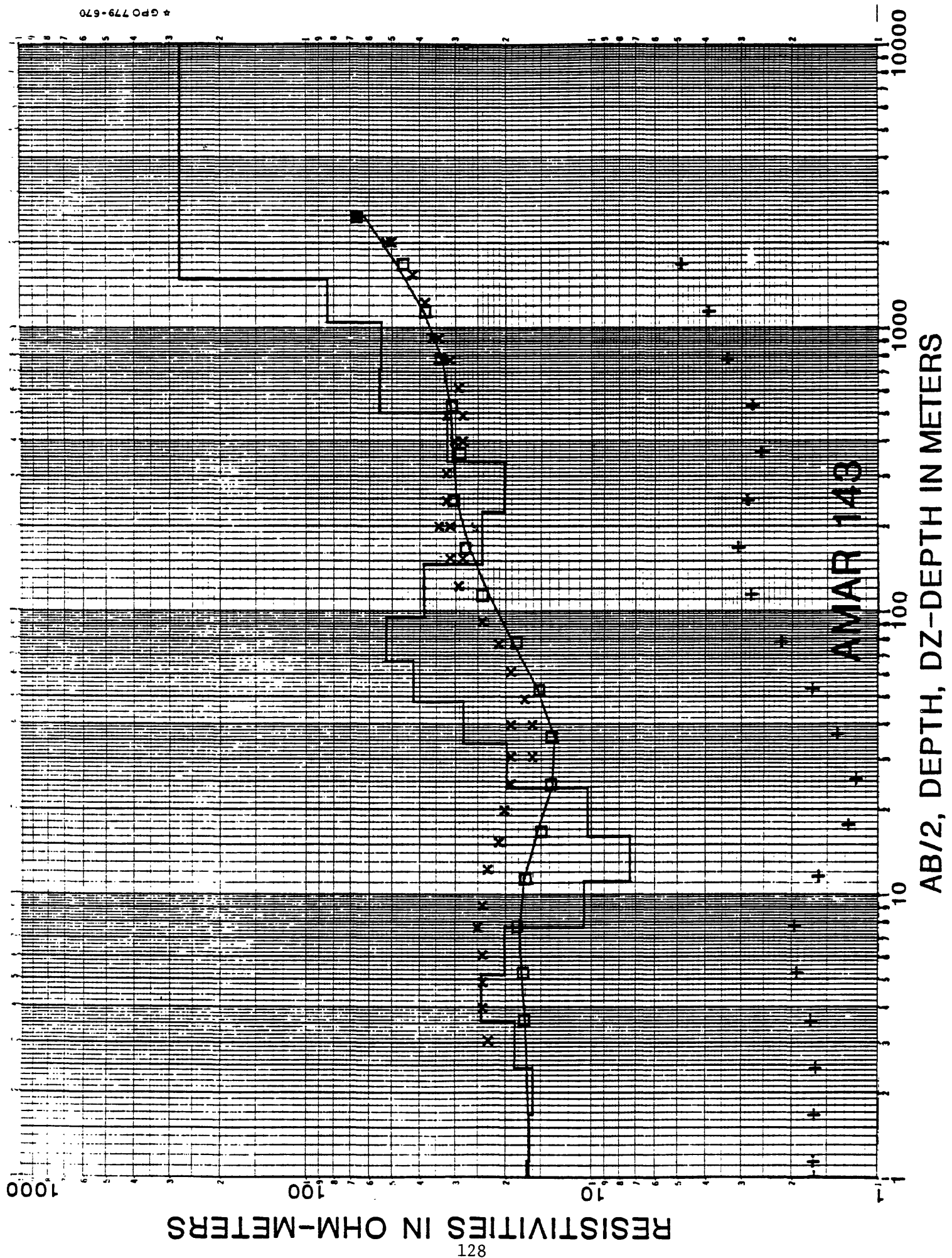
RESISTIVITIES IN OHM-METERS









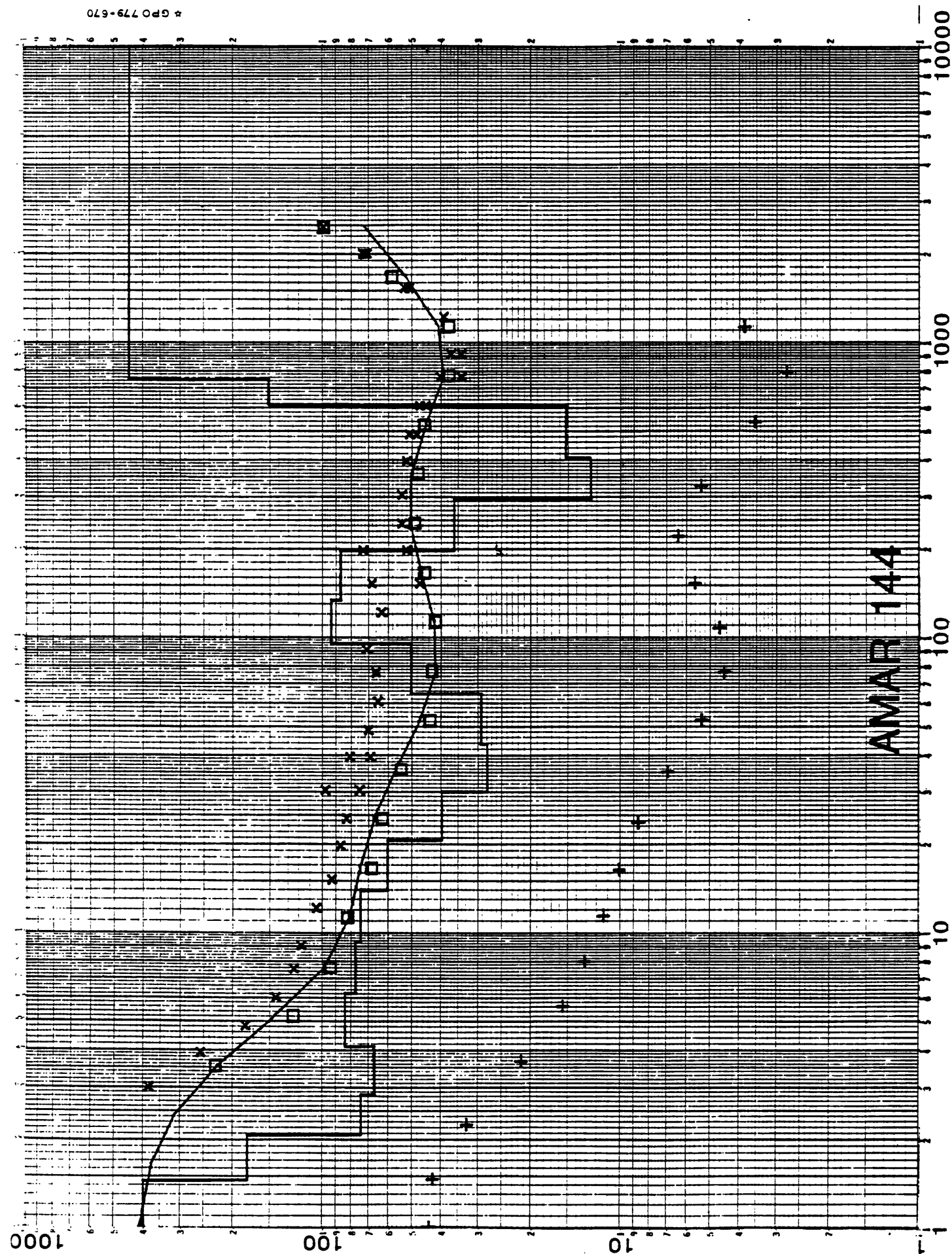


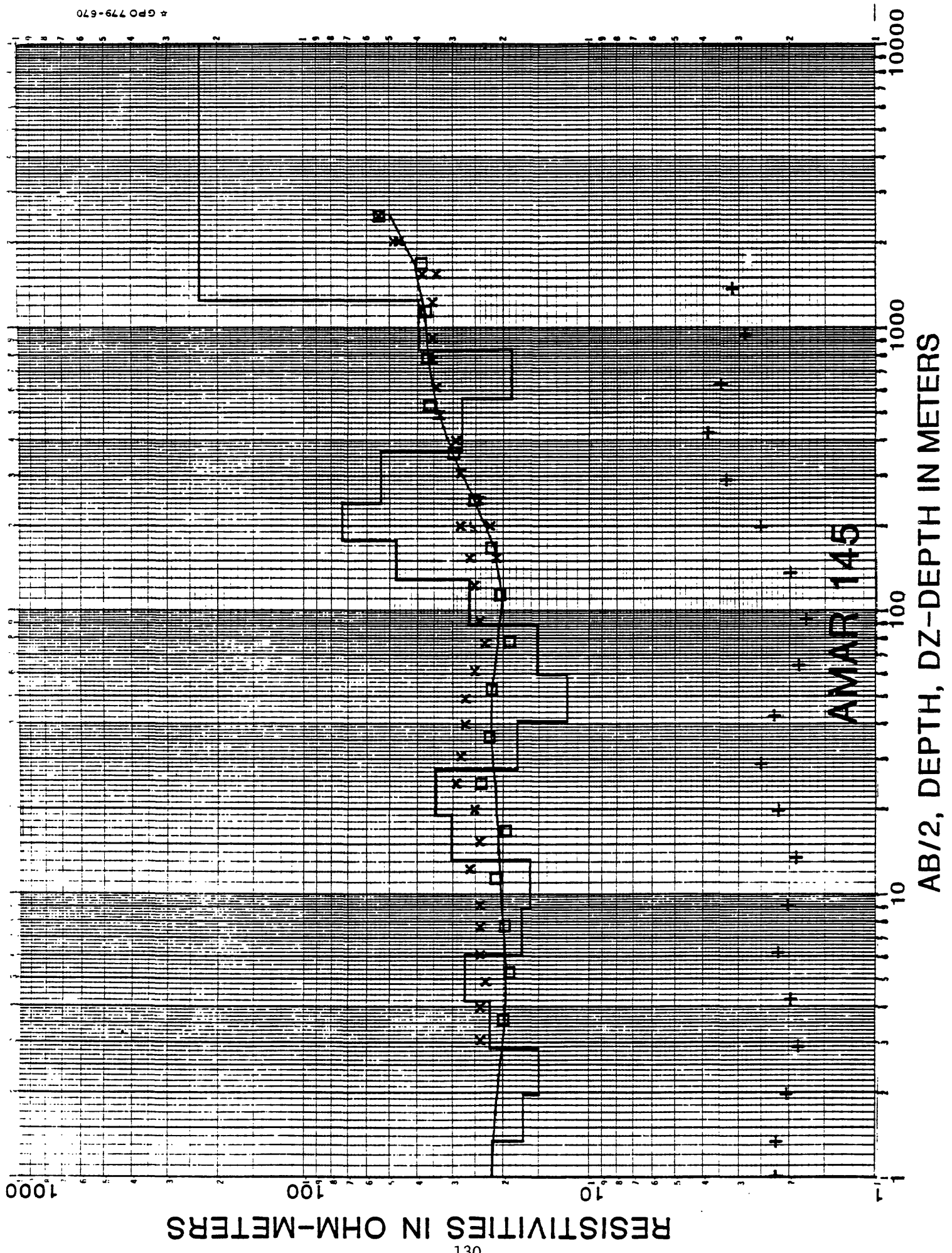
RESISTIVITIES IN OHM-METERS

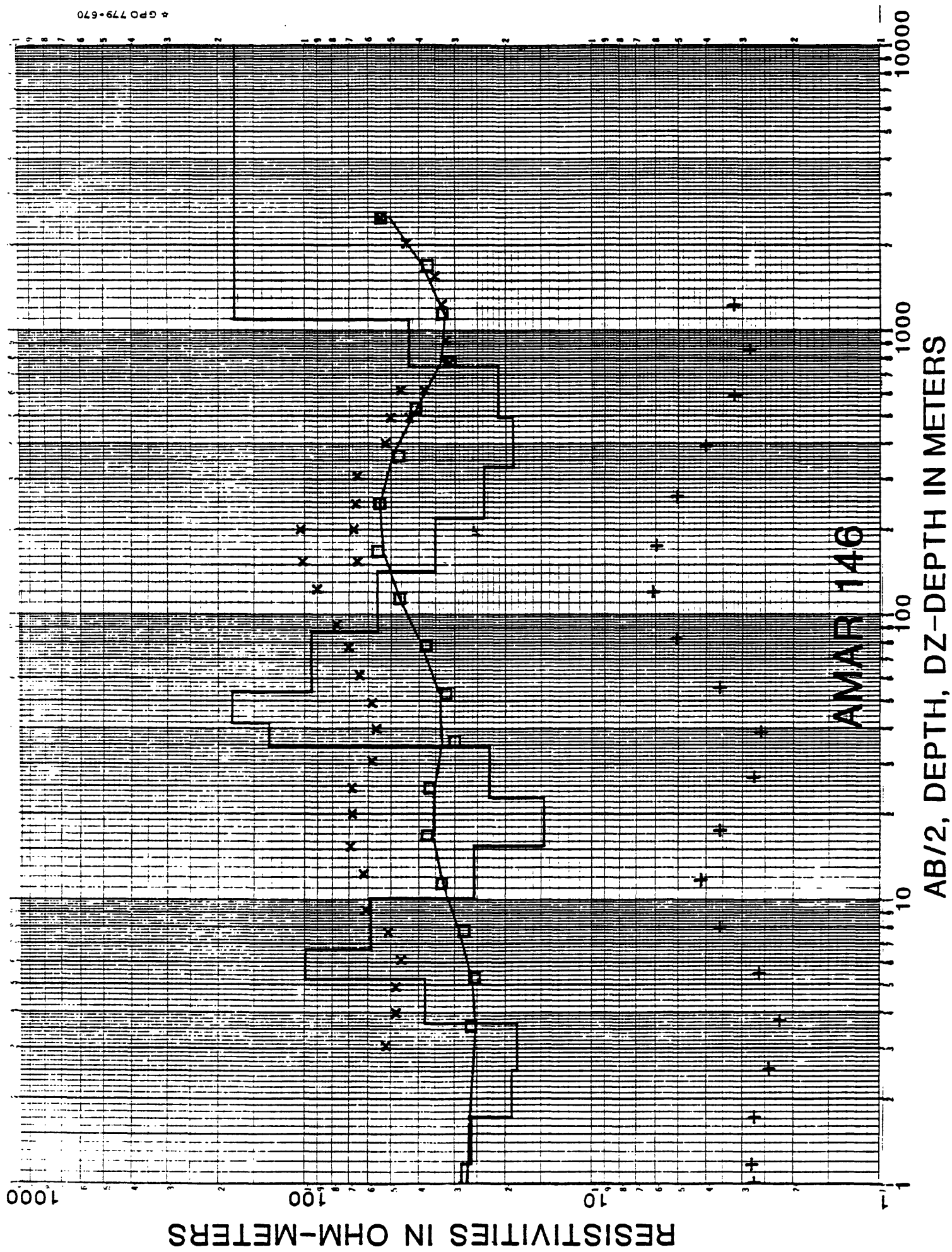
129

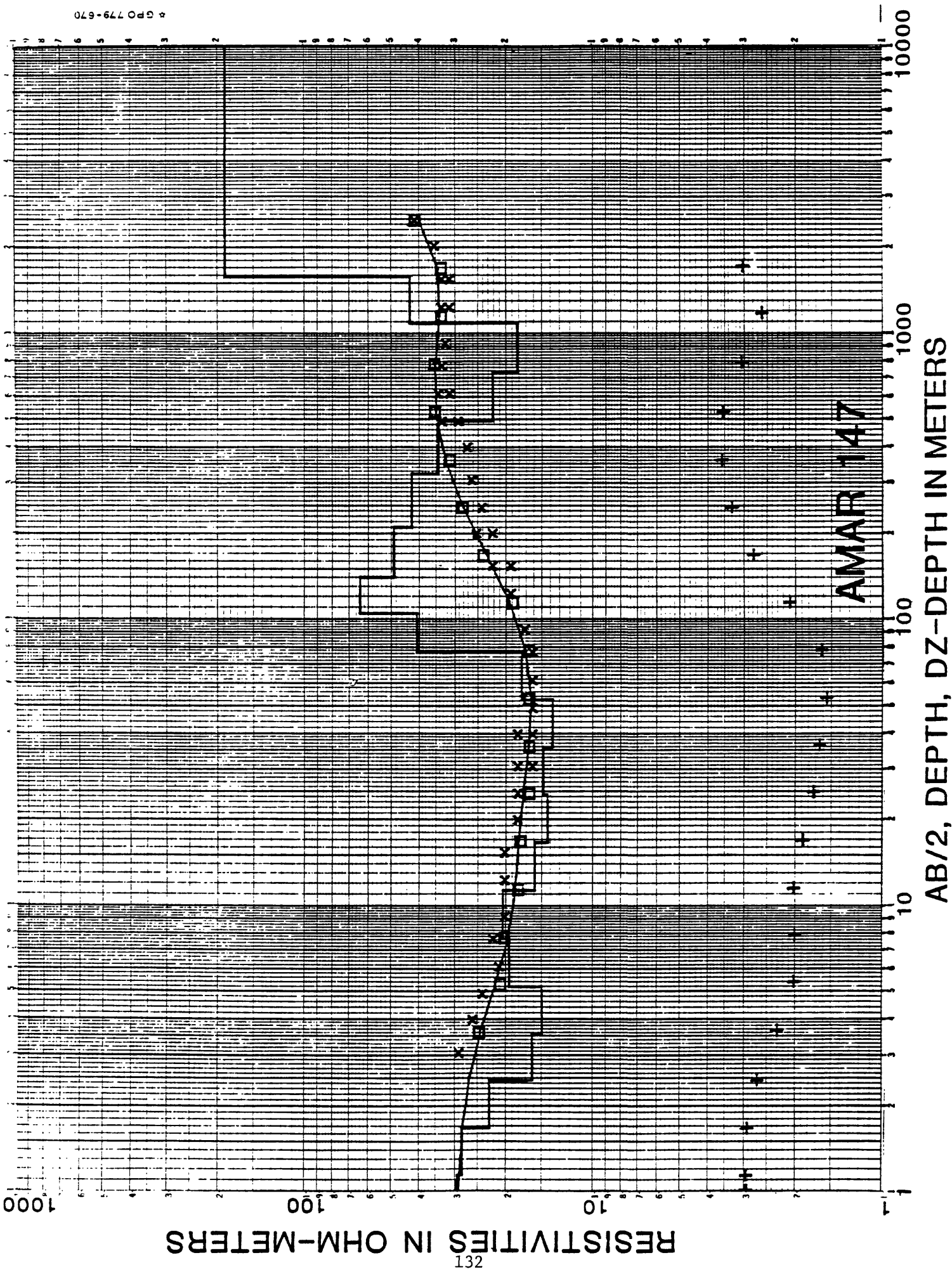
AMAR 144

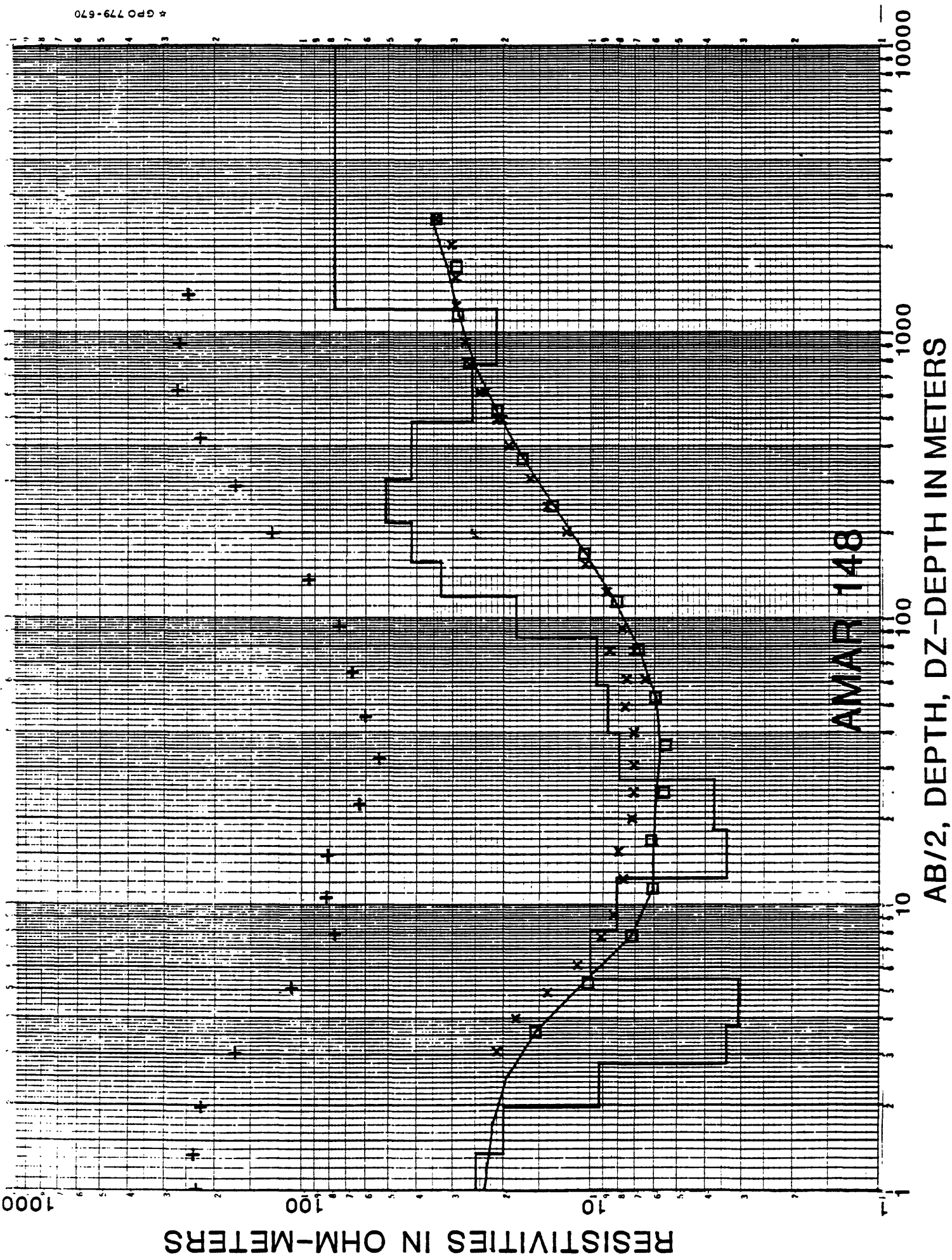
AB/2, DEPTH, DZ-DEPTH IN METERS

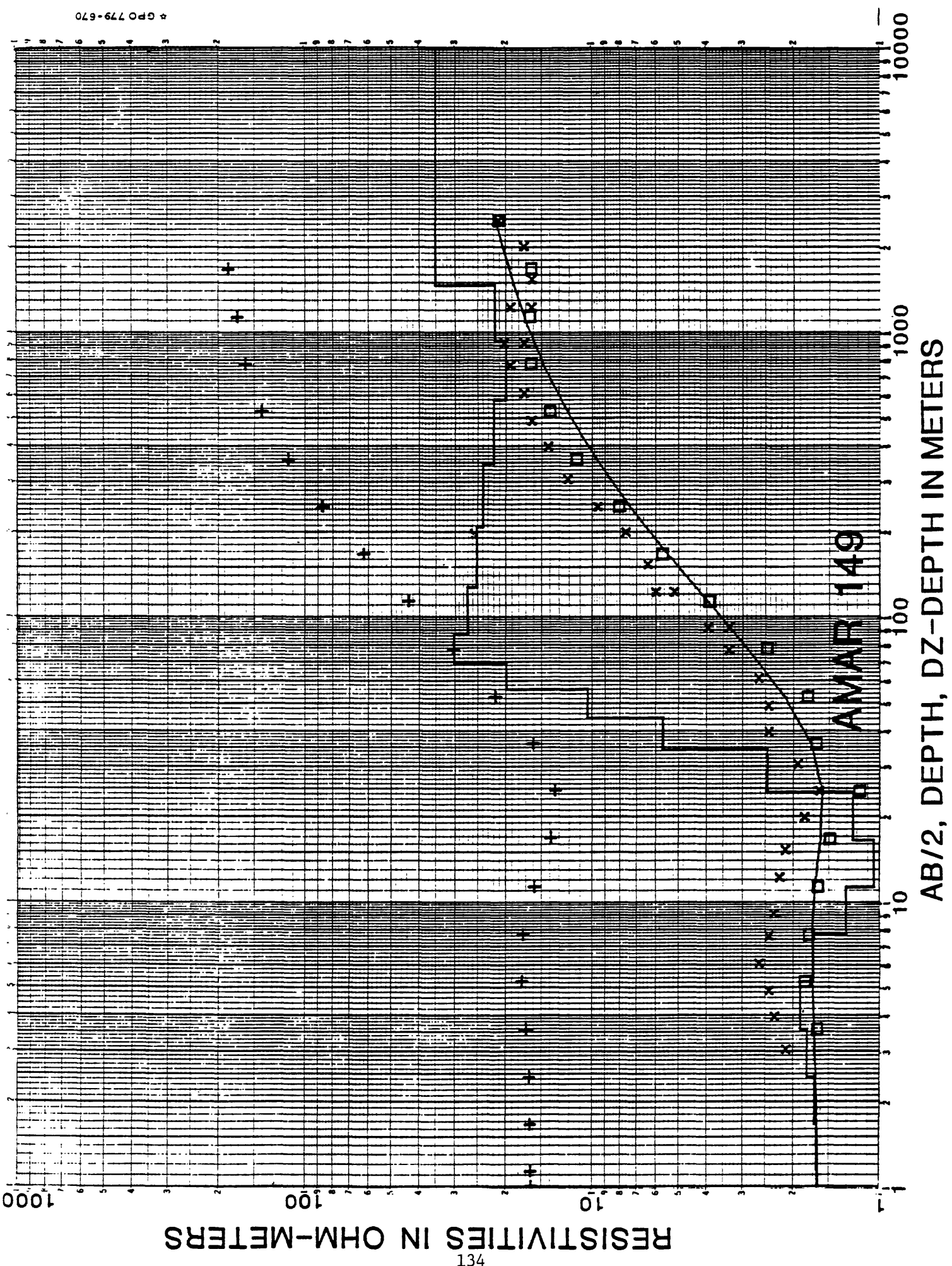


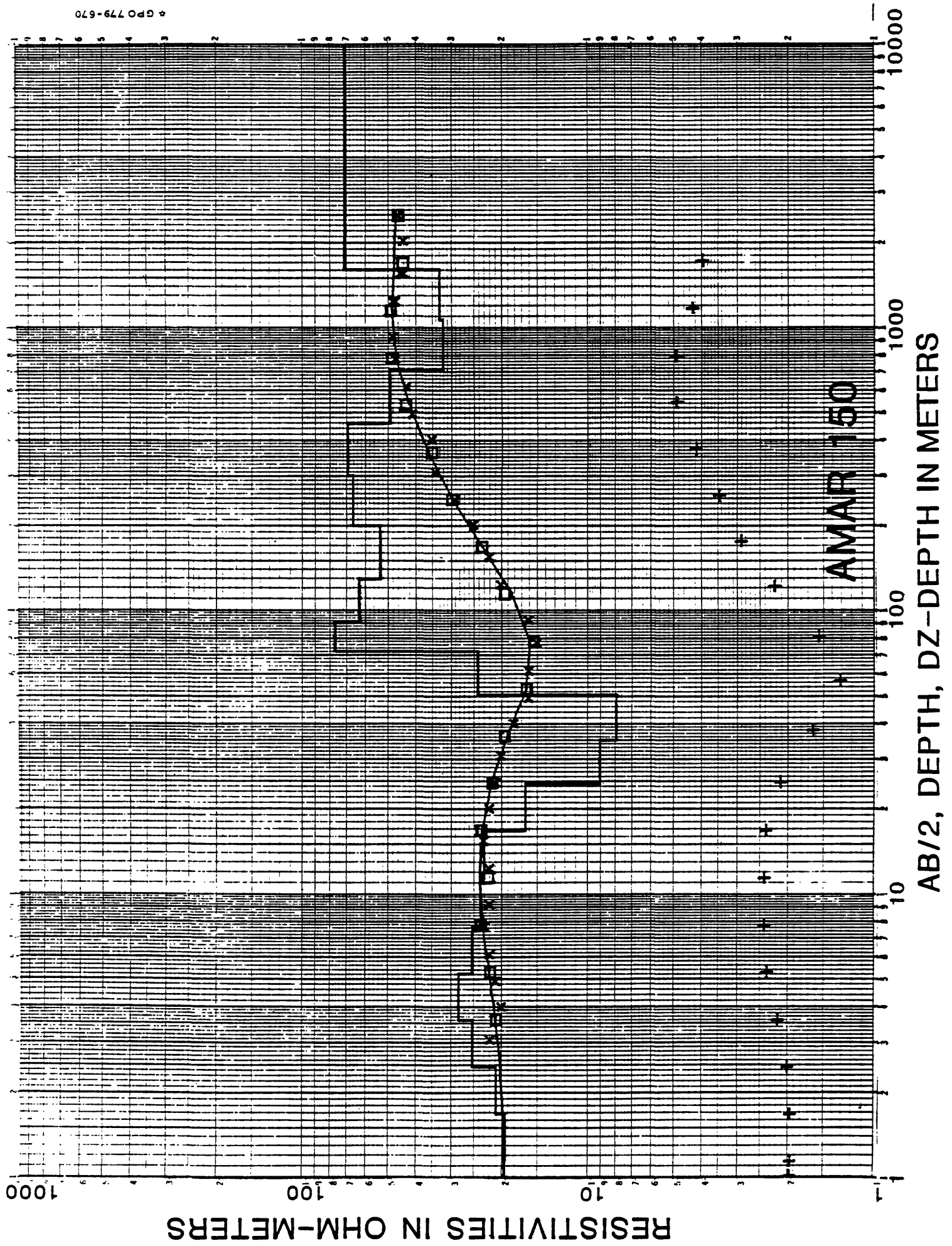


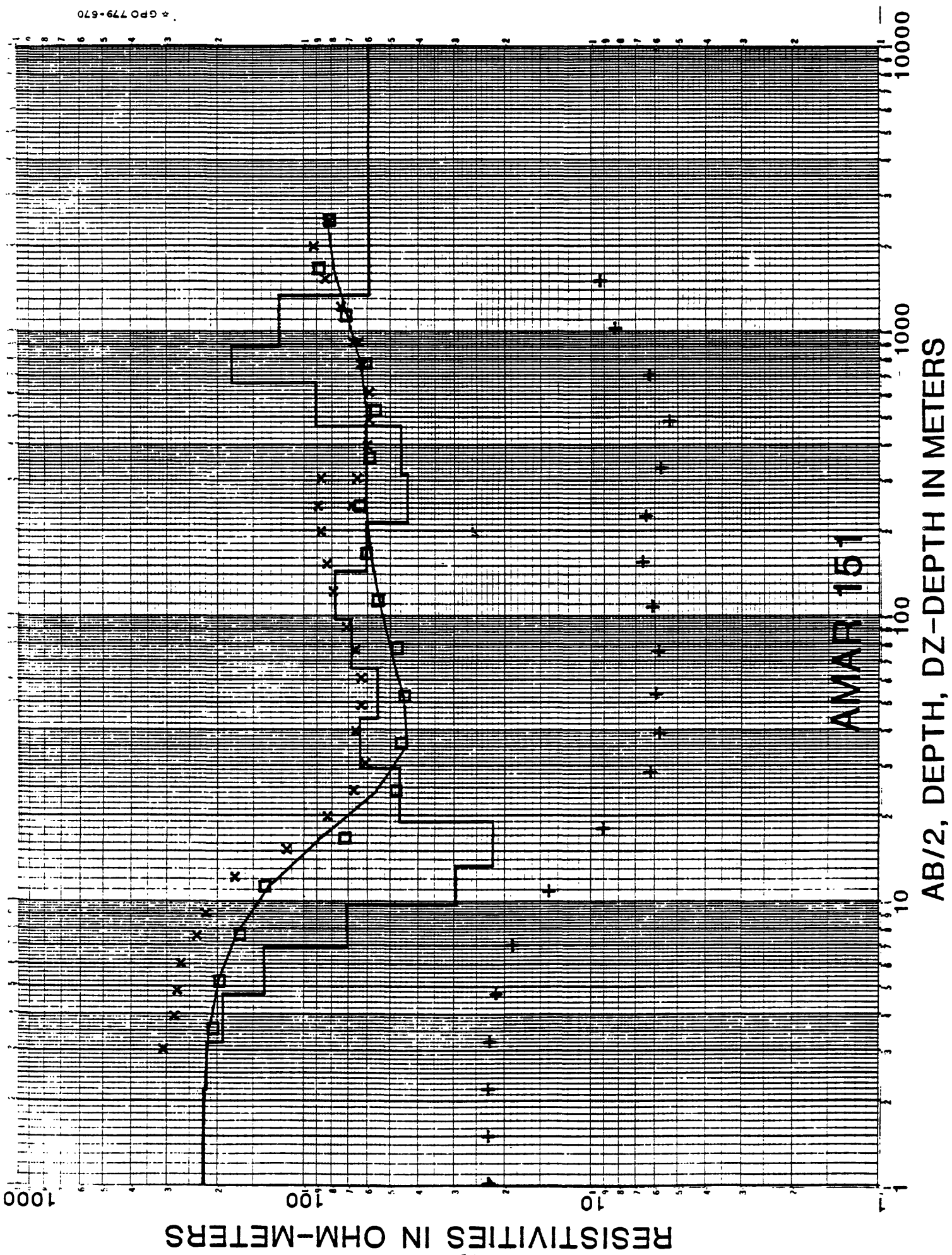


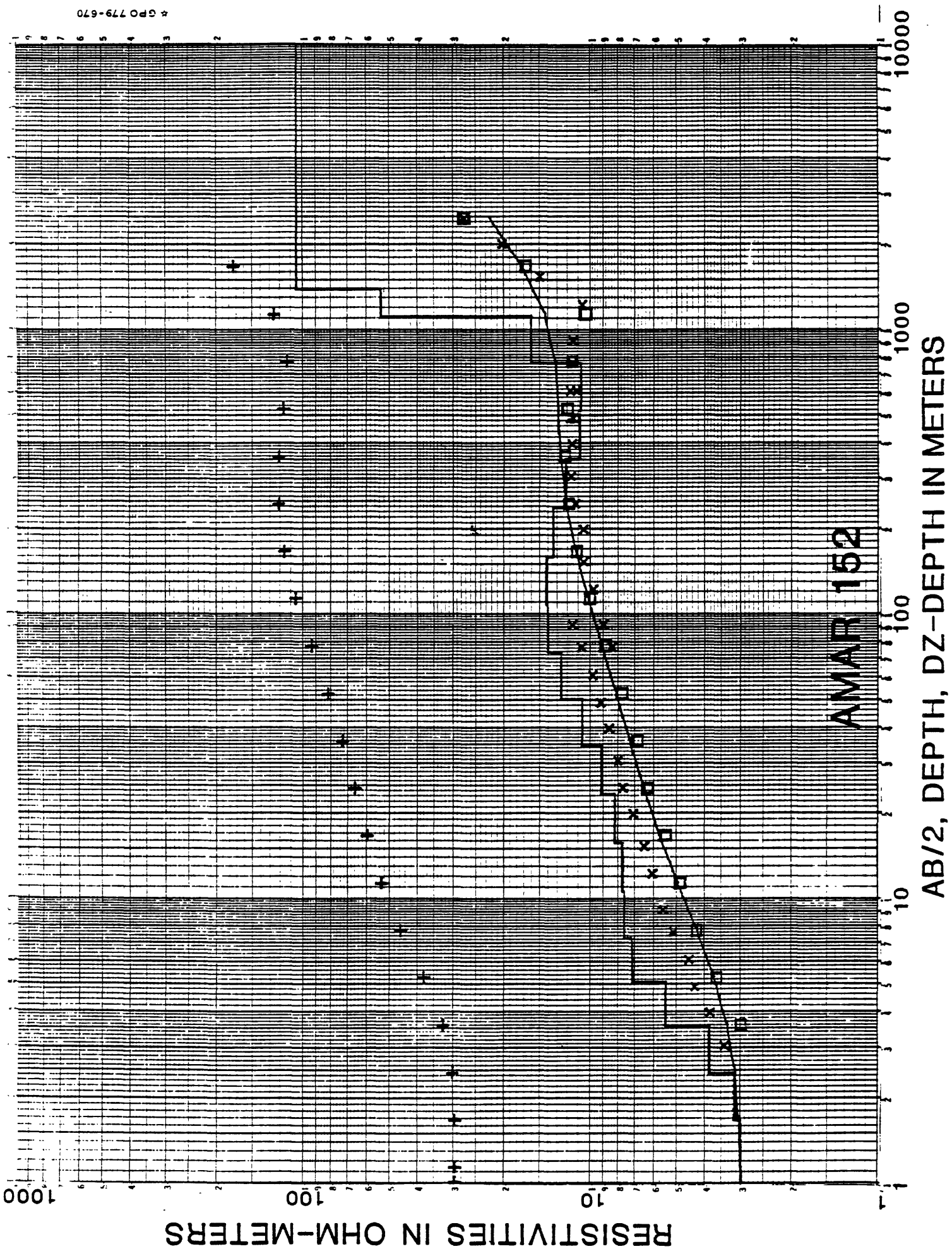


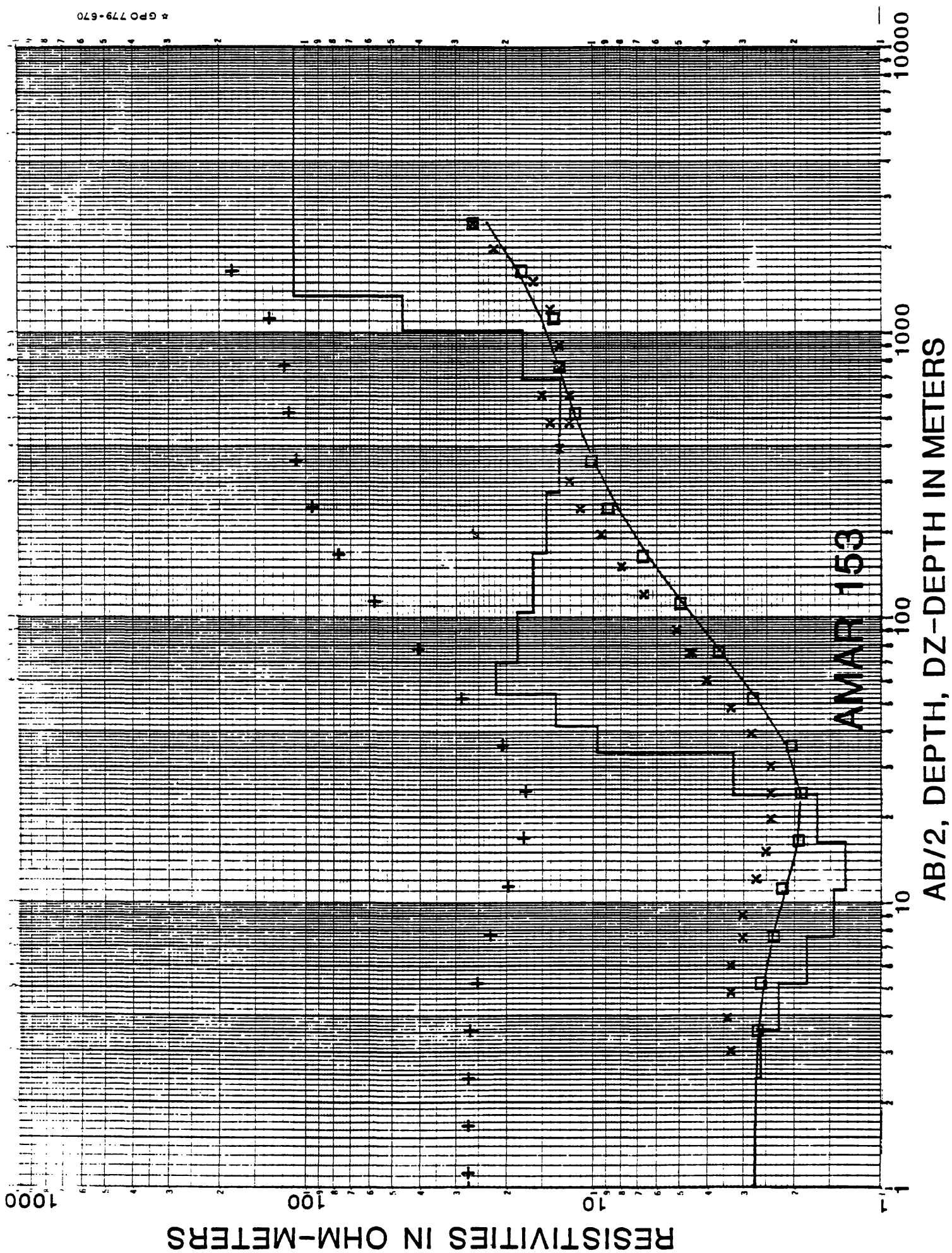


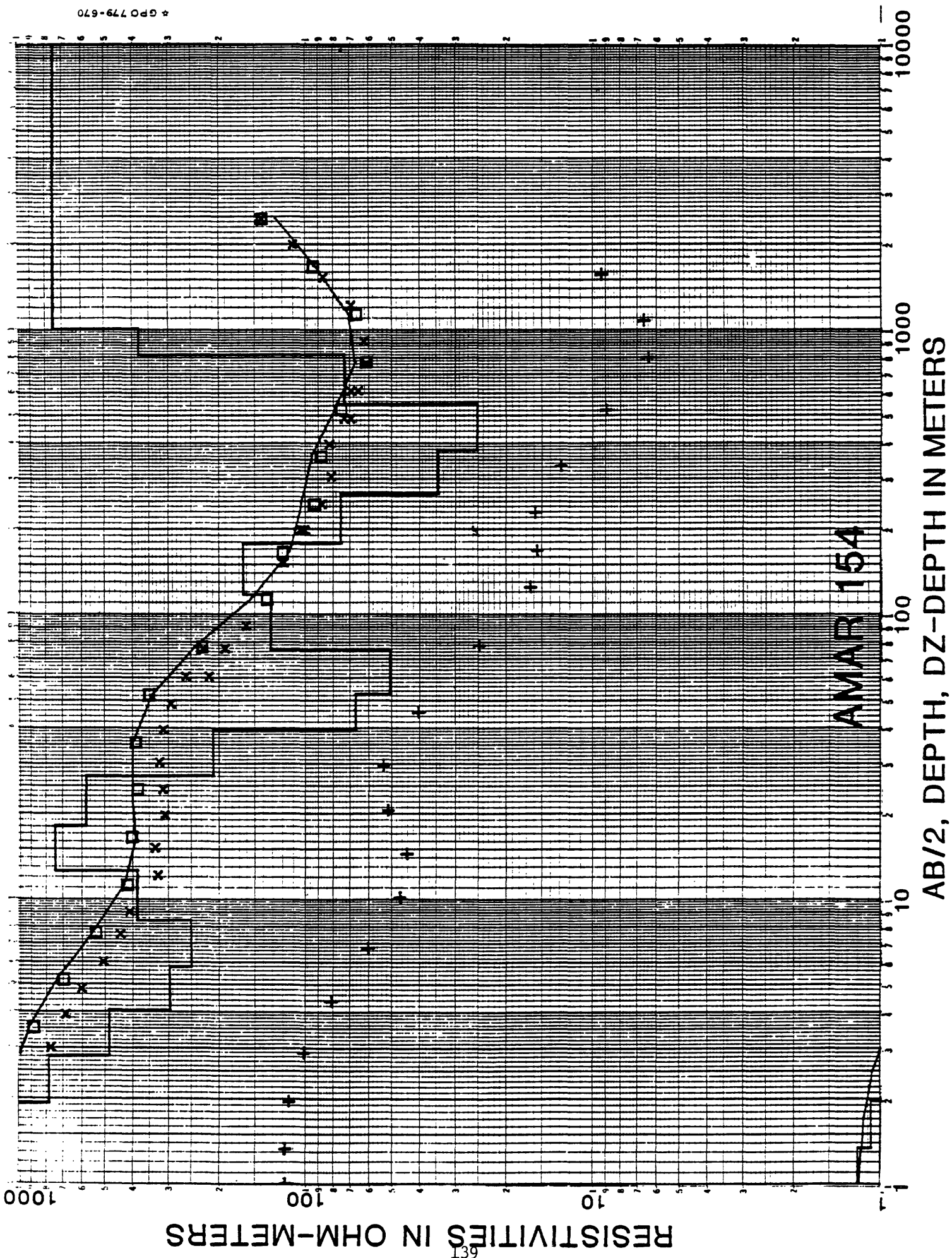


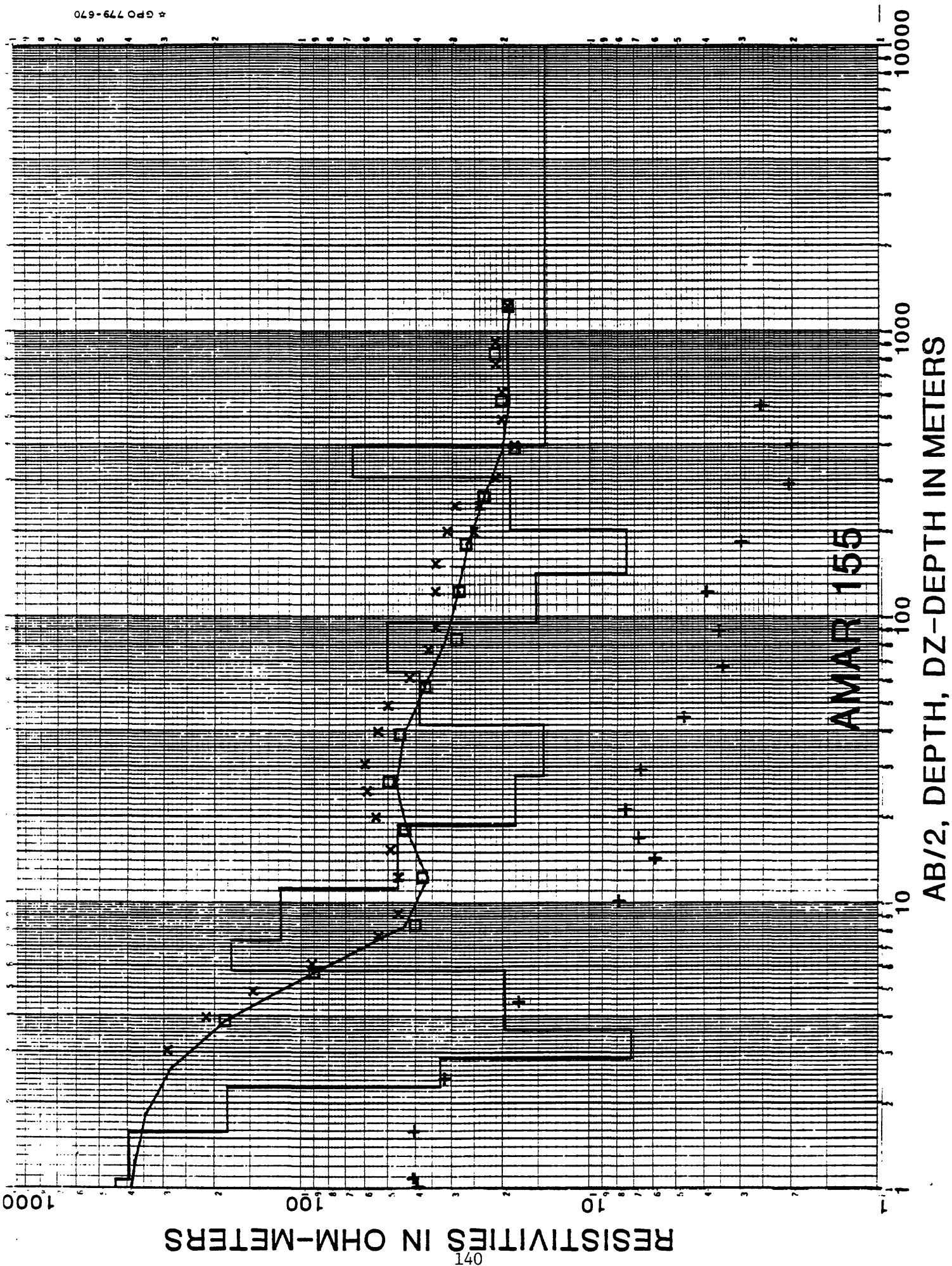


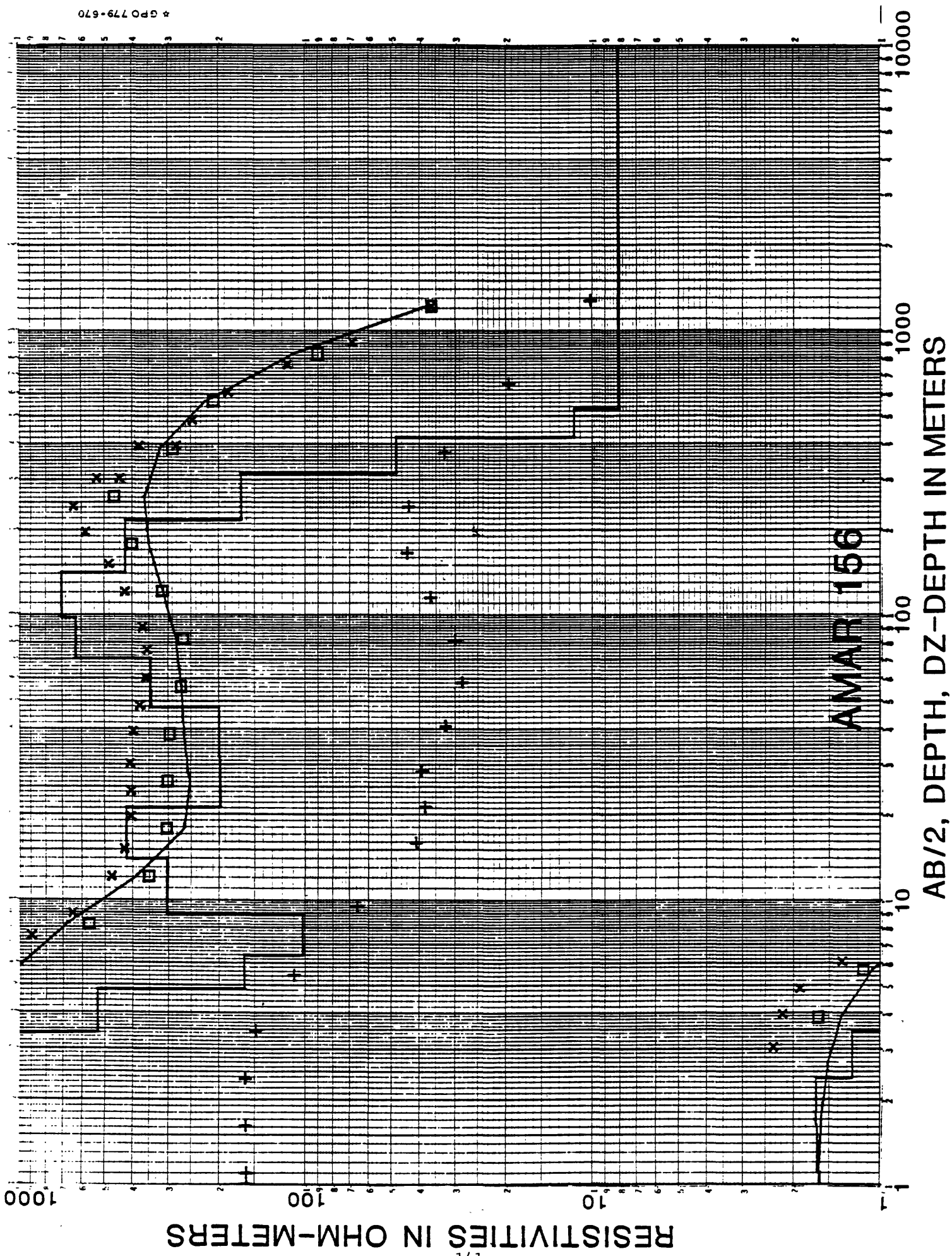


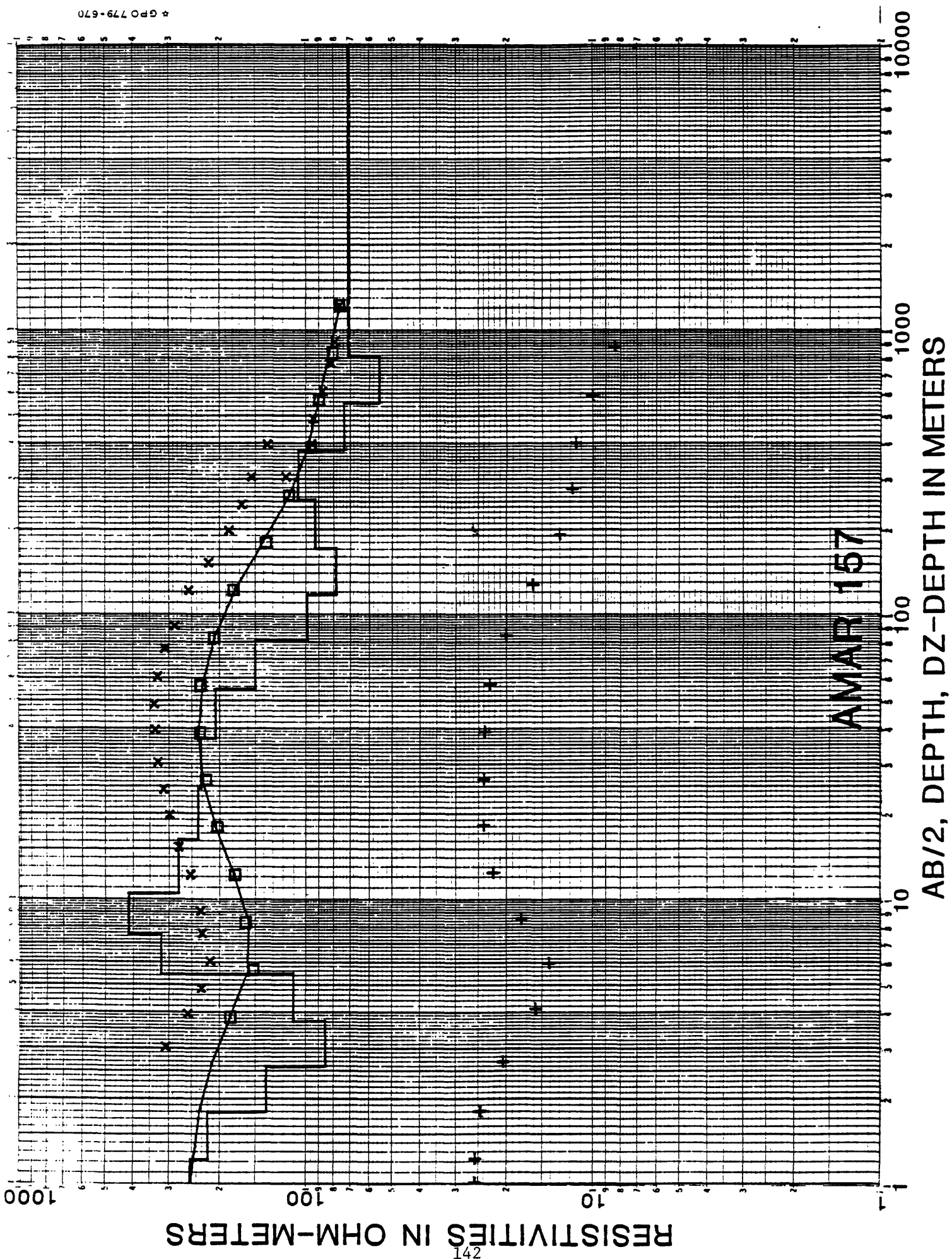


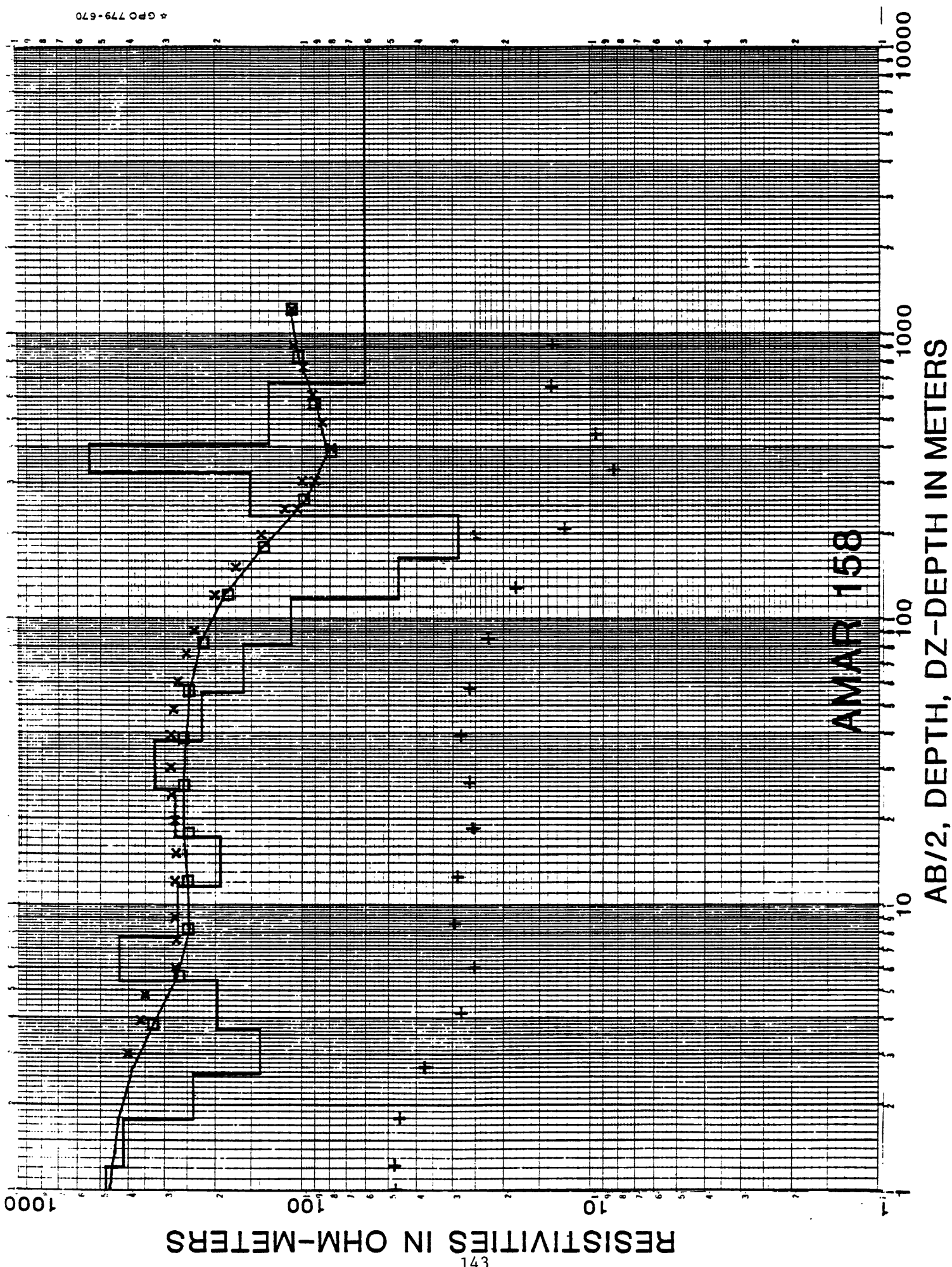


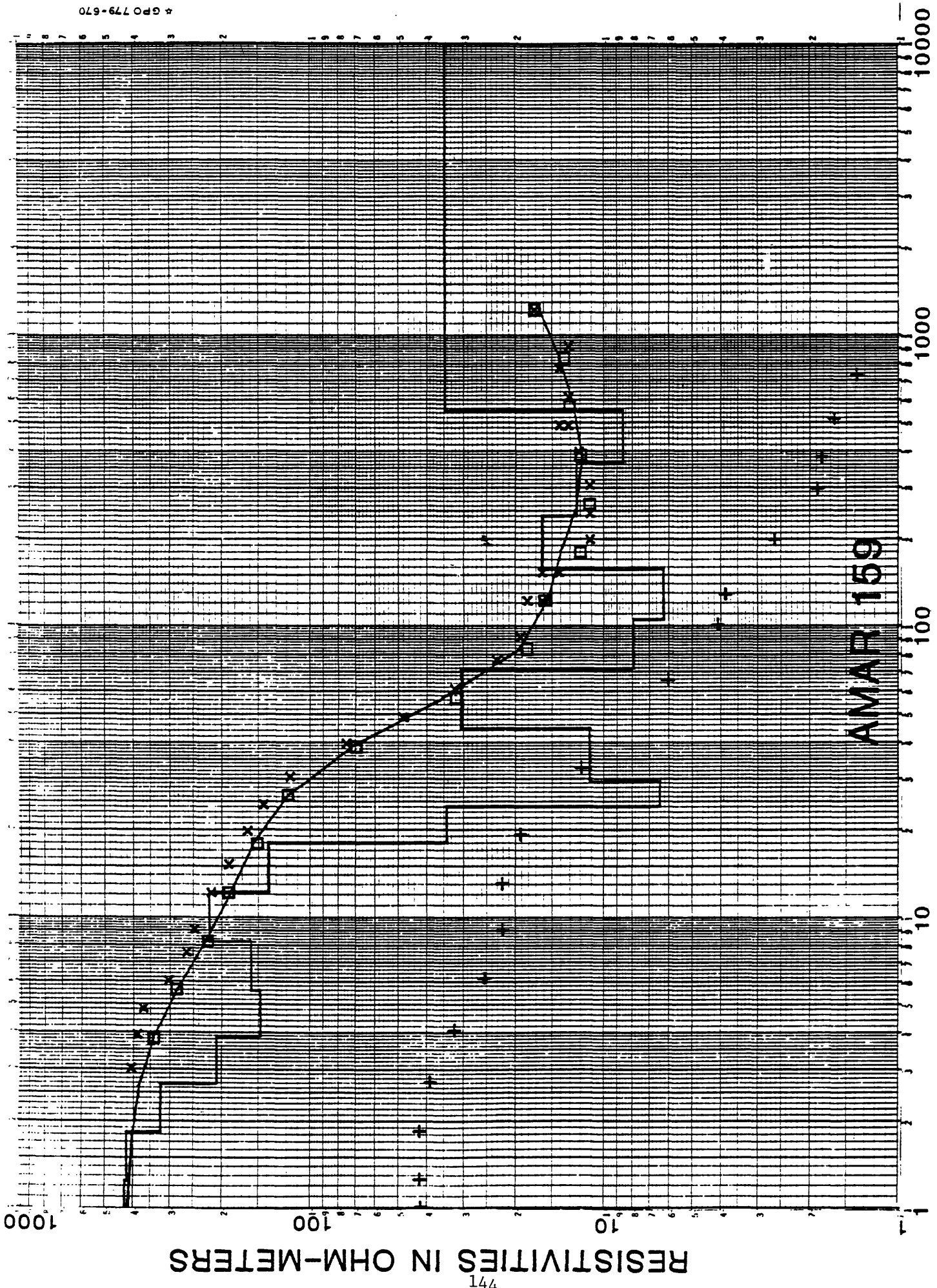












AMAR 159

AB/2, DEPTH, DZ-DEPTH IN METERS

RESISTIVITIES IN OHM-METERS

141

